

CRANFIELD UNIVERSITY

CRANFIELD DEFENCE AND SECURITY

CENTRE FOR DEFENCE ENGINEERING

PhD THESIS

Academic Year 2013-2014

Tamlin Whyte

**Adequacy of Test Standards in Evaluating Blast Overpressure (BOP)
Protection for the Torso**

Supervisor: Prof I Horsfall

June 2014

This thesis is submitted in partial fulfilment of the requirements for the Degree of
Doctor of Philosophy.

© Crown Copyright 2014. All rights reserved. No part of this publication may be
reproduced without the written permission of the copyright holder.

Abstract

The blast wave emanating from an explosion produces an almost instantaneous rise in pressure which can then cause Blast Overpressure (BOP) injuries to nearby persons. BOP injury criteria are specified in test standards to relate BOP measurements in a testing environment to a risk of BOP injury. This study considered the adequacy of test standards in evaluating BOP protection concepts for the torso.

Four potential BOP injury scenarios were studied to determine the likelihood of injury and the adequacy of test standards for appropriate protection concepts. In the case of vehicle blast, BOP injury is unlikely and test standards are adequate. In the scenario involving an explosive charge detonated within a vehicle, and the close proximity to a hand grenade scenario, test standards are not available. The demining scenario was identified as of importance as test standards are available, but do not mandate the evaluation of BOP protection.

A prototype South African Torso Surrogate (SATS) was developed to explore this scenario further. The SATS was required to be relatively inexpensive and robust. The SATS was cast from silicone (selected to represent body tissue characteristics) using a torso mould containing a steel frame and instrumented with chest face-on pressure transducer and accelerometer. The SATS was subjected to an Anti-Personnel (AP) mine test and the Chest Wall Velocity Predictor and Viscous Criterion were used to predict that BOP injuries would occur in a typical demining scenario. This result was confirmed by applying the injury criteria to empirical blast predictions from the Blast Effects Calculator Version 4 (BECV4).

Although limitations exist in the ability of injury criteria and measurement methods to accurately predict BOP injuries, generally a conservative approach should be taken. Thus, it is recommended that the risk of BOP injuries should be evaluated in demining personal protective equipment test standards.

ACKNOWLEDGEMENTS

This study was the outcome of working with many remarkable colleagues and mentors. I thank them all for sharing their expertise, opinions and passion for their various fields of interest.

Thanks to the Council for Scientific and Industrial Research (CSIR) who gave me the opportunity to work in the fascinating field of blast injuries. Thanks for showing faith in me and for providing funding for this study. Thanks to David Reinecke, for introducing me to the world of vehicle validation testing and providing me with opportunities to learn about the fields of injury biomechanics and blast injuries. Izak Snyman, thanks for being my mentor and CSIR study supervisor and providing feedback during the study. Thanks for sharing your valuable time with me. Thanks to Frikkie Mostert, Theo van Dyk, Philip Roach, Dave Roos, Jaap Lotter and Dave Engels, for inspiring me to believe in my opinions and for always having time to chat about ideas and theories to grow my thinking. Leon Broodryk, Deon Malherbe and Jimmy Hannan, thanks for assisting me with the practical design and manufacture of the South African Torso Surrogate (SATS). Geoff Turner, Jimmy Hannan, Piet Ramaloko, Martin Milwa and Tsepo Setlai, thanks for teaching me about the field of blast testing in general and for assisting with instrumentation and measurement for blast testing. Rayeesa Ahmed and Thanyani Pandelani, thanks for sharing the learning process with me.

To the Armaments Corporation of South Africa (ARMSCOR), thanks for providing funding for some of the testing in this study and specifically, Frans Beetge, for sharing his experience in the field of validation testing of landmine protected vehicles.

Thanks to the NATO HFM-148 working group (Piet-Jan Leerdam, Marike van der Horst, Mat Philippens, Frank Dosquet, José Manseau, Cynthia Bir, Denis Lafont, Lars Svensson, Ulf Aborelius and Ami Frydman). I was so privileged to meet regularly with such knowledgeable, open and inspiring people. Thanks for your guidance and discussion regarding BOP injuries and thoracic and abdominal injuries in particular. Thanks too for your friendship and support through the years. Thanks too to Marike for her mentorship and her reviews of my research over the years.

Wayne State University Department of Biomedical Engineering, thanks for welcoming me into your labs for your tests involving rats exposed to BOP. Special thanks to Cynthia Bir and Pamela van de Vord for making this opportunity possible. Thanks to Pamela van de Vord, Sujith Sajja, Dhananjeyan Thiruthalinathan, Alessandra Dal Cengio Leonardi, Evon Ereifej, Blake Mathie, Bin Wu, Li Mao, Andrea Kepsel and Richard Bolander for assisting me with the rat tissue processing and evaluation. Although it was ultimately decided that this work not be included, the insights into tests involving animal subjects expanded my outlook on injury criteria development.

Thanks to Cranfield University for assisting with funding for this study and to the library staff for their fantastic assistance in helping me as an off-campus student. They really went above and beyond to get me articles that I needed promptly.

Thanks to my thesis committee at Cranfield University and to Debra Carr in particular for her constructive feedback.

Many, many thanks to my thesis supervisor, Ian Horsfall, for taking me on as a distance learning part-time student. Thanks for your constant support during the years and for the great value that you have added to this thesis. I really appreciated our phone discussions that kept me on track and your understanding that life continues alongside PhD thesis.

To my wonderful family, thank you for providing me with and allowing me this privilege. To my parents, thanks for teaching me to value learning and for being my rock throughout the years. Thank you for giving me the freedom and the means to follow my own path. To my amazing husband, your support has no bounds! Thank you for sharing every up and down with me and for being there to discuss details and editing. Thank you for taking up the slack and giving me the time to pursue my studies. Finally, to my son, Matthew Vaughan Whyte, I'm so looking forward to spending more time exploring with you. My wish for you is that you continue to relish the joy of discovery and remember how to hold on to your convictions like only a 2 year old can! This is for you...

“Discovery consists of seeing what everybody has seen and thinking what nobody has thought.” – Albert von Szent-Györgyi.

TABLE OF CONTENTS

1	GENERAL INTRODUCTION	23
1.1	Blast Injury Mechanisms	24
1.2	Blast Scenarios Considered.....	25
1.3	Injury Criteria and Test Standards	26
1.4	Torso Surrogates	28
1.4.1	Why develop another torso surrogate?	29
1.5	Study outline	29
2	LITERATURE REVIEW AND BACKGROUND INFORMATION.....	33
2.1	Introduction.....	33
2.1.1	Chapter outline	33
2.2	Introduction to Blast Physics and Defining Blast Overpressure.....	34
2.2.1	Blast waves in free field environments.....	35
2.2.2	Blast waves in complex environments	39
2.2.3	Summary of terminology and defining BOP	40
2.3	Explosive Munitions and BOP Outputs.....	41
2.3.1	Classification of explosives	41
2.3.2	Scaling and TNT-equivalency of HE explosives	42
2.3.3	General explosive munitions	44
2.3.4	Description of explosive charges or munitions for blast scenarios considered in this study	45
2.4	BOP Measurements, Empirical Calculations and Numerical Simulations of Explosive Events.....	48
2.4.1	Measurement of blast effects	48
2.4.2	Predicting blast effects.....	50
2.5	Prevalence of Blast Injuries in Various Scenarios	60

2.5.1	Occurrence of blast injuries in general	60
2.5.2	Scenario A: Indirect BOP exposure within a vehicle (threat outside vehicle)	60
2.5.3	Scenario B: Direct BOP exposure within a vehicle or enclosed space (threat inside vehicle)	64
2.5.4	Scenario C: Direct BOP exposure through close contact with fragmentation munitions	65
2.5.5	Scenario D: Demining	65
2.6	BOP Injuries	67
2.6.1	Classification of BOP injuries	67
2.6.2	Susceptibility of different body regions to BOP injuries	68
2.6.3	Definition and scope of BOP injuries considered in this study	72
2.7	Identification and Severity Assessment of BOP Injuries to the Torso	73
2.7.1	Overview of thoracic and abdominal anatomy and physiology	73
2.7.2	Introduction to animal tests used to research BOP injuries	74
2.7.3	Identification and scoring of BOP lung injuries	75
2.7.4	Methods used to measure the severity of BOP injury	82
2.8	Injury Criteria	83
2.8.1	The Bowen/Bass injury criteria	84
2.8.2	The Chest Wall Velocity Predictor (CWVP)	85
2.8.3	Chest compression (C)	87
2.8.4	Viscous Criterion (VC)	87
2.9	Torso Surrogates	91
2.9.1	Torso surrogates and ATDs used in recognised test standards or in this study	91
2.9.2	Other torso surrogates and ATDs	95
2.10	Test Standards to Assess Blast Protection in Various Scenarios	97

2.10.1	Scenario A: Vehicle validation testing against IEDs and landmines (threat outside vehicle)	98
2.10.2	Scenario B: Explosive charge within a vehicle or enclosed space	101
2.10.3	Scenario C: Close proximity to a hand grenade in open space	101
2.10.4	Scenario D: Demining scenario	101
2.11	Summary and Study Aims	109
2.11.1	Summary	109
2.11.2	Thesis statement, study aims and delineations	113
3	ARMOURED VEHICLE VALIDATION TESTING: PRELIMINARY RESEARCH INTO RISK OF BOP INJURIES FOR SCENARIO A	115
3.1	Introduction	115
3.1.1	Chapter aims	115
3.1.2	Chapter outline	116
3.2	Method	116
3.2.1	General test setup and instrumentation for pressure measurement in vehicle validation tests	116
3.2.2	Data analysis and validation	118
3.2.3	BOP Injury Calculations	120
3.3	Results	121
3.4	BOP Injury Calculations and Analysis	123
3.5	Summary of Chapter Outputs	126
4	EXPLOSIVE CHARGE WITHIN A VEHICLE OR ENCLOSED SPACE: SCENARIO B	127
4.1	Introduction	127
4.1.1	Chapter aim	127
4.1.2	Chapter outline	128
4.2	Method	128

4.2.1	Introduction to ProSAir	128
4.2.2	Overview of simulation setup.....	128
4.2.3	BOP injury calculations.....	132
4.3	Results.....	134
4.4	BOP Injury Calculations and Analysis	138
4.4.1	Comparing side-on pressure profiles in vehicle (ProSAir simulation results) with predicted free-field pressures (BECV4 predicted results).....	138
4.4.2	BOP injury predictions at different positions in the vehicle (using the CWVP criterion)	142
4.4.3	Comparing CWV BOP injury predictions with Bowen/Bass injury risk curves for free field	145
4.4.4	Test standards for this scenario	147
4.5	Summary of Chapter Outputs	147
5	CLOSE PROXIMITY TO HAND GRENADE CASE STUDY: PRELIMINARY RESEARCH INTO RISK OF BOP INJURIES FOR SCENARIO C	149
5.1	Introduction.....	149
5.1.1	Chapter aims	151
5.1.2	Chapter outline	151
5.2	Method.....	151
5.2.1	Overview of method and declaration of work done	151
5.2.2	Summary of medical methodology [Meel: 2008]	151
5.2.3	Summary of computational modelling methodology [Snyman: 2008] ..	151
5.3	Results.....	152
5.3.1	Medical results from autopsies.....	152
5.3.2	Engineering results from computational modelling	152
5.4	BOP Injury Predictions and Analysis	153

5.4.1	Comparison of simulation of the M26 hand grenade and predicted pressures using BECV4 software	154
5.4.2	BOP injury predictions	156
5.4.3	Comparison of actual injuries and predicted injuries	158
5.4.4	Discussion of explosive event injury criteria and research applications	159
5.5	Summary of Chapter Outputs	160
6	THE SOUTH AFRICAN WATERMAN IN AN AP MINE SCENARIO: PRELIMINARY RESEARCH INTO THE RISK OF BOP INJURIES FOR SCENARIO D	161
6.1	Introduction.....	161
6.1.1	Background.....	161
6.1.2	Chapter aims	162
6.1.3	Chapter outline	162
6.2	Method.....	163
6.2.1	General test setup and instrumentation.....	163
6.2.2	Data analysis and BOP injury predictions.....	165
6.3	Results.....	166
6.4	BOP Injury Calculations and Analysis	170
6.4.1	Analysis of SA Waterman face-on pressure measurements and CWVP injury calculations	170
6.4.2	Analysis of free-field pencil probe side-on pressure measurement and injury predictions (using Bass <i>et al.</i> [2006a] BOP injury curves)	173
6.4.3	Analysis of SA Waterman #3 accelerometer measurement	173
6.4.4	Analysis of PPE test standards in the demining scenario.....	174
6.5	Summary of Chapter Outputs	174
7	DEVELOPMENT OF THE SOUTH AFRICAN TORSO SURROGATE (SATS) AND AP MINE SCENARIO INVESTIGATION (SCENARIO D).....	176

7.1	Introduction.....	176
7.1.1	Chapter aims	177
7.1.2	Chapter Outline	178
7.2	Method.....	178
7.2.1	Design and development of the SATS prototype	178
7.2.2	SATS instrumentation	185
7.2.3	Ethical considerations for AP mine test	189
7.2.4	AP mine and SATS test setup and data processing.....	189
7.3	Results.....	194
7.4	BOP Injury Predictions and Analysis	199
7.4.1	Correlation of SATS measurements and camera footage.....	199
7.4.2	BOP injury prediction based on experimental SATS test results.....	205
7.5	Summary of Chapter Outputs	206
8	GENERAL DISCUSSION OF CHAPTER OUTPUTS	208
8.1	Identification and Prevalence of BOP Injuries	209
8.2	Prediction of BOP Injuries in Background Scenario Investigations.....	211
8.2.1	BOP injury prediction in the validation testing of landmine protected vehicles (LPVs) or armoured vehicles (AVs)	211
8.2.2	Explosive charge within a vehicle or enclosed space.....	212
8.2.3	Case study involving a hand grenade explosion in very close proximity to people	213
8.2.4	The South African Waterman exposed to anti-personnel (AP) mine blast	213
8.3	Ability of Injury Criteria to Predict BOP Injuries in the Demining Scenario	216
8.3.1	Factors that influence the development of injury criteria.....	216
8.3.2	Injury predictions and comparison of injury criteria (using SATS test results)	217

8.4	Test Standards to Evaluate BOP Injury Risk in the Demining Scenario.....	228
8.4.1	National Institute of Justice (NIJ) Public Safety Bomb Suit Standard (NIJ Standard - 0117.00) [NIJ: 2012]	228
8.4.2	North Atlantic Treaty Organisation (NATO) Test Methodologies for PPE Against Anti-Personnel (AP) Mine Blast [NATO-RTO-TR-HFM-089: 2006]....	229
8.4.3	International Mine Action Standards (IMAS) 10.3 [2009] - Specifications for PPE to protect against unexploded ordnance (UXO) and AP landmines (And CEN workshop agreement (CWA 15756) [2007] (provisionally withdrawn)).....	230
8.5	Contradictions between Test Standard Specifications, Predicted BOP Injuries and Real BOP Injuries	232
8.5.1	Injury criteria inadequacy and incomplete understanding of BOP injury mechanisms	232
8.5.2	BOP injuries caused by AP mine incidents may be under-reported	233
8.5.3	Differences in pressure profiles predicted using empirical blast calculation software or computational fluid dynamics (CFD) simulation software.....	233
8.5.4	Real scenario differs from simulated or test scenario.....	235
8.6	Implications for Development and Testing of BOP Protection Strategies for the Demining Scenario	237
9	CONCLUSIONS	239
10	REFERENCES	240
11	APPENDICES.....	254
	APPENDIX A: SUPPLEMENTARY INFORMATION FOR CHAPTER 3	255
	APPENDIX B: SUPPLEMENTARY INFORMATION FOR CHAPTER 4	256
	APPENDIX C: SUPPLEMENTARY INFORMATION FOR CHAPTER 6	260
	APPENDIX D: SUPPLEMENTARY INFORMATION FOR CHAPTER 7	266
	APPENDIX E: PUBLICATIONS	273
	APPENDIX F: PERSONAL COMMUNICATION WITH S. FORTH AND M. SHARMA	274

LIST OF FIGURES

Figure 1: Diagram showing the evolution of theories on the dominant injury mechanism causing BOP injuries (as described by Cooper <i>et al.</i> [1991]).	25
Figure 2: Graphical representation of thesis outline.	32
Figure 3: Illustration of the pressure profile experienced by a stationary point in space from the time of detonation of the explosive charge until the pressure has returned to ambient pressure.	35
Figure 4: Diagram illustrating incident and reflected pressure measurements at the ground for an air burst explosion (burst height of 5.5 m) at different heights above the ground (diagram modified from original after Richmond <i>et al.</i> [1968]).	37
Figure 5: Diagram illustrating Mach Stem creation and the path of the Triple Point (after Iremonger [1997]).	38
Figure 6: Diagram illustrating static and dynamic pressure measurements recorded at a ground range of 20 ft for an air burst explosion (burst height of 3.7 m) (diagram modified from original after Richmond <i>et al.</i> [1968]).	39
Figure 7: Diagram of an M26 fragmentation hand grenade (after [Global Security .Org]).	47
Figure 8: Photograph of an M26 hand grenade (after [Denel]).	47
Figure 9: Photograph of an AP blast mine surrogate (208 g pentolite charge).	48
Figure 10: Example of BECV4 [2000] in EXCEL™ generated by the author by inputting 1 kg of TNT at a range of 1 m (altitude of 1000m and 21 degrees C) and the outputs are generated by the program. The parameters that are used in this thesis are annotated in red on the screen shot above.	57
Figure 11: Distribution and threats that caused accidental injury to humanitarian deminers (after NATO-RTO-TR-HFM-089 [2004]).	66
Figure 12: Diagram of the ribcage (left) and the underlying soft tissue organs, namely the heart and the lungs (right) (after Schmitt <i>et al.</i> [2004]).	73
Figure 13: Diagram of showing the abdominal organs (after Schmitt <i>et al.</i> [2004]).	74
Figure 14: Graphs showing the relationship between the lung weight to body weight ratio and peak BOP in rats (A) and guinea pig mortality (B) (after Elsayed [1997]).	82
Figure 15: Survival curves predicted for a 70 kg man applicable to a free field situation where the long axis of the body is perpendicular to the blast winds (after Bowen <i>et al.</i> [1968]).	84
Figure 16: Single chamber, one lung model, as described in Axelsson and Yelverton [1996].	86

Figure 17: Risk curve for AIS 4+ chest injury based on the Viscous Criterion for blunt frontal impact (after Lau and Viano [1986]).	88
Figure 18: Probability of AIS 2 or 3 thoracic injury for blunt ballistic impacts versus the VCmax as determined by logistic regression analysis from experimental cadaver data (after Bir <i>et al.</i> [2004]).	89
Figure 19: Continuum of VC values determined to predict a 25% risk of varying levels of injury in terms of frontal versus lateral and surrogate type (after Bir [2000]).	90
Figure 20: Photograph of a SA Waterman torso surrogate with a transducer package mounted on the chest area.	92
Figure 21: Hybrid III ATD with chest strap for pressure transducer plate (after AEP-55 [2006]).	94
Figure 22: Photograph of the SA Surrogate Leg prior to testing in a vehicle validation test.	95
Figure 23: Example of a BTD cylinder to record pressure measurements (after AEP-55 [2006]).	96
Figure 24: Diagram showing a typical vehicle validation test setup involving an AT landmine surrogate detonated beneath the wheel of an armoured vehicle.	117
Figure 25: Photographs of a Hybrid III ATD, SA Surrogate Legs and data acquisition units in a vehicle prior to the blast test.	118
Figure 26: SA Surrogate Leg #3 pressure measured during an AV landmine test indicating the section of interest for the expected explosive event pressure (circled in red).	119
Figure 27: Hybrid III ATD pressure measured during an AV landmine test.	120
Figure 28: CWV calculated by the author (left) and colleagues at TNO (right) in order to validate the CWVP calculation.	121
Figure 29: Peak overpressure measurements recorded during vehicle validation tests and corresponding calculated CWV values.	123
Figure 30: Peak overpressure measurements (below 25 kPa) recorded during vehicle validation tests and corresponding calculated CWV values.	124
Figure 31: SA Surrogate Leg #3 pressure measured during an IED Test (left) and a zoomed in view of the peak (right).	125
Figure 32: SA Surrogate Leg #3 CWV calculated during an IED Test (left) and zoomed in view of the peak (right).	125
Figure 33: Screen shots for ProSAir simulation of the vehicle showing the plane views and a diagram showing the dimensions of the vehicle from the z=0 cross-section [Peare: 2013].	130
Figure 34: Diagram showing the target points of interest based on would-be occupant positions within a simulated vehicle [Peare: 2013].	131

Figure 35: Graph showing the pressure multiplication factor obtained from BECV4 software for various distances from 160 g PE4 (C4) explosive charge.	134
Figure 36: Side-on pressure profile over 10 ms as recorded by Occupant 1 leg, abdomen and thorax target points.	136
Figure 37: Side-on pressure profile over 10 ms as recorded by Occupant 2 leg, abdomen and thorax target points.	136
Figure 38: Side-on pressure profile over 10 ms as recorded by Occupant 3 leg, abdomen and thorax target points.	137
Figure 39: Side-on pressure profile over 10 ms as recorded by Occupant 3 leg, abdomen and thorax target points.	137
Figure 40: Side-on pressure profiles over 10 ms for abdomen target points of all occupants.	138
Figure 41: Side-on pressure profiles over 10 ms for thorax target points of all occupants.	139
Figure 42: Time of arrival of pressure profiles at various distances from 160 g PE4 (C4) charge for the in-vehicle scenario (ProSAir simulations) and free-field scenario (BECV4 software calculations).	140
Figure 43: Peak side-on pressure at various distances from 160 g PE4 (C4) charge for the in-vehicle scenario (ProSAir simulations) and free-field scenario (BECV4 software calculations).	141
Figure 44: Peak side-on pressure at distances greater than 0.745 m from 160 g PE4 (C4) charge for the in-vehicle scenario (ProSAir simulations) and free-field scenario (BECV4 software calculations).	141
Figure 45: Peak reflected pressure recorded at various target positions within the vehicle and the corresponding calculated peak CWV values. Injury levels predicted using CWVP are indicated on the graph.	143
Figure 46: Distance between target points and explosive charge and the corresponding calculated peak CWV values for those target points.	144
Figure 47: Diagram showing the target points of interest and the associated CWV values resulting from a simulated blast within a vehicle.	145
Figure 48: Bass <i>et al.</i> [2006a] injury risk curve with indicators showing the predicted overpressure injuries at various distances from a 160 g C4 charge as determined using BECV4.	146
Figure 49: Graph showing simulated side-on pressure predictions at various distances from 160g spherical TNT charge.	153
Figure 50: Graph showing simulated reflected (face-on) pressure predictions at various distances from 160g spherical TNT charge.	153
Figure 51: Graph showing the predicted peak side-on BOP values at various distances from a 160 g TNT charge as by simulations and blast calculation software (BECV4).	155

Figure 52: Graph showing the predicted peak face-on (reflected) pressure values at various distances from a 160 g TNT charge as by simulations and in the literature.	155
Figure 53: Graph showing the simulated Chest Wall Velocity Predictions for the pressure profiles recorded at various distances from 160g spherical TNT charge.	156
Figure 54: Diagram showing the regions within which BOP injuries and fragmentation injuries caused by a M26 hand grenade may be expected.	158
Figure 55: Photograph of a SA Waterman torso surrogate with a bracket mounted on the chest area to protect the chest transducer plate from impact by clothing or PPE.	164
Figure 56: Photograph of the experimental setup of the four SA Waterman torso surrogates and pressure probe prior to the test (1. Foam (50mm thick closed cell polyurethane foam); 2. Lexin; 3. Uniform Only; 4. Aluminium Sheet).	164
Figure 57: Photograph of the four SA Waterman Surrogates and pressure probe after the test (1. Foam; 2. Lexin; 3. Uniform Only; 4. Aluminium Sheet).	167
Figure 58: Photograph of SA Waterman #3 (uniform only) after the test.	167
Figure 59: Photograph of the small hole in SA Waterman #4 after the test.	168
Figure 60: Graph of the face-on pressure profiles captured by transducers mounted on SA Waterman #1 (foam interface), SA Waterman #2 (lexin interface) and SA Waterman #3 (uniform only interface).	168
Figure 61: Side-on pressure measured with a pencil probe at approximately 0.7 m from the test charge.	169
Figure 62: Graph showing the acceleration signal recorded on SA Waterman #3 (behind the uniform only interface).	169
Figure 63: Graph of the pressure profiles captured by transducers mounted behind the foam (blue) and the uniform only (red) interfaces.	170
Figure 64: Graph showing the peak reflected and side on pressure values at various distances from a 100 g TNT charge as obtained from BECV4.	171
Figure 65: Graph of the calculated CWV using the pressure measured behind the uniform only interface.	172
Figure 66: A diagram showing the location of the pressure transducers and the structure of the “chest simulator” used to evaluate stackings of armour materials or lamination samples (From [Nerenberg <i>et al.</i> : 2000]).	180
Figure 67: The Mannequin for the Assessment of Blast Incapacitation and Lethality (MABIL) developed by Defence R&D Canada, Valcartier [Bouamoul <i>et al.</i> : 2007].	181
Figure 68: Photograph of the mould created in order to cast the abdominal insert of the SATS.	182

Figure 69: Photograph showing vacuum generated to remove air bubbles from the Dragon Skin™ mixture.	183
Figure 70: Photograph of the lungs and abdominal insert secured on a steel frame prior to casting the outer layer of the SATS.	184
Figure 71: Photograph of the abdominal insert prior to casting the outer layer of the SATS with the back PVDF transducer.	184
Figure 72: Photograph of the abdominal section of the SATS, after casting the outer layer, with the front PVDF transducer positioned (above the top of the middle PVDF transducer that cannot be seen here).	185
Figure 73: Labelled photograph of the SATS to show transducers.	186
Figure 74: Labelled photograph of the SATS chest plate to show the chest accelerometer, chest face-on pressure sensor and the chest side-on pressure sensor with vent hole through the torso.	188
Figure 75: Labelled photograph of the SATS to show transducers.	188
Figure 76: Photograph showing the positioning of the SATS (wearing protective clothing) and the stand in relation to the AP mine and the splinter proof shelter.	190
Figure 77: Photograph of the 208 g pentolite charge.	190
Figure 78: Photograph of the SATS covered with a Mutton cloth layer to test for any penetration effects.	190
Figure 79: Photograph of the mobile splinter proof shelter in which the data acquisition equipment was placed.	191
Figure 80: Labelled photograph of the data acquisition equipment inside the mobile splinter proof shelter.	191
Figure 81: Photograph of the test setup in relation to the main splinter proof shelter and to the camera.	193
Figure 82: Photograph of the SATS after the AP mine test.	194
Figure 83: Photograph of the SATS with protective clothing removed to enable the Mutton cloth layer to be inspected for signs of penetrations.	195
Figure 84: Photograph showing a penetration of the Mutton cloth layer by a small stone on the right shoulder of the SATS.	195
Figure 85: Photograph of damaged triaxial head accelerometer.	196
Figure 86: Graph of abdominal PVDF signals (front – blue; middle – red; back – green).	197
Figure 87: Graph of chest PVDF signals (front – blue; middle – red; back – green).	197
Figure 88: Graph showing the chest plate acceleration signal recorded by both the Scope1 (blue) and the Graphtec (red) data acquisition units.	198
Figure 89: Pressure profile obtained from the SATS chest plate face-on pressure sensor.	198

Figure 90: Graph showing the chest plate acceleration signal recorded by both the Scope 1 (blue) and the Graphtec (red) data acquisition units (zoomed in view).	199
Figure 91: Still frames of the camera footage from the blast at 0.9 ms (left) and 2 ms (right).	200
Figure 92: Still frames of the camera footage from the blast at - 0.05 ms (left) and 0 ms (right).	201
Figure 93: Graph of abdominal PVDF signals (front – blue; middle – red; back – green) zoomed in view of the first 1 ms.	202
Figure 94: Graph of chest PVDF signals (front – blue; middle – red; back – green) zoomed in view of the first 3 ms.	203
Figure 95: Graph of front chest PVDF signals (blue) and chest plate acceleration (red) zoomed in view of the first 3 ms (both captured by Scope 1).	204
Figure 96: Graph of chest plate pressure signals (cyan) and chest plate acceleration (black) zoomed in view of the first 7 ms (both captured by the Graphtec data acquisition unit).	204
Figure 97: Pressure profile obtained from the SATS chest plate face-on pressure sensor.	205
Figure 98: Calculated CWV from the pressure profile obtained from the SATS chest plate face-on pressure sensor.	206
Figure 99: Mortality curves for different animal species exposed to “short” duration reflected pressures (after Richmond <i>et al.</i> [1968]).	216
Figure 100: Acceleration signal recorded by the SATS chest plate accelerometer during an AP mine test.	218
Figure 101: Calculated chest plate velocity from the SATS chest plate accelerometer.	219
Figure 102: Calculated chest plate displacement from the SATS chest plate accelerometer.	220
Figure 103: Injury risk curve for Hybrid III sterna deflection and associated 95% confidence bands for AIS 3+ thoracic injury (after Mertz <i>et al.</i> [1991]).	221
Figure 104: V(t)C(t) calculated based on the SATS rig acceleration data in order to obtain VCmax.	222
Figure 105: Calculated nonlinear logistic regression model for survival or threshold for injury for a 70 kg man using scaled duration and side-on pressure (after Bass <i>et al.</i> [2006a]) applicable to a free field situation where the long axis of the body is perpendicular to the blast winds with indicators showing the predicted overpressure injuries at various distances from a 240 g TNT charge as determined in Table 22.	224

LIST OF TABLES

Table 1: Description of blast event scenarios considered in this study and the associated and threat descriptions.	26
Table 2: Table showing the number of explosive tests upon which the Kingery-Bulmash curves [Kingery and Bulmash: 1984] were based (modified from Swisdak [1994]).	53
Table 3: AIS or injury severity rating for common blast and blunt trauma injuries to the thorax (descriptions from Schmitt <i>et al.</i> [2004] and AAAM [2005]).	77
Table 4: Description of injury scoring system (after Carneal <i>et al.</i> [2012]).	81
Table 5: Summary of scenario descriptions, threats and dominant injury mechanisms.	112
Table 6: Details of Pressure Transducers used in Vehicle Validation Tests	118
Table 7: Peak pressures recorded during vehicle validation tests	122
Table 8: Table showing the distance between target points (of each occupant) and the explosive charge within the vehicle.	131
Table 9: Peak side-on pressure, peak reflected pressure and the resulting pressure multiplication factor for each target point specified by the distance from the charge as predicted by the BECV4 software.	133
Table 10: ProSAir simulation results showing peak side-on pressure and the time at which that pressure occurs for each of the target points considered.	135
Table 11: Peak side-on pressure, peak reflected pressure and the calculated Chest Wall Velocity (CWV) for the abdominal and thoracic target points of each vehicle occupant.	142
Table 12: Peak side-on pressure and positive phase duration for the thoracic target points specified by the distance from the charge as predicted by the BECV4 software.	146
Table 13: Peak overpressure and positive phase duration at various distances from a 160 g TNT charge from BECV4.	154
Table 14: Descriptions of primary injury levels predicted at various distances from the 106 g spherical TNT charge.	159
Table 15: Details of instrumentation and clothing or PPE mounted on the SA Waterman torso surrogates.	165
Table 16: Peak face-on pressure, peak side-on pressure and positive phase duration at various distances from a 100 g TNT charge from BECV4.	171
Table 17: Summary of comments on applicability of test standards and BOP injury criteria applied in the various scenarios described in this study.	176
Table 18: Sensor specification for the SATS.	186
Table 19: DBEL Safe Operating Procedure (SOP) specifications	189

Table 20: Record of data acquisition unit and channel number associated with each SATS transducer for the AP mine test.	192
Table 21: Summary of the outcomes regarding the available test standards and injury criteria based on the scenario investigations.	215
Table 22: Peak face-on pressure, peak side-on pressure and positive phase duration at various distances from a 240 g TNT charge from BECV4 [2000].	223
Table 23: Chance of survival due to BOP injury as predicted using empirical BECV4 pressure profiles and Bowen <i>et al.</i> [1968] and Bass <i>et al.</i> [2006a] injury criteria at various distances from a 240 g TNT charge.	225
Table 24: Chance of survival due to BOP injury as predicted by empirical BECV4 pressure profiles for a 240 g TNT spherical charge and 208 g pentolite charge at 0.6 m.	227

ABBREVIATIONS AND ACRONYMS

AAAM	Association for the Advancement of Automotive Medicine
AEP	Allied Engineering Publication
AIS	Abbreviated Injury Scale
AP	Anti-Personnel
ASII	Adjusted Severity of Injury Index
AT	Anti-Tank
ATD	Anthropomorphic Test Device
AV	Armoured Vehicle
BECV4	Blast Effects Calculation (Version 4)
BOP	Blast Overpressure
BTD	Blast Test Device
C	Chest Compression
CEN	(European) Committee for Standardisation
CFD	Computational Fluid Dynamics
CONWEP	Conventional Weapons Effects Program
CSIR	Council for Scientific and Industrial Research
CWVP	Chest Wall Velocity Predictor
DDAS	Database of Demining Accidents
DDESB	Department of Defense Explosives Safety Board
DBEL	Detonics, Ballistics and Explosives Laboratory
DOD	Department of Defence

DRDC	Defence R&D Canada
EFP	Explosively Formed Projectiles
EOD	Explosive Ordnance Disposal
ERW	Explosive Remnants of War
FAE	Fuel-Air Explosives
GICHD	Geneva International Centre for Humanitarian Demining
HE	High-order Explosives
HFM	Human Factors and Medicine
IED	Improvised Explosive Device
IMAS	International Mine Action Standards
ISS	Injury Severity Score
ITEP	International Test and Evaluation Program for Humanitarian Demining
LPV	Landmine Protected Vehicle
MABIL	Mannequin for the Assessment of Blast Incapacitation and Lethality
mTBI	mild Traumatic Brain Injury
NATO	North Atlantic Treaty Organisation
NIJ	National Institute of Justice
PMHS	Post Mortem Human Surrogate
PPE	Personal Protective Equipment
ProSAir	Propagation of Shocks in Air
PVDF	polyvinylidene flouride
RTO	Research and Technology Organisation (NATO)

SA	South African
SATS	South African Torso Surrogate
STANAG	Standardisation Agreement (NATO)
TBI	Traumatic Brain Injury
TNO	Toegepast Natuurwetenschappelijk Onderzoek
TNT	Trinitrotoluene
UFC	Unified Facilities Criteria
UNMAS	United Nations Mine Action Service
VC	Viscous Criterion
WSU	Wayne State University
fps	frames per second
g	grams
kg	kilograms
kHz	kilohertz
kPa	kilopascals
m	meters
mm	millimetres
ms	milliseconds
m/s	meters per second

1 GENERAL INTRODUCTION

“The blast wave is a shot without a bullet, a slash without a sword. It is present everywhere within its range. Blast would be as dreaded a weapon as chemical warfare, if its range, when explosives are used were not limited to small areas. However it would be premature to believe that this situation will always remain the same.”

- Theodor Benzinger 1950 (in Horrocks [2001])

The rapid release of energy due to an explosion results in an almost instantaneous rise in pressure. As this pressure wave moves outwards from the explosion it may cause blast overpressure (BOP) injuries to nearby persons. The incidence of BOP injury is greater in confined spaces near reflecting surfaces which makes blast weapons particularly dangerous in built up areas. In addition, there are reports of new weapons systems that focus on enhanced blast technology which makes specific use of BOP effects [Wildegger-Gasissmaier: 2003]. Kirkman *et al.* [2011] suggest that the occurrence of BOP injuries may be underestimated in current military casualties as blast lung injuries are often excluded when they co-exist with other injury types (such as fragment injuries to the torso or broken ribs).

BOP injuries caused by explosions in Northern Ireland were highlighted in Cooper [1996]. Eleven percent of the dead soldiers sustained BOP injuries with no other apparent injuries. More recently, BOP injuries sustained by UK Military personnel in operations in Iraq and Afghanistan accounted for 4% of blast related fatalities. A combination of BOP and fragmentation effects accounted for 31% of the blast related fatalities [Lewis: 2006].

1.1 Blast Injury Mechanisms

Injuries due to blast have been defined as direct or indirect injuries [White: 1968; Zuckerman: 1941] and very commonly, although less logically (as will be explained later), into primary, secondary, tertiary or quaternary (or miscellaneous) injuries [White: 1968; Kirkman *et al.*: 2011]:

- **Direct** or **primary** effects are caused by the variations in the environmental pressure due to the explosive event. These injuries are also known as **blast overpressure (BOP) injuries** as they relate to the actual physical interaction between the body of the victim and the detonation products, defined by the physical boundaries of the fireball, and/or the blast wave generated by the explosion [NATO RTO-TR-HFM-089: 2004]. They have most commonly been shown to affect the hollow air-containing organs such as the ears, upper respiratory tract, lungs and gastrointestinal tract. However, the role of BOP in causing injuries to the heart, solid abdominal organs [Axelsson and Yelverton: 1996; Carneal *et al.*: 2012] and the brain (traumatic brain injury (TBI)) has also been studied [Taber *et al.*: 2006]. Traumatic amputations or mutilating injuries are also most often referred to as primary injuries [Wolf *et al.*: 2009; Hull and Cooper: 1996].
- **Indirect** effects of the explosive event cause secondary, tertiary and quaternary or miscellaneous injuries. **Secondary** injuries are caused by fragments, soil ejecta or other flying debris energised by the blast. **Tertiary** injuries are caused by whole body displacement by the blast wind [National Center for Injury Prevention and Control]. **Miscellaneous or quaternary** injuries cover all other injuries from the blast, including burns, toxic gas inhalation [Smith *et al.*: 1996], crushing injuries caused by structural collapses [Wightman and Gladish: 2001] and exacerbations of chronic illness [CDC CS218119-A: no date]. Recently, a **quinary** injury pattern has been suggested to cover a hyperinflammatory state following an explosion [Wolf *et al.*: 2009; Kluger *et al.*: 2007].

The focus of this study is on blast overpressure (BOP) injuries.

The hollow, gas containing organs, namely the ears, upper respiratory tract, lungs and gastrointestinal tract are most susceptible to BOP injuries. These injuries could result in immediate death or a delayed progression of injury severity with little or no external visual indication of injury. Even minor BOP injuries to the lungs or gastrointestinal tract may add complications in patients with other blast injuries and may cause a patient to deteriorate very rapidly, the first signs of which are subtle findings such as elevated heart rate and narrowed pulse pressure [Stewart: 2006].

BOP injuries observed during World War II were shown to be a result of the impact of the blast wave upon the chest wall and not as a result of the blast wave passing down the trachea as was previously hypothesised [Cooper *et al.*: 1991]. It was shown in [Cooper *et al.*: 1991] that rather than gross compression of the thorax the dominant injury mechanism was direct transmission of stress waves into the thorax (See Figure 1).

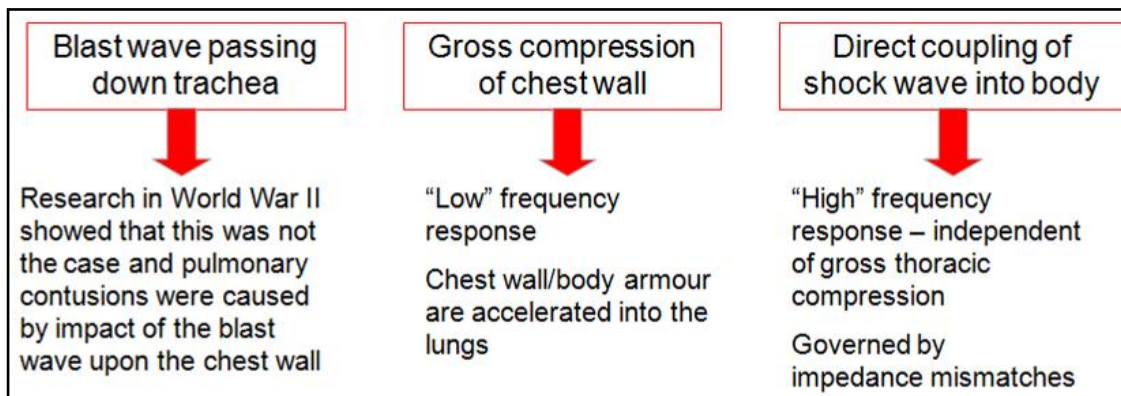


Figure 1: Diagram showing the evolution of theories on the dominant injury mechanism causing BOP injuries (as described by Cooper *et al.* [1991]).

The materials or armour applied to the thoracic wall of animal test subjects were found to have a large influence on lung overpressure injury outcomes and an acoustic transmission model was suggested to identify decoupling materials/armours which could reduce the probability of injuries caused by this mechanism [Cooper *et al.*: 1991].

1.2 Blast Scenarios Considered

The first step in this study was to determine in which blast event scenarios BOP injuries were most likely to occur. Table 1 shows the scenarios that were selected for consideration in this study.

Table 1: Description of blast event scenarios considered in this study and the associated and threat descriptions.

Scenario Name	Scenario Description	Threat Descriptions
Scenario A	Vehicle validation testing against IEDs and landmines (threat outside vehicle)	AT blast mine, IED or roadside bomb
Scenario B	Explosive charge within a vehicle or enclosed space	IED, terrorist bombing on bus/train etc.
Scenario C	Close proximity to a hand grenade in open space	IEDs, terrorist bombings, hand grenades
Scenario D	Demining : Direct exposure to blast munitions (mainly blast rather than fragmentation munitions)	AP mines, bombs, IEDs, accidental explosions

The profile of a measured pressure resulting from an explosive event has been used to predict BOP injuries. It is well known that the higher the peak pressure, the more severe the injuries caused by this pressure will be. It is also accepted that longer positive phase pressure durations result in more severe injuries than if the duration was shorter. In addition, BOP injuries are more severe in complex wave environments or near reflecting surfaces.

1.3 Injury Criteria and Test Standards

BOP injury criteria are used to predict the risk and severity of BOP injuries based on the measured pressure profile. Commonly used injury criteria for predicting BOP injuries include the Bowen criterion [Bowen *et al.*: 1968], Bass *et al.* [2006] criterion (for short duration BOP) and the Chest Wall Velocity Predictor (CWVP) [Axelsson and Yelverton: 1996]. The Viscous Criterion (VC) and the chest compression are injury criteria typically used to predict impact injuries in the automotive environment, but they have been included in the North Atlantic Treaty Organisation (NATO) armoured vehicle (AV) test standard to assess the protection of AVs against IEDs and landmines [van der Horst *et al.*: 2010; NATO, Research and Technology Organisation (RTO), Human Factors and Medicine Panel (HFM) Task Group TG-148 (NATO-RTO-TR-HFM-148): 2012]. Even though the VC was developed for use in the automotive

environment, it has been shown to be valid over a number of different loading rates [Bir: 2000]. Not all injury criteria are applicable for use in all BOP scenarios and the validity of these criteria when applied to short duration BOP is of particular concern. This will be discussed further in the literature review.

Test standards are used to evaluate the level of protection provided against BOP injuries in the various scenarios. Protection concepts that have been developed include structures (such as walls or buildings), vehicles (such as armoured vehicles) and Personal Protection Equipment (PPE) (such as demining body armour or bomb suits). Test standards used to evaluate these protection concepts prescribe a controlled (as far as is practically possible) test setup representing an operational scenario, with a surrogate explosive charge (standardised to provide consistency) and measurement devices. They specify the measurements that must be taken and the injury criteria that must be applied to determine the risk of BOP injury. Thus, an indication of the level of protection offered by the protection concept under evaluation is obtained. However, protection solutions that may protect against penetrating injuries may in fact increase the risk and severity of BOP injuries. For example, if an explosive charge penetrates or detonates within a vehicle or an enclosed space, the reflections would result in more severe BOP injuries; or certain materials used in PPE may couple the blast wave into the body tissues resulting in increased severity of BOP injury to the lungs and gastrointestinal tract. Test standards are only as good as the accuracy with which they are able to evaluate a wide range of conventional and novel protection concepts. Contradictions were found in the currently available test standards [National Institute of Justice (NIJ): 2012; NATO-RTO-TR-HFM-089: 2004; International Mine Action Standards (IMAS) 10.3: 2009; Allied Engineering Publication (AEP)-55: 2006] regarding methodologies to be used, the measurements to be taken and the injury criteria to be used to evaluate the protection capabilities against the BOP effects of a blast. Some even questioned the relevance of testing protection against BOP effects in the first place [NIJ (Standard-0101.06): 2008; NIJ (Standard-0117.00): 2008; NATO-RTO-TR-HFM-089: 2004; IMAS 10.3: 2009]. Even the most recent Public Safety Bomb Suit Standard NIJ Standard-0117.00 [NIJ: 2012] states that,

“This standard addresses blast overpressure only in terms of bomb suit integrity; i.e., only in terms of the bomb suit’s remaining intact when subjected to an explosion. At present, research and data related to the effects of blast overpressure are limited. The following aspects of blast overpressure will not be addressed until the necessary research is complete: blast head trauma, blast thoracic injury, blunt thoracic injury, blunt lower neck trauma, other neck injury, and blast ear injury. NIJ anticipates publishing addenda or revisions to this standard when the necessary data are available and applicable requirements and test methods are defined.” The assumption that the bomb suit remains intact will offer protection against BOP injury will be explored in this study.

1.4 Torso Surrogates

Anthropomorphic test devices (ATDs), also known as crash test dummies, or torso surrogates are instrumented mechanical surrogates representing a human body. They are instrumented with sensors and the recorded measurements can then be used, together with injury criteria, to determine the risk of injury.

The Hybrid III 50th percentile male ATD was developed in the automotive crash testing environment and is the apparatus specified for use (together with the EuroSID-2re ATD for side impact scenarios) in vehicle validation testing of AVs against IEDs and landmines [van der Horst *et al.*: 2010]. In the demining scenario, where a person is directly exposed to an explosive event, the NATO standard for testing PPE against anti-personnel (AP) mine blast recommends the use of a Hybrid II or a Hybrid III ATD [NATO-RTO-TR-HFM-089: 2004]. Torso surrogates (other than the Hybrid III ATD) have been developed for use in blast testing, but are not mandated in internationally recognised standards to evaluate PPE for the demining or explosive ordnance disposal (EOD) operational environments. These include, to mention but a couple, the thoracic rig developed by the Chemical and Biological Defence Establishment, Porton Down, UK [Cooper *et al.*:1996] and the Mannequin for the Assessment of Blast Incapacitation and Lethality (MABIL) developed by Defence R&D Canada, Valcartier [Bouamoul *et al.*: 2007].

It is difficult for a test authority to specify a test surrogate and methodology when there are contradictions in the literature regarding, not only the essential measurements which

must be recorded, but even the very relevance of testing protection capabilities against BOP injuries in the first place.

1.4.1 Why develop another torso surrogate?

As the NATO standard for testing PPE against AP mine blast recommends the use of a Hybrid II or a Hybrid III anthropomorphic test device (ATD), it would be sensible to use the same torso surrogate to explore BOP effects in this scenario. However, the Hybrid III ATD is an expensive measurement device, requiring regular calibration, which may be easily damaged in the harsh blast testing environment. Thus, a Hybrid III ATD was not available for use in this study. The validity of injury prediction made using Hybrid III ATD measurements is also debated due to the high loading rate resulting from explosive events [NATO-RTO-TR-HFM-090: 2007].

Thus, the South African Torso Surrogate (SATS) was developed to be used in blast tests to provide insights as to whether the assessment of BOP injury should be included in PPE test standards. The prototype SATS was not designed for use in a PPE test standard, but rather was developed as a research apparatus.

1.5 Study outline

A review of the literature highlighted contradictions in BOP injury predictions and test standards used to evaluate protection against BOP injuries. This is a multidisciplinary study in which aspects of blast physics, injury biomechanics and physiology and engineering test, measurement and evaluation standards, were required. The literature review thus forms the base of this study and enabled the aim of the thesis to be defined.

Studies were conducted to determine the significance of BOP injuries in different explosive threat scenarios. Currently available test standards, injury criteria, experimental BOP measurements and empirical BOP predictions were used to determine the risk of BOP injury in the following scenarios:

- Indirect exposure to an explosive event: validation testing of landmine protected vehicles (LPVs) or AVs (Chapter 3).

Pressure measurements were recorded in a number of vehicle validation tests and these were documented, together with BOP injury predictions. The results

do not show evidence that BOP injuries would occur if the vehicle hull remains intact during the blast, thus the risk of BOP injuries is adequately covered by the current test standards.

- Direct exposure to an explosive event within a confined environment: Simulation of detonation within an AV (Chapter 4).

Pressure profiles generated by ProSAir (Propagation of Shocks in Air) simulations (email communications with Alan Peare [Peare: 2013] were used to determine the risk of BOP injuries from a 160g PE4 charge detonation within a vehicle. The simulation results were used together with the chest wall velocity predictor (CWVP) (using MATLAB SimulinkTM) to calculate the risk of BOP occupants at various locations within the vehicle

- Direct exposure to an explosive event (i.e. not protected by a vehicle) in free field: a case study involving a hand grenade explosion in very close proximity to people (Chapter 5).

Although the BOP injuries would influence the severity of injury (as in this study, the victims were extremely close to the explosive device), the high velocity fragments expelled by the hand grenade (up to a range of 230 m) would be the main concern when protection against such a threat is concerned.

- Direct exposure to an explosive event in free field: an experimental test setup representing a demining scenario (Chapter 6).

The final preliminary study explored the scenario where BOP, rather than fragments, was the dominant injury mechanism. The South African Waterman (a plastic container filled with water in the shape of a human torso which was used in the past to occupy seats in vehicles during testing against anti-tank mines) was instrumented and the recorded pressure measurements were used to calculate the risk of BOP injury. Although the results predicted no risk of BOP injuries (possibly as the sample rate was too low and thus the actual peak may not have been captured), empirical predictions (based on pressure parameters

obtained from the Blast Effects Calculator (Version 4) (BECV4) [Swisdak: 2000]) reflected that the threshold for lung injury would be exceeded.

In order to conduct further research into test standards and injury criteria for the evaluation of PPE in the demining scenario, an improved torso surrogate was developed. Chapter 7 describes the development of the South African Torso Surrogate (SATS) and an AP mine test to further investigate the contradiction between empirical BOP injury predictions and the lack of mandatory assessment of PPE for BOP protection in currently recognised test standards. Secondary injuries were noted (as it was necessary to protect the SATS transducers from fragments/soil ejecta from the blast) but tertiary injuries such as behind armour blunt trauma, injuries caused by the global movement of the body as it is thrown backwards or burn injuries were not considered in this study. SATS pressure measurements were used to calculate the CWVP to predict the risk of BOP injuries.

The discussion in Chapter 8 combines the information from the previous chapters to draw conclusions regarding the adequacy of test standards in evaluating BOP protection. The velocity and displacement of the chest plate was calculated from the chest plate accelerometer and compared to the CWVP calculated using the chest plate face-on pressure. The risk of BOP injury was also assessed using empirical BECV4 side-on pressure profiles and the Bass *et al.* [2006a] curves for predicting BOP injuries from short-duration blasts. Chapter 9 lists the conclusions derived from this work.

Figure 2 illustrates the outline of this thesis.

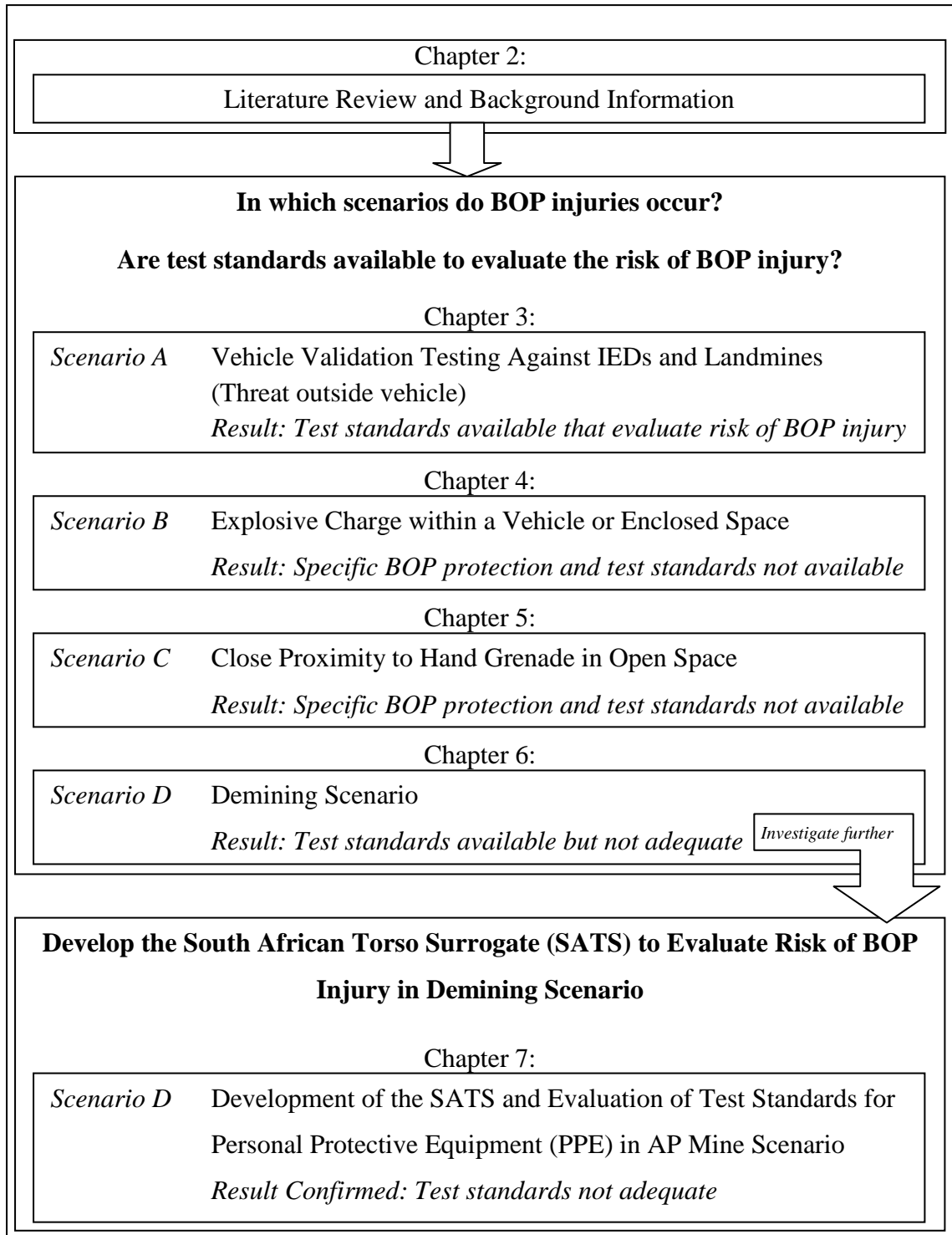


Figure 2: Graphical representation of thesis outline.

2 LITERATURE REVIEW AND BACKGROUND INFORMATION

2.1 Introduction

Explosive events may occur due to natural causes, such as a lightning strike or volcanic eruptions, or they could be artificial. Artificial explosions could be accidental – For example, failure of pressurised gas containers or dust or vapour cloud explosions in the coal mining, grain storage (such as corn dust, wheat dust and soya bean dust) and the woodworking and paper industries [Stewart: 2006; Dearden: 2001] – or intentional as in the case of military high explosive weapons or nuclear weapons [Iremonger: 1997]. In this study the focus is on explosive events due to high explosive weapons, such as hand grenades, landmines or IEDs.

When an explosive charge detonates, the physical space occupied by the explosive material is transformed, almost instantaneously, into a gas that fills the same volume within a few microseconds and thus the particles are under an extremely high pressure [Wightman and Gladish: 2001]. This results in a blast or pressure wave that expands outward. This will be referred to as the blast overpressure (BOP).

Pressure measurements are used to relate the BOP to a risk of injury to a person or destruction of a structure when exposed to an explosive event. The pressure dose to which a person is exposed is dependent on the scenario in which the explosive event occurs. The scenarios considered in this study were outlined in Table 1 (Section 1.2).

Predicting the risk of BOP injury in the various scenarios required a multidisciplinary approach. The literature review provides a base upon which the aims of the study can be defined. The relevant aspects of blast physics, injury biomechanics and physiology and engineering test, measurement and evaluation standards, are provided in this chapter.

2.1.1 Chapter outline

This chapter provides the background information to allow the specific aims of the thesis to be defined.

Firstly, a brief introduction to blast physics leads to important definitions used to describe the explosive event and BOP.

The types of explosive munitions that cause BOP injuries and the explosive munitions used in this study were described in Section 2.3.

Section 2.4 looked at how BOP outputs can be measured and predicted using empirical calculations or numerical simulations and the limitations of obtaining BOP profiles using these methods.

The prevalence of blast injuries in general and in the various scenarios considered in this study was ascertained to allow the reality of problem of BOP injuries to be understood.

Section 2.6 hones in on BOP injuries, how they are classified and defined within the scope of this study.

The physiological identification and severity assessment of BOP injuries is considered in Section 2.7 in order to understand the influence that injury identification and severity assessment methods have on the prevalence that is reported for BOP injuries and the injury criteria that are developed using animal subjects exposed to BOP.

Section 2.8 further explores the injury criteria that can used to predict BOP injuries.

Torso surrogates and anthropomorphic test devices (ATDs) that measure parameters of the blast wave to allow BOP injuries to be predicted are described in Section 2.9.

Finally, section 2.10 provides an initial evaluation of test standards used to assess blast protection in the various scenarios. This leads to a summary of the outcomes of the literature review and the explanation of the aims of this thesis.

2.2 Introduction to Blast Physics and Defining Blast Overpressure

In this section, the blast physics behind and the basic terminology used to describe a simple, theoretical, free field blast wave is defined. In reality, blast waves interact with the ground or other surfaces in the environment. An overview of how blast waves interact with surfaces in different scenarios is thus provided. As the terminology may be ambiguous, based on how blast events in the selected scenarios are described and how the definition of terms differs between sources, a summary of commonly used terminology and the terminology selected for this document is provided.

Specifically the term BOP injury will be delineated as it is used in this thesis. However, the theme of understanding exactly what BOP injuries are, and how they can be measured and quantified through the use of test standards (specifying the test scenario, injury criteria, ATD/torso surrogate, measurement methods, explosive surrogate type), is an underlying subject of investigation throughout this thesis.

2.2.1 Blast waves in free field environments

In its simplest form, if the blast wave is viewed by a stationary point in space (See Figure 3), the blast wave will reach the point at time, t_a , also known as the time of arrival, where the pressure jumps abruptly from ambient pressure to a maximum pressure known as peak overpressure. The leading edge of the blast wave is known as the shock front (also known as blast front). The peak overpressure then decays exponentially back to ambient pressure where the positive phase duration, t_+ , is a characteristic of the blast wave. The pressure proceeds to drop below the ambient pressure due to the after-flow (also known as the underpressure), or negative phase and after the negative phase duration, t_- , the pressure returns to ambient pressure [Held: 1983].

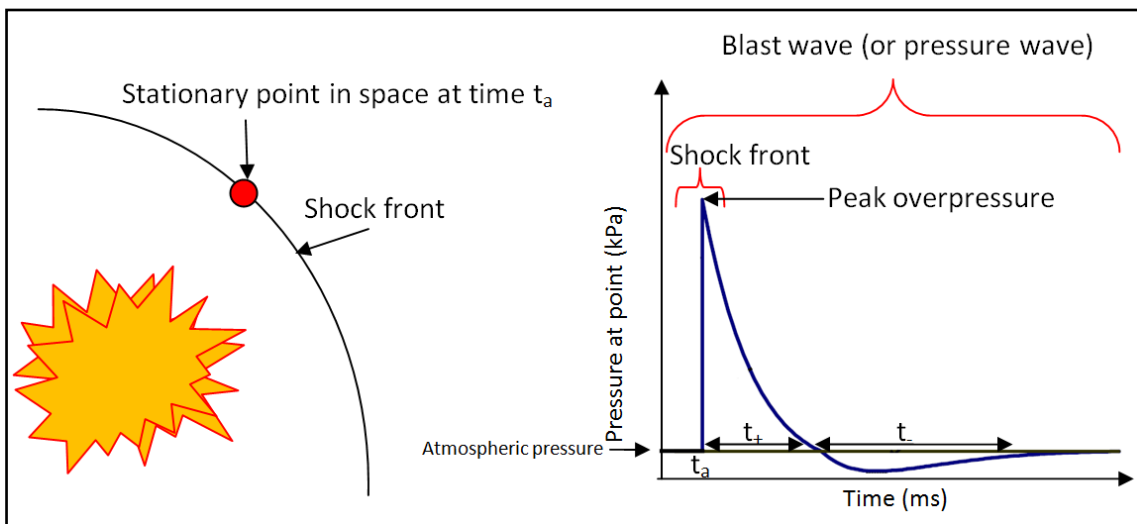


Figure 3: Illustration of the pressure profile experienced by a stationary point in space from the time of detonation of the explosive charge until the pressure has returned to ambient pressure.

The blast wave shown in Figure 3 is also known as an ideal blast wave (often described as a Friedlander waveform).

When reflecting surfaces are present, the blast wave differs from the ideal blast waveform and the terminology that can be used to describe the blast wave becomes more complicated.

Figure 4 shows the pressure-time curves measured in different places in space and time resulting from an above ground detonation of a spherical Trinitrotoluene (TNT) charge (modified from [Richmond *et al.*: 1968]). As the waveform travels outwards from the detonation point, before any obstructions or surfaces are encountered, it is referred to as the incident pressure. When the incident wave encounters the ground (or other obstructions), a reflected pressure wave that propagates away from the surface is created. The peak reflected pressure wave is two or more times greater than the peak incident pressure wave due to the build up of gas molecules at the surface. Gauge (a) in Figure 4, mounted at the surface, measures the incident pressure and the reflected pressures as a single peak. Gauges (b) and (c) measure the incident and reflected pressures as two distinct peaks separated by different time intervals indicating the respective distances of the gauges from the explosive charge and the surface. Gauges (b) and (c) measure the side-on or static pressure as the sensing surface is oriented parallel to the direction of propagation of the wave and is unaffected by any kinetic energy in the travelling wave front and thus measures the air compression that is active in all directions due to the thermal motion of the gas particles [Stuhmiller *et al.*: 1991]. The rush of air caused by the net motion of the gas (which is related mainly to the particle velocity of the air, rather than the pressure at which the air particles are at the shock front of the pressure wave) is called the blast wind [Stuhmiller *et al.*: 1991].

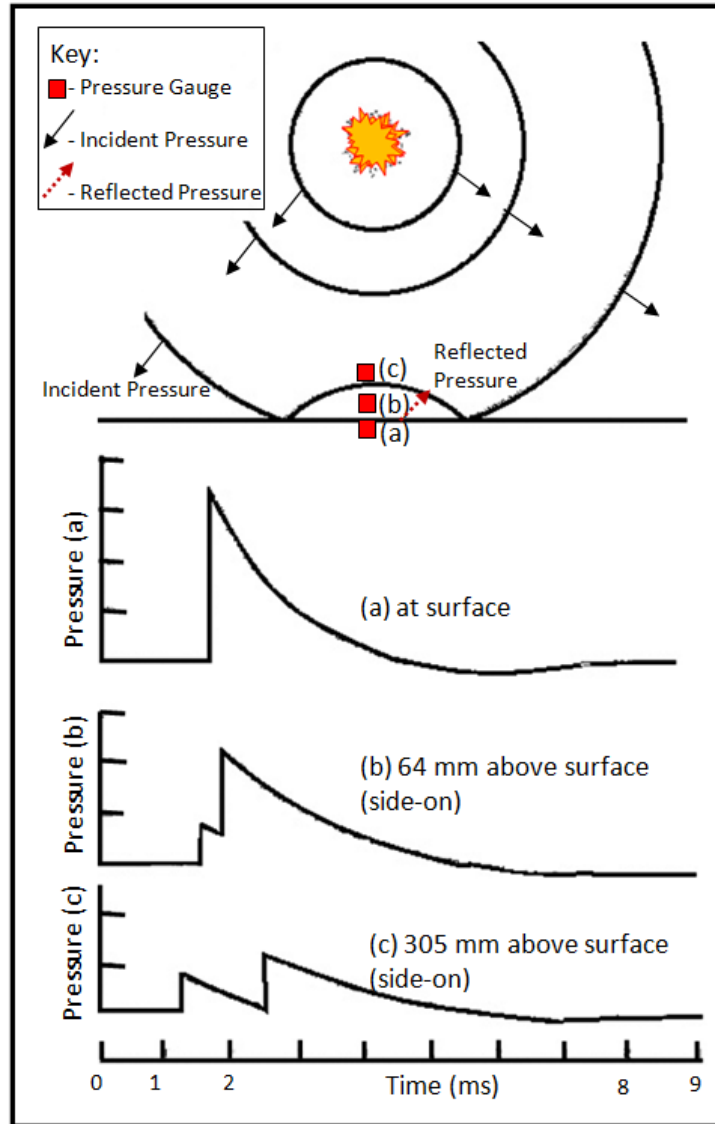


Figure 4: Diagram illustrating incident and reflected pressure measurements at the ground for an air burst explosion (burst height of 5.5 m) at different heights above the ground (diagram modified from original after Richmond *et al.* [1968]).

The incident and reflected pressures continue to propagate away from the point of detonation and the surface respectively (See Figure 6). At a certain time, the reflected shock overtakes the incident shock to form a Mach stem and the flow of the Mach stem becomes parallel with the surface (See Figure 5). The point at which the reflected pressure wave and the incident pressure wave intersect with the Mach stem is called the triple point. The triple point is significant as when the height of the triple point is greater than the height of the target, the target is considered to be subjected to a plane wave (uniform pressure over target surface). If the target is above the triple point, then

it will be exposed to the incident and reflected waves separately. The pressure profile (variation in the pressure-time curve) of the Mach front is similar to that of the incident pressure wave, but the magnitude of the blast parameters of the Mach front are larger than those of the incident wave [Unified Facilities Criteria (UFC): 2008]. So, for a “worst case” scenario in the testing and evaluation environment, it is important to ensure that the target is sufficiently far from the origin of the explosion (and the height of the explosion origin is sufficiently close to the ground) to be below the triple point (i.e. Exposed to the Mach front). Practically, this also simplifies the positioning of pressure transducers as the target will be exposed to a uniform pressure. The height of the triple point can be obtained using a graph of the scaled height of the triple point.

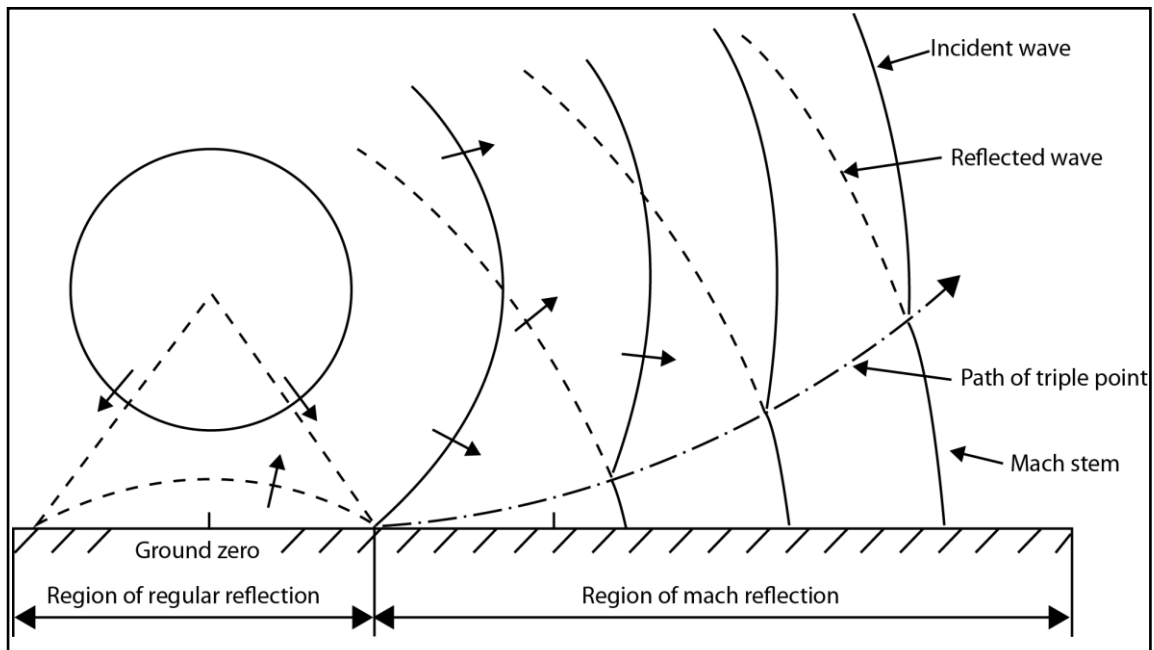


Figure 5: Diagram illustrating Mach Stem creation and the path of the Triple Point (after Iremonger [1997]).

Looking in more depth at the concept of reflected pressure, it can be referred to as face-on pressure as illustrated in Figure 6. Gauge (d) in Figure 6 is mounted face-on to the flow and records the static pressure plus the dynamic pressure (due to the sensor stopping the net air motion at the sensor surface). The dynamic pressure is the force associated with the blast wind (the movement of air particles at the leading edge of the shock wave) and is the difference between the side-on (Gauge (e) is mounted side-on in the surface or at right angles to the flow of the Mach stem) and face-on pressure measurements [Stuhmiller *et al.*: 1991].

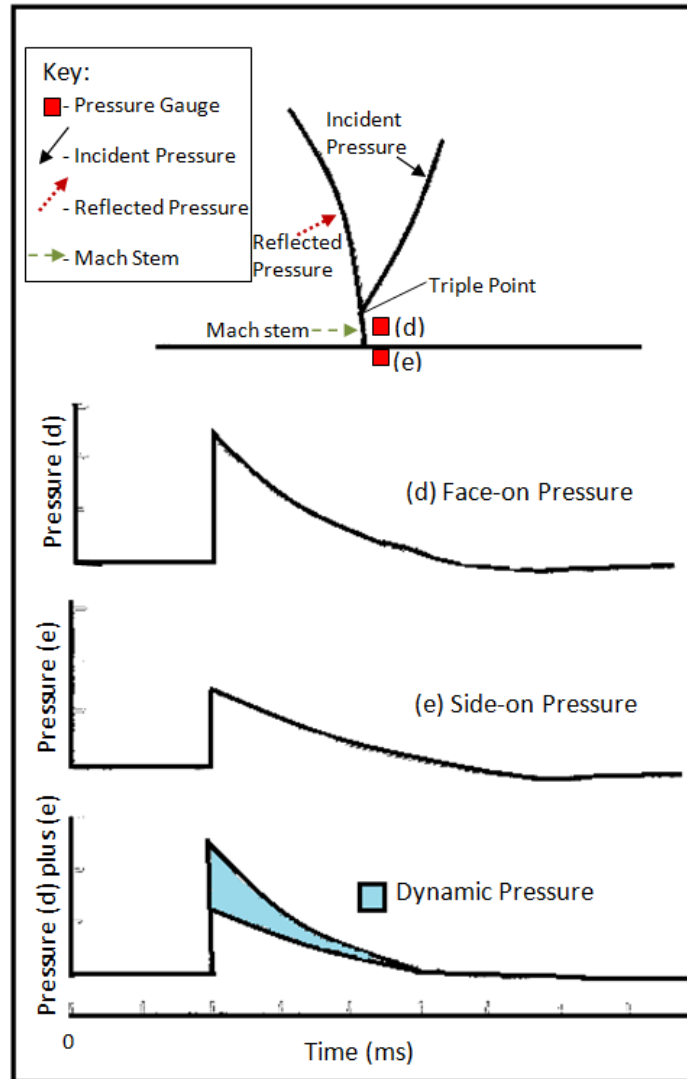


Figure 6: Diagram illustrating static and dynamic pressure measurements recorded at a ground range of 20 ft for an air burst explosion (burst height of 3.7 m) (diagram modified from original after Richmond *et al.* [1968]).

2.2.2 Blast waves in complex environments

Complex wave environments occur when the blast wave is reflected from various surfaces before reaching the point of interest (structure/person or animal). Walls, structures, vehicles or other large objects in the vicinity of the explosion can reflect and amplify the incident wave. This can result in higher injury levels than expected for equivalent (same charge and standoff distance) free field conditions [Dionne and Makris: 2011].

2.2.3 Summary of terminology and defining BOP

Unfortunately, the terminology used to describe the blast wave in various scenarios is often confusing and differs between sources. Thus, the terminology that will be used throughout this study will be defined in this section.

In this study, face-on and/or side-on pressure measurements are recorded depending on the sensors that are used and their orientation to the blast wave. In order to predict BOP injuries, injury criteria can be used based on either the side-on overpressure profile or the face-on pressure profiles. These terms will be used throughout this study and the terms *incident pressure*, *reflected pressure*, *total pressure*, *dynamic pressure* or *effective pressure* will only be specified when the blast wave environment ensures that their use is unambiguous.

Side-on pressure is the effect of the pressure wave is measured without any obstruction.

Face-on pressure is the effect at the location where the pressure wave is obstructed by a surface (reflected pressure). The peak reflected pressure is between 2 and 8 times the peak side-on pressure (according to [Swisdak: 1975]).

The term BOP is defined to distinguish this kind of injury from impact or tertiary blast injuries (due to blast wind). In this study it is assumed that by the time the body starts to experience whole body displacement, the BOP injuries will have already been inflicted. Thus, the focus will be on the section of measurements that are recorded before the whole body starts to move. However, whilst this may be sufficient to define the phase of BOP injuries in the free field scenario, in a complex scenario (For example, in a building or a vehicle or near a reflecting surface), this will become more complicated as face-on reflected pressures and the build up of gas particles prevent the pressure from dispersing as quickly as in a free field environment. The implication will be longer times to which a person will be subjected to pressures which may cause BOP injuries. This means that even though the person may start to move, the pressure to which they are exposed may still be significant enough to influence BOP injuries.

The definition of BOP for this study is the pressure profile measured at the point where BOP injuries are to be calculated. BOP injuries can be calculated using side-on or

face-on pressure measurements together with appropriate injury criteria (which will be discussed in Section 2.9).

2.3 Explosive Munitions and BOP Outputs

The type of explosive threat to which a person is exposed will influence the nature and severity of possible BOP injuries. The type of explosive compound, casing and configuration of the compound, along with the situation in which the explosion occurs will all influence the injury outcomes. This section includes:

- An introduction to how explosives are classified;
- A brief explanation of how the outputs of different types of explosives can be related to one another through the application of scaling laws and TNT-equivalency;
- An overview of the types of explosive munitions and devices;
- A description of the specific threats that were considered in this thesis.

2.3.1 Classification of explosives

Explosives are categorised as low-order explosives or high-order explosives (HE) depending on the rate at which energy is released. Low-order explosives or propellants (e.g. gunpowder) burn (or deflagrate) with a velocity of less than 1000 m/s and produce large volumes of gas that will only explode if confined (e.g. pipe bomb, “pressure cooker” bomb). HE detonate due to a chemical reaction where the explosive (liquid or solid depending on the type of explosive) is almost instantaneously converted into a gas that moves outwards and produces a blast or pressure wave (even if not confined) [Wightman and Gladish: 2001; Stewart: 2006; Wolf *et al.*: 2009].

HE are also classified as primary and secondary explosives. Primary explosives can be detonated by mechanical shock, friction or heat, where secondary explosives usually need an initiating explosion to result in a detonation [Wolf *et al.*: 2009]. Small quantities of primary explosives are thus often used to initiate the detonation of larger quantities of secondary explosives (which are safer to handle (including moulding or casting into specific configurations) and transport than primary explosives). General

purpose explosive munitions usually consist of a detonator or a fuse that contains a sensitive primary explosive, a booster of a relatively sensitive secondary explosive and a main charge of an insensitive secondary explosive [Stuhmiller *et al.*: 1991].

2.3.2 Scaling and TNT-equivalency of HE explosives

In order to predict BOP profiles for a given explosive charge, mathematical relationships are used to relate the various conditions to one another. These are called scaling laws. If the BOP is measured at various distances from a single weight of explosive, the BOP due to any other amount of that explosive at any distance can be estimated without conducting further blast tests.

Cube root scaling or the Hopkinson's Rule states that the magnitudes of distance and time are scaled in proportion to the relative dimensions of explosive charges detonated in the same atmosphere [Iremonger: 1997]. The relative volumes of two spheres are proportional to the cubes of their diameters and the weight or energy of an explosive charge is proportional to its volume. Thus, the scaled distances and times are proportional to the cube root of the explosive weight [Iremonger: 1997]. The equation below shows the scaled distance Z , where:

$$Z = R/W^{1/3}$$

where R is the distance from the centre of the explosion and W is the energy of the explosive (usually this is the weight of a standard explosive such as TNT) [Iremonger: 1997]. A graph or look-up table can then be used to read the parameter of interest, such as peak pressure, positive impulse, positive phase duration or time of arrival [Stuhmiller *et al.*: 1991].

The TNT-equivalency (based on the yield of an explosive expressed in terms of an equivalent weight of TNT [Iremonger: 1997]), allows the cube root scaling procedure to be followed for other types of explosives [Stuhmiller *et al.*: 1991]. Even though this procedure is greatly simplified and has limitations (as the BOP profile is dependent on many other parameters such as altitude, weather conditions, shape of the charge), it can provide a quick and simple way of obtaining a first approximation of what to expect

from certain explosive charges at certain distances. However, it should be noted that there are specific conditions for which the BOP parameters will be valid.

Although nuclear explosions are not considered in this study, it is interesting to note that, as described in [Iremonger: 1997], only 50% of the energy of a nuclear explosion is released into the blast wave (the remainder is converted into thermal and nuclear radiation), compared to chemical explosions (such as TNT explosions) in which nearly 100% of the energy is converted into blast energy. Thus, this scaling law does not apply when converting from chemical to nuclear explosions or vice versa.

HE chemical explosives mentioned or used in this study and their respective TNT-equivalencies include:

- *Nitroglycerin* (NG) – was the first HE discovered in 1846. In 1867, Alfred Nobel combined the inherently unstable and dangerous nitroglycerin with inert materials which gave rise to *dynamite*. Dynamite is widely used in the demolition, mining and construction industries and it has been used in terrorist attacks such as the 2004 train bombing in Madrid, Spain [Wolf *et al.*: 2009]. (Equivalent wt of NG relative to TNT – 1.48 [Iremonger: 1997]).
- *Trinitrotoluene* (TNT).
- *Cyclotrimethylenetrinitramine* or *Cyclonite* (Royal Demolition Explosive (RDX) [Stewart: 2006]) (Equivalent wt relative to TNT – 1.19 [Stuhmiller *et al.*: 1991] [Iremonger: 1997]).
- *Pentaethyltrinitride* (PETN) (Equivalent wt relative to TNT – 1.27 [Stuhmiller *et al.*: 1991])(1.28 according to [Iremonger: 1997]).
- *Composition B* - consists of RDX and TNT (trinitrotoluene) in the ratio 60:40 [Köhler and Meyer, 1993]. (Equivalent wt relative to TNT – 1.11 [Stuhmiller *et al.*: 1991]) (1.15 according to [Iremonger: 1997]).
- *Composition C4* – consists of 91% RDX, 2.1% rubber, oil 1.6% and 5.3% plasticiser [Stuhmiller *et al.*: 1991]. *Plastic explosives* (such as Composition C4) are made by combining a HE explosive with plasticisers which make these

explosives easy to mould. Thus, they are often used in explosive demolition and by military forces. They were historically difficult to detect by security authorities and thus they were used by terrorists in, for example, the 1988 Pan Am Flight 103 downing in the UK, the 2000 attack on the USS Cole warship in Yemen, and the 2002 Mumbai train bombing in India [Wolf *et al.*: 2009]. (Equivalent wt relative to TNT – 1.37 [Stuhmiller *et al.*: 1991]; 1.08 according to [Iremonger: 1997], this discrepancy may be due to different mass of plasticiser, although both had 91% RDX, the C4 in [Iremonger: 1997] consisted of 9% plasticiser.

- *Pentolite* – 50% TNT and 50% PETN (Equivalent wt relative to TNT – 1.42 [Stuhmiller *et al.*: 1991]; 1.13 according to [Iremonger: 1997], although the density and detonation velocities were the same).

2.3.3 General explosive munitions

The configuration of the explosive threat is dependent on the purpose for which it was made.

Many explosive blast munitions rely on the explosive charge to create and/or propel the fragments, rather than to injure by means of the BOP generated by detonation. Generally, fragmenting munitions will have a lethal range that is much larger than the lethal radius generated by the BOP alone (much of the energy generated by the detonation goes into creating and/or dispersing the fragments). Examples of conventional fragmenting munitions are hand grenades, mortars and shells [Dearden: 2001].

Improvised explosive devices (IEDs) also often (but not always) contain fragmenting materials such as ball-bearings, rocks or scrap metal to increase the injury radius of the explosive device. The term IED describes any makeshift incendiary device constructed to injure, incapacitate, harass, or distract [Wolf *et al.*: 2009].

Shaped charges, explosively formed projectiles (EFPs) and EFP- IEDs make use of the explosive charge to produce a directional projectile threat and are mainly used to defeat armour (rather than for attacking personnel) [Dearden: 2001]. EFPs are related to

shaped charges, but form a fragment (or symmetric projectile from various metal liner shapes) rather than a jet [Stewart: 2006].

Dearden [2001] describes a move towards weapon systems that use blast (or BOP as opposed to fragments energised by the blast overpressure) as the main damage or injury mechanism. He explains that when collateral damage is a principal concern, the use of fragmenting munitions is limited due to the indiscriminate nature of the fragment throw. Blast weapons have a well defined and limited range of effectiveness as the BOP wave decays rapidly as it moves out from the source of the detonation. Obstacles such as walls or trenches provide significant protection against fragments and thus in built up areas, blast weapons would be more dangerous due to reflected waves and the fact that BOP can travel around corners.

Enhanced blast weapon systems utilise the BOP output rather than fragmenting effects. Thermobaric or fuel-air explosives (FAE) result in enhanced blast output as the BOP waves are of a relatively long duration (compared to the short duration of BOP waves from a TNT explosion) and the temperature can be more than twice that generated by a conventional explosive. FAE occur in both military scenarios and industrial accidents. In military scenarios, a vapour cloud of fuel can be dispersed in the air and then ignited over a target.

2.3.4 Description of explosive charges or munitions for blast scenarios considered in this study

It is beyond the scope of this thesis to cover all blast weapons in detail, but the explosive threats associated with the scenarios that were considered in this study were reviewed.

The background on the actual threat in each scenario is described, followed by the details of the simulated or surrogate blast threat (where applicable).

A simulated threat is an approximation of the actual threat that is created for research purposes to produce a BOP output as similar as possible to the actual threat. This is done to ensure a ready supply of simulated threats to use in blast tests and to ensure that the blast tests are as repeatable as possible (often actual threats can produce variable BOP outputs and, in the case of IEDs, the threats themselves vary widely). A simulated

threat also allows different test authorities to subject test items to the same threat level. The details of the simulated threats are specified in test standards to allow test authorities to make use of standardised threat levels.

Anti-tank (AT) blast mine surrogate – Scenario A

For the scenario where occupants are in an armoured vehicle that is subjected to an AT landmine, a simulated AT blast mine or an AT blast mine surrogate is the threat considered in this thesis.

The NATO STANAG 4569 Allied Engineering Publication (AEP) – 55 Volume 2 (Edition 1) [AEP-55 vol.2: 2006] covers the “Procedures for Evaluating the Protection Level of Logistic and Light Armoured Vehicles – Mine Threat.” The mine threat in AEP-55 vol. 2 (Edition 1) [2006] is defined as follows:

- Threat level 1 represents hand grenades, unexploded artillery fragmentation submunitions, or other small anti-personnel explosive devices detonated anywhere under the vehicle.
- Threat levels 2 to 4 are based on representative buried anti-vehicular blast landmines (commonly known as Anti-Tank (AT) mines) detonated under a wheel/track or anywhere under the vehicle. These representative mines are referred to as surrogate mines. A threat level 2 specifies a 6 kg TNT blast mine surrogate, a threat level 3 specifies an 8 kg TNT blast mine surrogate and a level 4 threat specifies a 10 kg TNT blast mine surrogate.

M26 hand grenade - Scenario C

The M26 grenade was designed to produce casualties through the high velocity fragments that it expels [Global Security .Org: no date].

M26 hand grenades were used to supplement small arms fire against enemy in close combat. The grenade is 113 mm in length with a diameter of 60 mm [Denel: no date] and is filled with 160 g of high-energy Composition B charge. The total weight of the grenade is 465 g and it produces approximately 1000 small fragments weighing about 200 mg each [Denel: no date]. It has a 50% casualty radius of 15 m, however, the

fragments can disperse out to 230 m [Denel: no date]. The grenades can be identified by an olive drab body with a single yellow band at the top with yellow markings which are indicative of the high-explosive filler. A diagram of the M26 grenade can be seen in Figure 7 and a photograph of the grenade is shown in Figure 8.

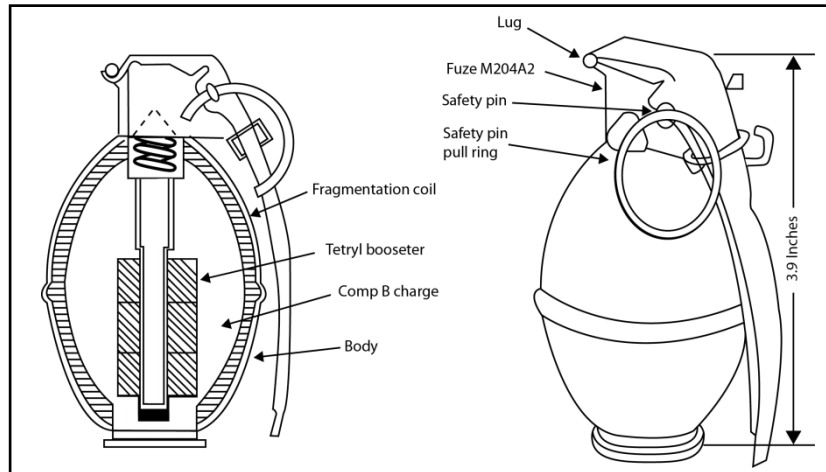


Figure 7: Diagram of an M26 fragmentation hand grenade (after [Global Security .Org]).



Figure 8: Photograph of an M26 hand grenade (after [Denel]).

Anti-personnel (AP) blast landmine – Scenario D

The actual threat in this scenario is the PMN blast mine. This AP mine was involved in 43% of blast mine accidents reported in a 1998 survey of 232 mine accidents in the field of humanitarian demining, which shows a very high prevalence of this threat, although it may be an artefact of the contribution of a large amount of data from organisations in Afghanistan [NATO-RTO-TR-HFM-089: 2004].

The PMN mine is the largest of all blast mines with 240 g of TNT, so use as the basis for a surrogate used in testing should be a “worst case” scenario.

The AP mine surrogate that was used for this scenario in this study was a cylindrical 208 g pentolite charge with a diameter of 0.1 m and a height of 0.02 m (See Figure 9).



Figure 9: Photograph of an AP blast mine surrogate (208 g pentolite charge).

2.4 BOP Measurements, Empirical Calculations and Numerical Simulations of Explosive Events

As previously mentioned, the pressure profile or BOP generated by an explosive charge can be related to a risk of injury to a person (or damage to a building or vehicle). It is thus useful to know the pressure-time history for various types of explosive charges. For each type of explosive, every combination of weight and distance from the explosion produces a specific pressure-time history or BOP profile.

The BOP profile can be obtained directly by taking measurements of the blast in a test environment. The BOP profile can be predicted using empirical blast calculation software or numerical simulation software.

This section outlines the limitations involved when using BOP measurements or BOP calculations to determine the risk of and severity of blast injury that could occur due to an explosive event.

2.4.1 Measurement of blast effects

Measurements that are typically used to predict blast injuries are pressures, forces, accelerations and displacements. The measurements can be obtained using sensors mounted on torso surrogates or ATDs or the sensors can be mounted on pencil probes or

surfaces of interest. The sensors that are selected are usually chosen based on which measures are associated with established blast injury criteria. Injury criteria and ATDs used in explosive events are reviewed in Sections 2.8 and 2.9.

Pressure can be measured using piezoelectric and piezoresistive sensors. The Greek word “piezein” means “to squeeze” and piezoelectric materials produce a voltage when strained, whilst piezoresistive materials exhibit a change in resistance when subjected to pressure.

In the experimental trials conducted in this study, piezoresistive pressure transducers were used. Piezoresistive materials have a high sensitivity and better low frequency response than piezoelectric materials [Loiseau *et al.*: 2009].

The standard practice in blast measurement is to record the static component of the pressure (side-on measurement) and to present that measurement in terms of the peak overpressure and the positive-phase duration [Stuhmiller *et al.*: 1991].

In reality, the measured BOP is influenced by the rate at which the signal is sampled (must be at least 200 kHz), charge parameters such as shape and depth of burial, the altitude at the test site (although this effect is only obvious far from the test charge or for small peak BOP [UFC: 2008]), the orientation and location of the pressure transducer and the target size and shape. It also becomes difficult to obtain repeatable measurements close to the origin of the explosion and within the fireball due to the harsh nature of the test environment and the poor repeatability when considering phenomena such as soil ejecta and jets of hot gasses [NATO-RTO-TR-HFM-089: 2004]. Unintentional loading of the transducer can also produce unexpected results, such as impact by debris or a safety belt.

These parameters highlight the difficulties inherent in measuring BOP in practice. It is thus important to validate experimental results with expected empirical or predicted results.

2.4.2 Predicting blast effects

Blast load predictions have been used in blast injury research for various reasons, including:

- To establish injury criteria which relate a combination of measured and predicted blast wave parameters to a risk of BOP injury.
- To allow appropriate sensors to be selected for use in blast tests.
- To provide confidence in blast test results where the number of repeat tests may be limited due to the destructive nature of blast testing (or the cost of many repeat tests is too high).

The methods used for predicting blast loads or BOP can be empirical (or analytical), semi-empirical or numerical (or first-principle) methods [Remennikov: 2003]. Empirical methods are correlations with experimental data. They are limited by the extent of the underlying experimental data. Semi-empirical methods use simplified models of physical phenomena and aim to model the underlying physical processes in a simplified way. They rely on extensive data and case study [Remennikov: 2003].

Numerical methods are based on mathematical equations that describe the basic laws of physics governing a problem. These models are commonly termed computational fluid dynamics models [Remennikov: 2003].

Empirical blast calculation software

Commonly referenced blast calculation protocols or software are reviewed here in terms the background to their developed (i.e. what data are they based on and what assumptions have been made), the limitations of their applicability to various blast scenarios and how they have been used in this thesis.

Some of the protocols or blast calculation software that are available include the following:

- Unified Facilities Criteria (UFC) Structures to Resist the Effect of Accidental Explosions (UFC 3-340-02) [2008]

Background

This standard supersedes the army TM 5-1300, navy NAVFAC P-397 and Air Force AFR 88-22. The document is referenced by the DOD Ammunition and Explosives Safety Standards (DOD 6055.09-STD) and contains design procedures to achieve personnel protection, protect facilities and equipment, and prevent the propagation of accidental explosions [UFC: 2008]. It is one of the most widely used publications available to both military and civilian sectors for designing structures to provide protection against the blast effects of explosions [Remennikov: 2003]. The UFC provides extensive information and BOP profiles for blast loading in different scenarios (e.g. free air burst or surface burst, different kinds of explosives and different explosive shapes).

Limitations:

It was stated that not all the terms used were standardised throughout the document and, as with most documents, the terminology for describing the blast wave was sometimes contradictory. Even so, many of the definitions used in this thesis were obtained from the UFC [2008], in particular, the terms used to describe the different blast scenarios.

Although a detailed bibliography is provided at the end of each chapter of the UFC, the individual graphs, the associated data sources and the empirical equations are not attributed to individual references. This makes it difficult to see which data has actually been used to make the blast predictions. The document bibliography lists Goodman [1960], Swisdak [1975] and Kingery and Bulmash [1984] (which are discussed as sources of data under the remaining bullet points in this section), among others. The bibliography does not contain

entries of documents dated later than 1986 for the blast references, thus it is assumed that these predictions are based on data gathered in 1986 or before.

Due to the amount of content necessary to describe structures that resist blast, the author found the document difficult to navigate and find the relevant information. The document has a high level of detail and complexity and was not as straight forward to use as computerised blast calculation software.

Applications in this study:

This document was used to gain an understanding of how blast waves interact with structures. The terminology was helpful in describing the blast scenarios defined in this thesis.

- Conventional Weapons Effects Program (CONWEP) and the TM5-855-1

Background:

The CONWEP program [Hyde: 1992] is often used for blast predictions in the BOP injury criteria research field (e.g. Bass *et al.* [2006a] and Teland and van Doormaal [2012]) and for predicting free-field pressures and loads on structures.

As CONWEP is restricted (along with the TM5-855-1) the author did not have access to this software. Thus, CONWEP is discussed in terms of what other authors have written on the subject.

CONWEP is a computer program based on the Kingery-Bulmash equations [Kingery and Bulmash: 1984] that can also be found in graphical form in TM5-855-1. The TM5-855-1, however, used an approximate equivalent triangular pulse to represent the decay of the incident and reflected pressure, whereas CONWEP used a more realistic exponential decay of the pressure with time as represented by the Friedlander equation [Remennikov: 2003].

The Kingery-Bulmash curves were derived from only four explosive events (See Table 2) that were conducted in Canada between 1959 and 1964 and air blast parameters were recorded by representatives from the United States, Canada and the United Kingdom [Swisdak: 1994].

Table 2: Table showing the number of explosive tests upon which the Kingery-Bulmash curves [Kingery and Bulmash: 1984] were based (modified from Swisdak [1994]).

Event number	Nominal yield of TNT	Date (year in which the test took place)
1	4536 kg (5 tons)	1959
2	18144 kg (20 tons)	1960
3	90719 kg (100 tons)	1961
4	453592 kg (500 tons)	1964

It is quoted in Swisdak [1994] that Kingery [1966] states that, “The data from all four tests were first processed to obtain the as read values of peak BOP, arrival time, positive duration and positive impulse. The cube root scaling and altitude corrections were applied to these values to bring them to standard sea-level conditions and the equivalent of a one-pound [0.45 kg] charge. The scaled values were then used to determine the curves in this report.” This scaling already introduced possible inaccuracies. Then, in Kingery and Bulmash [1984] the same data was re-examined and information on reflected pressure, reflected impulse and shock front velocity was included, where these parameters were not measured, but calculated. The reflected pressure was calculated using the peak overpressure and variable specific heat ratio, the reflected impulse was calculated from free air TNT reflected impulse data and the shock front velocity was calculated from the peak overpressure [Swisdak: 1994].

Limitations:

The Kingery-Bulmash curves do not, for example, take into account weather effects (e.g. atmospheric pressure (other than altitude correction), wind, temperature) and are based on a limited data set (with very large charges at a distance). Weather effects may significantly influence low pressure measurements and thus results may differ significantly from the empirical Kingery-Bulmash curves [Swisdak: 1994].

CONWEP has been found to be non-conservative in predicting blast outputs when the target is close to the explosive charge [Johnson and Claber: 2000].

Johnson and Claber [2000] also conducted a series of experiments and discovered that there are variations in TNT equivalencies of both plastic explosive PE4 and TNT itself which will influence the applicability of the outputs of the CONWEP calculations.

Applications in this study:

Teland and van Doormaal [2012] quote the original Kingery and Bulmash [1984] report wherein Kingery and Bulmash express doubts about the accuracy of the experimental data for the positive phase duration as, "...it is very difficult to determine the time of which the overpressure changes to an underpressure. There can be large variations in the individual interpretations of the positive duration of the blast wave." This will directly affect BOP injury predictions that rely on CONWEP to obtain the peak BOP and the positive phase duration.

The positive phase duration data was also used in the development of the Bass *et al.* [2006a] BOP injury criterion itself (See Section 2.9 for more information on the development and limitation of this injury criterion).

It is useful to know that CONWEP may under predict BOP outputs for smaller charges and close-in targets (as discussed in Johnson and Claber [2000]) as this may make injury criteria that are based on these inputs non-conservative. This could be dangerous as the risk of and severity of BOP injuries that are predicted may be less than could actually occur.

- The Department of Defense Explosives Safety Board (DDESB) Blast Effects Computer – Version 4.0 (BECV4) [2000]

Background:

As discussed in Swisdak [1994], the original curve fits for the Blast Effects Computer (BEC) were requested by the DDESB to provide simplified equations of the Kingery and Bulmash hemispherical TNT compilation [1984]. The results needed to be within 1% of the original results and the incident pressure curves were to be extended to lower levels based on data gathered by Kingery and Pannill [1964]. It was explicitly stated that the limitations of the Kingery-

Bulmash data (as described under the CONWEP bullet point above) would also apply to these curves and thus the curves should not be used as an absolute standard [Swisdak: 1994].

The BEC has been updated since the first circular slide released in 1978, to the BECV1 which was implemented in EXCEL™ in 1997 [Swisdak and Ward: 1998]. The BECV2 was released in 1998 and incorporated updated air blast information for earth-covered magazines and hardened aircraft shelter, updated air blast algorithms for MK82, MK83, MK84 and M117 bombs and M107 155mm projectiles. In 1999, BECV3 was released with additional Potential Explosion Sites (PES) and algorithms for predicting dynamic pressure and dynamic pressure impulse and for estimating the probability of ear drum rupture and probability of lethality due to lung damage. BECV4 was released in 2000 to include structures such as a High Performance Magazine and revised algorithms for predicting the effects from Aboveground Sites (AGS). The effects of altitude were also included in BECV4 in accordance with [Swisdak: 1975]. An improvement of the low pressure yield estimates was made (resulting in improved air blast predictions at pressures below 1 psi) [Swisdak *et al.*: 2000]. This modification was based on a 40-tonne trial conducted in Australia to update the aboveground sites algorithm which revealed the low-pressure hemispherical yields used by the BEC were too low and thus the predicted pressure and impulses were lower than the measured values [Swisdak and Absil: 2000].

According to the BECV4 author/sponsor in presenting the calculation software [Swisdak *et al.*: 2000], the BECV4 is superior to CONWEP as it takes into account the effects of the potential explosion site, the type of weapon and the TNT equivalence of the explosive, whereas CONWEP assumes all weapons are spheres or hemispheres and only makes a correction for TNT equivalence. Practically, CONWEP does not consider the weapon case or shape or the effects of any structure that may exist around the explosion source.

Although a version 6 of the Blast Effects Computer has been released, this version, along with the user manual and documentation, is not freely available (Description obtained at [DDESB: no date]).

Limitations:

Similar limitations to that of CONWEP in that it is based on limited data consisting of much larger charges than those considered in this thesis 4536 kg (5 tons) TNT is the smallest charge size upon which the blast calculators are based, whereas this thesis considers charges in the range of 0.240 kg TNT to 50 kg TNT). However, unlike CONWEP that is only for spherical or hemispherical charges in free field, BECV4 takes into account the weapon case, shape and the effects of any structure that may exist around the explosion source.

Applications in this study:

As mentioned above, the latest version of the software, version 6, is not freely available. Thus, the author has made use of a previous version of the software, version 4 [BECV4: 2000], that is freely available online, for the blast predictions in this thesis. Figure 10 shows an example of data input into BECV4 in EXCELTM and the outputs generated by the program.

Hydrocodes or numerical simulation software

Computational fluid dynamics programs are available for modelling blast waves. The benefit of computational simulation software is that the required number expensive and destructive explosive blast tests could be reduced. In addition, if a sufficient animal model was developed, this could allow the number of tests involving animals to be reduced which has great ethical benefits. However, simulation software is limited by, for example, material properties at high strain rates, and the validity of the software outputs can only be as good as the understanding of the event which occurs. ANSYS AUTODYN2D and Propagation of Shocks in Air (ProSAir) (formerly Air3D) are simulation programs which were used to obtain results that were used in this thesis. These are discussed further in section 8.5.3 of this study.

INPUT SECTION			
Metric Units (kg, m, kPa, Pa-s, ms)			
Select Potential Explosion Site (PES)	Select Number of Weapons or Total NEQ	Enter initial range for Summary Table	Select Atmospheric Description
Open Storage	Total NEQ (kg)	0.1	Altitude (meters)
Select Type of Weapon	Enter Total NEQ (kg)	1.0	Enter Altitude (m)
Bulk/Light Cased			1 000.00
Select Type of Explosive	Range (m)	1.0	Enter Temperature (°C)
TNT			21.00
OUTPUT SECTION			
EXPLOSIVE PARAMETERS		ATMOSPHERE PARAMETERS	
Total NEQ (kg)	1.0	Pressure (mbar)	897.4
NEW per weapon (kg)	1.000	Temperature (°C)	21.00
TNT Equivalence	1.00	Pressure (S _p)	0.8857
		Distance (S _d)	1.0413
Equivalent Hemispherical Weight (kg)	1.0	Time (S _t)	1.0306
Effective Yield (kg)	1.0	Impulse (S _i)	0.9128
(N.B.: Both Weight and Yield are in kg of TNT)			
AIRBLAST SEA LEVEL		PARAMETERS ALTITUDE (meters)	
			1000
Range (m)	1.0		0.9
Time of Arrival at Range (msec)	0.47		0.5
Over-Pressure at Range (kPa)	1353.91		1199.2
Reflected Press. at Range (kPa)	8117.55		7189.9
Positive Phase Duration at Range (ms)	1.7		1.8
Positive Phase Impulse at Range (Pa-s)	236.3		215.7
Reflected Impulse at Range (Pa-s)	884.8		807.7
Dynamic Overpressure at Range (kPa)	2268.5		2009.29
Dynamic Overpressure Impulse at Range (Pa-s)	185.0		168.9
OTHER INFORMATION			
Probability of Window Breakage (percent) at Range (note: dimensions are cm)	Area = 0.186 m ² 30.5 x 61.0 x 0.223 Float annealed	100.0	Area = 1.626 m ² 152.4 x 106.7 x 0.559 Plate annealed
	Area = 0.372 m ² 61.0 x 61.0 x 0.223 Float annealed	100.0	Area = 2.787 m ² 182.9 x 152.4 x 0.559 Plate annealed
	Area = 0.975 m ² 106.7 x 91.4 x 0.305 Float annealed	100.0	Area = 4.645 m ² 304.8 x 152.4 x 0.762 Plate annealed
Probability of Eardrum Rupture (percent) at Range		100.0 (Maccan)	
		100.0 (Eisenberg)	
Probability of lethality due to lung damage (percent) at Range		0.0	

Parameters used in this thesis:

- Time of arrival
- Peak overpressure (side-on)
- Peak reflected pressure (face-on)
- Positive phase duration

Figure 10: Example of BECV4 [2000] in EXCEL™ generated by the author by inputting 1 kg of TNT at a range of 1 m (altitude of 1000m and 21 degrees C) and the outputs are generated by the program. The parameters that are used in this thesis are annotated in red on the screen shot above.

Considerations when using blast calculators or numerical simulations to predict BOP profiles

When reviewing blast calculators, the author found it concerning that a number of different methods of determining BOP profiles (computer blast calculators or documents on how to calculate blast parameters) are currently in use by the US Defence Department. It is stated in UFC [2008] that other complimentary manuals and computer programs are available from the appropriate representatives of the US Army, the US Navy, the US Air Force and the DDESB. The author of this thesis suggests that the multiple manuals and computer codes that are available may be due to the various defence bodies that developed them. The TM55-855-1 (and CONWEP) is linked to the US Army and the DDESB BECV4 is linked to the US Navy.

For the purpose of predicting BOP parameters in this thesis, the BECV4 software was selected over the UFC [2008] document and CONWEP as:

- The original sources of the individual curves used for predictions in UFC [2008] are not specifically referenced; the document is not as straight forward to use as computerised blast calculation software; and the document is not commonly used in the field of BOP injury predictions, but rather in the field of structural response to blast.
- Although CONWEP is widely used in the field of BOP injury predictions, it is restricted and thus not available to the author.
- BECV4 claims to be superior to CONWEP (See details above).
- Although BECV6 (version 6) has been released, it was not available to the author and thus BECV4 was used.

Limitations of empirical blast calculation software include:

- Uncertainties in empirical formulae for blast wave parameters results in differences in predicted injuries for very short duration, high amplitude blast waves [Teland and van Doormaal: 2012].

- They are based on actual experimental measurements that may be influenced by test site conditions that vary from day to day. There are many different scaling laws to correct for different parameters that will influence the BOP profile generated by an explosive charge, for example, temperature or altitude correction (See Petes [1968] for a number of scaling examples).
- If an explosive charge type, other than TNT is used, it must be converted to a TNT equivalent mass. The use of TNT-equivalencies also introduces inaccuracies (See [Held: 1983] for full discussion of the limitations of TNT-equivalence approximations).

In summary, the limitations of these blast calculators must be considered when using setups that vary from those under which the underlying experimental data is based. When this is not the case, one should keep in mind that the algorithms used to for example, scale the data or account for alternative weather conditions, are not absolute values, but rather approximations that may be based on limited data. The empirical data was gathered from a limited set of data which was collected during the detonation of very large charges. Thus, the accuracy of empirical equations decreases as the explosive event becomes increasingly near field [Remennikov: 2003].

In the field of BOP injury research, the charges are usually much smaller than those used in the development of the blast calculation software and they are positioned close to the subject. This is important when reviewing injury criteria that were developed making use of these calculators and when comparing experimental blast results to those predicted by the blast calculators for relatively small charges that are close to the subject.

The importance of conducting actual blast trials or experiments is acknowledged as there is still much debate as to the accuracy of empirical blast calculators, especially when looking at small charges, close-in, as is the case in this thesis. It would be dangerous if only blast calculators were used to predict BOP injuries as the BOP outputs are sometimes under-predicted which could lead to a higher risk of more severe BOP injuries for a particular scenario.

However, blast calculators are useful to allow comparisons with experimental results, provided the limitations of the blast calculators are understood.

2.5 Prevalence of Blast Injuries in Various Scenarios

People involved in explosive events (such as landmine or improvised explosive device (IED) incidents in military scenarios or terrorist bombings in civilian scenarios) may be killed or injured in a number of different ways which depends largely on the scenario in which the event occurs. In most blast scenarios, a number of different blast injury mechanisms occur simultaneously which makes it difficult to assess the true effect of BOP. In addition, the methodology used to assess the injuries will influence which injuries are detected [Mayorga: 1997]. A review of the injury mechanisms that may be involved in various scenarios and the prevalence of blast and BOP injuries in those scenarios, provides an indication of the scope of BOP injuries. The prevalence of blast injuries in general, and in the scenarios defined in for this thesis, are described below.

2.5.1 Occurrence of blast injuries in general

Blast lung was reported as a common injury amongst soldiers killed by explosions in Northern Ireland, where 11% of them sustained lung damage with no other apparent injuries [Cooper: 1996]. More recently, blast overpressure injuries, sustained by UK Military personnel in operations in Iraq and Afghanistan, accounted for 4% of blast related fatalities, but a combination of blast overpressure and fragmentation effects accounted for 31% of the blast related fatalities [Lewis: 2006]. Kirkman *et al.* [2011] suggests that the occurrence of BOP (blast lung) injuries may be underestimated in current military casualties as blast lung injuries are often excluded when they co-exist with other injury types (such as fragment injuries to the torso or broken ribs).

Blast injuries have an overall lethality of about 7.8% in open spaces which jumps to 49% when the blast occurs in a confined space or built up area [Stewart: 2006]. Traumatic amputations occur in about 11% of cases.

2.5.2 Scenario A: Indirect BOP exposure within a vehicle (threat outside vehicle)

Anti-vehicle (AV) or anti-tank (AT) landmines and improvised explosive devices (IEDs) present a threat to vehicle occupants and their humanitarian impact extends into

the future as the mines are often not cleared. IEDs/mines prevent humanitarian organisations from gaining access to populations in need of aid and the clearing of these landmines is time-consuming and costly [Geneva International Centre for Humanitarian Demining (GICHD): no date; Gondusky and Reiter: 2005]. AVs are designed to minimise the risk of injury to the occupants during times of conflict as well as to protect members of humanitarian organisations to allow them to bring aid to post-conflict countries.

Although not a large percentage of occupants of AVs are injured, those that are injured tend to have very severe or fatal injuries [Stiff: 1986; Medin *et al.*: 1998; Radonic *et al.*: 2004]. The prevalence and nature of injuries sustained within vehicles subjected to blast is difficult to ascertain as much of this information is restricted so as not to expose weak areas in AVs which may put vehicle occupants at more risk of targeted attacks. Few publications are available detailing AT landmine / IED (road-side bomb) incidents and even fewer describe the injuries in detail.

The book by Stiff [1986] presents a large number of AT landmine incidents that occurred during the Rhodesian War (December 1972 to January 1980), but only the number of people killed or injured are reported on. The specific injuries are not described, as is the case with most documentation concerning AT landmine incidents. Anecdotal evidence from the author's discussions with people who had been involved in the Rhodesian conflict suggested that most injuries sustained during AT landmine incidents were caused by people being thrown from the vehicle during the explosive event (as they often stood on the seats and looked out the top of the roofless vehicles) or due to the vehicle rolling after being damaged by an AT landmine.

Papers that do describe the nature of injuries sustained by occupants of vehicles involved in an AT mine explosions are Medin *et al.* [1998] and Radonic *et al.* [2004].

An AT landmine (6.5 kg TNT) incident involving a Swedish armoured personnel carrier in Bosnia in January 1996 [Medin *et al.*: 1998]. Of the nine occupants, two needed below knee amputations, three suffered from heel bone fractures, one sustained a ligament injury of the knee and three others sustained no physical injuries. It must be noted that the occupants were standing and not sitting at the time of the incident.

Radonic *et al.* [2004] analysed antitank mine casualties in South Croatia from 1991 to 1995. Of 464 occupants, there were 42 victims and 12 fatalities. Brain injuries were the most common injuries amongst the fatalities (which they attributed mainly due to lack of restraint systems or not using restraint systems which resulted in head impact with the roof), followed by vessel injuries and massive thoracic injuries. They conclude that although injuries from antitank mines are frequently fatal, a large percentage of occupants survived their injuries or were unharmed.

IEDs or road-side bombs pose the most prevalent single threat to UK and Coalition troops operating in Iraq and Afghanistan [Ramasamy *et al.*: 2011]. IEDs cause multiple casualties with injuries requiring multi-disciplinary intervention and thus place a significant burden on field hospital surgical facilities. With improved torso PPE, enhanced pre-hospital care and rapid access to medical attention, more people are surviving with extremity or non-penetrating torso injuries.

An example of an IED incident in Afghanistan in 2003 that caused a hull rupture was provided in Dosquet *et al.* [2004]. Four soldiers were killed and 29 were injured. BOP injuries included 24 eardrum injuries of 18 soldiers that had to be reconstructed. The cause of death of two of the soldiers was BOP injury (lung rupture, pulmonary (lung) haemorrhage and edema).

Case reports of close proximity blast injury patterns from IEDs in Iraq in 2004 were described in Nelson *et al.* [2008]. The cases included victims within vehicles and dismounted soldiers. The BOP injuries sustained by a victim who was in an armoured vehicle that was subjected to an IED explosion under the vehicle, were discussed in detail. The patient was sent to recovery, but later developed hypoxia (low oxygen) and was returned to the operating room. The doctors found small stellate lacerations (star-shaped or branching tears) on the liver and spleen and multiple small areas of petechial haemorrhage along the serosa of the small bowel and colon.. The patient subsequently arrested and was noted to have an avulsion of the right reno-vascular pedicle with a contained retroperitoneal hematoma. A general observation was that the majority of patients who died demonstrated early hemodynamic stability after initial resuscitation, but showed an abrupt and immediate drop in blood pressure without an increase in pulse rate 45 – 90 minutes after presentation. Some patients showed instability after

intubation that may have developed secondary to alveolar-venous fistulae. The increase in severity of BOP injuries as time passes after an explosive event is suggested by these case studies.

In the scenario where vehicle occupants are involved in an IED or AT mine incident, the injury mechanisms can still be due to direct blast effects (mainly due to BOP caused by the expanding detonation products which interact with the vehicle) and indirect blast effects (due to fragments (secondary effects), whole body motion and relative displacement of body parts (tertiary effects), burn injuries, smoke inhalation (miscellaneous effects)) [van der Horst *et al.*: 2010]. Ramasamy *et al.* [2011] provide a good overview of the interactions of buried landmine/IED explosions on vehicles and their occupants. The three phases that are described are the explosive interacting with the soil, the gas expanding and pushing material outwards from the soil surface and the soil ejecta interacting with the vehicle. They regard the soil ejecta interacting with the vehicle and causing local deformation of the vehicle floor (resulting in mainly lower limb injuries) as a tertiary blast injury mechanism and the most significant injury mechanism if the hull remains intact. Overall, fragmentation effects have the highest lethality risk in IED incidents Dosquet *et al.* [2004].

If the vehicle integrity is assured (i.e. No breach of the occupant compartment; no fragments enter the occupant compartment and loose objects within the vehicle are not accelerated so as to become penetrating projectiles), then the effects of BOP, fragments, gasses and heat will not have major physical effects on the vehicle occupants. The most likely injuries to the thorax would then be blunt trauma injuries. Blunt trauma injuries could occur if the thorax is loaded via the seat, seat belt, objects in the vehicle or vehicle components (e.g. steering column) moving into the occupant or if the occupant is propelled into objects in the vehicle or vehicle components. Unfortunately limited data is available regarding thoracic injuries due to an IED or landmine incident, thus injuries occurring in the automotive environment have been studied as many of the injury mechanisms in this environment may be similar.

The focus of this study is on BOP injuries or injuries due to direct blast effects. However, deciding which injuries are due to direct BOP effects, and which are due to indirect blast effects, becomes difficult in certain scenarios. The time spans of the

signals recorded when a person within a vehicle is exposed to an explosive event are different from that of a person exposed directly to an explosive event. A vehicle occupant could be injured by the local effect (shock and deformation) and the global effect (vehicle motion) of the mine detonation process [Leerdam: 2002].

2.5.3 Scenario B: Direct BOP exposure within a vehicle or enclosed space (threat inside vehicle)

This scenario describes an explosive event within a vehicle or enclosed space. Examples could include terrorist attacks such as bombs or IEDs detonated within busses, cars or trains. These incidents result in a high number of BOP injuries (most often along with mutilating and/or penetrating injuries).

Katz *et al.* [1989] described injuries due to a 6 kg TNT bomb explosion in a civilian bus in Jerusalem. Of the passengers, 3 people died, 55 survived and of those 55 people, 29 were hospitalised. Of the 29 people in hospital, BOP injuries were found in many of them, with 76% showing ear drum perforations, 38% showing blast lung and 14% with abdominal blast injuries (including bowel perforations).

In the Madrid train bombings in 2004, 10 terrorist bomb explosions occurred in four commuter trains resulting in 191 deaths and over 2000 people being injured. Ear blast injuries were identified in 67% and blast lung injuries were reported in 63% of critically ill patients [de Ceballos *et al.*: 2005].

Other examples of this scenario are the London Underground train and bus bombings on 7 July 2005 (often referred to as 7/7) where 52 victims and four bombers died and many more casualties (either during the initial blast or the subsequent effects) [Hepper *et al.*: 2011].

In the military scenario, shaped charges or explosively formed projectiles (EFPs) may bring the blast into the vehicle, however, the peak BOP measured experimentally are too low to cause significant BOP injuries [Jacobson and Schmidt: 1999; Held: 2008].

2.5.4 Scenario C: Direct BOP exposure through close contact with fragmentation munitions

The threat considered for this scenario was the M26 hand grenade, thus the prevalence of blast injuries due to this hand grenade in South Africa was reviewed.

Eleven hand grenade incidents were reported in the Mthatha area the media between 1998 and 2007. There were thirteen explosive devices involved in which thirteen children and five adults were killed. The South African manufactured M26 hand grenade was the most common threat identified in these incidents (Details of the review can be found in Meel *et al.* [2009]).

Although this information indicates how often people are killed by hand grenades, details of the injuries were not provided. However, the main injury mechanism of fragmentation munitions is the high velocity fragments that are expelled and that have a kill radius greater than that of the BOP effects. But, BOP effects may complicate existing injuries, and as discussed above, traumatic amputation or mutilating blast injuries (if a person is very close to the origin of a blast), are in fact BOP effects.

2.5.5 Scenario D: Demining

The injury mechanisms and prevalence of BOP Injuries in a demining scenario were reviewed as inputs to this study.

As with injuries caused by AT mines to vehicle occupants, injuries caused to dismounted soldiers are not widely publicised [NATO-RTO-TR-HFM-089: 2004]. However, a survey reported in [NATO-RTO-TR-HFM-089: 2004] was conducted in 1998 that looked at the distribution of threats and injuries in the field of humanitarian demining. The study included 232 mine accidents with 295 victims.

Figure 11 shows that the majority of injuries resulted from AP blast mines, more than three times the number of people that were injured by fragmentation mines. However, only 7% of the victims that were injured by AP blast mines died, compared to 38% of the victims that died due to injuries from fragmentation mines [NATO-RTO-TR-HFM-089: 2004]. This illustrates the aim of AP blast mines to injure and maim victims (rather than kill them) to place a burden on the medical systems and psychological outlook of the opposing force.

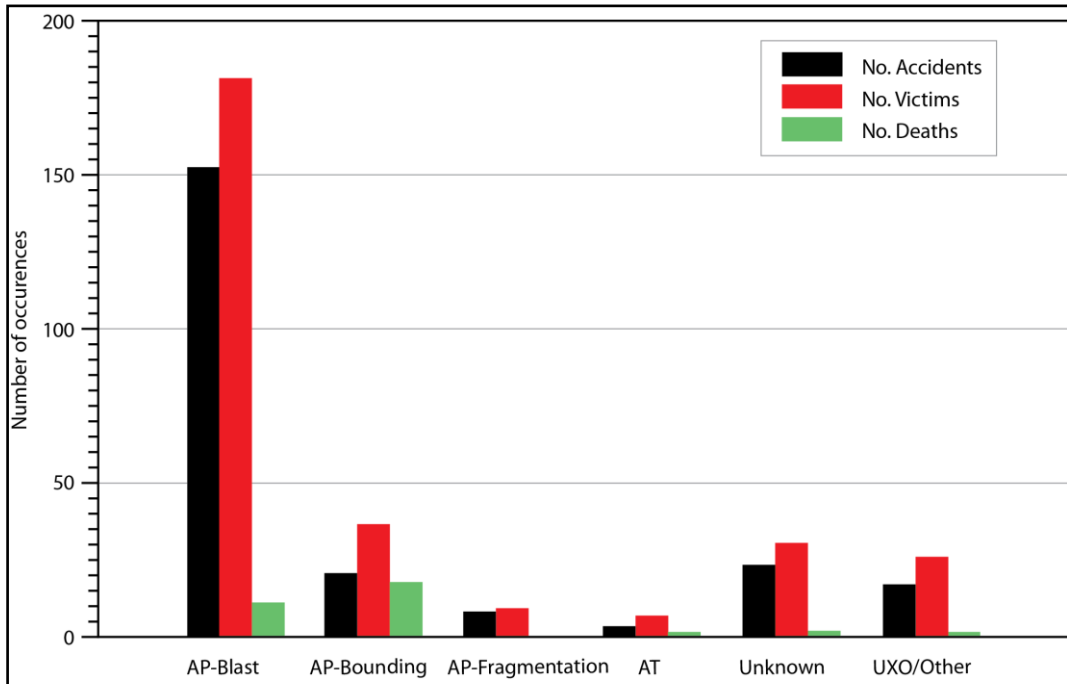


Figure 11: Distribution and threats that caused accidental injury to humanitarian deminers (after NATO-RTO-TR-HFM-089 [2004]).

AP blast mines are designed to cause blast injury near the mine, rather than AP fragmentation mines that have a much greater kill and injury radius due to the high velocity fragments that are expelled.

AP blast mines mainly use the direct effects of blast on human tissue [NATO-RTO-TR-HFM-089: 2004]. The dominant injury mechanism is believed to be the expansion of the detonation products (the mass of hot high-pressure gas formed by the chemical reaction that transformed the solid explosive into a gas almost instantaneously (in about 5 μ s)). When the detonation wave reaches the physical boundaries of the explosive, it is partly transmitted to the surroundings. If the explosive device is in direct contact with an object, the stresses generated by the transmitted wave can easily exceed the strength of the receptor material and cause it to fail. This process, called brisance, refers to the ability of the explosive to shatter materials [NATO-RTO-TR-HFM-089: 2004]. It is believed that brisance is related to the extent of injury of a soldier that steps on a mine buried flush with the ground as the shattering high-pressure wave is transmitted directly into the lower limb. The effect of the brisance diminishes rapidly as the standoff distance between the explosive and the target increases [NATO-RTO-TR-HFM-089: 2004].

Looking at the torso body region, the torso is normally not as close to or in contact with the explosive device (as the lower limb would be if a victim stood on a mine). The injury mechanisms described in NATO-RTO-TR-HFM-089 [2004] are burns, BOP and fragmentation, where direct injuries include respiratory tract injuries, ear injuries. Indirect injuries include those due to the elastic deformation of PPE caused by the push of the air shock and detonation products, body translation and fragmentation NATO-RTO-TR-HFM-089: 2004]. The AP mine case and internal trigger mechanism become fragments that can cause injury and soil ejecta, small stones or other environmental debris can become secondary fragments as the blast propels them away from the origin of the blast [NATO-RTO-TR-HFM-089: 2004].

2.6 BOP Injuries

This section defines BOP injuries, explores BOP injury mechanisms and the susceptibility of different body regions to BOP injuries.

2.6.1 Classification of BOP injuries

The classification of blast injuries in general was described in the introduction. However, there is confusion in the literature regarding what is meant by BOP injuries.

Injuries due to blast have been defined as direct or indirect injuries [White: 1968; Zuckerman: 1941] and very commonly, although less logically, into primary, secondary, tertiary or quaternary (or miscellaneous) injuries [White: 1968; Kirkman *et al.*: 2011].

In this study, BOP injuries are taken to mean injuries due to direct or primary effects caused by the variation in the environmental pressure due to an explosive event. They relate to the actual physical interaction between the body of the victim and the detonation products, defined by the physical boundaries of the fireball, and/or the blast wave generated by the explosion [NATO RTO-TR-HFM-089: 2004].

In some literature sources, mutilating blast injuries are also considered BOP injuries. Stuhmiller *et al.* [1991] stated that “Mutilating blast injury (that is, traumatic amputation) occurs as a combination of secondary and tertiary blast effects.” Other researchers regard traumatic amputations as BOP injuries. They say traumatic amputations are caused by high BOP forces resulting in boney fractures while

concomitant strong blast winds rupture soft tissue structure, leading to partial or complete extremity amputations. Hull and Cooper [1996] investigated the mechanisms of fatal limb amputations in blast victims and used computer modelling and tests with a goat limb to show that these are direct BOP injuries caused by a shock wave rather than by disarticulation or by flying debris. The exact BOP needed to cause these injuries is not known [Wolf *et al.*: 2009].

Burns are classified as quaternary or miscellaneous injuries, even though they can also be caused by the direct thermal energy of the explosion (again another confusing point in the primary, secondary, tertiary and quaternary classification). Burns can also be caused by the secondary burning of structures, vehicles, clothes, or equipment (in these cases the quaternary, miscellaneous classification seems appropriate).

Focussing on contradictory meaning of the term *primary* when dealing with blast scenarios, it is sometimes taken to mean “dominant” or “main”. For example, when referring to vehicles perforated by shaped charges, Jacobson and Schmidt [1999] specified that the “primary damage mechanism is associated with residual warhead material and armor spall. However, there is also the potential for damage from secondary effects such as blast, flash, thermal pulse, and noxious gases.” Another example of confusion that could be introduced by using the term primary is when the term is used in the medical field such as in Tatic *et al.* [1996]. The primary and secondary perforations of the intestinal wall of rats exposed to blast, where primary perforations are those that occur immediately during the blast and secondary perforations are those that occur hours after the blast. However, they also use the term primary perforations to describe injuries caused by the effect of the direct pressure wave.

Thus, it was decided that in this thesis that the term BOP injuries would be used, rather than the more commonly used term *primary* blast injuries. In addition, mutilating blast injuries would not be form part of the focus of BOP injuries considered in this thesis.

2.6.2 Susceptibility of different body regions to BOP injuries

There are conflicting views on which organs are most susceptible to BOP effects. The aim is to clear up the confusion regarding which injuries are caused by direct BOP

effects versus which are caused by other blast effects (such as fragments). This information will then allow the author to motivate which organs have been selected for inclusion in this study and how BOP injuries have been defined.

It is usually stated that the hollow air-containing organs such as the ears, upper respiratory tract, lungs and gastrointestinal tract are most vulnerable to BOP injury (e.g. Kirkman *et al.* [2011]). However, recent studies have shown the solid abdominal organs may even be more vulnerable to BOP injury [Carneal *et al.*: 2012]. Wolf *et al.* [2009] provided a useful overview of how various body regions may be injured by the direct BOP effects of an explosive event, irrespective of whether these injuries may be formally, sometimes ambiguously, classified as primary, secondary, tertiary and quaternary/miscellaneous/quinary injuries. Thus, the author describes injuries due to the direct effects of explosive events which will be further delineated to provide a definition of BOP injuries at the end of the section.

Ears

Most commonly, it is stated that the ear is most susceptible to BOP [NATO-RTO-TR-HFM-090: 2007] and has been viewed as an indicator of BOP injury to the rest of the body. At a peak pressure of 35 kPa peak pressure, the eardrum may rupture, but at 100 kPa, almost all eardrums will rupture [Stewart: 2006]. However, studies have shown that an intact eardrum does not indicate the lack of blast lung (lung damage due to BOP). Peters [2011] stated that the use of the perforation of the eardrum as an indicator of a primary blast injury (BOP injury) missed a range of up to 50% of those suffering from blast lung. Wolf *et al.* [2009] presents conflicting evidence from authors regarding the relationship between eardrum damage and other BOP injuries; 94% of people with eardrum rupture will have other BOP injuries, but a substantial proportion of survivors with and without eardrum rupture have blast lung injury. Interestingly, recent studies suggest that eardrum rupture might be a predictor for concussive brain injury, although it may not be a predictor of other BOP injuries [Harrison *et al.*: 2006; Xydakis *et al.*: 2007].

Lungs

The lungs are particularly susceptible to damage due to BOP as there is a large air-lung tissue surface area [Stewart: 2006; Wolf *et al.*: 2009]. Wolf *et al.* [2009] reflected that of people exposed to explosions, 17%-47% of people who died had evidence of blast lung injury and 71% of those critically ill and hospitalised had blast lung injury. A recent retrospective study by Carneal *et al.* [2012], based on experiments using a sheep model, showed that the lungs were the most susceptible thoracic or abdominal organs to BOP injury and that they showed the highest sensitivity to changes in charge weight (or exposure to different BOP levels). However, it was noted that lung injury is normally more acute than abdominal injuries which may take longer to develop (manifestation of abdominal injuries usually occurs after 1 hour of exposure to blast, whereas manifestation of lung injuries usually occurs within 1 hour of exposure) [Carneal *et al.*: 2012]. The acute cause of death due to lung BOP injury is usually air emboli [Sharpnack *et al.*: 1991].

Upper respiratory tract (pharynx, larynx and trachea)

The upper respiratory tract was shown in Carneal *et al.* [2012] to be less susceptible to BOP injury than the lungs and showed less sensitivity to increasing BOP exposure levels than the lungs did.

Hollow abdominal organs (gastrointestinal tract)

The gastrointestinal tract has a high risk of BOP injury due to its air content [Wolf *et al.*: 2009] and that the incidence of abdominal BOP injury might be as high as 14% to 24%, although composite data suggests lower figures. However, a study on pigs exposed to BOP [Suneson: 1987] showed intestinal injuries with no lung damage. Cripps and Cooper [1997] investigated the risk of late perforation in intestinal contusions caused by BOP.

Mayorga [1997] indicated that in free-field single exposures, the susceptibility of the gastrointestinal tract was less than that of the lungs and the upper respiratory tract. But, for a single detonation under complex wave conditions there was no significant difference in the susceptibility, and for multiple detonations in a complex wave

environment, the gastrointestinal tract was more susceptible to injury than the lungs and upper respiratory tract.

Yelverton *et al.* [1996], Phillips and Richmond [1991] and Sharpnack *et al.* [1991] found that the hollow abdominal organs were more susceptible to BOP than the solid abdominal organs. However, Carneal *et al.* [2012] found that there was little difference in the injury response between the hollow and solid abdominal organs. A study based on clinical observations of blast victims with BOP injuries, as referred to by Carneal *et al.* [2012], confirmed that there was little difference in the susceptibility of the hollow and solid abdominal organs to BOP injury.

Carneal *et al.* [2012] found that the abdominal organs were susceptible to blast at low threat exposure levels, but had a reduced sensitivity to increasing BOP exposure levels.

Solid abdominal organs

As mentioned above, Carneal *et al.* [2012] found that the abdominal organs were susceptible to blast at low threat exposure levels, but had a reduced sensitivity to increasing BOP exposure levels. The hollow and solid abdominal organs had similar susceptibility to BOP injury at both high and low threat levels.

Brain

BOP injury to the brain (traumatic brain injury (TBI) or mild traumatic brain injury (mTBI)) has also been studied. Hoge *et al.* [2008] reflects that studies looking at brain injury as a BOP injury, rather than a secondary or tertiary injury, seldom use methodical clinical investigations and the results of diagnostic testing (e.g. neuroimaging, neuropsychological tests and serum biomarkers) are typically inconclusive and difficult to interpret. In the past, BOP effects on the brain were not even considered (were believed to be due to projectiles or inertial effects) (e.g. Sharpnack *et al.* [1991]). However, there is now a large ongoing research effort in many different countries and at various research institutions into the mechanisms of blast induced TBI [Courtney and Courtney: 2009; van de Vord *et al.*: 2012].

Musculoskeletal

Musculoskeletal injuries are the most common blast injuries [Hayda *et al.*: 2004].

Fractures could occur due to BOP loading of body, for example rib fractures of the thorax, but the ribs were found to be less susceptible to BOP injury than the lungs, upper respiratory tract, hollow abdominal organs and the solid abdominal organs [Carneal *et al.*:2012]. This indicates that skeletal injuries do not adequately predict soft-tissue injury due to BOP to the thorax and abdomen [Carneal *et al.*: 2012].

Common musculoskeletal injuries to the extremities are traumatic amputations and compartment syndromes [Wolf *et al.*: 2009].

Eyes (visual system)

Up to 10% of people injured by explosions have eye (ocular) trauma, but most of these are due to secondary blast effects. However, ruptured globes, hyphemas, conjunctival haemorrhage, serous rhinitis and orbital fractures have been reported as BOP injuries [Wolf *et al.*: 2009].

2.6.3 Definition and scope of BOP injuries considered in this study

In this study, BOP injuries are taken to mean injuries due to direct effects caused by the variation in the environmental pressure due to an explosive event. They relate to the actual physical interaction between the body of the victim and the detonation products, defined by the physical boundaries of the fireball, and/or the blast wave generated by the explosion [NATO RTO-TR-HFM-089: 2004].

In addition, mutilating blast injuries and burn injuries will not form part of the focus of BOP injuries considered in this thesis.

Other than mutilating blast injuries, the organs most often affected by BOP injuries are those found in the thorax and abdominal body regions. Thus, for the purpose of this thesis, only torso injuries will be considered.

2.7 Identification and Severity Assessment of BOP Injuries to the Torso

The previous section reviewed the susceptibility of various organs to BOP injury. There was some debate as to which organs were most susceptible to BOP. A possible reason for this was that the methodologies used to identify and quantify BOP injuries differ between researchers. A closer examination of what BOP injuries to the torso look like on a macro and microscopic scale is reviewed here, and how these injuries are quantified or scored by different research groups.

2.7.1 Overview of thoracic and abdominal anatomy and physiology

The thorax consists of the ribcage and the underlying soft tissue organs. The thorax extends from the base of the neck to the diaphragm which separates the thoracic and abdominal cavities. The major organs which are included in the thorax are the heart and the lungs.

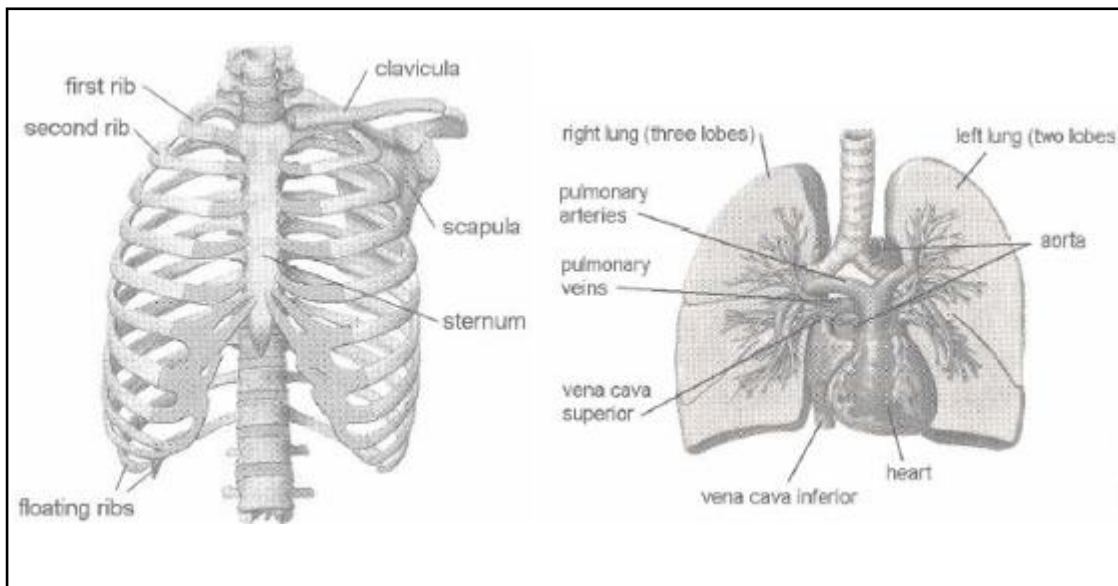


Figure 12: Diagram of the ribcage (left) and the underlying soft tissue organs, namely the heart and the lungs (right) (after Schmitt *et al.* [2004]).

The abdomen is bounded by the diaphragm and the pelvic bones (See Figure 13). On the front and sides of the abdomen, muscles surround the abdominal organs and, at the back, the lumbar spine bounds the abdomen (the lumbar spine itself is usually not considered part of the abdomen [Schmitt *et al.*: 2004] and is not considered in this study). The lower rib cage bounds the upper abdominal region which results in

different impact responses of the upper and the lower abdominal regions. The lower ribs influence injury outcomes particularly in rear and side impacts, but for frontal impacts, the organs directly in front of the spinal column are at higher risk of being damaged by compression than organs lateral to the spine [Schmitt *et al.*: 2004].

Abdominal organs are grouped into solid (liver, spleen, pancreas, kidneys, ovaries and adrenal glands) and hollow organs (stomach, large and small intestines, bladder and uterus) by the gross density of the organ (not the tissue density) [Schmitt *et al.*: 2004]. The solid organs contain fluid-filled vessels and the hollow organs are filled with air or digestive matter which results in the hollow organs being less dense than the solid organs.

The abdominal organs are not rigidly fixed to the abdominal wall or each other, but rather, they are embedded in fat (e.g. kidneys) or secured by the folds of the peritoneum which covers the inner abdominal walls and each organ [Schmitt *et al.*: 2004]. The lubricating peritoneum adds to the high mobility of the abdominal organs may help them to escape injury due to mechanical loads [Johannsen and Schindler: 2006].

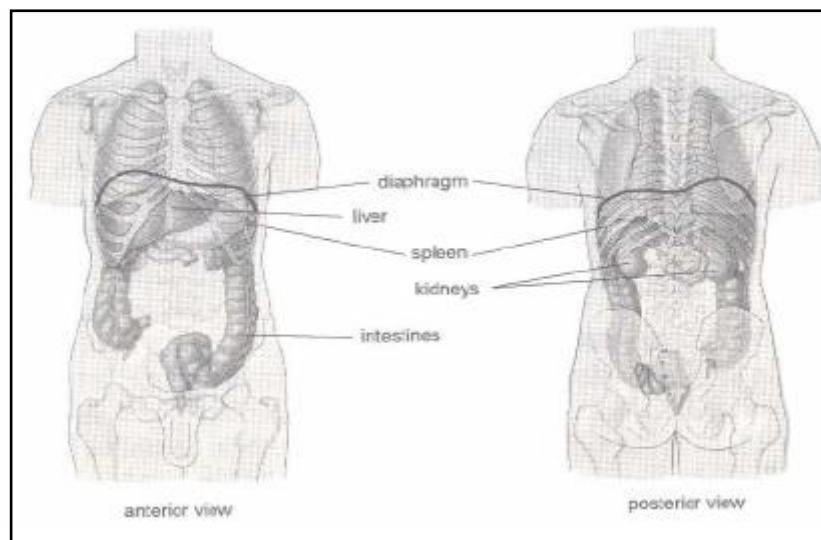


Figure 13: Diagram of showing the abdominal organs (after Schmitt *et al.* [2004]).

2.7.2 Introduction to animal tests used to research BOP injuries

Research into BOP injuries is achieved by clinical observations of blast victim or by making use of biological system testing [Carneal *et al.*: 2012]. The biological system testing or animal studies are often conducted using explosives or shock tubes in a lab

environment. BOP profiles can be simulated in a laboratory using compressed air-driven shock tubes [Elsayed: 1997].

Many different animals have been used to study BOP injuries, including, rats, mice, guinea pigs, rabbits, sheep, pigs, and monkeys [Elsayed: 1997]. The animals are anesthetized during the exposure and given pain relief if they are allowed to wake up following the exposure. Ethical approval is obtained prior to testing with animal models.

Contradictory information regarding BOP injuries may arise when using different animal models, post mortem human surrogates (PMHS) or data derived from case studies (Mayorga [1997]). The gastrointestinal tract was affected less frequently than the lung in [Katz *et al.*: 1989], where people were involved, but the gastrointestinal tract was shown to be more susceptible to BOP exposure in sheep studies [Stuhmiller *et al.*: 1991]. Mayorga [1997] attributed this difference to the difference between sheep, that are ruminants, and humans that are not. Thus, the air content of the gastrointestinal tract may differ. When guinea pigs were used (also non-ruminants) the solid organs were shown to be injured at the same time as the lung, but this may be due to the fragility of the young guinea pig solid organs.

2.7.3 Identification and scoring of BOP lung injuries

Injury scales are used to describe the type and severity of an injury and are based on medical diagnosis [Schmitt *et al.*: 2004]. Examples of anatomic injury scales are the Abbreviated Injury Scale (AIS), the Injury Severity Score (ISS), the Probability of Death (POD) and the Occupant Injury Classification (OIC) [AAAM: 2005].

The Abbreviated Injury Scale (AIS)

In trauma research, the most commonly used scale is the Abbreviated Injury Scale (AIS) [Schmitt *et al.*: 2004]. The AIS dates back to 1971 to fill a need for a standardised system for classifying the type and severity of injuries resulting from vehicular crashes [AAAM: 2005]. The AIS has been revised over the years to describe more injuries and the latest version is AIS 2005. In [AAAM: 2005] the AIS is defined as “an anatomically-based, consensus-derived, global severity scoring system that classifies each injury by body region according to its relative importance on a 6-point ordinal

scale.” In the AIS code the injury is given a number which describes the specific injury and a severity rating from 1 to 6, where 1 is considered a minor injury and 6 is an untreatable or fatal injury. The AIS code is described by seven numbers, ab(cd)(ef).g, where a is the body region, b is the type of anatomical structure, cd is the specific anatomical structure, ef is the level and g is the severity of the score. However, the severity of the AIS score may change over time as a once untreatable and fatal injury becomes a survivable injury due to improved medical interventions [Clasper: 2014].

In the current military standard for the evaluation of occupant safety within AVs [AEP-55 vol. 2 (Edition 1): 2006] the accepted injury risk is less than 10% chance of an AIS 2+ injury (where an AIS 2+ injury could be an AIS 2, AIS 3, AIS 4, AIS 5 or AIS 6 injury and an AIS 2 injury is a moderate severity injury with a 0.1 to 0.4% fatality range).

Examples of AIS injury severity rating for common blast and blunt trauma injuries to the thorax and abdomen are described in Table 3. It is interesting to note that whilst blast lung is specified in AIS 2005, BOP injuries are not listed for abdominal, trachea or digestive tract overpressure injuries, even though BOP intestinal injuries are seen without lung injuries.

Table 3: AIS or injury severity rating for common blast and blunt trauma injuries to the thorax (descriptions from Schmitt *et al.* [2004] and AAAM [2005]).

AIS	Injury severity	Thoracic Skeletal Injury	Thoracic and Abdominal Soft Tissue Injury
1	Minor	1 rib fracture	Contusion of bronchus Abdominal skin or muscle contusion (hematoma)
2	Moderate	2-3 rib fractures Sternum fracture	Partial thickness bronchus tear Spleen or liver contusion (<50% surface area)
3	Serious	4 or more rib fracture on one side 2-3 rib fractures with hemo/pneumothorax	Lung contusion Minor heart contusion Mild blast lung injury Major kidney contusion; spleen rupture
4	Severe	Flail chest 4 or more rib fractures on each side 4 or more rib fractures with hemo/pneumothorax	Bilateral lung laceration Minor aortic laceration Major heart contusion Moderate uni/bilateral blast lung injury with peripheral pulmonary haemorrhage Minor laceration of abdominal aorta; kidney or liver rupture
5	Critical	Bilateral flail chest	Major aortic laceration Lung laceration with tension Pneumothorax Severe bilateral blast lung injury with air embolus Total destruction of kidney and its vascular system
6	Maximum		Aortic laceration with haemorrhage not confined to mediastinum Hepatic avulsion (total separation of all vascular attachments)

The Severity of Injury Index (SII) and the Adjusted Severity of Injury Index (ASII)

A severity scoring system that has been used extensively in BOP injury research is the Severity of Injury Index (SII). This pathology scoring system was initially developed by the Walter Reed Army Institute of Research in collaboration with the Lovelace Biomedical and Environmental Research Institute [Dodd *et al.*: 1990; Yelverton: 1996; Elsayed: 1997]. The SII was developed by exposing 265 sheep [Yelverton: 1996] to 0.114 kg to 1.361 kg of C4 explosive [Axelsson and Yelverton: 1996].

Axelsson and Yelverton [1996] modified the SII by not adjusting the scoring for a fatality, but rather focussing on the injuries themselves. They called the scorings system the Adjusted Severity of Injury Index (ASII) for the assessment of non-auditory blast injury (which did not include burn or ear injuries). The ASII is described below for the body regions considered in this study.

Lungs:

- negative for no injury,
- trace for scattered surface petechiation or minimal ecchymoses involving less than 10% of the organ, slight for areas of extensive petechiation to scattered parenchymal hepatization involving less than 30% of the lungs,
- moderate for areas of heamorrhage ranging from isolated parenchymal contusions to confluent hepatization involving less than 30% of the lungs, and
- extensive for isolated parenchymal contusions and confluent hepatised regions encompassing areas equal to or greater than 30% of the organ.

Pharynx/larynx and trachea:

- negative for no injury,
- trace for scattered petechiation to isolated spots of ecchymosis less than one layer deep covering less than 10% of the organ,
- slight for scattered petechiation to confluent contusions one to two layers deep involving less than 30% of the organ,
- moderate for lesions ranging from ecchymotic spots to confluent contusions two layers deep encompassing less than 60% of the available surface area, and

extensive for areas of confluent contusions two or more layers deep covering 60% or more of the organ, and

- extensive for when haemorrhage and edema reduced the lumen diameter of the organ, making it difficult to breathe. In subjects with extensive lung haemorrhage, confluent parenchymal hepatization with bleeding into the bronchi and trachea was present.

Gastrointestinal tract:

- negative for no injury,
- trace for minor contusions with intact mucosa with no more than two gut layers or two organs involved with the contusions distributed over an area of less than 10 cm²,
- slight for scattered contusions generally distributed over an area of 10-20 cm² with some mucosal ulcerations, moderate for multiple transmural contusions with mucosal ulcerations encompassing an area 21-30 cm², and
- extensive for areas of more than 30 cm² of transmural contusions with concomitant perforation of the gut wall.

Solid intraabdominal organ injuries:

- negative for no injury, trace for small subcapsular contusions or haematomas involving less than 10% of one or two organs,
- slight for subcapsular contusions or haematomas involving less than 30% of one or more organs with slight tears in the organ possible,
- moderate for deep tears in the liver and/or maceration of the spleen with up to 60% of the organ damaged, and
- extensive for deep tears in the liver, maceration of the spleen, or both with more than 60% of the organ traumatized.

The SSI was visited again recently by Carneal *et al.* [2012] where the main difference from the original SSI was the exclusion of surface, head, external/inner ears and burns as they found insufficient pathological information for those areas. The re-analysis of the original pathology scoring sheets showed that the system showed increasing injury

severity with increasing threat or BOP levels and that some organs were more sensitive to variations in BOP than others [Carneal *et al.* :2012].

The following points from Carneal *et al.* [2012] are of relevance to this study:

- The contribution of abdominal injuries to long-term survival outcomes may be under-predicted as they have a delayed manifestation, but the study only considered the injuries apparent at 1 hour after the blast (at which point the animals were sacrificed).
- The ribs were the least susceptible to injury onset which indicated that the initiation of soft-tissue injury is not adequately predicted by skeletal injuries for the blast environment.
- The lungs were most susceptible to BOP injury and showed most sensitivity to varying threat levels.
- The orientation of the targets with respect to the blast influence the injury outcomes with the side facing the incident blast wave receiving lower injury scores than the reflected blast wave.
- In terms of the actual scoring system, the injury “extent” scores were most insensitive to increasing threat level, while the “depth” and “grade” scores were the most sensitive (See Table 4 for details of the injury scoring system). However, Raghavendran *et al.* [2005] noted that there is often little direct correlation between the anatomic extent of contused lung and the degree of hypoxemia. This finding is worth noting, however, their test series involved blunt trauma rather than blast and the main cause of immediate death following BOP exposure is air embolism.

Table 4: Description of injury scoring system (after Carneal *et al.* [2012]).

Extent:	Extent of injury in terms of component parts to organ or system				
Left ribs	Left ribs				
Right ribs	Right ribs				
Upper respiratory	Larynx, pharynx, trachea				
Left lungs	Apical/cranial, cardiac/middle, caudal/diaphragmatic				
Right lungs	Apical/cranial, cardiac/middle, caudal/diaphragmatic, intermediate/accessory				
HAO	Rumen, reticulum,omasum, abomasum, duodenum, jejunum, ileum, caecum, large colon, spiralis, rectum, gallbladder				
SAO	Liver, spleen, pancreas, kidneys				
Grade	Surface area of lesion or percentage of organ traumatize, number of fractures for skeleton system				
ORGANS	1	2	3	4	5
Left ribs (number of fractures)	1	2	3	>4	
Right ribs (number of fractures)	1	2	3	>4	
Upper respiratory (percentage of organ)	<10	11-30	31-60	>60	
Left lungs (percentage of organ)	<10	11-30	31-60	>60	
Right lungs (percentage of organ)	<10	11-30	31-60	>60	
HAO (area of lesion)	0-1	2-10	11-20	21-30	>30
SAO (percentage of organ)	<10	11-30	31-60	>60	
Type	Classification of worst-case lesion to organ system				
ORGANS	1	2	3	4	5
Left ribs	Incomplete	Complete	Compound		
Right ribs	Incomplete	Complete	Compound		
Upper respiratory	1-5 petechiae	>6 petechiae	Ecchymosis	Confluent Contusions	
Left lungs	Petechiae	Ecchymosis or blebs	Isolated haemorrhages	Confluent haemorrhages	Puncture/rupture
Right lungs	Petechiae	Ecchymosis or blebs	Isolated haemorrhages	Confluent haemorrhages	Puncture/rupture
HAO	Serosa or mucosa	Two layers	Transmural		
SAO	Subcapsular contusion	Subcapsular hematoma			
Depth	Depth or degree of disruption of the worst-case lesion				
ORGANS	1	2	3	4	5
Left ribs	Closed	Open			
Right ribs	Closed	Open			
Upper respiratory	1 layer	2 layers	Transmural	Hematoma decreasing lumen	Puncture/rupture
Left lungs	Pleural/subpleural	Parenchymal	Scattered hepatization	Confluent hepatization	
Right lungs	Pleural/subpleural	Parenchymal	Scattered hepatization	Confluent hepatization	
HAO	Mucosa intact	Mucosal ulceration	Rupture/puncture		
SAO	Capsule intact	Superficial laceration	Deep laceration	Maceration of parenchyma	
Maximum Organ Injury Scores (Extent + Grade + Type) x Depth					
Organ	Extent	Grade	Type	Depth	Total Organ
Left ribs	12	4	3	2	38
Right ribs	12	4	3	2	38
Upper respiratory	3	4	4	5	55
Left lungs	3	4	5	4	48
Right lungs	4	4	5	4	52
HAO	12	5	3	3	60
SAO	4	4	2	4	40

2.7.4 Methods used to measure the severity of BOP injury

Lung weight to body weight ratio as a measure of severity of BOP injury

Another gross index of lung injury is the lung weight normalised to the body weight or the lung to body weight ratio, but this index is not uniformly accepted [Elsayed: 1997]. This measure is based on the premise that the weight of the lungs will increase as blood and edema fluid accumulates in the alveolar spaces when exposed to BOP (See Figure 14).

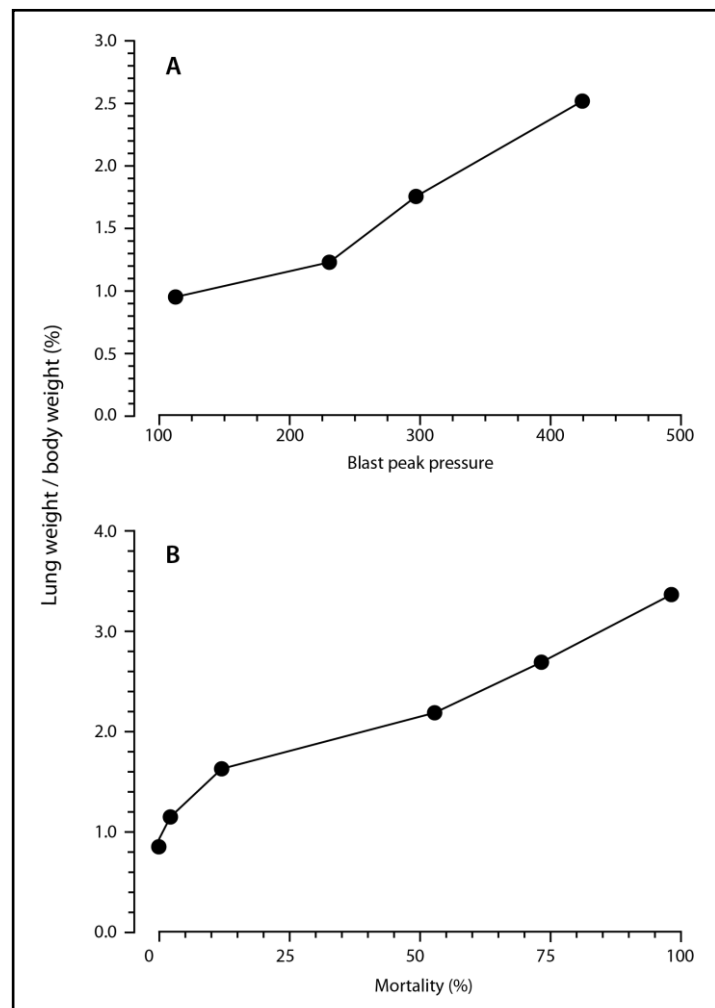


Figure 14: Graphs showing the relationship between the lung weight to body weight ratio and peak BOP in rats (A) and guinea pig mortality (B) (after Elsayed [1997]).

Stuhmiller [1995] states that the lung to body weight ratio is not sensitive to small pathologies under the circumstances where the animal is sacrificed shortly after exposure. The lung to body weight ratio was found to be a poor predictor of BOP

injury by others such as Junkui *et al.* [1996]. This may be due to small discrepancies in experimental protocol which lead to different outcomes regarding the efficacy of various methods of determining BOP injury.

Other measures for scoring the severity of BOP injuries

Behavioural, neuronal and biochemical measures are available to assess the severity of BOP injury, but these are beyond the scope of this study. For further information regarding these see Sharpnack *et al.* [1991], Elsayed [1997], van der Vord *et al.* [2012] for behavioural and neuronal indicators and Elsayed [1997], Elsayed and Gorbunov [2006] for biochemical indicators.

2.8 Injury Criteria

Injury criteria have been developed using animal, post mortem human surrogates (PMHS or cadavers) and mechanical and frangible surrogates that can relate measurements recorded during an explosive event to a risk of injury to the torso body region. Test standards rely on the torso surrogates that are available and the injury criteria that have been developed to determine the risk and severity of blast injury that could occur in a particular scenario. There is much debate surrounding many injury criteria that are used today and it is agreed, worldwide, that much research is still needed to revise these criteria. The scenarios for which these criteria are valid and the practicalities of using various torso surrogates in test standards are assessed.

The profile of a measured pressure resulting from an explosive event has been used to predict the risk and severity of BOP Injury. It is well known that the higher the peak pressure, the more severe the injuries caused by this pressure will be. It is also accepted that longer positive phase pressure durations result in more severe injuries than if the duration was shorter [Bowen *et al.*: 1968; Axelsson and Yelverton: 1996; Cooper: 1996; White: 1968; Bouamoul *et al.*: 2007]. Injury criteria developed for use in the automotive industry include the Force Criterion [Patrick *et al.*: 1965], the Acceleration Criterion [Mertz and Gadd: 1971], chest compression [Kroell *et al.*: 1971], the Thoracic Trauma Index (TTI) [Eppinger *et al.*: 1984], the Viscous Criterion [Viano and Lau: 1985] and the Combined Thoracic Index (CTI) [Kleinberger *et al.*: 1998]. The injury criteria that have been developed specifically for blast scenarios will be reviewed in this

section, as well as possibly applicable blunt trauma injury criteria originating in the automotive industry (namely the chest compression and VC). Although the applicability of blunt trauma injury criteria may be limited to certain scenarios, the predictions may be valid under certain conditions.

2.8.1 The Bowen/Bass injury criteria

The Bowen criterion [Bowen *et al.*: 1968] is used to predict lung injuries caused by explosive events in a free field environment (i.e. not in an enclosure or near objects which may cause complex reflected waves to interact with the subject). The criterion was derived from mortality studies conducted on 2097 animals of 13 different species performed at the Lovelace Foundation during the 1960s [Teland and van Doormaal: 2012]. Risk curves were produced to predict human injuries for various peak incident (side-on) overpressures and positive-phase durations of the blast wave [Yelverton: 1997]. The risk curves produced in Bowen *et al.* [1968] are shown in Figure 15.

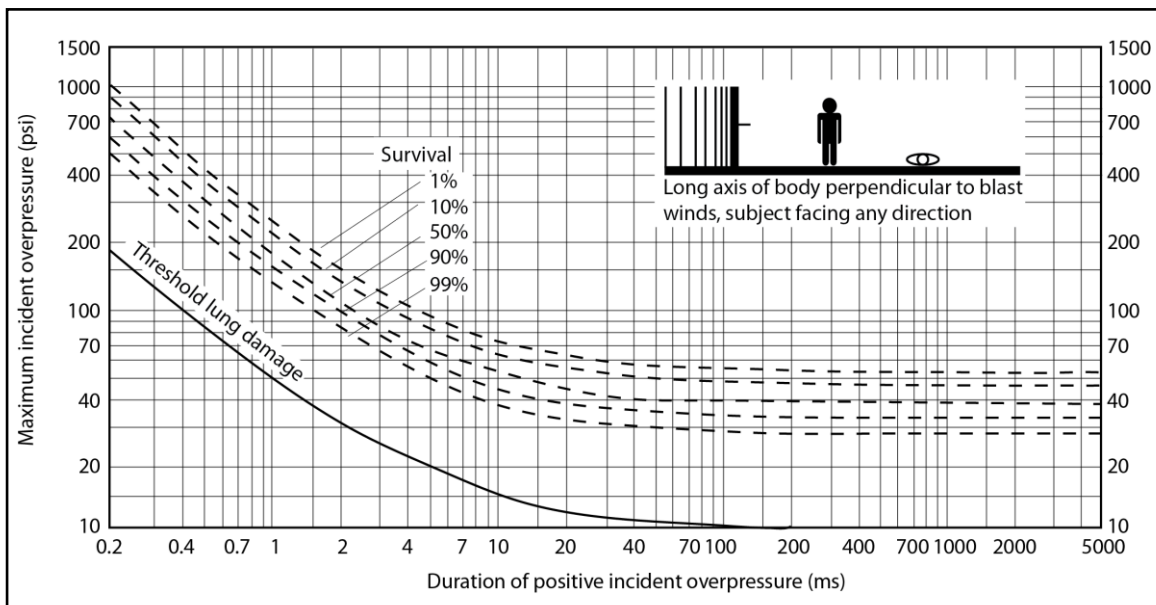


Figure 15: Survival curves predicted for a 70 kg man applicable to a free field situation where the long axis of the body is perpendicular to the blast winds (after Bowen *et al.* [1968]).

Limitations of the Bowen *et al.* [1968] curves are, that they are only strictly valid for the situation where a subject is standing against a wall unless certain assumptions are made [Teland and van Doormaal: 2012], they are not applicable to complex blast wave scenarios, for short blast wave durations, there is uncertainty in the data (as the

durations were obtained from now dated empirical data from Goodman [Goodman: 1960].

Revised lung injury risk curves for short-duration blasts were provided by Bass [Bass *et al.*: 2006a] by reanalysing existing blast literature, including the data used in the development of the Bowen curves and more recent test data. However, the Kingery-Bulmash or CONWEP empirical data (based on very large charges at a distance) was used and thus there is still uncertainty in the curves for short durations [Teland and van Doormaal: 2012].

Neither of these criteria are mandated by any currently available and internationally recognised test standards, but the original Bowen curves were used by test setups reported in the NATO PPE test standard [NATO-RTO-TR-HFM-089: 2004].

2.8.2 The Chest Wall Velocity Predictor (CWVP)

An alternative to the Bowen or Bass criteria is the CWVP [Axelsson and Yelverton: 1996] which takes into account the upper respiratory tract, gastrointestinal tract and solid intra-abdominal organs, in addition to the lungs which were also considered in [Bowen *et al.*: 1968]. This criterion was developed to take into account complex blast waves (as one might find if an explosive was to detonated in an enclosed space or near reflecting surfaces) and thus the reflected or face-on pressure measurement is required to calculate this criterion. It is also valid for free field scenarios.

The criterion was developed by exposing sheep to explosive events in various size enclosures. The sheep were then removed and BOP injuries noted. The tests were then repeated but the sheep were replaced with aluminium instrumented cylinders approximating the shize of a sheep. The cylinders or Blast Test Device (BTD) were instrumented with four pressure gauges to record the pressure waves from four different directions within the enclosure. A mathematical model of the thorax was then used to relate the pressure measurements to a risk of BOP injury using a single degree of freedom system in which chest wall response (displacement, velocity and acceleration) and intra-thoracic (lung) pressure can be calculated for different loading conditions (See Figure 16).

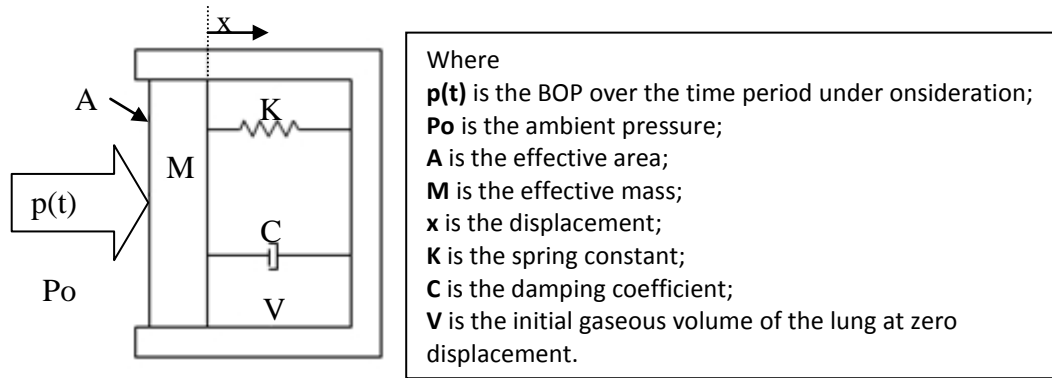


Figure 16: Single chamber, one lung model, as described in Axelsson and Yelverton [1996].

The equation for the model is the following:

$$M \cdot \frac{d^2x}{dt^2} + C \cdot \frac{dx}{dt} + K \cdot x = A \cdot [p(t) + P_0 - \left(\frac{V}{V - A \cdot x}\right)^\gamma \cdot P_0]$$

For a 70 kg mammal,

M, the effective mass, is set to 2.03 kg;

C, the damping coefficient, is set to 969 Ns/m;

K, the spring coefficient, is set to 989 N/m;

A, the effective area, is set to 0.082 m²;

V, the initial gaseous volume of the lung at zero displacement, is set to 0,00182 m³;

And γ , the polytropic exponent for gas in the lungs, is set to 1.2.

Thus, for a given input pressure, p(t), that can be measured experimentally and a recorded atmospheric or ambient pressure Po, the chest wall velocity (represented by $\frac{dx}{dt}$ in the above equation) can be calculated.

It is unclear if the CWVP is valid for positive-phase durations of less than 0.4 ms as the data set included only pressure profiles with positive-phase durations greater than 0.4 ms.

The CWVP is the only BOP specific criterion currently included in an international test standard. The CWVP is a mandated criterion in the NATO vehicle protection assessment against landmines and IED threats standard [AEP-55: 2006; NATO-RTO-TR-HFM-148: 2012].

2.8.3 Chest compression (C)

The chest compression (C) criterion arose from study by Kroell *et al.* [1971; 1974] that concluded that maximum thorax compression correlated well with the AIS injury severity score while force and acceleration did not.

Thus, defining compression C as the chest deformation divided by the thickness of the thorax, the following relationship was established:

$$AIS = -3.78 + 19.56 C.$$

Mertz *et al.* [1991] refined this criterion for use with the Hybrid III ATD to determine risk of injury due to seat belt loading in the automotive field. Thus measuring 92 mm thorax deflection for the 230 mm chest of the 50th percentile male gives a compression (C) of 40% and predicts AIS4 injuries. A 30% compression predicts to AIS2 injuries.

2.8.4 Viscous Criterion (VC)

The Viscous Criterion (VC) is also called the velocity of compression or soft tissue criterion as it takes into account that soft tissue injury is both compression and rate dependent [Schmitt *et al.*: 2004]. The VC was developed by [Viano and Lau: 1985] where tests were conducted on rabbits with impact velocities of 5 to 22 m/s and maximum thoracic compressions of 4 to 55%. The chest compression (C) was defined as the displacement of the chest in relationship to the spine, normalized by the initial thickness of the thorax. The VC is the maximum of the momentary product of the thorax deformation speed (V) and the thorax deformation (C).

The VC was further validated by [Viano and Lau: 1988] through the reanalysis of cadaver data which demonstrated that the maximum viscous response was highly correlated to the risk of severe soft tissue and internal organ injury. A guided mass impacted the cadavers at velocities of 5 to 15 m/s, resulting in chest compressions from 22 to 49%. The VC was found in various studies to predict injuries such as heart rupture [Kroel *et al.*: 1986], cardiac arrhythmia [Bir and Viano: 1999] and severe liver lacerations [Horsch *et al.*: 1985].

A tolerance level of a VCmax value of 1.00 m/s was established in [Lau and Viano: 1986] that correlated to a 25% probability of severe to fatal (AIS 4+) injury for frontal chest impacts (See Figure 17).

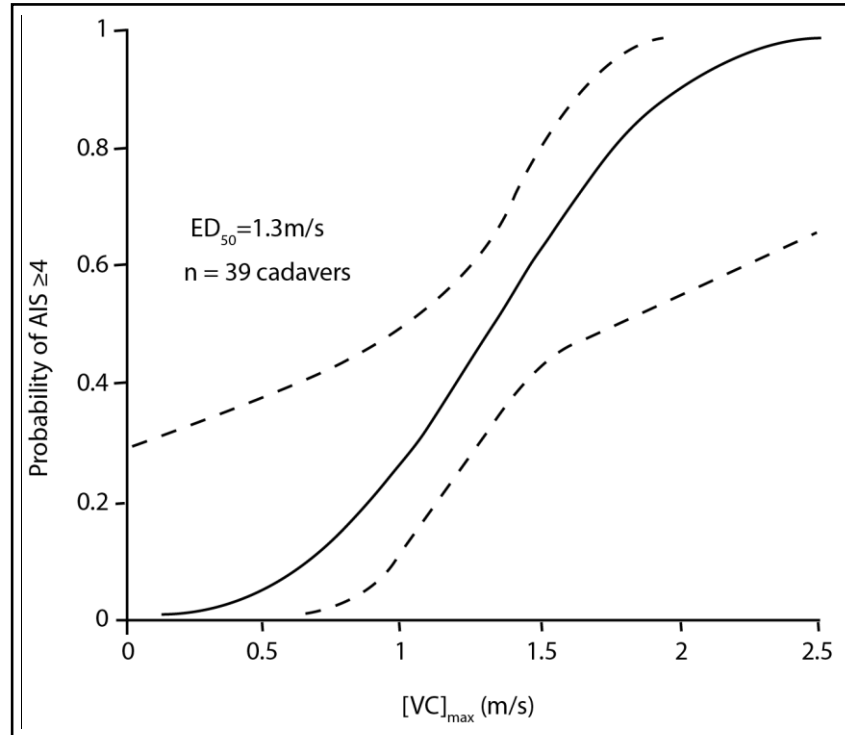


Figure 17: Risk curve for AIS 4+ chest injury based on the Viscous Criterion for blunt frontal impact (after Lau and Viano [1986]).

In order to identify an applicable injury criterion and threshold value, the mechanism of injury must be determined [Bir: 2000]. In the automotive industry, it has been determined that at impact velocities of less than 1 m/s, the injury is mainly due to a crush mechanism [Lau and Viano: 1986] where the Compression Criterion is best predictor of injury. When the impact velocity is between 3 and 30 m/s, the injury tolerance becomes rate sensitive and the VC has thus been proven to best predict these injuries [Lau and Viano: 1986; Horsh *et al.*: 1985]. When the velocity of deformation is above 30 m/s, the injuries are due to a blast mechanism [Jonsson *et al.*: 1979] and it was shown in [Bir: 2000] that the VC is able to predict these injuries (although the velocity component will dominate over the compression component).

Work conducted at Wayne State University on the determination of injury criteria for use with kinetic less-lethal technologies in blunt ballistic impacts used a 37 mm diameter baton under the following test conditions: 140 g mass at 20 m/s, 140 g mass at

40 m/s and 30 g mass at 60 m/s [Bir *et al.*: 2004]. The impacts to the thorax produced VC threshold values for probabilities of AIS 2-3 thoracic injuries. The sigmoidal curve is shown in Figure 18.

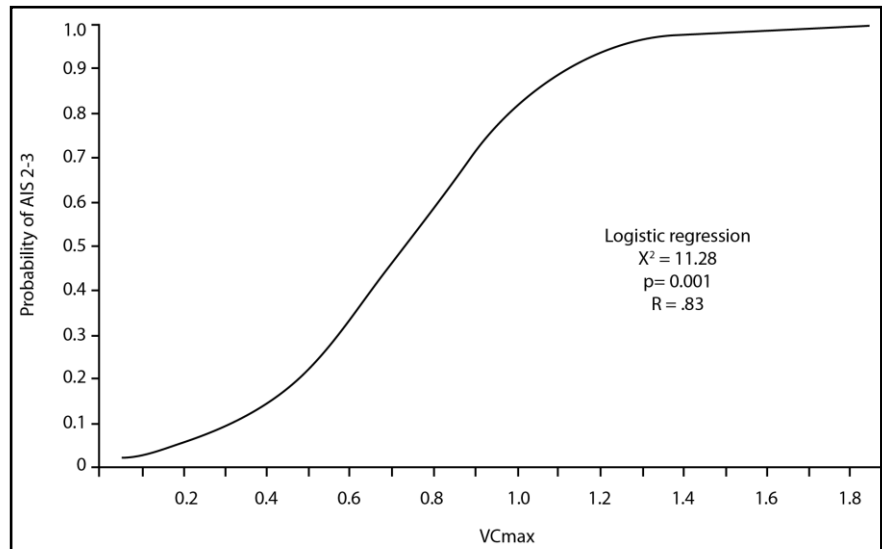


Figure 18: Probability of AIS 2 or 3 thoracic injury for blunt ballistic impacts versus the VCmax as determined by logistic regression analysis from experimental cadaver data (after Bir *et al.* [2004]).

A VCmax of 0.8 m/s or 0.6 m/s will result in a 50% or 25% chance respectively of sustaining a thoracic skeletal injury of AIS 2 or 3 [Bir *et al.*: 2004]. The required VCmax value for a 10% probability of an AIS 2+ injury to the thorax is approximately 0.3 m/s as determined from the data in [Bir *et al.*: 2004]. Although this value seems promising, it may be too conservative for the more distributed loading expected by seat belts and other systems in contact with large body areas of the occupant. The continuum of VC values determined to predict a 25% risk of varying levels of injury from the research fields of blunt ballistic trauma [Bir *et al.*: 2004], automotive [Lau and Viano: 1986] and lung injury was summarised in [Bir: 2000] (See Figure 19).

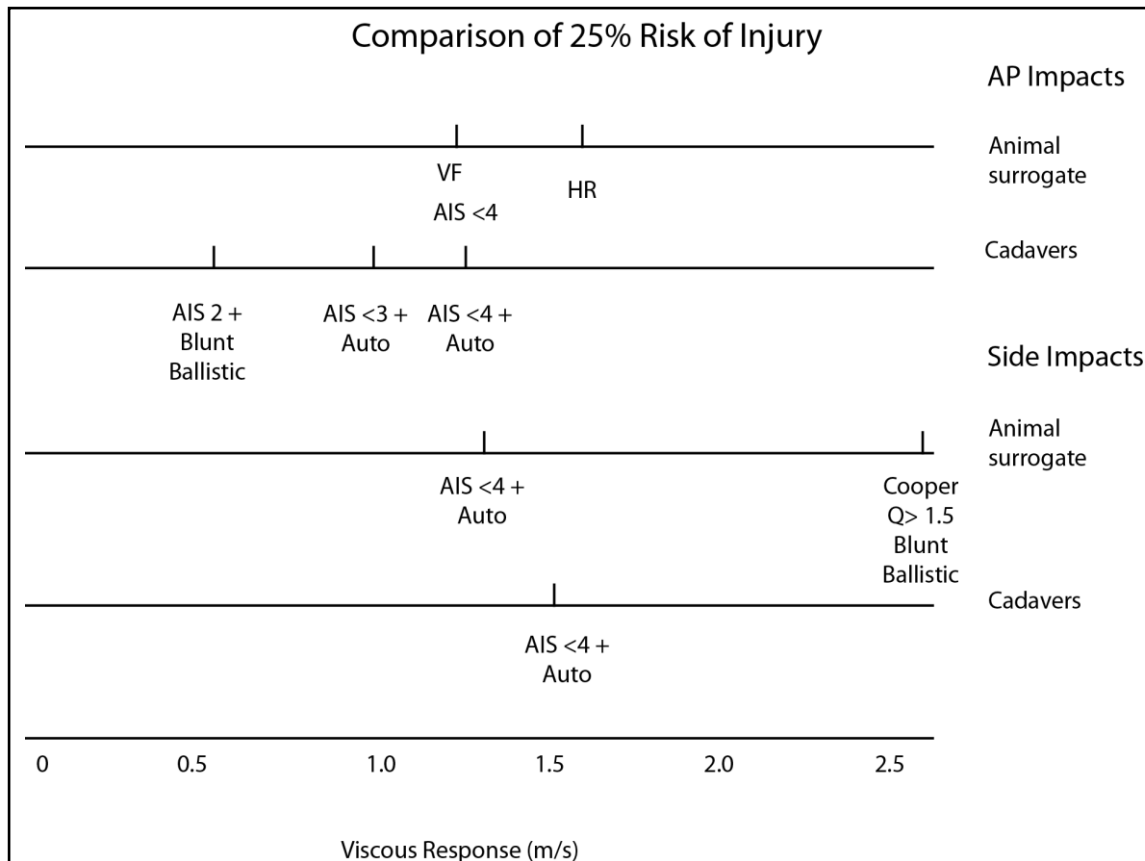


Figure 19: Continuum of VC values determined to predict a 25% risk of varying levels of injury in terms of frontal versus lateral and surrogate type (after Bir [2000]).

The VC values and corresponding injury levels appear to correlate across the various research fields and impact conditions. Injuries seen with blunt ballistic impacts occurred at higher compression velocities, but with less maximum compression than in the automotive area where the velocities were lower, but the compression was greater. However, it is not possible to determine exact VC values across the entire continuum consisting of various loading regimes without further research [Bir: 2000].

It was recommended by the NATO-RTO-TR-HFM-148 [2012] that the VC_{max} for AIS 4+ injury to the thorax (for frontal impact) [Lau and Viano: 1986] be applied as these values have been proven for blunt impacts in the automotive research area. A VC_{max} threshold of 0.7 m/s was thus chosen by the NATO-RTO-TR-HFM-148 [2012] as it reflects a 10% chance of an AIS 4+ injury to the thorax (See Figure 17).

2.9 Torso Surrogates

When humans are exposed to forces, accelerations or pressures they may sustain injuries. As humans obviously cannot be exposed to possibly harmful experiments, anthropomorphic test devices (ATDs) and other sensors are used in experiments to collect data which can then be related to possible injury levels. ATDs are mechanical models that represent the human body [Begeman and Prasad: 1990].

This section describes available mechanical torso surrogates that are used to investigate the effects of BOP on the torso body region. The mechanical torso surrogates that originate from the automotive environment will be referred to as ATDs, which represent the human body as a whole, whereas models used to represent just the torso section of the body will be referred to as torso surrogates. The ATDs represent the human body, but, unlike the human body, they are robust enough to withstand a high number of tests and loading that would cause damage to the human body [Schmitt *et al.*: 2004]. The results obtained using ATDs must be repeatable and reproducible to allow test results to be compared. There are many different ATDs that have been developed, mainly for use in automotive safety testing (See [Schmitt *et al.*: 2004; National Highway Traffic Safety Administration (NHTSA): no date]), but the Hybrid III 50th percentile ATD, representing the average adult male, is the most widely used dummy in frontal crash and automotive safety restraint testing.

This section first describes the torso surrogates used in this study, followed by alternative torso surrogates or ATDs. These ATDs have been used in blast scenarios constructed by researchers are mentioned to form a more complete picture of what is currently available (although they may not yet be prescribed in a recognised test standard which takes longer to be accepted internationally).

2.9.1 Torso surrogates and ATDs used in recognised test standards or in this study

The torso surrogates that were available at the Council for Scientific and Industrial Research (CSIR) during the experimental phase of this study were the South African Waterman, the Hybrid III 50th percentile male ATD [Backaitis and Mertz: 1994] and the South African (SA) Surrogate Leg. Data gathered from all three of these torso surrogates are presented in this dissertation.

South African (SA) Waterman

The SA Waterman is a torso surrogate that was used in South Africa in the past to provide a representative mass of a person in a landmine protected vehicle (LPV) and to give an indication of the impulse experienced by an occupant in an LPV during a landmine blast test.

It is a plastic container that resembles a human torso (See Figure 20) and is moulded to enable it to be strapped into a vehicle. The SA Waterman weights 72 kg when full of water. It was designed to burst at a vertical impulse of 600 kg.m/s which is half the lethal dose of 1200 kg.m/s that was determined by recreating the lethal impulse experienced by an occupant in a triple mine detonation incident that occurred in 1978 [Joynt: 2008]. The 1200 kg.m/s impulse that was used in the design is based on the fact that an occupant that was dead experienced this impulse, but, the half value of 600 kg.m/s (or even a lower value) could also have resulted in the death of the occupant as one cannot measure different levels of “dead”. Thus, it was determined in that the SA Waterman should not be used to validate the protection offered by LPVs, but only to simulate mass and to test seatbelts and seat structures. In this study the SA Waterman was used as a torso surrogate (of representative mass of a person) on which to mount transducers and various clothing and PPE related test items (See Chapter 6). Accelerometers and pressure transducers were mounted in a hard plastic plate (in a similar manner to how they are mounted when used with the ATDs in vehicle validation testing as prescribed by AEP-55 [2006]).



Figure 20: Photograph of a SA Waterman torso surrogate with a transducer package mounted on the chest area.

Hybrid III 50th percentile male ATD

The Hybrid III 50th percentile was originally developed by General Motors for vehicle safety purposes and over the years, improvements have been made to make it more human-like [NHTSA: no date]. This ATD represents the average male of a USA-population between the 1970s and the 1980s with a height of 1.72 m, an erect sitting height of 0.88 m and a weight of 78 kg. The weights of the Hybrid III upper and lower torso are 17.2 kg (37.9 lbs) and 23.0 kg (50.8 lbs) respectively [NHTSA: no date] (Total torso weight: 40.2 kg). The upper torso contains 6 high strength steel ribs with polymer based damping material to simulate human chest force-deflection characteristics and the standard instrumentation includes a thorax rotary potentiometer to measure the chest deflection (or sternum deflection). The lower torso contains an abdominal insert of urethane foam with a vinyl skin that can be removed to access the lumbar spine instrumentation. The standard abdominal insert does not contain instrumentation.

The great benefit of using the Hybrid III ATD is that the automotive industry has conducted a large amount of research into the measurements and related injury criteria and in particular how these can be used to predict a risk of injury to a certain body region. The Hybrid III ATDs have set maintenance and calibration procedures in place which ensure that results are reliable in the automotive crash testing environment.

However, as these ATDs were developed for use in the automotive environment for the evaluation of crush injuries rather than blast injuries which raises questions regarding the suitability of these ATDs (and the applicability of the measurements they provide) for use in blast tests [NATO-RTO-TR-HFM-089: 2004; AEP-55: 2006]. There have been modifications made in recent years to the Hybrid III ATD to increase the suitability for use inside AVs in the blast testing environment (e.g. MIL-Lx leg [McKay *et al.*: 2010; van der Horst *et al.*: 2010; NATO-RTO-TR-HFM-148: 2012]). These modifications focussed on the lower leg as lower tibia forces commonly exceed the injury threshold value during the validation testing of AVs [Whyte: 2007]. However, modifications to the torso region have not been included in recognised blast test standards. The NATO-RTO-TR-HFM-148 [2012] makes use of the Hybrid III chest potentiometer to measure the displacement of the sternum and a pressure measurement

device is strapped onto the outside of the clothed ATD to be used to predict BOP injuries (See Figure 21). It is recommended that a face-on pressure transducer be mounted in a thin hard plastic material that weight as little as possible to avoid inertia problems in the ATD response [AEP-55: 2006]. In some test protocols, ad hoc sensors such as accelerometers and pressure sensors have been mounted on and in the Hybrid III torso, but these protocols are not internationally recognised and the sensors were mainly used for research purposes.

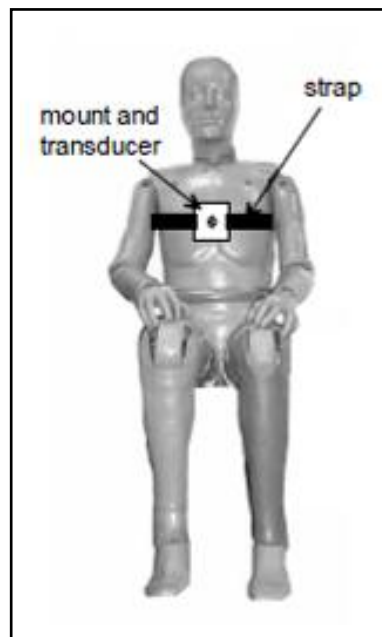


Figure 21: Hybrid III ATD with chest strap for pressure transducer plate (after AEP-55 [2006]).

Looking at the disadvantages of the Hybrid III ATD, it is an expensive measurement device which may be easily damaged in a harsh blast testing environment. The sensors must be recalibrated at a certified laboratory if the threshold values are exceeded. This could mean sending the ATD away for weeks at a time, which would mean it is unavailable for other tests. However, Chinchester *et al.* [2001] found the Hybrid III ATD to be a robust and repeatable during a large AP mine test series as no significant mechanical failures occurred.

SA Surrogate Leg

The SA Surrogate Leg (See Figure 22) was developed for use in the testing of LPVs. It provides a representative mass of a person to occupy seats in a vehicle (as did the SA Waterman), but it also includes an instrumented leg to measure tibia forces during

vehicle validation tests. For the purpose of this thesis, pressure transducer plates (similar to those used on the Hybrid III ATDs) were mounted on the chest position of the SA Surrogate Leg to provide additional face-on pressure measurements during vehicle validation tests.



Figure 22: Photograph of the SA Surrogate Leg prior to testing in a vehicle validation test.

2.9.2 Other torso surrogates and ATDs

In the vehicle validation testing scenario (Scenario A in this thesis), where a person is inside an AV that is subjected to an AT mine or IED, the Hybrid III 50th percentile male ATD and the EuroSID-2re ATD are required by the NATO test standards [AEP-55: 2006; NATO-RTO-TR-HFM-148: 2012].

The original blast test device (BTD), as described by Axelsson and Yelverton [1996], is recommended in AEP-55 vol. 2 (Edition 1) [2006] to determine risk of BOP injuries if an appropriate ATD is not available on which to mount a pressure measurement device. The BTD was used in the development of the chest wall velocity predictor (CWVP) which is the injury criterion used to determine possible BOP injuries and vehicle hull integrity in AEP-55 vol. 2 (Edition 1) and NATO-RTO-TR-HFM-148 [2012]. The BTD was not used in this study as ATDs were available for the vehicle testing scenario that was considered, but a diagram of the device is shown below as it is relevant to the CWVP injury criterion which is used throughout this thesis. The BTD consists of a

cylinder that represents the human torso, on which four pressure transducers can be mounted (See Figure 23). The AEP-55 vol.2 specifies at least one pressure transducer mounted in the same frontal position (in the same manner as with an ATD).

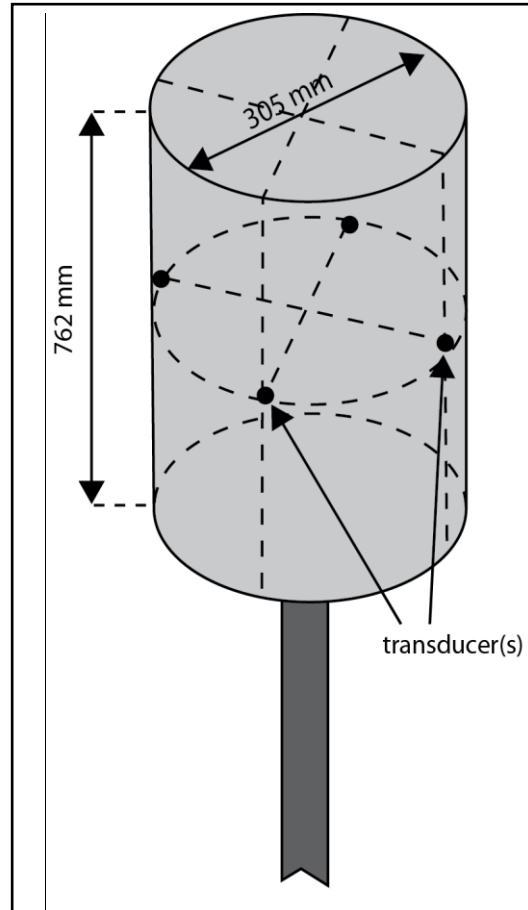


Figure 23: Example of a BTD cylinder to record pressure measurements (after AEP-55 [2006]).

In the demining scenario (Scenario D in this thesis), where a person is directly exposed to an explosive event, the NATO standard for testing PPE against anti-personnel (AP) mine blast recommends the use of a Hybrid II or a Hybrid III ATD [NATO-RTO-TR-HFM-089: 2004].

Other ATDs used in blast tests include:

- The thoracic rig developed by the Chemical and Biological Defence Establishment, Porton Down, UK [Cooper *et al.*: 1996].

- The Mannequin for the Assessment of Blast Incapacitation and Lethality (MABIL) developed by Defence R&D Canada, Valcartier [Anctil *et al.*: 2004; Oullet and Williams: 2008; Bouamoul *et al.*: 2007].
- The plate “chest simulator” developed by Med-Eng Systems Inc. was used to evaluate stackings of armour materials or lamination samples in Nerenberg *et al.* [2000].

2.10 Test Standards to Assess Blast Protection in Various Scenarios

Test standards are used to evaluate the level of protection provided against blast threats in various scenarios in which blast injuries typically occur. Protection against blast effects in the form of structures (such as walls or buildings), vehicles (such as armoured vehicles) and PPE (such as demining body armour or bomb suits) have been developed. One of the main challenges in developing a protocol is to balance the need to reproduce threat scenarios, that represent actual scenarios encountered in the field, with the need for a controlled, repeatable, practical method whereby the results from different test authorities can be compared to one another. In order for the technical and scientific data produced by a standard or test protocol to be internationally accepted, the results obtained by one test authority should be able to be reproduced by another test authority [Ceh *et al.*: 2005].

Most test standards focus on assessing the ballistic performance offered by protection solutions [NIJ: 2008; NIJ: 2012; NATO RTO TR-HFM-089: 2004; International Mine Action Standards (IMAS): 2009]. However, these solutions that may protect against penetrating injuries may in fact increase the risk and severity of BOP injuries (For example, if an explosive charge detonates within a structure designed to prevent fragments from entering, for example in a trench, dugout or wall, the reflections could result in more severe BOP injuries; or certain materials used in PPE may couple the blast wave into the body tissues resulting in increased severity of BOP injury to the lungs and gastrointestinal tract). Whilst it is acknowledged that it is essential to protect against fragment or ballistic threats, BOP may cause serious injuries even in the absence of any secondary or tertiary injuries. Test standards are only as good as the accuracy with which they are able to evaluate a wide range of conventional and novel protection concepts.

Contradictions were found in a number of currently available, and internationally accepted, test standards [NIJ: 2012; NATO-RTO-TR-HFM-089: 2004; IMAS: 2009; AEP55: 2006] regarding the methodologies to be used, the measurements to be taken and the injury criteria to be used to evaluate the protection capabilities against the BOP effects of a blast. Some even questioned the relevance of testing protection against BOP effects in the first place [NIJ: 2012; NATO-RTO-TR-HFM-089: 2004; IMAS: 2009]. When the standards do include specifications to test for BOP injuries, different methods and different injury criteria are used, depending on the environment in which they are applied and the preferences of the test authority involved. This becomes problematic when selecting the most appropriate manner of evaluating the level of protection offered against BOP injuries across the different application areas.

In this section, internationally recognised test standards for selected blast scenarios are reviewed. The parameters that have been selected by different internationally accepted standards and the motivation for the choices are discussed in this section. For each threat scenario that has been defined, the specifications outlined in available test standards are described. This includes the threat and setup scenario specification (based on the typical threat scenario for which the protection concept has been developed), the measurements required (including the instrumentation required in the ATDs) and the method used to determine the risk and severity of possible injuries to the torso body region. The risk and severity of possible injuries that may be sustained is determined using injury criteria and injury threshold values. Whilst these are required for many other body regions, the torso body region is the focus of this study and thus, only these measurements and injury criteria will be discussed in detail.

The internationally recognised blast test standards for all scenarios are compared in the final section of this literature review.

2.10.1 Scenario A: Vehicle validation testing against IEDs and landmines (threat outside vehicle)

Landmine Protected Vehicles (LPVs) or Armoured Vehicles (AVs) incorporate protection mechanisms aimed at minimising the risk of severe injury to occupants should the vehicle be involved in a landmine or IED incident. Much work has gone into testing and improving the protection capability of these vehicles.

Prior to being deployed in the field, AVs are tested to determine the level of threat against which they are likely to protect occupants. South Africa has a rich history in the development of LPVs [Stiff: 1986] and a military standard was developed for the validation testing of these vehicles against AT landmines. The internationally recognised standard is the NATO STANAG 4569 standard [AEP-55: 2006; van der Horst *et al.*: 2006]. The injury assessment criteria and tolerance levels were based on the efforts of the NATO HFM-090/TG25 between 2001 and 2004. A follow up to this group was the NATO HFM-148/Research Task Group (RTG) which was requested by the STANAG 4569 to select procedures and injury criteria which would be relevant for the blast IED threat, as well as the landmine threat [van der Horst *et al.*: 2010; NATO-RTO-TR-HFM-148: 2012]. The group met regularly between 2006 and 2009. The author was fortunate enough to be a member of this RTG and was responsible for reviewing injury criteria for the thoracic and abdominal body regions. The AEP-55 vol.2 (Edition 2) was published in 2011 and a summary of the outcomes of the NATO-RTO-TR-HFM-148 [2012] was presented in van der Horst *et al.* [2010]. The research and discussions from this group participation greatly helped to shape the author's views in the testing of AVs and specifically of the significance of BOP injuries in the scenario of vehicle validation testing.

NATO Standardisation Agreement (STANAG) 4569 Allied Engineering Publication (AEP) – 55 Volume 2 (Edition 1 and Edition 2), Procedures for evaluating the protection level of logistic and light armoured vehicles – mine and IED threat

The NATO Standardization Agreement (STANAG) 4569 covers the standards for the “Protection Levels for Occupants of Logistic and Light Armoured Vehicles.” The NATO STANAG 4569 Allied Engineering Publication (AEP) – 55 Volume 2 (Edition 1) [AEP-55: 2006] covers the “Procedures for Evaluating the Protection Level of Logistic and Light Armoured Vehicles – Mine Threat.” The NATO-RTO-TR-HFM-148 was published in 2012 to cover the threat to vehicles from IEDs.

Threat and test scenario description:

The AEP-55 vol. 2 (Edition 1) [2006] describes the threat definitions, test conditions and crew casualty or injury criteria of vehicle occupants to be used when determining the protection level of vehicles subjected to a grenade or blast mine threats.

Measurements Methods and Torso Surrogates:

In the vehicle validation testing scenario (Scenario A in this thesis), where a person is inside an AV that is subjected to an AT mine or IED, the Hybrid III 50th percentile male ATD and the EuroSID-2re ATD are required by the NATO test standards [AEP-55: 2006; NATO-RTO-TR-HFM-148: 2012].

The original blast test device (BTD), as described by Axelsson and Yelverton [1996], is recommended in AEP-55, vol. 2 (Edition 1) [2006] to determine risk of BOP injuries if an appropriate ATD is not available on which to mount a pressure measurement device.

Injury Criteria and Injury Risk Assessment for the Torso Body Region:

To assess the risk of blunt trauma injury to the thorax, the Thoracic Compression Criterion (TCCfrontal) and the Viscous Criterion (VCfrontal) were applied based on the sternal displacement measured by the H3 ATD and the Rib Deflection Criterion (RDClateral) and the Viscous Criterion (VClateral) were applied based on the upper/middle/lower rib deflections of the ES-2re. In terms of the abdominal injury risk, the Hybrid III ATD does not contain measurement transducers in this region, but the Abdominal Peak Force (Ftotal) is applied to the front/middle/rear abdominal force measurements recorded by the ES-2re [NATO-RTO-TR-HFM-148: 2012].

Both the AEP-55 vol. 2 (Edition 1) and NATO-RTO-TR-HFM-148 [2012] require at least two pressure measurements (sampled at 200 kHz or higher). These measurements are then used to calculate the chest wall velocity predictor (CWVP) [Axelsson and Yelverton: 1996], which indicates the level of possible BOP injury to vehicle occupants.

2.10.2 Scenario B: Explosive charge within a vehicle or enclosed space

This scenario is not directly covered by test standards. Generally, test standards specify that the vehicle must ensure that it is not penetrated or otherwise compromised by an external threat. If the threat is inside the vehicle, BOP injuries would be enhanced due to reflections.

2.10.3 Scenario C: Close proximity to a hand grenade in open space

Standards for this threat do not evaluate BOP injuries but rather focus on ballistic or fragmentation effects.

IMAS 10.30 [2009] states that “the fragmentation danger from most fragmentation mines and unexploded sub-munitions cannot be protected against with lightweight and practical PPE. This emphasises the need to minimise risk through the use of inherently safe procedures. Although the level of protection may not be sufficient, PPE provided to reduce the risk from fragmentation mines shall be at least that used as protection against blast hazards described.”

2.10.4 Scenario D: Demining scenario

Test standards or safety standards are available for a number of different application areas within this general scenario where a person may be directly exposed to BOP from blast munitions. These include:

- Standards used to evaluate protection offered by demining PPE against AP mines (e.g. in humanitarian demining operations),
- Standards for evaluating protection offered by bomb suit worn by EOD operators,
- Health and safety standards specifying safe distances from explosive charges where explosive tests are conducted or explosive devices are stored (these usually focus on hearing protection as life-threatening incidents are less common than hearing damage in the work place).

Whilst health and safety standards play an important role in preventing possible BOP injuries in controlled environments (such as on blast ranges or demolition sites), it is not always possible to prevent blast incidents from occurring in operational environments.

Where the risk of injury due to direct contact with blast munitions is high, bomb suits (for EOD operators) and PPE (for humanitarian demining or military personnel) are the main protection concepts available. The IMAS 10.30 [2009] states that, “PPE should be regarded as a “last resort” to protect against the effects of mine and ERW hazards. It should be the final protective measure after all planning, training and procedural efforts to reduce risk have been taken.”

In the EOD/IED scenario the main internationally recognised test and evaluation standard for bomb suits is the *Public Safety Bomb Suit Standard National Institute of Justice (NIJ) Standard-0117.00* [NIJ: 2012]. In the demining scenario the internationally recognised standards are the *North Atlantic Treaty Organisation (NATO)* [NATO-RTO-TR-HFM-089: 2006] and the *International Mine Action Standards (IMAS) 10.3* [2009].

National Institute of Justice (NIJ) Public Safety Bomb Suit Standard (NIJ Standard - 0117.00) [NIJ: 2012]

The National Institute of Justice (NIJ) Standards and Testing Program (which falls under the U.S. Department of Justice) develop and publish equipment standards that specifically address the needs of law enforcement, corrections and other criminal justice agencies. According to their website, the NIJ standards aim to be voluntary but influential as they articulate best practice and enable testing in a valid and consistently replicable manner.

Public Safety Bomb Suit Standard (NIJ Standard – 0117.00) and Public Safety Bomb Suit Certification Program Requirements (NIJ CR-0117.00) [NIJ: 2012] is a voluntary performance standard for bomb suits for use by certified public safety bomb technicians while performing render-safe procedures and disposal activities. It was developed by a panel of practitioners, technical experts and others with experience in standards development and conformity assessment.

Of the standards described above, it is the Public Safety Bomb Suit Standard (NIJ Standard -0117.00) that is most relevant (as the ballistic protection is not a focus of this study) and thus this standard will be discussed further.

The NIJ Draft Bomb Suit Standard for Law Enforcement (NIJ Standard – 0117.00) [2008] was developed to evaluate the protection offered by bomb suits against IEDs (and the foreword stated that this version only applied to bomb suits providing protection against IEDs. This standard did not include the evaluation blast overpressure injury protection, however in an NIJ TechBEAT report in 2009 [NIJ TechBeat: 2009] it was stated that blast overpressure will be fully addressed in future versions of the standard when the relevant research has been provided to the NIJ. A further NIJ fact sheet published in June 2010 [NIJ Fact Sheet: 2010] announced release of the NIJ Bomb Suit Standard for Public Safety, which is reported to define the minimum requirements for blast overpressure protection by the performance of a bomb suit integrity test [NIJ TechBeat: 2009]. Subsequently, the final *Public Safety Bomb Suit Standard NIJ Standard-0117.00* [NIJ: 2012] was released and states that,

“This standard addresses blast overpressure only in terms of bomb suit integrity; i.e., only in terms of the bomb suit’s remaining intact when subjected to an explosion. At present, research and data related to the effects of blast overpressure are limited. The following aspects of blast overpressure will not be addressed until the necessary research is complete: blast head trauma, blast thoracic injury, blunt thoracic injury, blunt lower neck trauma, other neck injury, and blast ear injury. NIJ anticipates publishing addenda or revisions to this standard when the necessary data are available and applicable requirements and test methods are defined.”

The assumption that the bomb suit’s remaining intact will offer protection against BOP injury will be explored in this study.

Procedure for testing:

Hybrid III 50th percentile male, positioning fixture for kneeling posture, 2 free field side-on blast overpressure gauges at 1.52 m from charge and ht of 0.77 m to record BOP values for reference data only. Data was sampled at a frequency of 500 kHz, one C4 plastic explosive, cylindrical cardboard tube length to diameter ratio of one to one. The exterior of the bomb suit is 0.6 m from the test charge (however, the reference point on the bomb suit is not specified. The charge is at 0.77 m from its horizontal centre to the ground. One bomb suit and one charge are used in testing.

Injury Criteria and Injury Risk Assessment for the Torso Body Region:

Integrity test – all protective elements must remain secured on the surrogate, protective elements covering the thorax/abdomen and pelvis shall remain attached to the bomb suit in the donned position. These protective elements shall maintain shape integrity and show no evidence of collapse. Cosmetic damage is permissible as long as such damage does not compromise the integrity of the protective layers within the bomb suit. Rips or holes are permissible as long as they do not perforate the innermost fabric ballistic protection layer. No gaps that expose the surface of the test surrogate are allowed.

Spine protection – in this case the bomb suit component designed to mitigate severity from direct impacts between the spine (thoracolumbar region) and solid objects - makes use of Canadian Standards Association CSA/CAN Z617-06 personal protective equipment (PPE) for Blunt Trauma. 2006. Mississauga, Ontario.

Fragmentation requirements v50 (also mobility requirements, ergonomics, optics, flammability, electrostatic discharge, head protection (impact in accordance with FMVSS no. 218), drag rescue, label durability and optional foot protection slip resistance).

Body armor - ballistic resistance, NIJ Standard-0101.06 [2008]

Body armor - ballistic resistance, NIJ Standard-0101.06 [2008] (Supersedes the 2005 interim requirements and the NIJ standard 0101.04 [2000] and a measurement and fitting guide is underway by American Society for Testing and Materials (ASTM International) is used to determine the ballistic resistance of personal body armour.

North Atlantic Treaty Organisation (NATO) Test Methodologies for PPE Against Anti-Personnel (AP) Mine Blast [NATO-RTO-TR-HFM-089: 2006]

As in the case of the EOD/bomb suits application area, the focus of test standards in the demining application area is also on the ballistic performance of the PPE. In 2001, the North Atlantic Treaty Organisation (NATO) Research and Technology Organisation (RTO) established a Task Group (TG)-024 to review how various countries test PPE against AP mines and to define common test conditions, methodology and surrogates [NATO-RTO-TR-HFM-089: 2006]. The current NATO standard, “Test Methodologies

for PPE Against Anti-Personnel (AP) Mine Blast (RTO-TR-HFM-089),” was published in 2006.

The NATO-RTO-TR-HFM-089 focuses on footwear and upper body PPE against AP mines and test conditions were described for three main scenarios, namely, “fragmentation mine tests”, “blast mine tests against footwear” and “blast mine test against the upper body”. The protocol relevant to this study is the “blast mine test against the upper body,” which specified the use of a Hybrid III ATD, with head, neck and chest instrumentation as a minimum; Mine surrogate consisting of C4 or PE4 explosive packed in cylindrical containers with prescribed detonation point; specified soil conditions and a test rig to position the ATD relative to the charge and blast cone.

The current NATO standard (NATO-RTO-TR-HFM-089 [2006]) does not mandate the evaluation of possible BOP injuries. It was stated in NATO-RTO-TR-HFM-089 [2006] that, “The loads generated by an AP mine, for the body positions considered, were well below the threshold required for blast lung injury,” however, “Ear pressure was found to often exceed the acceptable threshold for eardrum rupture...current helmet designs can increase the overpressure at the ear level...presence of a visor was found to lessen these effects significantly.”

Procedure for testing:

Component testing can be an efficient way to test specific PPE items, but it is important that the threat is realistically modelled, the PPE is mounted as it would be on a person and that the surrogate (with the protection) be located and oriented appropriately relative to the blast cone.

The recommended explosive threat is 100 g to 200 g C4 or PE4, short cylinder (35% height to diameter ratio), plastic casing with 2 mm max thickness, 20 mm overburden depth of burial.

Data should be samples at a rate of 200 kHz or more so that the data can be filtered with a 40 kHz low-pass filter during post-processing. The duration of sampling should be 100 ms or more.

The standard uses a Hybrid III ATD surrogate positioned using a test rig to minimise handling difficulties and allow the ATD to be placed in a kneeling position. The minimum required instrumentation includes head acceleration, neck forces and moments and acceleration of the chest centre of gravity. Recommended measurements include free-field side-on overpressure be measured to monitor the repeatability and quality of the explosive charges.

Injury Criteria and Injury Risk Assessment for the Torso Body Region:

No injury criteria were specified specifically for the torso body region (only head, neck and whole body acceleration (derived from the chest centre of gravity acceleration measurement) injury criteria were required).

However, each participant of the HFM-089/TG-024 that contributed to the development of this standard provided test setup examples for various trials that they had performed. The ATDs, measurements and injury criteria that were used by these contributors are described below.

MREL and DRDC Suffield: Recorded pressure at chest location, side of head, early tests used Hybrid II ATD and later made use of a Hybrid III ATD.

DRDC Suffield, Canada: Used a Hybrid III ATD and measured pressure at sides of head, free field side-on.

TNO, Netherlands: Measured Hybrid III ATD chest displacement and pressure using gauges located near the ATD

Aberdeen test centre, USA: Measured Hybrid III ATD chest displacement, chest pressure and side of head pressure (kneeling with nose 65 cm from mine and prone with nose 45 cm from mine)

WTD 91, Meppen Germany: Tested an EOD suit with Hybrid III ATD instrumented with two pressure gauges at the chest (inside suit) and two pressure gauges at the chest (outside suit). A 5 kg TNT was positioned at 1m above ground with the ATD at distances of 1 m, 3 m and 5 m from the charge. Torso injuries were predicted using Bowen and whole body acceleration.

DSTL Porton down: Used a thoracic rig (1999) with concept decoupler which measured the chest wall acceleration and used 100 g of PE4 charge to test with.

Selected test setups suggested the use of the Bowen *et al.* [1968] risk curves. However, these curves do not take into account the complex wave environment existing behind body armour or the ability of certain armour materials to enhance or reduce the coupling of the stress wave into the thorax and abdomen.

International Mine Action Standards (IMAS) 10.3 [2009] describes specifications for PPE to protect against unexploded ordnance (UXO) and AP landmines. And the CEN workshop agreement (CWA 15756) (provisionally withdrawn) [2007]

The International Mine Action Standards (IMAS) 10.3 [2009] describes specifications for PPE to protect against unexploded ordnance (UXO) and AP landmines. It was originally developed by a United Nations (UN) working group and the first edition was issued by the UN Mine Action Service (UNMAS) in March 1997. The standard was last updated in April 2009 with the assistance of the Geneva International Centre for Humanitarian Demining (GICHD). It is stated that the minimum requirement for demining PPE is that it, “Shall be capable of protecting the parts of the body that are covered against the blast effects of 240 g of TNT at distances appropriate to the wearer’s activity.” The minimum requirements for protection of the torso body region are:

- Protection against fragments as outlined in STANAG 2920 [NATO STANAG 2920: 2003] for V50 rating (dry) of 450 m/s for 1.102g fragments.
- Protection of the chest, abdomen and groin area against blast effects of 240 g of TNT at 0.6 m from the closest part of the body.

Eye protection, blast resistant footwear and hearing protection is also mentioned.

The IMAS 10.3 [2009] referred to The European Committee for Standardisation (CEN) Workshop Agreement [2007] for guidance on the test and evaluation of PPE. The CEN is the European standards body that operates parallel to the International Organisation for Standardisation (ISO) [Wilkinson: 2003]. In the field of Humanitarian Mine Action, the CEN collaborates with the United Nation Mine Action Standards (UNMAS), the

Geneva International Centre for Humanitarian Demining (GICHD), the EC Joint Research Centre of ISPRRA and the International Test and Evaluation Program for Humanitarian Demining (ITEP). The CEN Workshop Agreement [2007] agreement was provisionally withdrawn by the CEN as “The measurement of the quantity of explosive, necessary to carry out the tests, is inaccurate. Pending the recalculation of this parameter, a revised CEN Workshop Agreement in which the incriminated clause will be removed will be soon posted on this web page. New tests will have to be carried out before a complete CEN Workshop Agreement can be finalized and published.” However, at the time of submitting this thesis, the document had not been updated and the CEN Workshop Agreement [2007], or any later or previous version, was not available online. As this standard provided guidelines focussing on the testing of PPE for mine action against AP blast mines, it was considered to be worth discussing.

Procedure for testing:

Aim of PPE to be tested is to minimise the risk of fatal and critical (life-threatening) injuries and injuries affecting the vision.

Based on “effectiveness of PPE for use in demining AP landmines” – Chinchester *et al.* [2001] UXO conference, the CEN Workshop Agreement [2006] stated that “blunt trauma on the torso has been demonstrated not to be critical with a chest-mine distance of 60 cm. This appears to be reinforced with the data from the DDAS.”

Or again, “the blunt trauma from a blast has not been demonstrated to be a significant contributing (life threatening) factor, for the conditions tested, to deminer injuries, as presented in “A methodology for evaluating demining PPE for AP landmines. A number of simplifications have, therefore, been made to ensure more effective application for the mine action environment. The threat increases with proximity to the charge and the assumption is made that a reasonable distance is maintained between the deminer and the hazard.”

In terms of fragment protection it is stated that, “All regions to be protected should have ballistic protection that will withstand secondary fragments from exploding AP blast mines (For the purposes of this document and related testing, secondary fragments are

fragments that are picked up and ejected from the seat of the explosion including remains from parts of AP blast mines).”

A Hybrid III ATD is positioned as if it were a kneeling operator, with the tip of the nose 550 ± 10 mm from the simulated mine at an angle of 70 ± 2 degrees from horizontal to top centre.

The hazard level was set on a PMN mine surrogate with an explosive content of 240 g TNT (where the TNT is cast into a container of urethane plastic or equivalent, with minimum 70 Shore D hardness and with an outer diameter of 110 ± 2 mm and a thickness of 2 ± 0.5 mm), buried with an overburden of 20 ± 2 mm of sand.

The blast test involves applying a witness sheet of woven cotton fibre and cling film to the ATD to be worn beneath the PPE.

The blast test is carried out twice, if either test is a failure, the test undertaken once more, if this is a failure, the PPE ensemble has failed the test. Failure is defined as any penetration in facial or neck area with no margin of error and the torso region with 25 mm margin of error from the marked edge of the torso.

Other test standards that are not internationally recognised

Other non-internationally recognised test protocols include those developed by Bass *et al.* [2006a] for testing EOD suits and Chichester *et al.* [2001] for assessing demining PPE.

2.11 Summary and Study Aims

A review of the literature highlighted contradictions in BOP injury predictions and test standards used to evaluate protection against BOP injuries. This leads to the reason for this study which will be summarised in this section, followed by the thesis statement and designation of the study aims.

2.11.1 Summary

The rapid release of energy due to an explosion results in an almost instantaneous rise in pressure. This pressure wave moves outwards from the explosion which may cause BOP injuries to nearby persons. The incidence of BOP injury is greater in confined

spaces near reflecting surfaces which makes blast weapons particularly dangerous in built up areas. In addition, there are reports of new weapons systems that focus on enhanced blast technology which makes specific use of BOP effects [Wildegger-Gasissmaier: 2003].

BOP was defined as the pressure profile measured at the point where BOP injuries are to be calculated. BOP injuries are calculated using side-on or face-on pressure measurements, depending on the sensors that are used and their orientation to the blast wave.

The scenario in which the explosive event occurs will influence the risk and severity of BOP injuries. The explosive threats considered in this study were reviewed along with the relevant test standards where available.

The incidence of BOP injury is greater in confined spaces near reflecting surfaces which makes blast weapons particularly dangerous in built up areas. In addition, there are reports of new weapons systems that focus on enhanced blast technology which makes specific use of BOP effects [Wildegger-Gasissmaier: 2003]. The prevalence of blast injuries in general and in the various scenarios considered in this study was ascertained to allow the reality of problem of BOP injuries to be understood. Kirkman *et al.* [2011] suggest that the occurrence of BOP injuries may be underestimated in current military casualties as blast lung injuries are often excluded when they co-exist with other injury types (such as fragment injuries to the torso or broken ribs).

Another limitation in the assessment of BOP injuries was how BOP outputs are measured or predicted using empirical calculations or numerical simulations. Experimental measurements are influenced by practical limitations such as sample rate, experimental protocol, repeatability of explosive events and difficulties in obtaining close in measurements (e.g. sensors can be impacted by blast debris). Empirical blast calculators were based on only a few tests conducted with large charges and using fairly old measurement equipment, thus, the predictions for close in, short duration blasts, the prediction accuracy is limited. Blast simulations are based on a complete understanding of material properties (including biological materials), which are incomplete for very short duration blasts. Even though they cannot be taken to be infallible, empirical blast

calculations and blast simulations are able to provide data with which to validate experimental results. The empirical calculation software selected by the author was the BECV4. Numerical simulations were conducted to assist the author in validating experimental results using the ProSAir software (Cranfield University) [Peare: 2013] and ANSYS AUTODYN (CSIR) [Snyman: 2008].

BOP measurements and empirical blast calculation software also influence the validity of BOP injury criteria. This will be discussed further in Chapter 8.

The initial review of test standards, particularly in the demining scenario, indicated that BOP injuries do occur, but BOP injuries are not evaluated in all available test standards.

To investigate these contradictions further, BOP measurements, blast predictions and BOP injury calculations will be performed for the scenarios described in Table 5.

In order to explore the contradictions in the literature regarding the demining scenario, in particular, a new torso surrogate (the South African Torso Surrogate (SATS)) will be developed in Chapter 7. This was necessary as many torso surrogates and anthropomorphic test devices (ATDs) that measure parameters of the blast wave to allow BOP injuries to be predicted are expensive and may not be designed specifically for blast scenarios. Results obtained from the scenario investigation will lead to conclusions regarding the adequacy of test standards to evaluate the risk of BOP injuries.

Table 5: Summary of scenario descriptions, threats and dominant injury mechanisms.

Scenario Name	Scenario Description	Threat Descriptions	Dominant Blast Injury Mechanisms
Scenario A	Vehicle validation testing against IEDs and landmines (threat outside vehicle).	AT blast mine, IED or roadside bomb.	Blunt trauma (if vehicle hull remains intact).
Scenario B	Explosive charge within a vehicle or enclosed space <i>e.g. confined spaces, in vehicle/bus or building, in trench.</i>	IED, terrorist bombing on bus/train.	BOP, blunt trauma (head and lower limbs), fragments, burns, traumatic amputation/mutilating injuries.
Scenario C	Close proximity to hand grenade in open space.	IEDs, terrorist bombs, hand grenades.	For very close contact mutilating blast injuries would occur due to expanding products of detonation. If beyond the range of direct injury from the products of detonation, fragments are the main injury mechanism, but BOP injuries would also occur if sufficiently close to the origin of the detonation.
Scenario D	Demining Scenario.	Blast AP mines, bombs, IEDs, accidental explosions.	Fragment injuries (e.g. soil ejecta) occur unless ballistic protection is provided. BOP injuries occur if sufficiently close to the origin of the detonation. Mutilating blast injury or traumatic amputation if in contact the products of the detonation (e.g. standing on AP mine).

2.11.2 Thesis statement, study aims and delineations

Based on the study of the literature, the thesis statement is defined as follows:

Internationally accepted test standards are not adequate in the evaluation of protection against BOP injuries in the demining scenario.

To arrive at conclusions regarding this statement, the aim of the study is specified as follows:

The aim of the study is to evaluate the adequacy of internationally accepted test standards in determining the level of protection offered against blast overpressure injuries.

A test standard will be deemed *adequate* if:

- BOP injuries are not predicted in the scenario under consideration, thus the evaluation of protection against these injuries is not necessary;
- OR

The test standard mandates that the risk of BOP injury be determined using currently available measurement methods and injury criteria for the scenario under consideration

AND

the limitations of the test standard are fully described/disclosed. (i.e. the reasons for selecting the best available injury criteria, whether they under or over predict injuries for certain scenarios, for which conditions they are strictly valid, the assumptions made when test charge surrogates/torso surrogates are used, for which conditions the test scenario reflects the operational scenario).

The scope of the study is delineated as follows:

- Although BOP injuries may occur to other body regions, the focus of this study is only on the torso.

- Only BOP injuries are considered (not all injuries caused by the blast, such as fragment injuries or burn injuries).
- Only internationally recognised test standards will be evaluated.

3 ARMoured VEHICLE VALIDATION TESTING: PRELIMINARY RESEARCH INTO RISK OF BOP INJURIES FOR SCENARIO A

3.1 Introduction

Armoured Vehicle (AV) validation tests are conducted to assess the risk of injury to vehicle occupants when the vehicle is exposed to a landmine or improvised explosive device (IED). Full scale testing (involving a complete vehicle) of AVs is expensive as the vehicles being tested are often damaged during testing, thus the setup and preparation, data capture and processing for these tests is crucial.

Although many measurements used for injury predictions are recorded during testing, the risk of blast overpressure (BOP) injury is determined using pressure measurements and the chest wall velocity predictor (CWVP) [Axelsson and Yelverton: 1996] criterion.

The general experience indicates that AVs seldom fail a validation test based on BOP injury levels that exceed the allowable limit as defined by the CWVP (when the vehicle structure does not fail and if the hatches and doors remained sealed). It is typically assumed that if the hull of the vehicle was not breached, penetrated or structurally compromised by the blast, the pressure increase caused by the blast would not affect the vehicle occupants. However, BOP effects should be covered to assure the integrity of the vehicle safety cell [van der Horst *et al.*: 2010]. The author had not seen an AV fail based on the CWVP value when testing for protection against landmines. However, when the blast IED threat (simulated by a TNT charge) was incorporated into AV test standards, a vehicle did fail due to BOP recorded in the vehicle hull caused by a window failure. This sparked the author's interest in the investigation of BOP effects within the AV validation testing scenario.

3.1.1 Chapter aims

The aims of this study were to determine whether:

- BOP injuries could occur in AVs during a landmine or blast IED incident.
- Current AV validation test standards adequately evaluate the risk of BOP injuries occurring to vehicle occupants.

3.1.2 Chapter outline

This chapter describes how BOP measurements from AV validation tests are recorded, processed and validated.

The MATLAB SimulinkTM code that was developed by the author to calculate the risk of BOP injury to vehicle occupants, based on the CWVP criterion, is presented and the validation thereof is explained.

The BOP values recorded during actual AV validation tests are provided and the resulting risk of BOP injury for calculated for these tests are discussed.

3.2 Method

The pressure measurements used in this section of the study were recorded during vehicle validation tests carried out at the Council for Scientific and Industrial Research (CSIR) Detonics, Ballistics and Explosives Laboratory (DBEL) test range. Although a number of force, displacement and acceleration measurements were used to calculate injury risks for all body regions of the anthropomorphic test devices (ATDs), only those measurements relating to the risk of BOP injuries (i.e. pressure measurements) will be discussed here.

The data was processed to take into account the sensitivities of the transducers and the gains of the data acquisition units. The signals were then validated to determine whether the sensors were operating correctly (signal anomalies were studied to ensure data integrity and explained in the test report).

The pressure signals were used as input to the CWVP which was calculated in a program written in MATLAB SimulinkTM. This program was written by the author and validated by comparing predictions with colleagues performing similar testing at TNO (Toegepast Natuurwetenschappelijk Onderzoek) in the Netherlands.

3.2.1 General test setup and instrumentation for pressure measurement in vehicle validation tests

The basic test setup for a vehicle validation test involves either a surrogate landmine positioned beneath the vehicle hull or the wheel of the vehicle or a surrogate blast IED

which was positioned to the side of the vehicle. Figure 24 shows a diagram of a typical vehicle validation test setup.

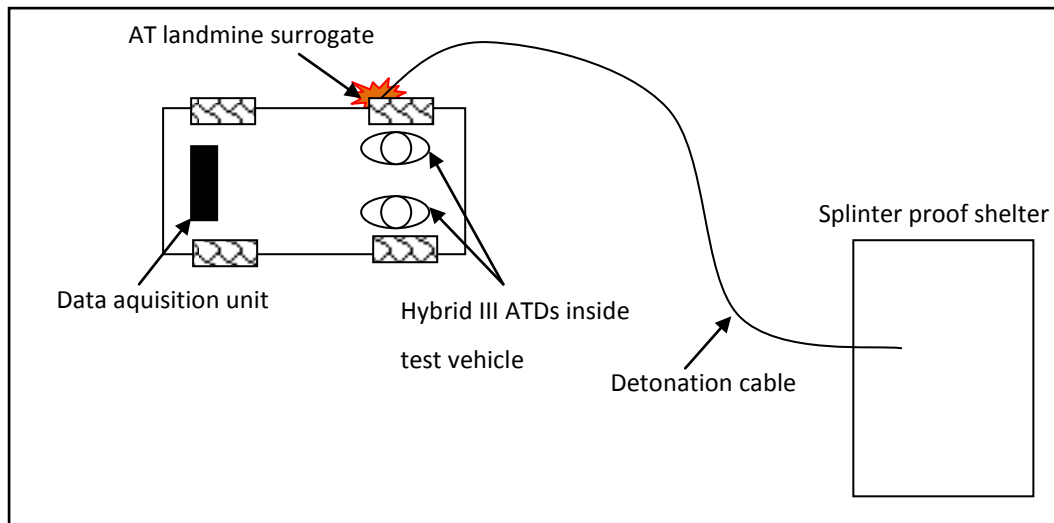


Figure 24: Diagram showing a typical vehicle validation test setup involving an AT landmine surrogate detonated beneath the wheel of an armoured vehicle.

In addition to Hybrid III ATDs, which are internationally recognized in AV validation test standards, the CSIR makes use of the South African (SA) Surrogate Leg (See Literature Review Section 2.9.1 for more details). In addition to measuring lower tibia axial forces (which are not relevant to this study), the SA Surrogate Leg was used to mount a pressure transducer in a similar way to how the chest transducers are mounted on the Hybrid III ATDs (See Section 2.9.1).

The pressure transducers mounted on the ATDs or the SA Surrogate Leg were sampled at 10 kHz using the custom built data acquisition unit which consists of a 24 channel signal conditioning unit and a Compact RIO™ embedded controller from National Instruments™. The data acquisition unit was programmed to acquire 0.25 seconds of pre-trigger data and 1.75 seconds of post trigger data at a sample rate of 10 kHz. This gives a total of 2×10^4 samples per channel.

The data acquisition units, Hybrid III ATDs and/or SA Surrogate Leg were positioned in the vehicle (See Figure 25) and the IED or landmine was detonated remotely from a splinter proof shelter (from where the test team observed the event). After the test, the positions of the ATDs and the condition of the vehicle were documented and the data was downloaded for analysis and injury calculations.

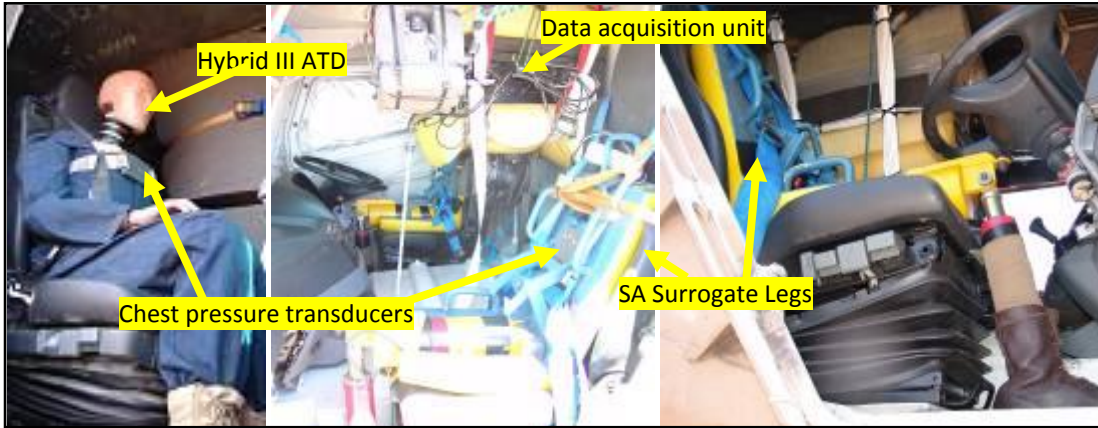


Figure 25: Photographs of a Hybrid III ATD, SA Surrogate Legs and data acquisition units in a vehicle prior to the blast test.

The SA Surrogate Leg that was instrumented with a pressure transducer was SA Surrogate Leg #3 and the two Hybrid III ATDs that were used had serial numbers 0200 0222 and 0200 0294. The transducers fitted in the SA Surrogate Leg and the Hybrid III ATDs to measure pressure profiles are detailed in Table 8.

Table 6: Details of Pressure Transducers used in Vehicle Validation Tests

Make	Model	Serial Number	Sensitivity	Location of Transducer
Endevco	8515C-50	K15630	0.2575 mV/kPa	SA Surrogate Leg #3 Chest Plate
ICSensors	1471-250A	P4_2	0.0377 mV/kPa	ATD 02000222 Right Ear
Endevco	8515C-50	K15644	0.3030 mV/kPa	ATD 02000222 Chest Plate
ICSensors	1451	P4_1	0.1450 mV/kPa	ATD 02000294 Right Ear
ICSensors	1471-250A	P4_3	0.0377 mV/kPa	ATD 02000294 Chest Plate

3.2.2 Data analysis and validation

The data files were processed in MATLAB™ to account for the data acquisition gains and the sensitivity of the transducers. The pressure profiles were then analysed to check

for anomalies which may indicate a faulty transducer or an error somewhere in the measurement or processing chain. Pressures recorded during the same test can also be compared to one another.

An example of an analysis of a pressure signal with interference recorded by SA Surrogate Leg #3 in a vehicle during a landmine test is shown in Figure 26. The spikes at approximately 0.5 s and 1.2 s were concerning as they did not correspond to typical pressure signals which record the peak pressure shortly after the detonation. In addition, the spikes were not reflected in the pressure signal recorded by the Hybrid III ATD which was also in the vehicle during the test (See Figure 26).

Possible explanations for the spikes include:

- Mechanical loading of the connectors or of the device via the mounting.
- Impact by debris or perhaps the safety belt.

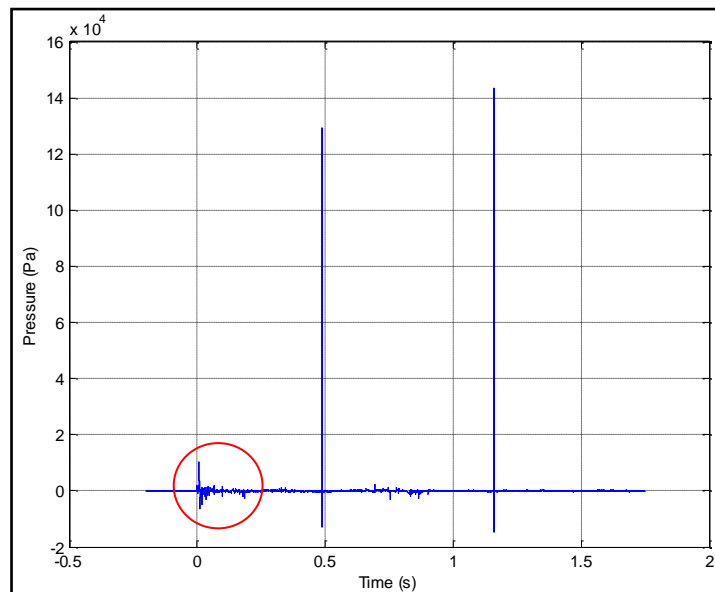


Figure 26: SA Surrogate Leg #3 pressure measured during an AV landmine test indicating the section of interest for the expected explosive event pressure (circled in red).

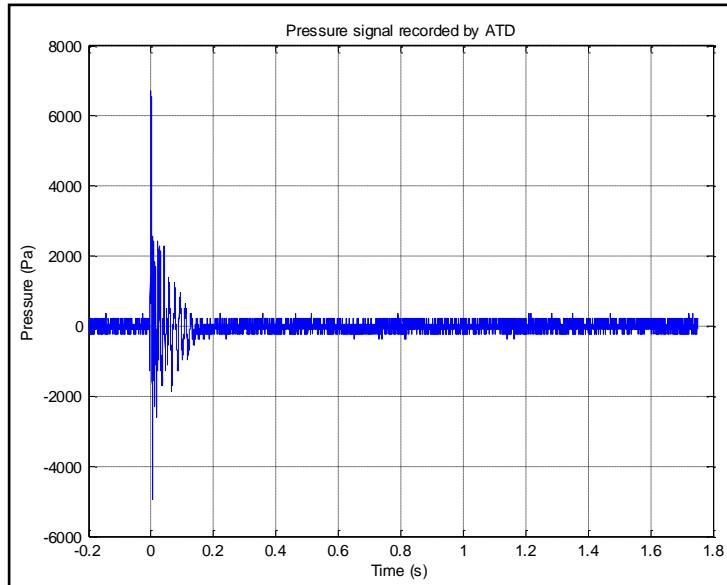


Figure 27: Hybrid III ATD pressure measured during an AV landmine test.

The pressure sensor and cables required careful checking prior to further tests to ensure that the anomaly did not occur again. This example illustrated the importance of analysing the signals after the test before the injury calculations are performed to prevent errors due to transducer readings which do not accurately reflect the explosive pressure of interest (i.e. Due to the sensor reacting to influences other than that for which it was designed such as impact by loose objects in the vehicle).

3.2.3 BOP Injury Calculations

As mentioned before, all the vehicle validation test standards covered in this chapter require the use of the CWVP criterion to determine whether the vehicle protects the occupants against BOP injuries. The CWVP criterion is discussed in the literature review, however, on attempting to apply this criterion, the author found the describing equation difficult to solve as a number of approximating iterations were necessary. An easier and more accurate (as many iterations can be computed in a short amount of time) solution was to program a feedback loop representing the equation which was possible using MATLAB Simulink™ (the resulting Simulink™ diagram can be found in Appendix A1). In simple terms, the recorded pressure signal, the sample rate and the ambient pressure recorded at the test site on the day of testing, are input into the simulation. After a number of iterations, the CWV for the same time duration is

available and can be plotted. The CWVP can then be determined by taking the maximum absolute value of the CWV curve.

After this procedure for calculating the CWVP was determined by the author, it was necessary to validate or check the accuracy of the calculation. This was done by comparing predictions with colleagues performing similar AV validation testing at TNO in the Netherlands. The results were found to be the same to within at least 0.01 m/s, which is adequate as the CWVP threshold for lung damage is 3.7 m/s and would thus require accuracy to within at least 0.1 m/s. The calculated CWV for a given pressure profile is shown in Figure 28, together with the CWV profile that was calculated (for the same pressure profile) by colleagues at TNO.

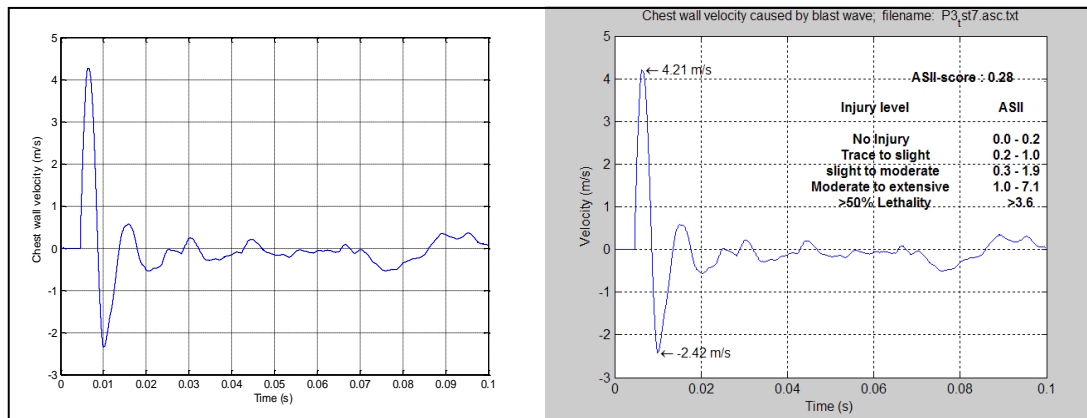


Figure 28: CWV calculated by the author (left) and colleagues at TNO (right) in order to validate the CWVP calculation.

3.3 Results

The peak pressure values recorded during a number of vehicle validation tests are presented in Table 7. In order to maintain the confidentiality of these tests, details such as the dates of the tests, the specific threats involved and the names of the vehicles being tested, are not provided. The pressure profiles were used to calculate the CWVP (whilst also dependent on the positive phase duration of the pressure profile, it is mainly dependent on the peak pressure) which provides an indication of the vulnerability of vehicle occupants to BOP injuries.

Table 7: Peak pressures recorded during vehicle validation tests

Threat Description	Test Surrogate Description	Recorded Peak Pressure (kPa)
Landmine	ATD 020000294	6.8
Landmine	SA Surrogate Leg #3	11.0
Landmine	ATD 020000294	5.5
Landmine	SA Surrogate Leg #3	10.5
IED	SA Surrogate Leg #3	2.8
Landmine	ATD 020000222	11.5
Landmine	ATD 020000222 (ear location)	15.5
Landmine	SA Surrogate Leg #3	21.2
Landmine	ATD 020000222	4.8
Landmine	ATD 020000222 (ear location)	5.2
Landmine	SA Surrogate Leg #3	13.5
IED	SA Surrogate Leg #3	11.0
IED	ATD 020000222	6.9
IED	ATD 020000222 (ear location)	8.8
IED	ATD 020000294	11.5
IED	SA Surrogate Leg #3	250.0
Landmine	ATD 020000222 (ear location)	3.0
Landmine	SA Surrogate Leg #3	4.8
Landmine	ATD 020000222	8.0
Landmine	SA Surrogate Leg #3	20.5
Landmine	ATD 020000222	4.0
Landmine	ATD 020000294	5.1
Landmine	ATD 020000222	3.9
Landmine	ATD 020000294	5.8
Landmine	SA Surrogate Leg #3	12.5
Landmine	ATD 020000294	8.7

Threat Description	Test Surrogate Description	Recorded Peak Pressure (kPa)
Landmine	SA Surrogate Leg #3	8.4
Landmine	ATD 020000222	12.4
Landmine	ATD 020000294	4.9
Landmine	ATD 020000222	5.2
Landmine	ATD 020000294	10.0

3.4 BOP Injury Calculations and Analysis

The CWV was calculated using the recorded pressure profile as described above. The graph in Figure 29 shows the peak overpressure measurements (from Table 9) plotted against the CWV that was calculated for each pressure profile. Figure 30 shows a zoomed in view of all peak overpressure measurements below 25 kPa and the corresponding CWV values that were calculated. Although Figure 29 and Figure 30 show that the relationship between peak overpressure and CWV is not a direct relationship (as the entire pressure/time profile is used in the calculation of the CWV), the graphs illustrate that most pressures recorded in vehicle validation tests result in CWV values that are well below the threshold for lung damage of 3.7 m/s.

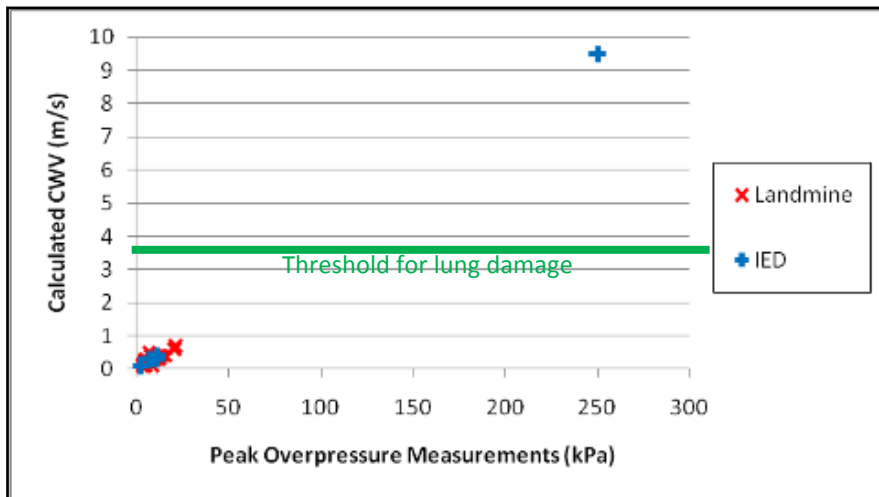


Figure 29: Peak overpressure measurements recorded during vehicle validation tests and corresponding calculated CWV values.

The outlier in Figure 29 at 250 kPa represents the only test where the CWVP criterion indicated that threshold for lung injury had been exceeded. This data point occurred during a 50 kg IED test where the vehicle was 1 m from the explosive charge. The vehicle suffered a hull breach during the blast.

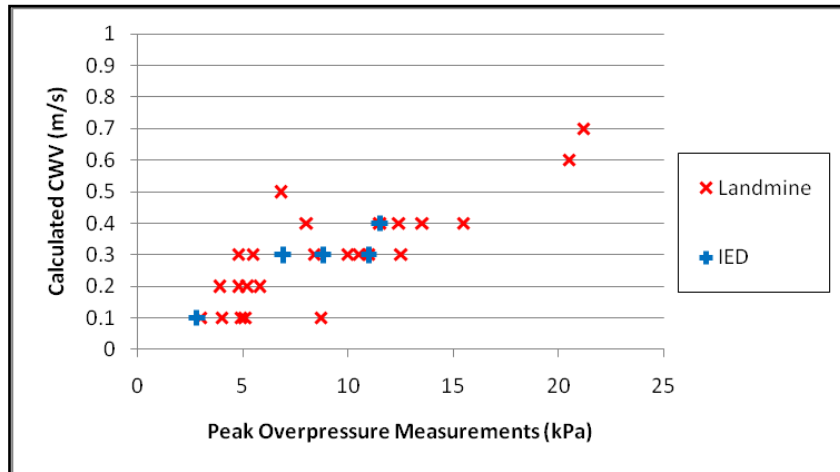


Figure 30: Peak overpressure measurements (below 25 kPa) recorded during vehicle validation tests and corresponding calculated CWV values.

The pressure transducer mounted on the chest of SA Surrogate Leg #3 recorded the signal shown in Figure 31. This graph shows that the pressure transducer saturated at just less than 250 kPa for approximately 5 ms. In order to check the validity of this signal (i.e. that the transducer was not faulty) the BECV4 data base was used to predict the peak incident pressure¹ and positive phase duration of the pressure signal at 5 m from a 50 kg TNT spherical charge. The peak was predicted to be 693 kPa for duration of 8 ms. It seems reasonable that the pressure measured inside the vehicle would be less than that predicted at the side of the vehicle when the pressure wave makes contact with the vehicle. The predicted time of arrival of the signal at the side of the vehicle is about 3 ms, so the time of arrival of the signal at the chest transducer of about 4 ms, also seems reasonable. Thus, the signal was deemed to be valid (although it would actually have been higher had the transducer not saturated at 250 kPa) and thus the CWV

¹ The peak incident (or side-on) pressure was used rather than the reflected pressure as the chest transducer would be in a side-on orientation to the blast as the SA Surrogate Leg was positioned in a seated position in the vehicle driver

(reflecting a minimum value) could be calculated using the available pressure signal² (See Figure 32).

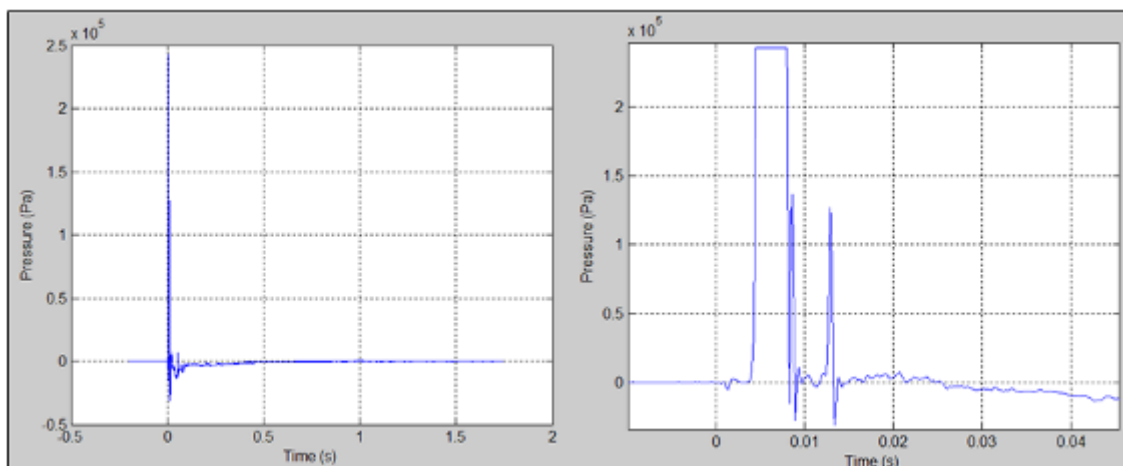


Figure 31: SA Surrogate Leg #3 pressure measured during an IED Test (left) and a zoomed in view of the peak (right).

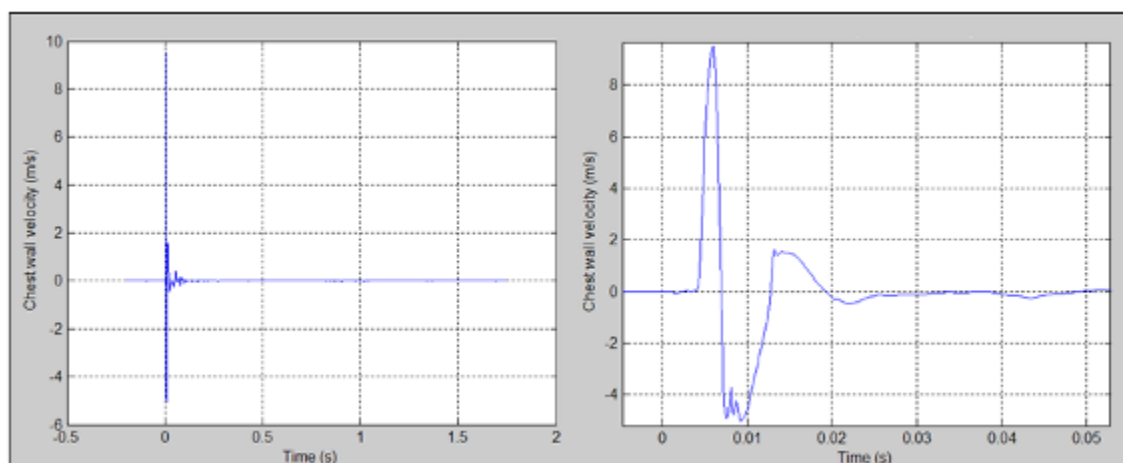


Figure 32: SA Surrogate Leg #3 CWV calculated during an IED Test (left) and zoomed in view of the peak (right).

AEP-55 volume 2 [2006] includes a general criterion that the integrity of the vehicle crew compartment (or the vehicle hull) is assured during the explosive event. BOP injuries are primarily covered as a fail-safe to assure the integrity of the vehicle crew compartment. Thus, in this example, irrespective of the fact that the CWVP criterion

² In order to investigate the effect of the discontinuity of the pressure signal in calculating the CWV, the discontinuity was manipulated by hand so that it increased gradually to a peak value of 273 kPa. The maximum CWV that was calculated using this manipulated pressure signal was 10.0 m/s, which is greater than the 9.5 m/s that was calculated for the saturated pressure transducer signal. This provides confidence that the value of 9.5 m/s is in fact the minimum CWV and the actual value, had the transducer not saturated at 250 kPa) would have been higher.

exceeded the allowable limit, as the vehicle compartment was breached by the blast, the vehicle would fail the validation test anyway.

It is important to note that due to the current data acquisition setup the ATD signals were sampled at 10 kHz, which is below the AEP-55 recommended rate of 200 kHz. This means that although all the measured peak pressures were lower than expected (and thus BOP injuries are not predicted), the true peaks could be missed due to the below optimal data acquisition sample rate. However, anecdotal evidence from other test authorities, who do sample their pressure signals at 200 kHz or more, suggests that there is no reason to believe that BOP injuries would occur without a hull breach.

3.5 Summary of Chapter Outputs

The outputs of this chapter regarding the risk of BOP injuries predicted in the AV validation testing scenario are as follows:

- BOP injuries could be a problem in armoured vehicles if the occupant compartment (or hull) is compromised by the blast.
- A MATLAB Simulink™ program was written and shown to accurately calculate the CWVP based on recorded pressure measurements.
- Current vehicle validation test standards (AEP-55 Volume 2 (Edition 1) [2006]; NATO-RTO-TR-HFM-148 [2012]) do adequately evaluate the risk of BOP injuries as there is no reason to believe that BOP injuries would occur without a hull breach.

The implications of these outputs on the adequacy of test standards in evaluating BOP protection are further discussed in Chapter 8.

4 EXPLOSIVE CHARGE WITHIN A VEHICLE OR ENCLOSED SPACE: SCENARIO B

4.1 Introduction

The armoured vehicle (AV) validation tests in the previous chapter considered the effects on vehicle occupants when an explosive charge detonates outside the vehicle. However, if an explosive charge detonates within an enclosed space (such as inside an AV), the many reflecting surfaces (a complex wave environment) will be more likely to cause BOP injuries to blast victims than if the blast occurred out in the open. This provides an illustration of the influence of a complex wave environment on the risk of BOP injuries.

Pressure measurements in complex wave environments are highly dependent on the exact orientation of the pressure gauge and its position within the vehicle. The BOP injuries sustained by vehicle occupants are also very specific depending on their position within the vehicle and relative to the explosive charge. It is hoped that a simulation a blast within a vehicle will enable the pressure profile at various locations (and gauge orientations) within the vehicle to be examined (without the need for numerous destructive blast tests which are expensive, not completely repeatable and it would not be feasible to do as many different setups to compare variables).

There are currently no test standards available that consider protection against BOP injuries within vehicles as the standards focus on ensuring that threats outside the vehicle do not penetrate the occupant compartment.

4.1.1 Chapter aim

The aim of this study was to determine whether:

- BOP injuries could occur inside an AV when an explosive charge detonates within the vehicle.

This will allow the author to discuss the relevance of the lack of test standards to evaluate possible protection concepts for this scenario.

4.1.2 Chapter outline

It was decided that ProSAir (Propagation of Shocks in Air) could be used to model the blast within a vehicle. Thus, a test scenario and vehicle geometry was decided upon and the model was assembled and run by staff at Cranfield University [Peare: 2013]. The model produced raw data of the side-on BOP which was then used as the input to the study detailed here.

The measurements were to calculate the chest wall velocity predictor (CWVP) (using MATLAB SimulinkTM). This gave an indication of BOP injury risk to vehicle occupants at various locations within the vehicle.

4.2 Method

An introduction of ProSAir is provided, followed by an overview of the simulation setup and the method used to process the simulation results.

4.2.1 Introduction to ProSAir

ProSAir is a finite volume, compressible fluid dynamics solver that is mainly used for modelling air-blasts in and around structures and estimating the resultant structural loading [Forth: 2012]. The software was developed at Cranfield University and the predecessor to ProSAir is Air3d. ProSAir provides relatively fast run times (compared to other solvers such as ANSYS AUTODYN (See discussion section 8.5.3)). Disadvantages of ProSAir are that explosive charges are assumed as ideal, spherical charges with no afterburning. This may result in an underestimate of the actual impulse where explosives such as TNT (where afterburning does occur) are used.

4.2.2 Overview of simulation setup

The vehicle represented in these simulations was based on a generic protected patrol or armoured utility vehicle. The 160 g spherical PE4 charge was selected as it is a standard charge used at Cranfield University which allows the option of future comparative explosive test trials.

The dimensions of the vehicle are shown in screen shots and a diagram in Figure 33. A three dimensional diagram of the vehicle is shown in the Figure 34. The diagram shows the target points of interest, based on would-be occupant positions within a simulated

vehicle. Three target points were selected for each of the four occupant positions. These points represent the leg, abdomen and thorax of a person seated within the vehicle. The charge is positioned 0.2 m above the floor of the vehicle and the proximity of the charge to the target points is provided in Table 8. A mesh size of 1 mm was used for the spherical phase of the simulation and a 25 mm mesh size was used for the 3D phase of the simulation.

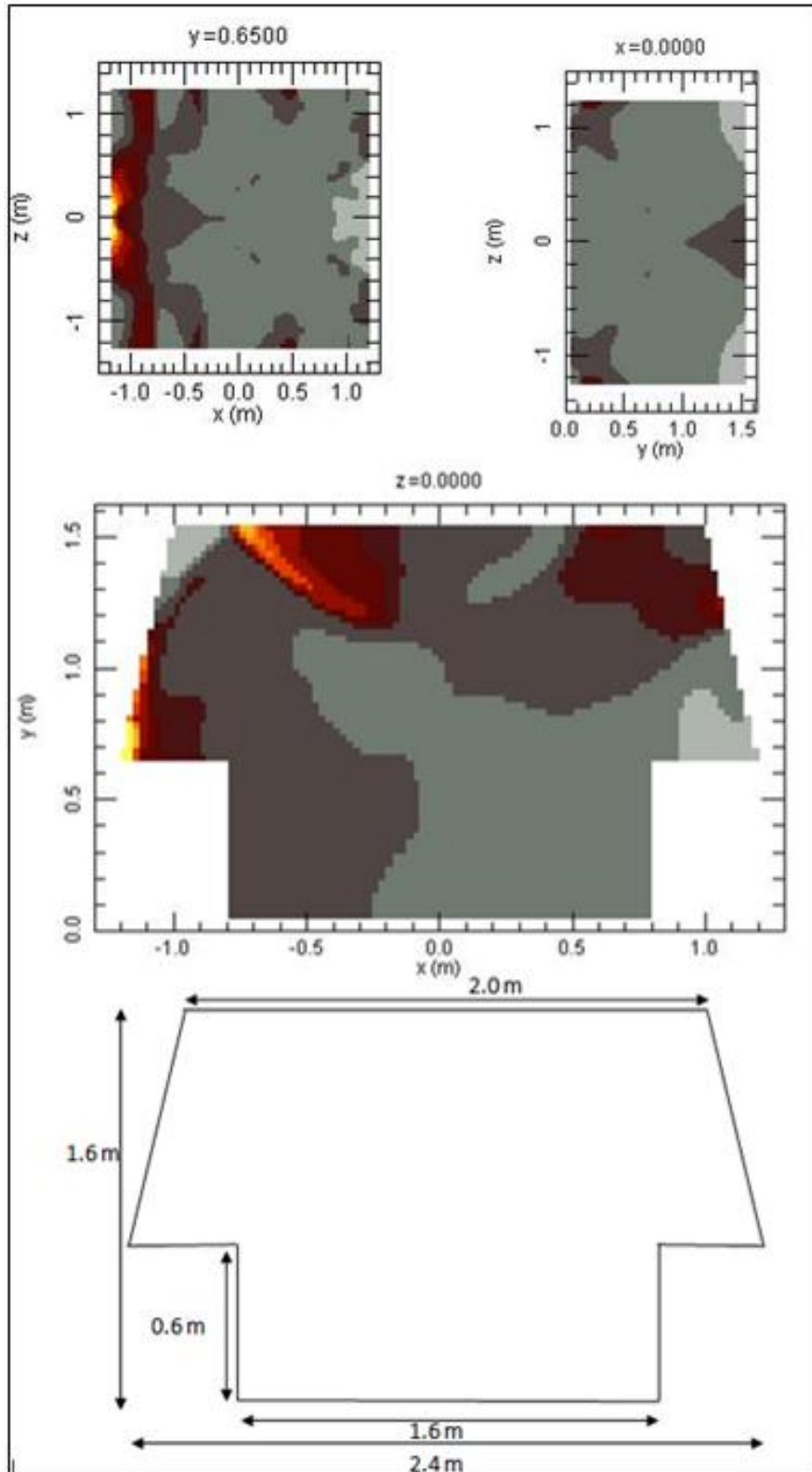


Figure 33: Screen shots for ProSAir simulation of the vehicle showing the plane views and a diagram showing the dimensions of the vehicle from the $z=0$ cross-section [Peare: 2013].

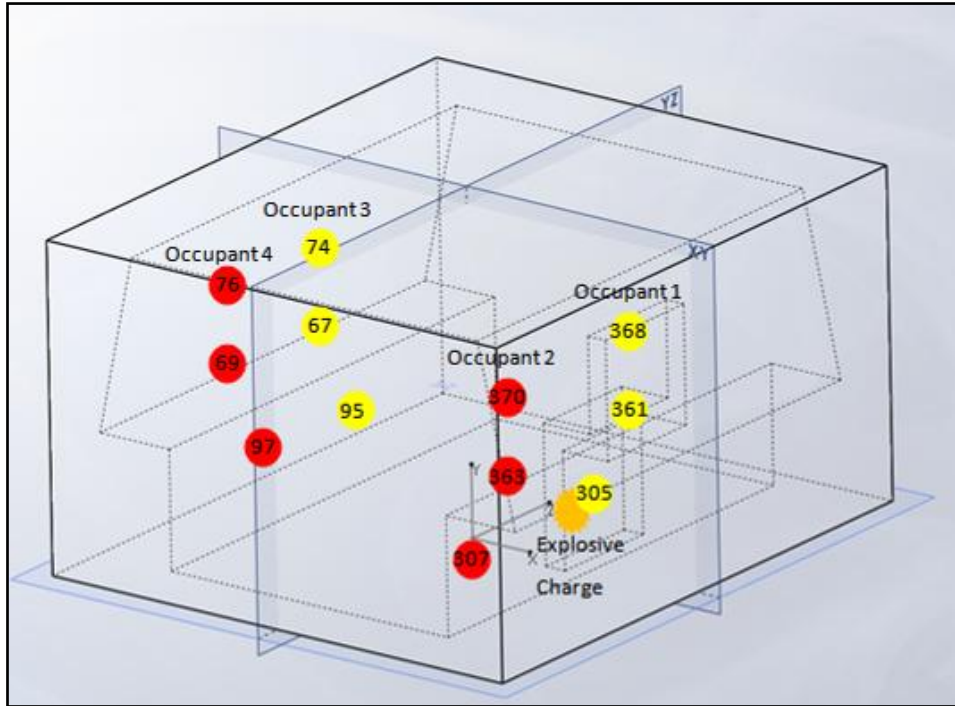


Figure 34: Diagram showing the target points of interest based on would-be occupant positions within a simulated vehicle [Peare: 2013].

Table 8: Table showing the distance between target points (of each occupant) and the explosive charge within the vehicle.

Target Description	Distance from Charge (m)
Occupant 1, closest to charge, thorax (Point 368)	1.005
Occupant 1, closest to charge, abdomen (Point 361)	0.745
Occupant 1, closest to charge, leg (Point 305)	0.143
Occupant 2, same side corner, thorax (Point 370)	1.261
Occupant 2, same side corner, abdomen (Point 363)	1.066
Occupant 2, same side corner, leg (Point 307)	0.776
Occupant 3, opposite side, thorax (Point 74)	1.772
Occupant 3, opposite side, abdomen (Point 67)	1.639
Occupant 3, opposite side, leg (Point 95)	1.245
Occupant 4, opposite side corner, thorax (Point 76)	1.929
Occupant 4, opposite side corner, abdomen (Point 69)	1.807
Occupant 4, opposite side corner, leg (Point 97)	1.460

4.2.3 BOP injury calculations

In order to make use of the CWVP criterion, the side-on pressure values obtained from the ProSAir simulation values needed to be converted to face-on or reflected pressure values.

As previously mentioned, there is much debate as to the accuracy of this type of conversion, particularly when the point of interest is very close to the explosive charge. The Rankine-Hugoniot equations state that for strong shocks (large BOP values), the reflected pressure is 8 times the side-on pressure and for weak shocks (low BOP values), the reflected pressure is twice the side-on pressure [Smith and Hetherington: 1994]. However, it is stated in Smith and Hetherington [1994] that “because of gas dissociation effects at close range (when the assumptions about the behaviour of air in the reflection process are not valid), measurements of reflected pressure of up to 12 or 13 times incident (or side-on) pressure have been made.” It is noted that the assumption is zero angle of incidence from an infinite reflecting surface which would produce the worst-case injury risk scenario.

The Blast Effects Calculator Version 4 (BECV4) software [Swisdak: 2000] was used to obtain pressure multiplication factors (to convert side-on pressure to face-on pressure values). It must be noted that these values are only strictly valid for free-field case. Table 11 shows the BECV4 values obtained for peak side-on pressure, peak reflected pressure and the resulting pressure multiplication factor for each target point specified by the distance from the charge. These results are also shown in Figure 35. The pressure multiplication factor increases when the target is closer to the charge and decreases to just over 2 when the target is further from the charge. This is in line with the Rankine-Hugoniot equations. At the target point closest to the charge, the pressure multiplication factor is 10.2. This is higher than the value of 8 which is the highest factor predicted by the Rankine-Hugoniot equations, but it is in line with measurements reported in [Smith and Hetherington: 1994] which state measured pressure multiplication factors at close range can be as high as 12 or 13.

The pressure multiplication factors listed in Table 9 were used to convert the side-on pressure profiles (from the ProSAir simulations) to reflected pressure profiles for each corresponding target point. This was achieved by multiplying each point of the side-on

pressure profile by the same pressure multiplication factor using MATLAB™ (the code can be found in Appendix B1).

Table 9: Peak side-on pressure, peak reflected pressure and the resulting pressure multiplication factor for each target point specified by the distance from the charge as predicted by the BECV4 software.

Target Description	Distance from Charge (m)	Peak Side-on Pressure (kPa)	Peak Reflected Pressure (kPa)	Pressure Multiplication Factor
Occupant 1, closest to charge, thorax (Point 368)	1.005	415.4	1749.9	4.2
Occupant 1, closest to charge, abdomen (Point 361)	0.745	822.9	4278.7	5.2
Occupant 1, closest to charge, leg (Point 305)	0.143	13520.7	137764.2	10.2
Occupant 2, same side corner, thorax (Point 370)	1.261	246.1	873.4	3.5
Occupant 2, same side corner, abdomen (Point 363)	1.066	363.4	1458.7	4.0
Occupant 2, same side corner, leg (Point 307)	0.776	751	3799.2	5.1
Occupant 3, opposite side, thorax (Point 74)	1.772	116.5	332.4	2.9
Occupant 3, opposite side, abdomen (Point 67)	1.639	137.5	410.2	3.0
Occupant 3, opposite side, leg (Point 95)	1.245	253.4	907.7	3.6
Occupant 4, opposite side corner, thorax (Point 76)	1.929	97.5	266.8	2.7
Occupant 4, opposite side corner, abdomen (Point 69)	1.807	111.8	315.8	2.8
Occupant 4, opposite side corner, leg (Point 97)	1.460	176.9	567.6	3.2

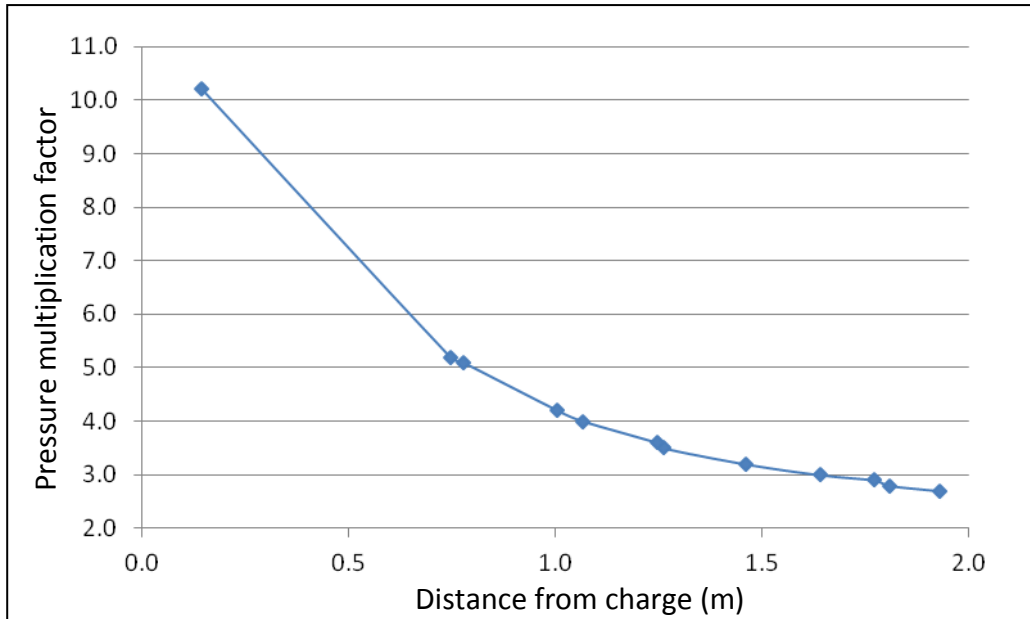


Figure 35: Graph showing the pressure multiplication factor obtained from BECV4 software for various distances from 160 g PE4 (C4) explosive charge.

The CWVP criterion was then calculated, using the reflected pressure profiles, to determine the risk of BOP injuries in this scenario. A MATLAB Simulink™ program was written to perform the CWV calculations that was similar to the program used in the previous chapter, but with the signal length and sample rates adjusted accordingly (the MATLAB files used in this section were saved as *plot_ProSAir_results.m* and *plot_ProSAir_cwv.m* can be found in Appendix B1).

4.3 Results

Table 10 shows the peak side-on pressure and the time at which the peak occurs.

Table 10: ProSAir simulation results showing peak side-on pressure and the time at which that pressure occurs for each of the target points considered.

Target Description	Peak Side-On Pressure (kPa)	Time at which Peak Occurs (ms)
Occupant 1, closest to charge, thorax (Point 368)	192.9	4.7
Occupant 1, closest to charge, abdomen (Point 361)	336.0	0.4
Occupant 1, closest to charge, leg (Point 305)	1303.1	0.1
Occupant 2, same side corner, thorax (Point 370)	179.4	8.1
Occupant 2, same side corner, abdomen (Point 363)	181.6	0.9
Occupant 2, same side corner, leg (Point 307)	927.5	0.5
Occupant 3, opposite side, thorax (Point 74)	388.0	5.4
Occupant 3, opposite side, abdomen (Point 67)	204.7	5.7
Occupant 3, opposite side, leg (Point 95)	310.5	4.4
Occupant 4, opposite side corner, thorax (Point 76)	308.8	4.0
Occupant 4, opposite side corner, abdomen (Point 69)	175.5	4.5
Occupant 4, opposite side corner, leg (Point 97)	176.2	2.1

Figure 36, Figure 37, Figure 38 and Figure 39 show the side-on pressure profiles for the leg, abdomen and thorax target points on Occupant 1, Occupant 2, Occupant 3 and Occupant 4 respectively.

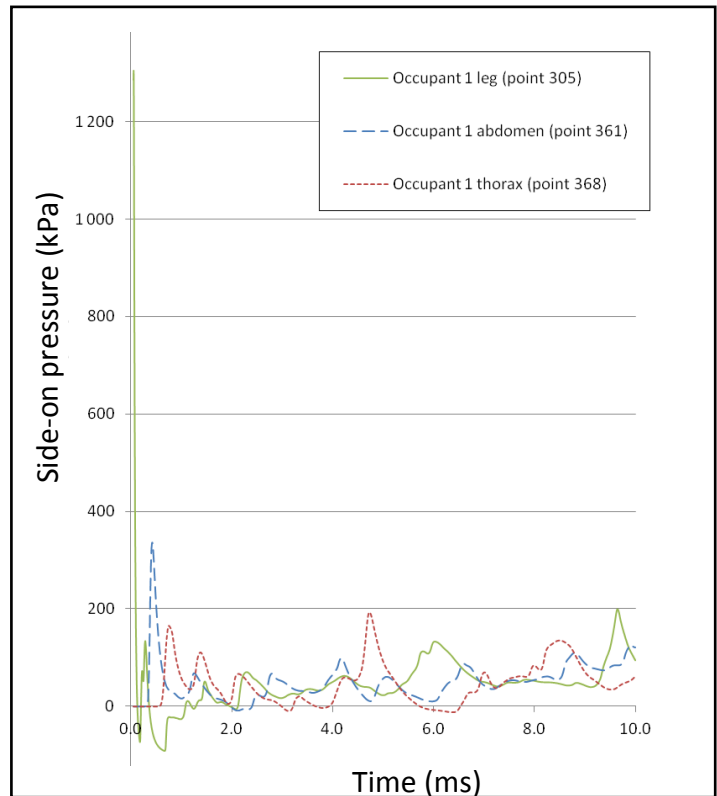


Figure 36: Side-on pressure profile over 10 ms as recorded by Occupant 1 leg, abdomen and thorax target points.

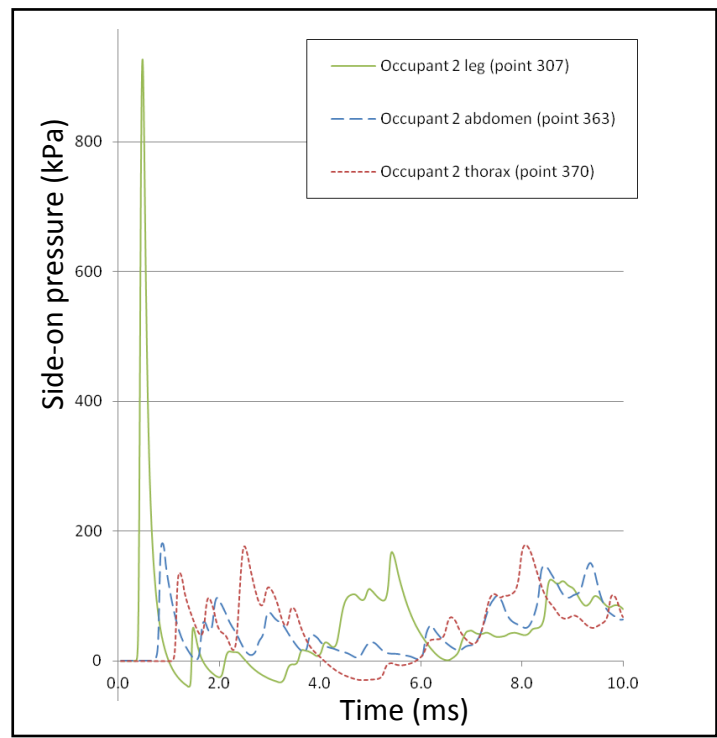


Figure 37: Side-on pressure profile over 10 ms as recorded by Occupant 2 leg, abdomen and thorax target points.

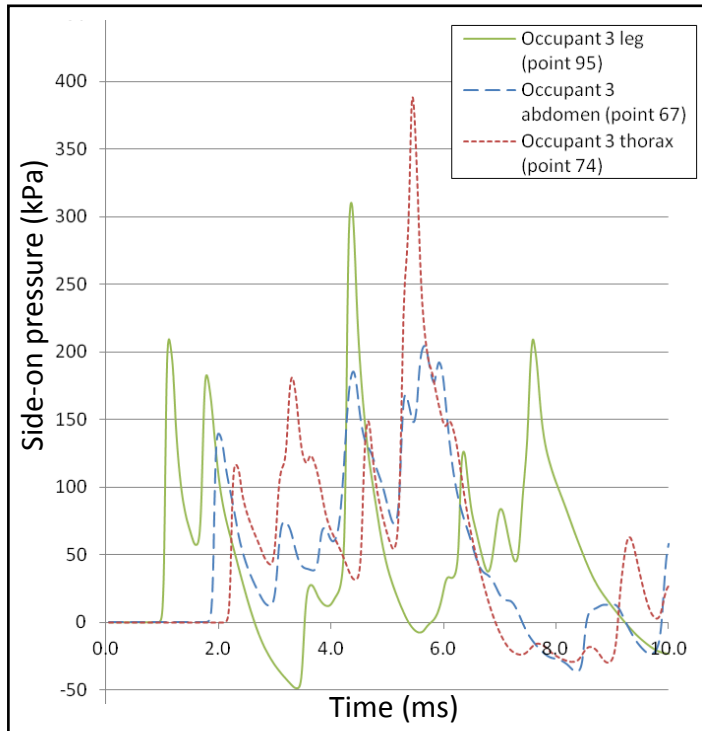


Figure 38: Side-on pressure profile over 10 ms as recorded by Occupant 3 leg, abdomen and thorax target points.

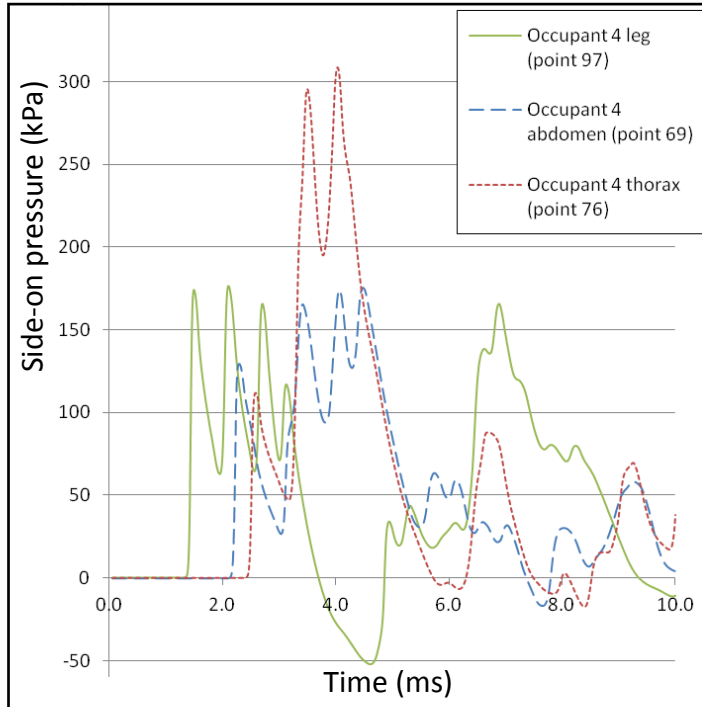


Figure 39: Side-on pressure profile over 10 ms as recorded by Occupant 3 leg, abdomen and thorax target points.

4.4 BOP Injury Calculations and Analysis

This section looks at the influence of the complex wave environment, established within the vehicle, on the pressure profiles observed at specific distances from the charge. This was done firstly by comparing the ProSAir simulation results with predicted results from BECV4 calculations. The CWV was then calculated for each abdomen and thorax target point to determine the risk of BOP injury at each point. The leg target points were not considered in this section as they are not relevant for the CWV injury calculations.

4.4.1 Comparing side-on pressure profiles in vehicle (ProSAir simulation results) with predicted free-field pressures (BECV4 predicted results)

Looking at the pressure profiles from the ProSAir simulations, observations can be made regarding the time of arrival of the pressure waves at various distances from the charge. Figure 40 and Figure 41 show the side-on pressure profiles for all occupants for the abdomen and thorax target points respectively.

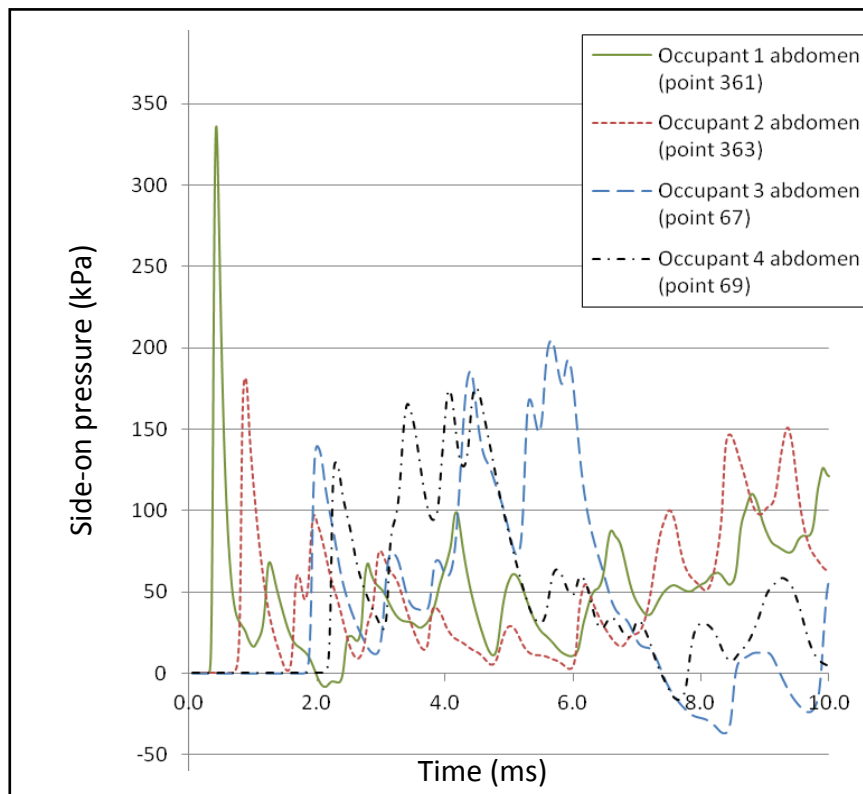


Figure 40: Side-on pressure profiles over 10 ms for abdomen target points of all occupants.

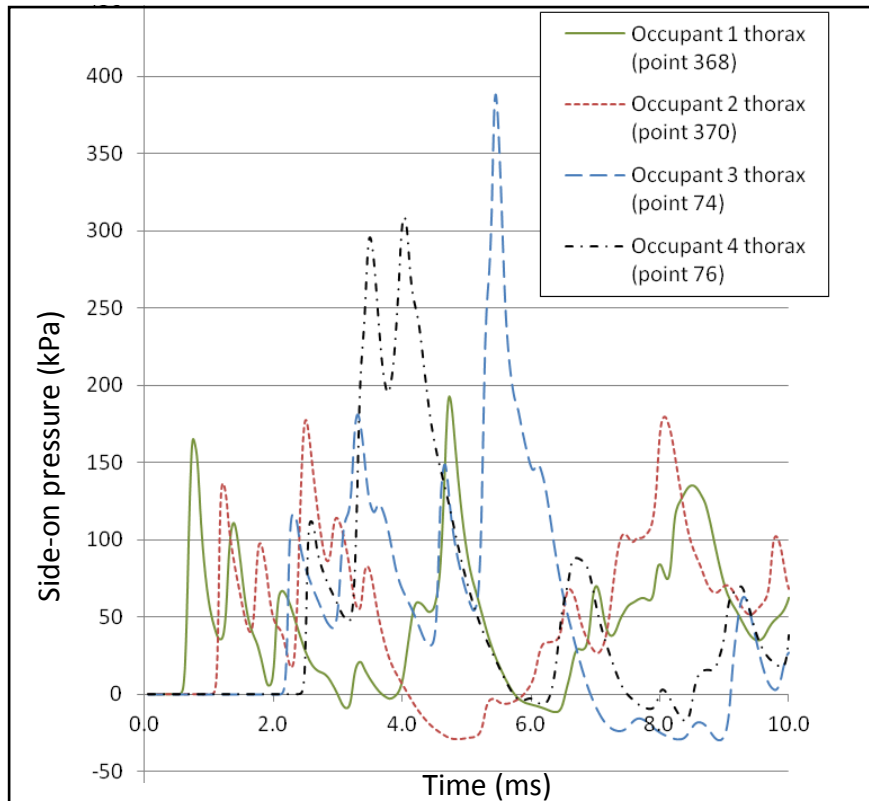


Figure 41: Side-on pressure profiles over 10 ms for thorax target points of all occupants.

In Figure 40 and Figure 41 the peak side-on pressures do not occur on arrival of the pressure wave, but rather a few milliseconds later due to reflections within the vehicle. This is different from a free-field pressure profile in which the pressure peaks almost immediately. Due to the complex wave environment, it is not possible to validate the maximum peak side-on pressure using the BECV4 software. However, the time of arrival of the pressure wave at the various target points should be comparable.

Figure 42 shows the time of arrival of the pressure wave at the thorax target points at various distances from the explosive charge from the ProSAir simulation and a free field prediction from BECV4 (Note: As PE4 explosive is not available in the BECV4 software, C4 was used instead as it has a similar TNT equivalency). The graph in Figure 42 shows that the time of arrival values from the ProSAir simulation and the BECV4 predictions are similar and follow a similar trend. This provides added confidence in the ProSAir simulation results.

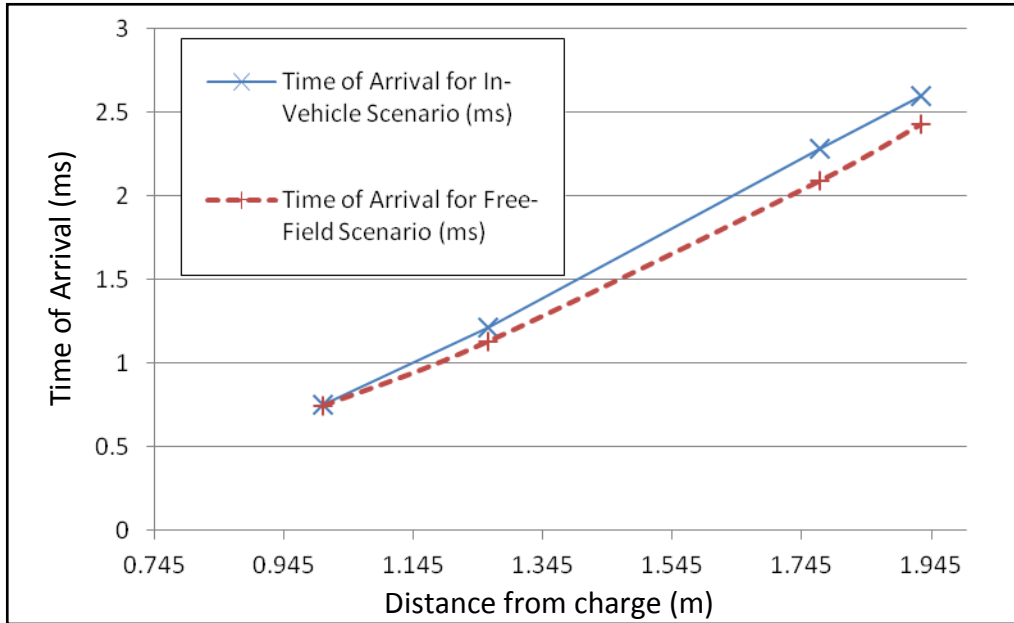


Figure 42: Time of arrival of pressure profiles at various distances from 160 g PE4 (C4) charge for the in-vehicle scenario (ProSAir simulations) and free-field scenario (BECV4 software calculations).

Although there is a correlation between the time of arrival of the initial peak of the pressure profiles in the ProSAir simulation results and the BECV4 software calculations, the maximum peak pressure from the ProSAir simulation occurred later in the pressure profile. In addition, the peak side-on pressure does not decrease exponentially as the distance from the charge increases, as is the case in the free field scenario (shown in the BECV4 calculations). Figure 43 shows the peak side-on pressure profiles within a vehicle (obtained in from the ProSAir simulations) and the peak side-on pressure profiles in free-field predicted using the BECV4 software.

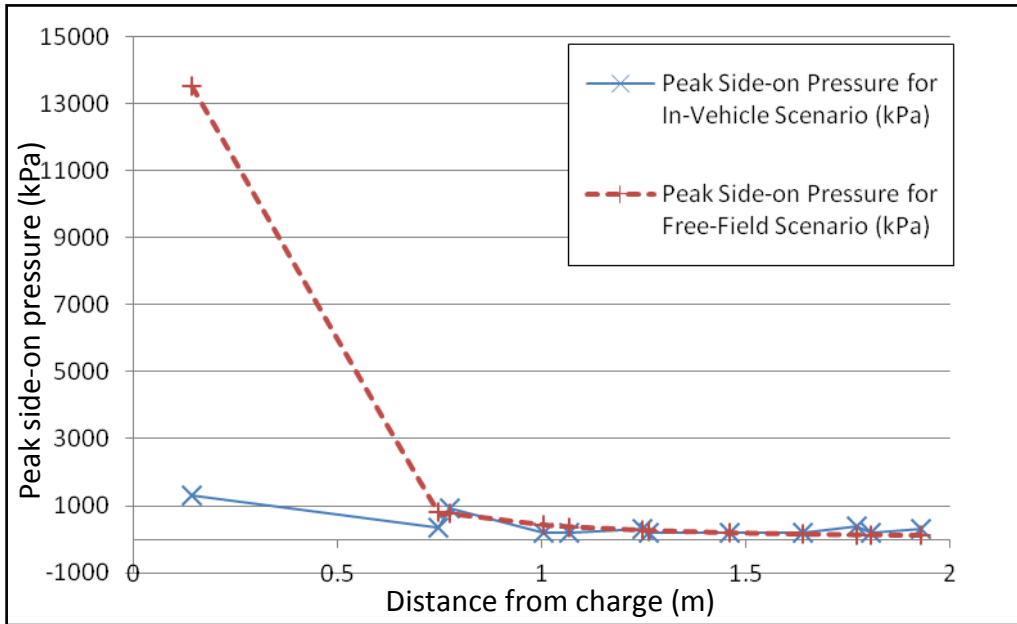


Figure 43: Peak side-on pressure at various distances from 160 g PE4 (C4) charge for the in-vehicle scenario (ProSAir simulations) and free-field scenario (BECV4 software calculations).

As both the ProSAir simulated and the BECV4 predicted results are not reliable in the very near field, the point closest to the charge (Occupant 1 leg) has been removed in Figure 44. The graph shows that in a complex wave environment, the peak pressure dose to a target (or vehicle occupant) cannot be estimated based on the distance between the target and the explosive charge.

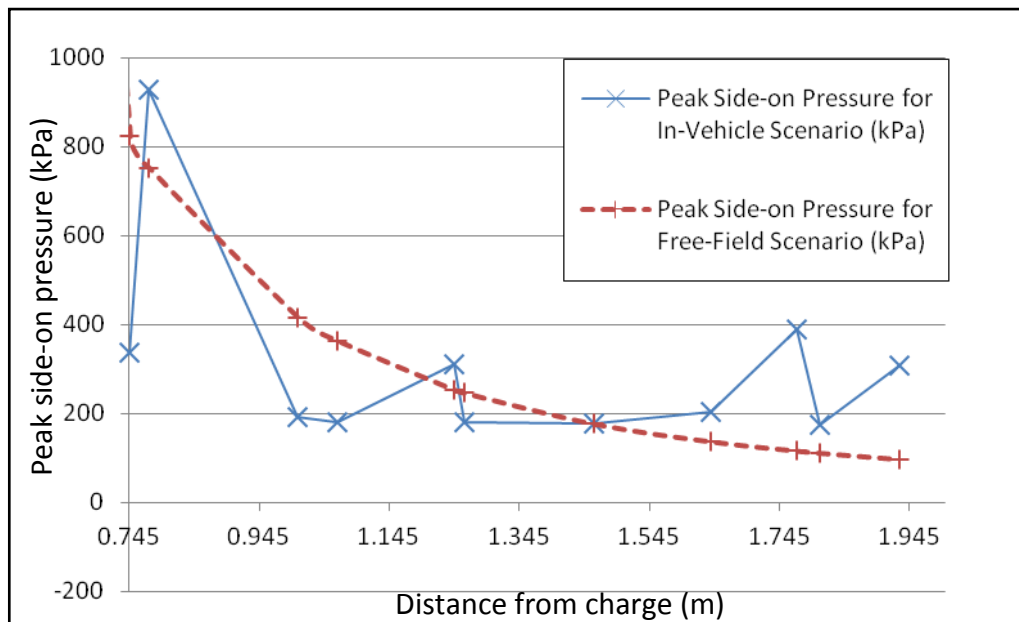


Figure 44: Peak side-on pressure at distances greater than 0.745 m from 160 g PE4 (C4) charge for the in-vehicle scenario (ProSAir simulations) and free-field scenario (BECV4 software calculations).

4.4.2 BOP injury predictions at different positions in the vehicle (using the CWVP criterion)

In free field, injuries correlate with peak pressure and positive phase duration. The CWV was calculated to provide injury predictions based on the pressure profiles obtained within the complex wave environment of the vehicle. The maximum CWV for each target point within the vehicle is shown in Table 11.

Table 11: Peak side-on pressure, peak reflected pressure and the calculated Chest Wall Velocity (CWV) for the abdominal and thoracic target points of each vehicle occupant.

Target Description	Distance from Charge (m)	Peak Side-on Pressure (kPa)	Peak Reflected Pressure (kPa)	Maximum Chest Wall Velocity (CWV) (m/s)
Occupant 1, closest to charge, thorax (Point 368)	1.005	192.9	810.4	12.5
Occupant 1, closest to charge, abdomen (Point 361)	0.745	336.0	1747.2	17.9
Occupant 2, same side corner, thorax (Point 370)	1.261	179.4	627.9	18.1+
Occupant 2, same side corner, abdomen (Point 363)	1.066	181.6	726.3	14.7+
Occupant 3, opposite side, thorax (Point 74)	1.772	388.0	1125.2	13.1
Occupant 3, opposite side, abdomen (Point 67)	1.639	204.7	614.2	9.9
Occupant 4, opposite side corner, thorax (Point 76)	1.929	308.8	833.7	22.4
Occupant 4, opposite side corner, abdomen (Point 69)	1.807	175.5	491.3	13.8

Figure 45 shows that there is no obvious relationship between the peak CWV and the peak reflected pressure in the complex wave environment within the vehicle.

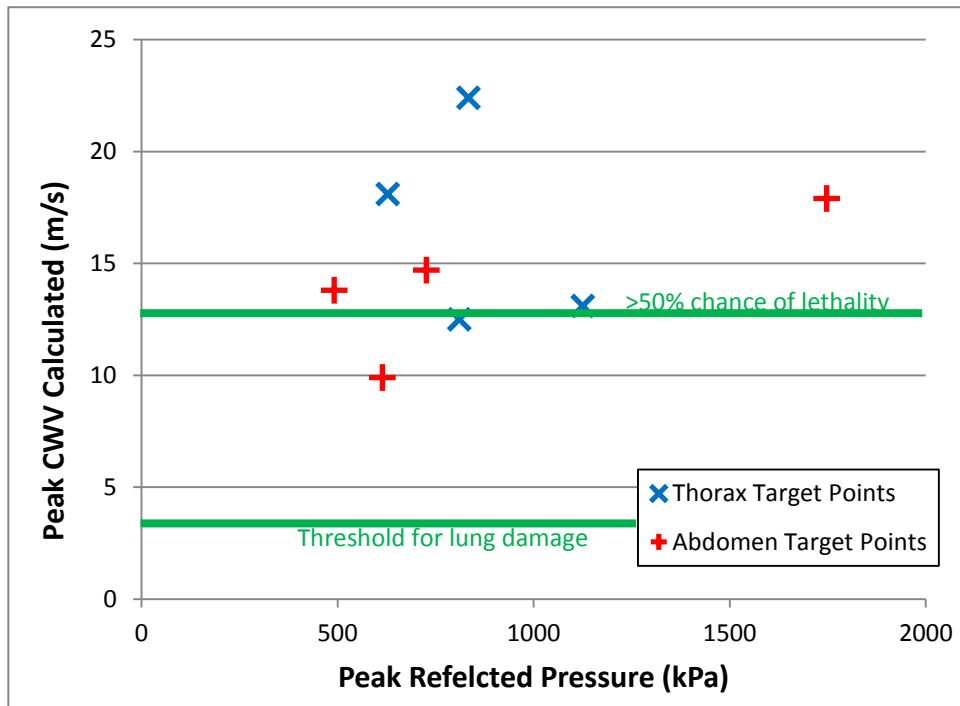


Figure 45: Peak reflected pressure recorded at various target positions within the vehicle and the corresponding calculated peak CWV values. Injury levels predicted using CWVP are indicated on the graph.

Figure 46 shows that there is also no obvious relationship between the peak CWV and the distance from the charge (as is the case in a free field scenario).

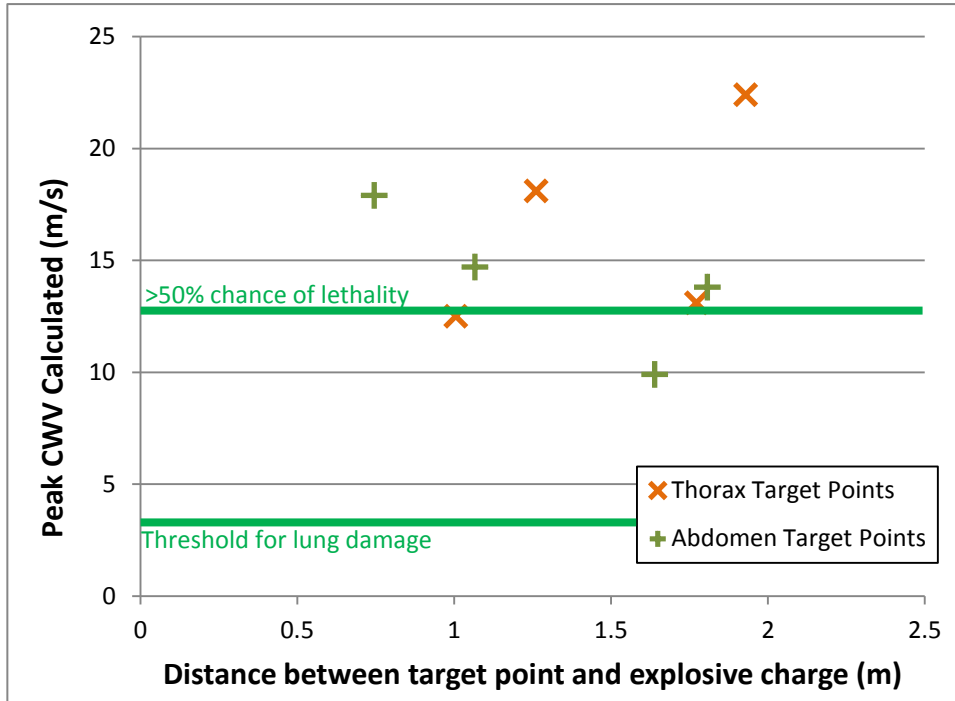


Figure 46: Distance between target points and explosive charge and the corresponding calculated peak CWV values for those target points.

The target positions within the vehicle and corresponding CWV values are illustrated in Figure 47. This example suggests that in a complex wave environment, occupants in corner positions have a higher risk of BOP injuries than occupants that are positioned closer to the explosive charge.

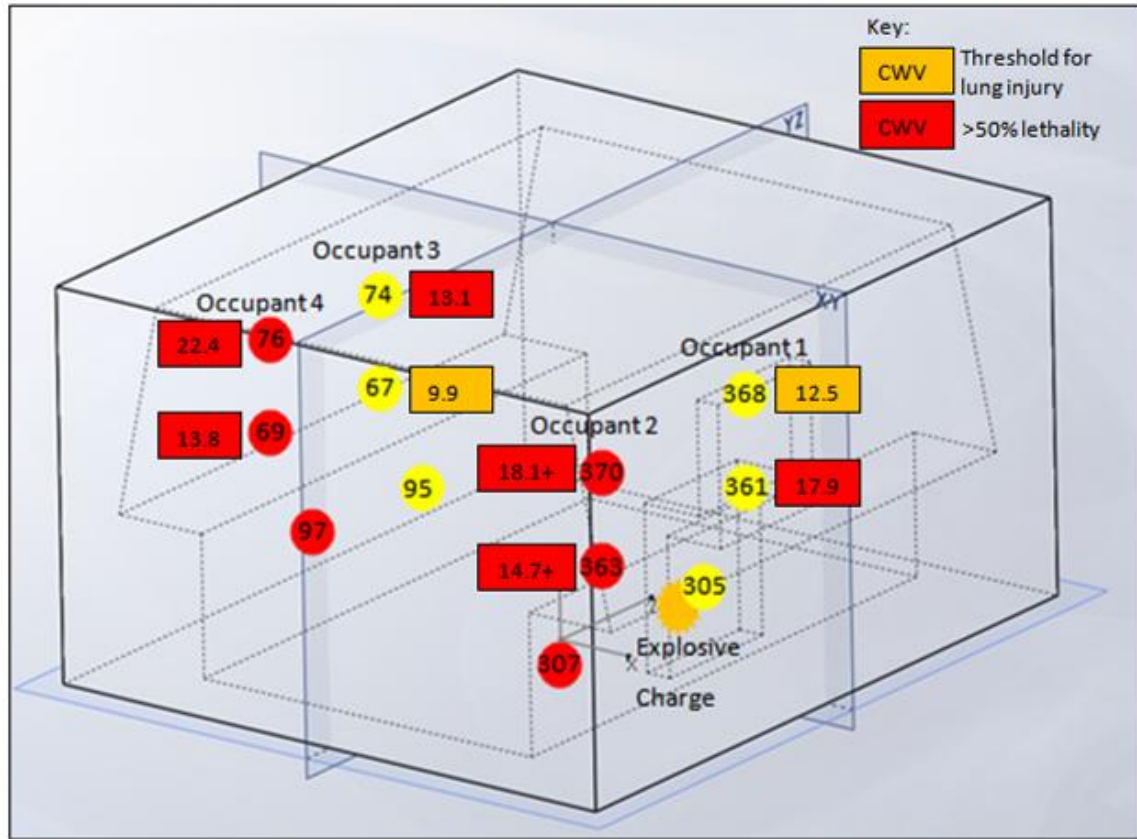


Figure 47: Diagram showing the target points of interest and the associated CWV values resulting from a simulated blast within a vehicle.

4.4.3 Comparing CWV BOP injury predictions with Bowen/Bass injury risk curves for free field

The Bowen *et al.* [1968] or Bass *et al.* [2006a; 2008] injury risk cannot be used in the complex wave environment within a vehicle. However, the Bowen/Bass curves can be applied to a theoretical free field scenario by inputting the explosive charge type and weight and the distances to the various target points in the BECV4 calculator. This provides a peak side-on pressure and a positive phase duration which can then be used with the Bowen/Bass curves to predict the risk of BOP injury in a scenario in which the vehicle is not present. Comparing the predicted risk of BOP injury with and without the vehicle gives an indication of the influence of the vehicle on severity of possible BOP injuries to vehicle occupants.

Table 12 shows the BECV4 predicted peak side-on pressure and the positive phase durations. These values were then used to obtain a risk of BOP injury to the vehicle

occupants or target points (if they were in free field). Figure 48 shows the Bass *et al.* [2006a] predictions (specifically for short-duration blasts).

Table 12: Peak side-on pressure and positive phase duration for the thoracic target points specified by the distance from the charge as predicted by the BECV4 software.

Target Description	Distance from Charge (m)	Peak Side-on Pressure (kPa)	Positive Phase Duration (ms)
Occupant 1, closest to charge, thorax (Point 368)	1.005	415.4	1.2
Occupant 2, same side corner, thorax (Point 370)	1.261	246.1	1.2
Occupant 3, opposite side, thorax (Point 74)	1.772	116.5	1.7
Occupant 4, opposite side corner, thorax (Point 76)	1.929	97.5	1.8

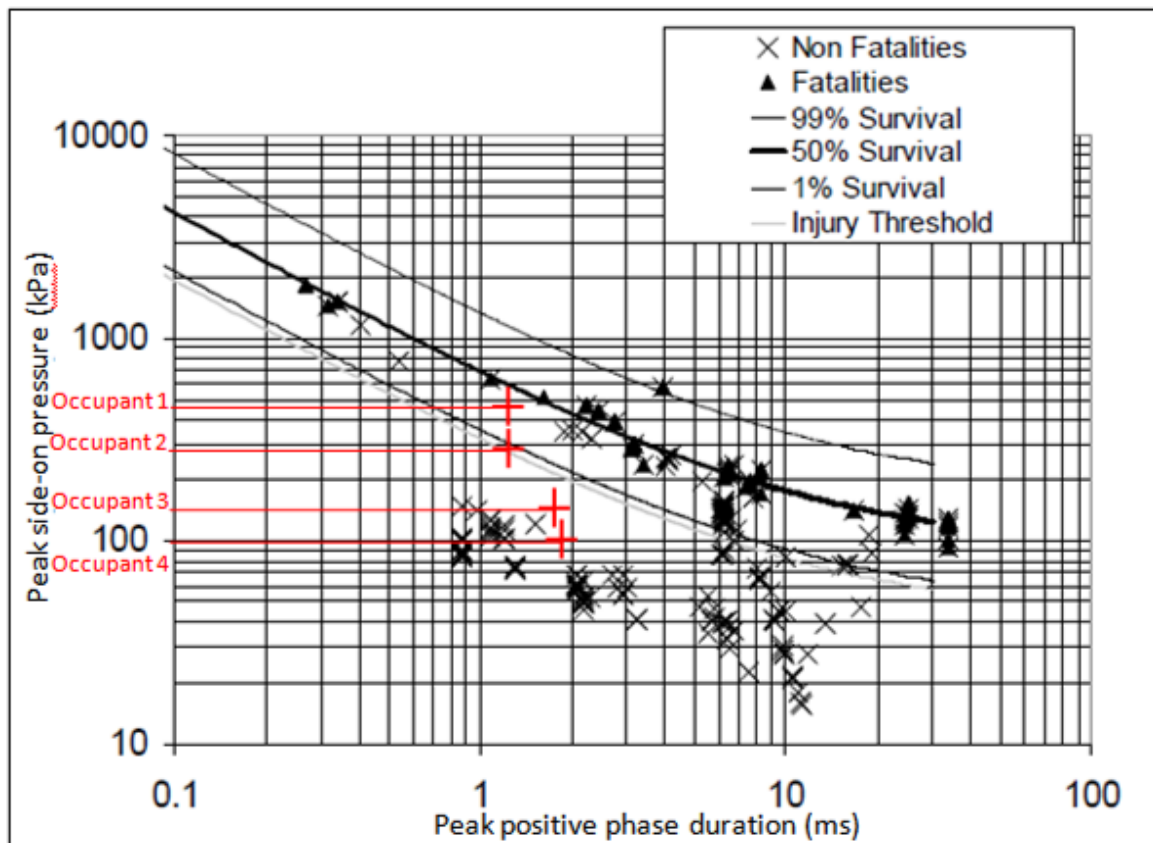


Figure 48: Bass *et al.* [2006a] injury risk curve with indicators showing the predicted overpressure injuries at various distances from a 160 g C4 charge as determined using BECV4.

The BOP injuries predicted for the free field scenario for the thorax target points all indicate a greater than 50% chance of survival (See Figure 48). The thorax point closest to the charge (Occupant 1) would have the highest risk of BOP injury (i.e. above the injury threshold, but between 50% and 99% chance of survival). The thorax point furthest from the charge (Occupant 4) has the lowest risk of BOP injury (i.e. below injury threshold).

At the same distances from the charge, but in a complex wave environment within a vehicle, all the thoracic target points predict the threshold for lung damage is exceeded. The thorax point closest to the charge (Occupant 1) sustains the least risk of BOP injury (the threshold for lung injury is exceeded, but greater than 50% chance of survival). The thorax point furthest from the charge, but in a corner (Occupant 4), has the highest risk of BOP injury and there is a greater than 50% chance of lethality.

Although many assumptions have been made in comparing the BECV4 free field scenario with the ProSAir simulated in-vehicle scenario, the example illustrates that it is essential to take into account the complex wave environment when assessing the risk of BOP injuries within a vehicle or enclosed space.

4.4.4 Test standards for this scenario

Current vehicle validation test standards (AEP-55 vol.2 [2006] and NATO-RTO-TR-HFM-148 [2012] and STANAG No. 4190 (Edition 2) [1998])) do not evaluate the risk of BOP injuries in the scenario where an explosive charge is detonated within a vehicle. If an explosive charge were to penetrate the vehicle, the vehicle would not pass based on the test standards.

4.5 Summary of Chapter Outputs

The outputs of this chapter regarding the risk of BOP injuries predicted in the complex wave environment within a vehicle are as follows:

- The risk of BOP injury is higher in a complex wave environment than in a free field environment.
- In free field, risk of BOP injuries correlate with peak pressure and positive phase duration. This is not necessarily the case in complex wave environments.

- In free field, risk of BOP injuries increases with proximity to the explosive charge. In a complex wave environment, the risk of BOP injuries is not obvious based on the pressure profile. In this scenario, occupants in the corner target positions within the vehicle are more vulnerable to BOP injuries than other target points which are closer to explosive charge.
- Current vehicle validation test standards (AEP-55 vol.2 (Edition 1) [2006], AEP-55 vol.2 (Edition 2) [2006] and NATO-RTO-TR-HFM-148 [2012]) do not evaluate the risk of BOP injuries in the scenario where an explosive charge is detonated within a vehicle. If an explosive charge were to penetrate the vehicle, the vehicle would not “pass” based on the test standards.

The implications of these outputs on the adequacy of test standards in evaluating BOP protection are further discussed in Chapter 8.

5 CLOSE PROXIMITY TO HAND GRENADE CASE STUDY: PRELIMINARY RESEARCH INTO RISK OF BOP INJURIES FOR SCENARIO C

5.1 Introduction

This preliminary investigation involves a case study of an M26 hand grenade incident that occurred just outside Mthatha, in the Eastern Cape of South Africa, in 1998. In this scenario the victims are in very close proximity to a fragmentation munition (i.e. a hand grenade) in an open space.

The M26 grenade is designed to produce casualties through the high velocity fragments that it expels. However, if one is close enough to the grenade BOP injuries (including mutilating injuries) will occur in addition to penetration injuries caused by the fragments. Simulations were conducted to obtain pressure profiles that could be produced by the explosive charge contained in the grenade. Injury predictions were then made using currently available injury criteria and compared one another and to the actual injuries that were sustained by the children. The validity of currently available pressure based injury criteria to predict injuries, when the subject is in very close proximity to the explosive charge, were explored. The significance of BOP injuries in this scenario was evaluated.

Background to collaborative research with Walter Sisulu University

This study came about when the author approached Professor B. Meel in the hope that collaboration could be established to obtain medical inputs into the field of human response to explosive events. The author came across Professor Meel's paper on lightning strike injuries [Meel: 2007] which are said to be similar in nature to blast injuries. He expressed interest in the field and mentioned an incident involving a hand grenade which resulted in the deaths of six children. Professor Meel is head of forensic medicine at Walter Sisulu University (WSU) (based in Mthatha in the Eastern Cape) and he conducted the autopsies of the children following this tragedy. He suggested combining inputs from engineering field, looking at injuries caused by explosive events, with his medical insights in order to create an improved understanding of the injuries caused by the hand grenade incident. Thus, a visit to WSU was arranged to discuss the

case in detail. This led to a paper published in the journal, South African Family Practice [Meel *et al.*: 2009] and a second paper, with more of an engineering focus, being presented at the CSIR Outcomes Conference 2008 [Whyte *et al.*: 2008]. This collaboration also led to a broader collaborative relationship being established between CSIR and WSU (where previously disadvantaged students were given bursaries and opportunities to work with CSIR scientists).

Overview of the incident

This incident involved eight children who were minding cattle when they found, and unintentionally detonated a M26 hand grenade. Six of the children died instantly, and the other two children, who were further away from the grenade when it was detonated, sustained minor injuries.

Blast injury mechanisms for the hand grenade scenario

A fragmentation grenade such as the M26 produces a complex set of injury mechanisms that produce injuries to humans within certain ranges. BOP injuries caused by the direct effects of the blast (blast induced variations in the environmental pressure could occur when the victim is in very close proximity to a grenade containing high-energy explosives. Secondary ballistic injuries due to fragmentation and flying debris will be touched on in this section as, although not the focus of this thesis, this is the mechanism by which the M26 grenade is intended to cause injury. Tertiary injuries, caused by whole body displacement, will not be considered in this section and burns and toxic fume inhalation, will not be considered in this section, but it is noted that burns could possibly be caused if the subject was in the fire ball resulting from an explosive event.

A case study, as is presented in this paper, provides researchers with an opportunity to gauge the validity of criteria that have been developed to predict injuries. As the children were handling the grenade directly at the time of detonation (which would not usually be the case as the grenade is designed to be thrown into the general vicinity of the enemy and relies on the fragments inflicting injury over a 15 m radius). Thus, in addition to the fragments causing serious injury, due to the close proximity of the children to the exploding device, BOP effects may also be observed or cause complications when treating the more visible blast injuries.

5.1.1 Chapter aims

- Are BOP injuries significant in the case of fragmentation ammunition, such as a hand grenade?
- Are currently available BOP injury criteria able to predict injuries at such close proximity to an explosive charge?

5.1.2 Chapter outline

This chapter describes how inputs from simulations (as referenced in personal communications [Snyman: 2008]) and post-mortem injury descriptions [Meel: 2008] were used to compare actual and predicted injuries caused by a hand grenade.

Firstly, the method section described the people responsible for producing simulation data and medical inputs to this study. The results were then described and used to predict BOP injury risk and compare to actual injuries sustained by the victims.

5.2 Method

5.2.1 Overview of method and declaration of work done

Inputs to this case study from the medical field were provided by Professor B. Meel who conducted the autopsies [Meel: 2008]. Dr I. Snyman conducted simulations of the hand grenade in order to obtain pressure profiles at various distances from the explosive charge [Snyman: 2008]. These pressure profiles were then used by the author, together profiles obtained from the literature and currently available injury criteria, to compare predicted BOP injuries with actual injuries.

5.2.2 Summary of medical methodology [Meel: 2008]

Professor B. Meel conducted autopsies on the six children who died during when the M26 hand grenade was detonated. He discussed the findings with the author and supplied a summary of his findings to the author.

5.2.3 Summary of computational modelling methodology [Snyman: 2008]

ANSYS AUTODYN2D software was used to calculate the pressure at three locations of a 160 g spherical TNT charge that approximates the M26 hand grenade [Snyman: 2008]. The explosive and air were modelled with the Euler Gudonov solver in an axial

symmetric geometry. The air and explosive gas were allowed to escape across the boundaries. The ideal gas equation of state models the air and the explosive was modelled with the Jones-Wilkens-Lee (JWL) [Lee *et al.*: 1968] equation of state. The side-on overpressure time histories were calculated at distances of 0.1 m, 0.2 m and 0.5 m from the simulated charge. The face-on or reflected pressure time histories were calculated at distances of 0.2 m, 0.5 m and 1.0 m from the simulated charge.

5.3 Results

5.3.1 Medical results from autopsies

Professor B. Meel noted the following when conducting autopsies on the children [Meel *et al.*: 2009]:

“All children had their ventral aspects mutilated or greatly lacerated. A bluish green substance was deposited over the abdomen and chest. The boy closest to the blast sustained abdominal and chest mutilation, while those near him sustained deep lacerations to the torso. The lungs and intestines were diffusely contused in three of the boys. The two boys who were a considerable distance from the grenade escaped with minor injuries.”

5.3.2 Engineering results from computational modelling

In Figure 49 the side-on BOP time histories at locations 0.1 m, 0.2 m and 0.5 m are shown. The face-on BOP time histories at 0.2 m, 0.5 m and 1.0 m are shown in Figure 50.

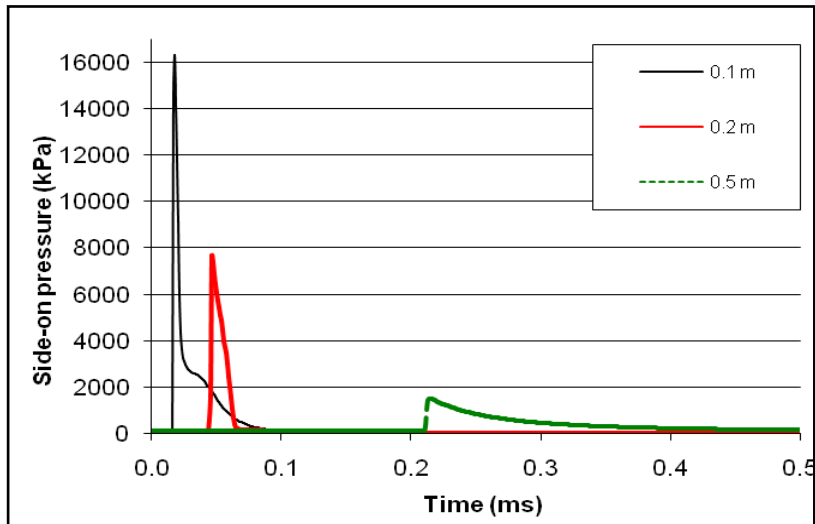


Figure 49: Graph showing simulated side-on pressure predictions at various distances from 160g spherical TNT charge.

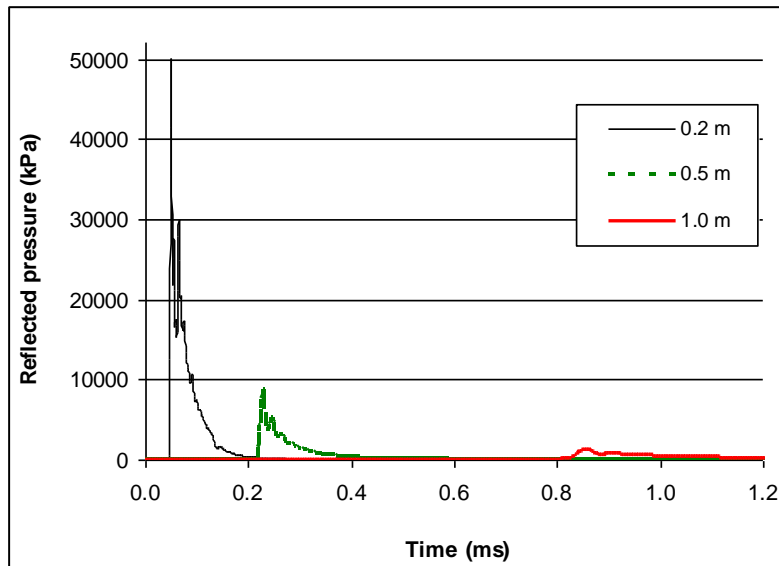


Figure 50: Graph showing simulated reflected (face-on) pressure predictions at various distances from 160g spherical TNT charge.

5.4 BOP Injury Predictions and Analysis

In order to predict BOP injuries, injury criteria can be used based on either the side-on overpressure profile or the reflected pressure profiles. Specifically, the peak pressure value and the positive phase duration of the pressure profiles at certain distances from the charge are required. The computational results were compared to results from the literature before being used, together with existing injury criteria, to predict BOP injury levels at various distances from the hand grenade.

5.4.1 Comparison of simulation of the M26 hand grenade and predicted pressures using BECV4 software

Peak pressure values were obtained from various formulae which, in turn, were derived from experimental results (e.g. [Petes: 1968; Swisdak: 1975; Kinney and Graham: 1985]). Peak side-on BOP values and positive phase durations from BECV4 database and the ANSYS AUTODYN simulations are shown in Table 13.

Table 13: Peak overpressure and positive phase duration at various distances from a 160 g TNT charge from BECV4.

Distance from charge (m)	BECV4 peak side-on BOP (kPa)	BECV4 positive phase duration (ms)	ANSYS AUTODYN peak side-on BOP (kPa)	ANSYS AUTODYN positive phase duration (ms)
0.1	-	-	16330	0.06
0.2	7704	0.1	7661	0.02
0.3	4155	0.2	-	-
0.4	2494	0.3	-	-
0.5	1607	0.7	1507	0.3
1	343	1.1	-	-
15	4	3.5	-	-

The positive phase durations appear fairly different between the predicted BECV4 values and the simulated values. This may be due in part to the threshold value set to determine the start and end of the positive phase. (i.e. The pressure may decrease to nearly 0 kPa, but not actually cross the x-axis for some time, even though the value is very small.)

The peak pressure values from the literature, together with the computational results are shown in Figure 51. One can see that the simulated and BECV4 predictions are very similar.

Note: The ANSYS AUTODYN simulations were based on a spherical 160 g TNT charge, whilst the BECV4 predictions are for a hemispherical 160 g TNT charge. The implications thereof will be discussed further in Chapter 8 Section 8.5.3, but BOP from a hemispherical charge are expected to be higher than those from a spherical charge of the same charge type and mass [Chichester *et al.*: 2001]. This is in line with the predictions in Table 13.

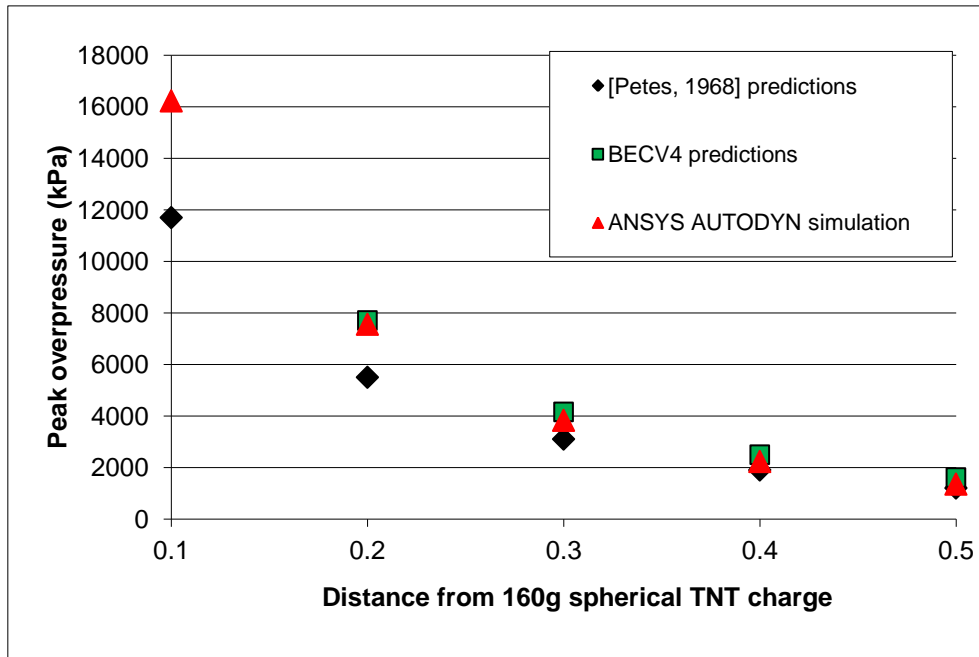


Figure 51: Graph showing the predicted peak side-on BOP values at various distances from a 160 g TNT charge as by simulations and blast calculation software (BECV4).

The computation of the peak reflected pressure at the various locations by ANSYS AUTODYN and from the BECV4 software are shown in Figure 52.

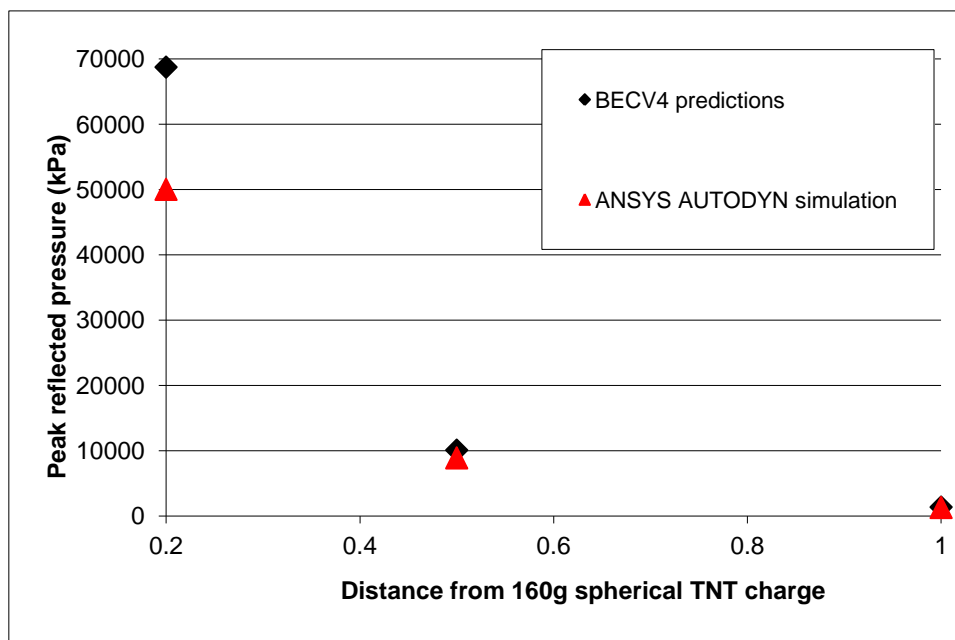


Figure 52: Graph showing the predicted peak face-on (reflected) pressure values at various distances from a 160 g TNT charge as by simulations and in the literature.

5.4.2 BOP injury predictions

The simulated peak side-on BOP and positive phase durations can be used to predict primary injuries at various distances from the grenade. Unfortunately the positive phase durations used in [Bowen *et al.*: 1968] only go down to 0.2 ms and the durations shown in Table 13 for distances less than 0.5 m from the grenade fall below 0.1 ms. However, at 0.5 m from the grenade the positive phase duration is approximately 0.3 ms. The peak overpressure at this distance is approximately 1507 kPa which is above the threshold for lung damage but below the 99% chance of survival curve (as deduced from the curves indicated in [Bowen *et al.*: 1968] for a 70kg man applicable to a free field situation where the long axis of the body is perpendicular to the blast winds.

Using the Bass *et al.* [2006a] criterion for short-duration blasts, at 0.5 m from the grenade (the peak overpressure is 1507 kPa and duration is 0.3 ms), the injury threshold is exceeded and a person would have a 50% chance of survival.

Although it is unclear if the CWVP criterion is valid for positive phase durations of less than 0.4 ms as tests were not conducted for that loading rate, MATLABTM simulations using this criterion were conducted. This was achieved through the use of the pressure profiles obtained from the simulations shown in Figure 50. The results are shown in Figure 53.

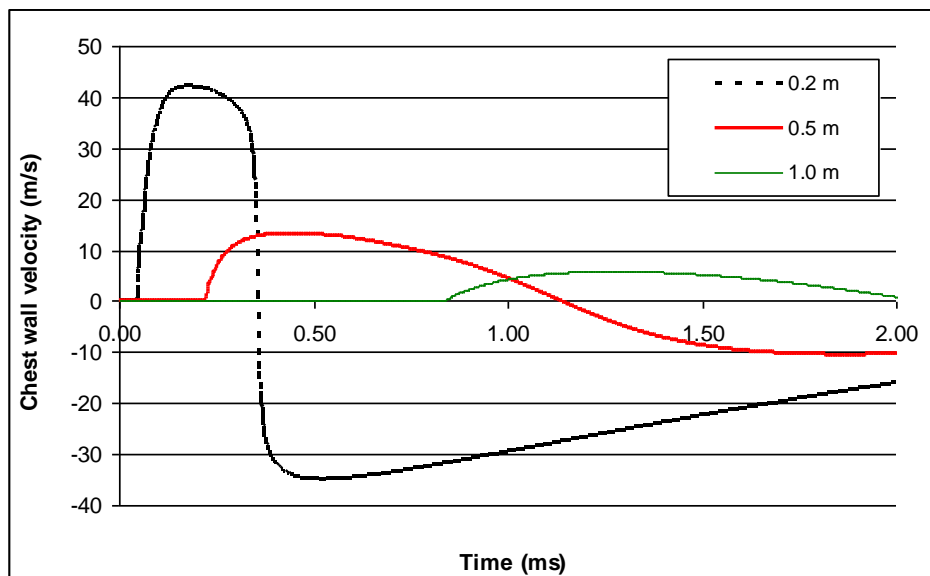


Figure 53: Graph showing the simulated Chest Wall Velocity Predictions for the pressure profiles recorded at various distances from 160g spherical TNT charge.

At a distance of less than or equal to 0.5 m the injury severity was moderate to extensive and corresponded to a greater than 50% chance of lethality [Axelsson and Yelverton: 1996]. At a distance of 1 m the severity decreases to trace to slight or slight to moderate [Axelsson and Yelverton: 1996].

Although the M26 hand grenade has been predicted to cause serious injury using the pressure profile criteria outlined above, as mentioned before, the grenade is primarily designed to produce injury via high velocity fragments. In the simulation conducted to predict the pressure profiles at various distances from the grenade, the velocities of the fragments were also measured. From 0.01 ms it was found that the fragments already achieved peak velocities in excess of 1400 m/s which they maintained until at least 0.3 ms at which stage they are approximately 0.5 m from the original centre of the grenade. The fragments cause damage by transferring kinetic energy to the body tissue which causes the tissue to be damaged [Zajtchuk: 1990]. These high velocity fragments result in the grenade having a 50% casualty radius of 15 m, however the fragments are able to disperse out to 230 m [Denel: no date].

The severity of injuries in very close proximity to the grenade would be more severe due to the dramatic increase in peak pressure values as the distance to the grenade decreases. However, this is speculation and further work to be conducted to understand the injury mechanisms when the body is exposed to excessive peak pressures with very short positive phase durations for which the currently used pressure based injury criteria may not be valid.

Figure 54 shows the regions within which injuries due to primary and secondary injuries caused by a M26 hand grenade may be expected. The grenade is positioned in the centre of the diagram. The orange circles indicate limits described for various levels of injury severity due to primary effects and the black circles indicate areas in which injuries caused by fragments could occur.

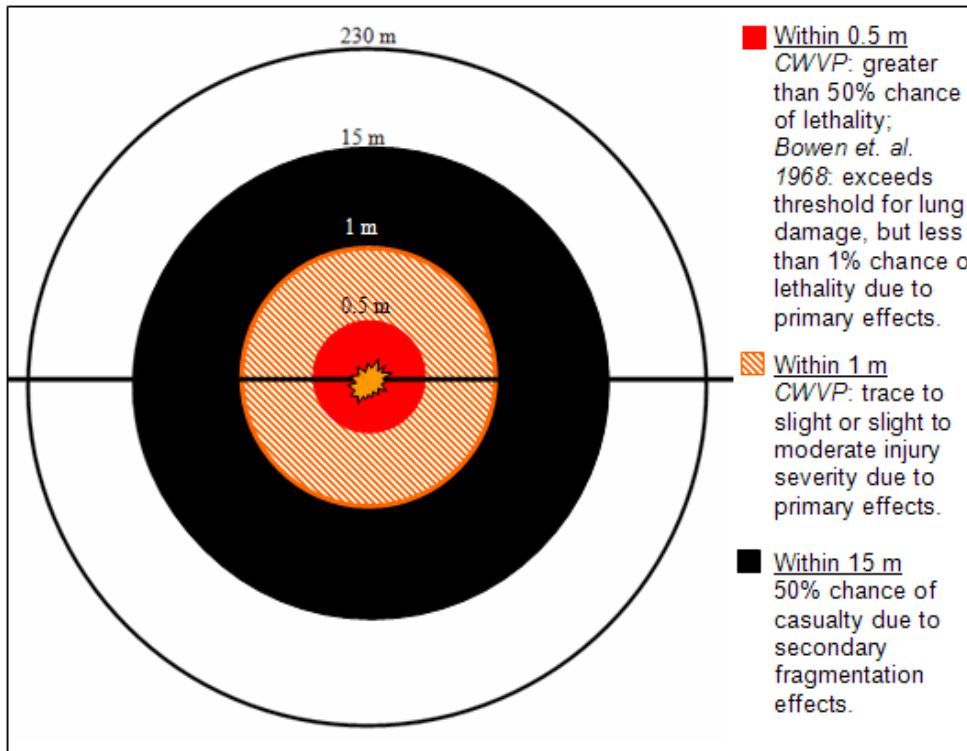


Figure 54: Diagram showing the regions within which BOP injuries and fragmentation injuries caused by a M26 hand grenade may be expected.

5.4.3 Comparison of actual injuries and predicted injuries

By speculating the proximity of the children to the grenade, one can correlate the injuries described in the autopsy reports with the predictions made surrounding the primary and secondary effects of the explosion.

The child holding the grenade could have been within 0.2 m of the grenade and another child could have been within 0.3 m of the grenade. Both **children in the inner circle** could thus have exceeded the threshold for lung damage (Using the Bowen criterion [Bowen *et al.*: 1968]) due to the primary effects of the explosive event. Using the CWVP criterion [Axelsson and Yelverton: 1996], within 0.3 m of the grenade, the children would have a 50% chance of lethality due to the primary injuries which they sustained. They were within the 50% casualty range due to the fragments produced by the grenade.

Four of the children may have crouched over the inner two and could have been within 0.3 m to 0.5 m of the grenade (**children in the outer circle**). At 0.5 m all of the children could have exceeded the threshold for lung damage, however they would have

a less than 1% chance of lethality due to the primary effects of the explosive event alone (Using the Bowen criterion [Bowen *et al.*: 1968]). Using the CWVP criterion [Axelsson and Yelverton: 1996], at 0.5 m the children would have a 50% chance of lethality due to the primary injuries which they sustained. They were all within the 50% casualty range due to the fragments produced by the grenade.

The two **children who witnessed the event** were outside the range of injury due to the primary effects of the blast, but the minor injuries which they sustained may have been due to the fragments which dispersed.

5.4.4 Discussion of explosive event injury criteria and research applications

It can be concluded that the injuries described in the autopsy reports correlate well with the predictions made surrounding the primary and secondary effects of the explosion.

This study focussed on predicting primary injuries caused by the explosive charge, which, although it is understood that the fragments are the intended injury mechanism of the M26 hand grenade, provide insight into the use of current pressure based injury criteria to predict injuries in very close proximity to explosive charges.

It was found that the Bowen criterion [Bowen *et al.*: 1968] and Bass *et al.* [2006a] predicted less severe injuries within a meter of the explosive charge than the CWVP criterion. The differences in severity are highlighted in Table 14.

Table 14: Descriptions of primary injury levels predicted at various distances from the 106 g spherical TNT charge.

Distance from charge	Bowen <i>et al.</i> [1968] predicted injury level	Bass <i>et al.</i> [2006a] predicted injury level	CWVP predicted injury level
0.5 m	Greater than 50% chance of survival	50% chance of survival	Less than 50% chance of survival
1 m	At the threshold for lung damage	Above the threshold for lung damage	Trace to moderate injury (Above threshold for lung damage)
15 m	No lung damage	Below injury threshold	No injury

Predictions of injury severities at distances of less than 0.5 m from the grenade are not included in Table 14 as simulated pressure profiles at 0.1 m and 0.2 m from the explosive charge have positive phase durations of less than 0.4 ms. The validity of the Bowen criterion for pressure profiles with positive phase durations less than 0.2 ms [Bowen *et al.*: 1968] or 0.4 ms for the CWVP criterion [Axelsson and Yelverton: 1996] has yet to be determined. The Bass *et al.* [2006a] criterion can be used for durations as short as 1 ms, but, as with the other criteria, there were few experiments with positive phase duration of less than 1 ms and limited experimental data across the range of durations and pressures for threshold injury tolerance [Bass *et al.*: 2006a]. Further research is required to develop criteria suitable for this loading regime.

5.5 Summary of Chapter Outputs

- Currently available BOP injury criteria are not able to accurately predict injuries at such close proximity to an explosive charge. If one is very close to an explosive charge, the positive phase duration of the pressure profile will be very short. Limited experimental data is available for positive phase durations of less than 1 ms and thus one should not have confidence in results obtained using injury criteria when the duration is this short.
- BOP injuries would influence the severity of injury when people are in very close proximity to the hand grenade (within 0.5 m), but the high velocity fragments that it expels (to a range of up to 230 m) would be the primary concern when protection against such a threat is considered.

6 THE SOUTH AFRICAN WATERMAN IN AN AP MINE SCENARIO: PRELIMINARY RESEARCH INTO THE RISK OF BOP INJURIES FOR SCENARIO D

6.1 Introduction

This preliminary study simulates the situation where a person is not protected by an armoured vehicle (AV), but rather relies on personal protective equipment (PPE) to protect the body against blast effects (or is totally unprotected). Test standards or safety standards are available for a number of different application areas such as

- evaluation of protection offered demining PPE used in the case of humanitarian demining operations,
- evaluation of protection offered to explosive ordnance disposal (EOD) operators who use bomb suits for protection,
- safety standards specifying safe distances from explosive charges where explosive tests are conducted or explosive devices are stored.

In this study, the demining scenario was simulated (with a medium size anti-personnel (AP) blast mine) and measurements were taken by attaching transducers to the South African (SA) Waterman.

6.1.1 Background

The two main test and evaluation standards for PPE in the demining scenario are the North Atlantic Treaty Organisation (NATO) [NATO-RTO-TR-HFM-089: 2006] and the International Mine Action Standards (IMAS) 10.3 [2009]. Both of these standards focus on the ballistic performance of PPE, rather than protection against BOP effects.

The NATO standard states that, “The loads generated by an AP mine, for the body positions considered, were well below the threshold required for blast lung injury” [NATO-RTO-TR-HFM-089: 2006]. The evaluation of BOP injuries is not mandated in the standard, but test setups used by various authorities to evaluate the risk of BOP injuries are provided in an annex to the document. If pressure is recorded in the setups, the Bowen *et al.* [1968] risk curves are then used to predict possible BOP injuries.

The IMAS 10.3 [2009] standard describes specifications for PPE to protect against UXO and AP landmines. It states that the minimum requirement for demining PPE is that it, “shall be capable of protecting the parts of the body that are covered against the blast effects of 240 g of TNT at distances appropriate to the wearer’s activity.” The minimum requirements are protection against fragment/ballistic (V50) at 0.6 m from the 240 g TNT charge, as well as eye and face protection at this distance. Blast resistant footwear and hearing protection is also mentioned. The reader is referred to The European Committee for Standardisation (CEN) Workshop Agreement 15756 [2007] for guidance on the test and evaluation of PPE in humanitarian mine action. This agreement has subsequently been provisionally withdrawn by the CEN due to an inaccurate measurement of the quantity of explosive necessary to carry out the tests [The European CEN Workshop Agreement Withdrawn: no date].

6.1.2 Chapter aims

- Become familiar with the SA Waterman to determine their possible usefulness in future AP blast mine experiments.
- Obtain pressure measurements and use these to calculate the risk of BOP injuries in the demining scenario.
- Use results to evaluate current test standards and methodologies used in the validation of PPE for use in the demining environment.
- Conduct a preliminary test into how different materials mounted on the torso may influence the pressure measurements and how pressure might practically be measured behind these materials (i.e. without the materials directly impacting the transducer, thus complicating the interpretation of the recorded signal).

6.1.3 Chapter outline

The test setup of the explosive charge and four SA Waterman torso surrogates was described, together with transducer details to capture pressure and acceleration measurements. The various materials or PPE that were mounted on the SA Waterman were also described in the method section.

The results were presented followed by an analysis of the validity of the measurements. The validated measurements were then used to calculate the risk of BOP injury and these were compared to empirical BECV4 predictions.

PPE test standards for the demining scenario were reviewed based on the BOP injury predictions.

6.2 Method

6.2.1 General test setup and instrumentation

The SA Waterman was used as a torso surrogate in these tests. The NATO standard for testing PPE against AP mine blast recommends the use of a Hybrid II or a Hybrid III anthropomorphic test device (ATD) [NATO-RTO-TR-HFM-089: 2004]. These ATDs were developed for use in the automotive environment for the evaluation of crush injuries rather than blast injuries and it is mentioned in [NATO-RTO-TR-HFM-089: 2004] that this raises questions regarding the suitability of these ATDs for use in mine tests. The Hybrid III ATD is an expensive measurement device, requiring regular calibration, which may be easily damaged if directly exposed to a blast. Thus, the author used the SA Waterman torso surrogate on which to mount transducers, rather than the Hybrid III ATD.

Accelerometers and pressure transducers were mounted in a hard plastic plate (in a similar manner to how they are mounted when used with the ATDs in vehicle validation testing as prescribed by AEP-55 Volume 2 (Edition 1) [2006] and NATO-RTO-TR-HFM-148 [2012]). This chest plate was then secured to the chest area of the SA Waterman with tape as shown in Figure 55. A steel bracket was manufactured for the SA Waterman to prevent the uniform or test material from directly impacting the pressure transducer which could make the measurement invalid. The bracket is shown mounted on a SA Waterman in Figure 55.



Figure 55: Photograph of a SA Waterman torso surrogate with a bracket mounted on the chest area to protect the chest transducer plate from impact by clothing or PPE.

The four SA Waterman torso surrogates were positioned with the centre of the chest 0.7 m from a 100g TNT-equivalent charge³ (See Figure 56).



Figure 56: Photograph of the experimental setup of the four SA Waterman torso surrogates and pressure probe prior to the test (1. Foam (50mm thick closed cell polyurethane foam); 2. Lexin; 3. Uniform Only; 4. Aluminium Sheet).

³ This mine was developed to represent a medium size AP mine (modelled on a PMA-2 mine). The mine consists of 87 g of pentolite cast in a plastic tube to ensure an explosive charge diameter to height ratio of 50 mm to 68 mm.

The four SA Waterman torso surrogates were instrumented and clothed as per Table 15.

Table 15: Details of instrumentation and clothing or PPE mounted on the SA Waterman torso surrogates.

Number of Waterman	Clothing/PPE	Pressure Transducer Details	Accelerometer Details
1	Uniform and 50mm thick closed cell polyurethane foam	Piezoresistive IC Sensors Model 1471 500 psi Face-on	None
2	Uniform and Lexin sheet	Piezoresistive IC Sensors Model 1471 250 psi Face-on	None
3	Uniform only	Piezoresistive IC Sensors Model 1471 250 psi Face-on	PCB Piezotronics Model 350B21 100000 g Shock accelerometer
4	Uniform and Aluminium sheet	Piezoresistive IC Sensors Model 1471 500 psi Face-on	None

A side-on pencil pressure probe was positioned between SA Waterman 1 and SA Waterman 2 with the sensor at a distance of 0.7 m from the test charge.

The pressure transducers mounted on the SA Waterman torso surrogates were sampled at 10 kHz using the custom built data acquisition unit which consists of a 24 channel signal conditioning unit and a cRIO™ embedded controller from National Instruments™. The data acquisition unit was programmed to acquire 0.25 seconds of pre-trigger data and 1.75 seconds of post trigger data at a sample rate of 10 kS/s. This gives a total of 2×10^4 samples per channel.

The accelerometer and pencil pressure probe data were captured using a Tektronics™ oscilloscope with a sample rate of 100 kHz.

6.2.2 Data analysis and BOP injury predictions

The reflected pressure measurements obtained from the SA Waterman Surrogates were compared to reflected pressures predicted by BECV4. The recorded pressure measurements were processed and plotted in MATLAB™ using the code saved as *watermen_viewer_version1.m* (See Appendix C1). The code for the BOP injury predictions, using the CWVP criterion, was described and validated previously in this

chapter. The input pressures were obtained from the SA Waterman torso surrogate pressure recordings and the ambient pressure on the day of testing (also required for the CWVP calculation) was recorded as 105.1 kPa. The MATLABTM file used for these calculations was saved as *cwvmodel_waterman.m* (See Appendix C1 for full code details and gain and sensitivity details of the data acquisition unit and the pressure transducers).

The accelerometer and pencil pressure probe were processed and plotted in ExcelTM.

The recorded pressures were compared to empirical pressures from BECV4 and both actual and empirical overpressures were used to determine the risk of BOP injury.

6.3 Results

After the test, the uniforms of SA Waterman #2, SA Waterman #3 and SA Waterman #4 had been blown upwards. The SA Waterman torso surrogates were not displaced by the blast (See Figure 57). The uniform of SA Waterman #3 was badly torn (See Figure 58). SA Waterman #1 was damaged by a small stone that caused a 2 mm diameter hole in the plastic of the waterman (See Figure 59). Data was obtained on for all transducers mounted on the SA Waterman torso surrogates, except for the pressure transducer mounted on SA Waterman #4 (the transducer appeared faulty). The accelerometer and pencil pressure probe data captured data.



Figure 57: Photograph of the four SA Waterman Surrogates and pressure probe after the test (1. Foam; 2. Lexin; 3. Uniform Only; 4. Aluminium Sheet).



Figure 58: Photograph of SA Waterman #3 (uniform only) after the test.



Figure 59: Photograph of the small hole in SA Waterman #4 after the test.

The results of the reflected pressure profiles recorded by SA Waterman #1 (foam interface), SA Waterman #2 (lexin interface) and SA Waterman #3 (uniform only interface) are shown in Figure 60.

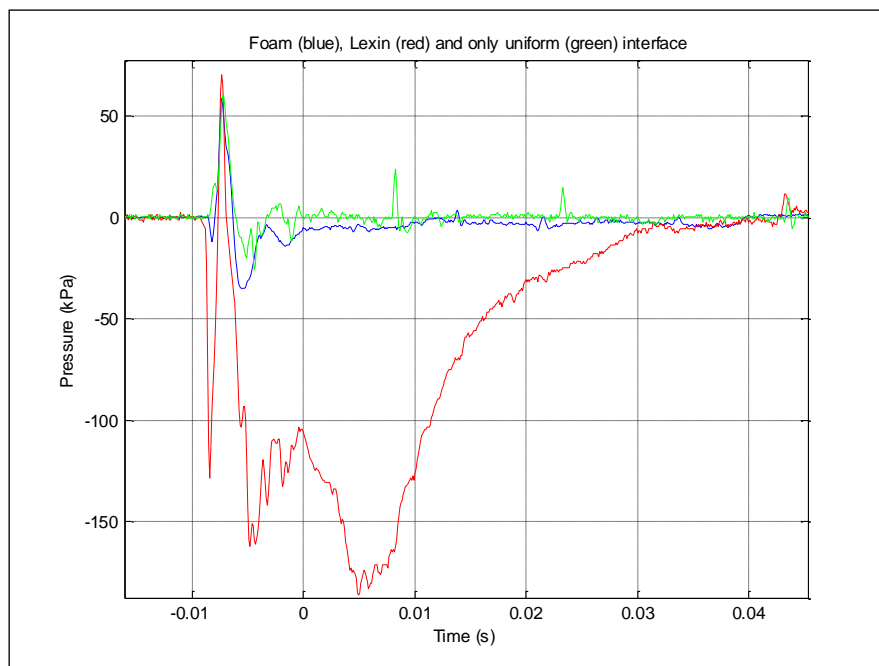


Figure 60: Graph of the face-on pressure profiles captured by transducers mounted on SA Waterman #1 (foam interface), SA Waterman #2 (lexin interface) and SA Waterman #3 (uniform only interface).

The free-field pencil probe recorded a peak pressure of approximately 270 kPa. The signal is shown in Figure 61.

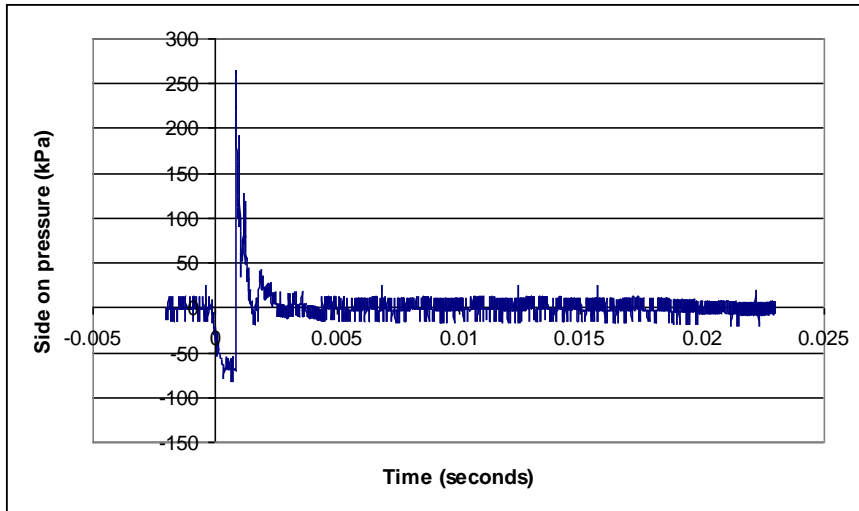


Figure 61: Side-on pressure measured with a pencil probe at approximately 0.7 m from the test charge.

The accelerometer mounted on SA Waterman #3 (behind the uniform) recorded a signal shown in Figure 62.

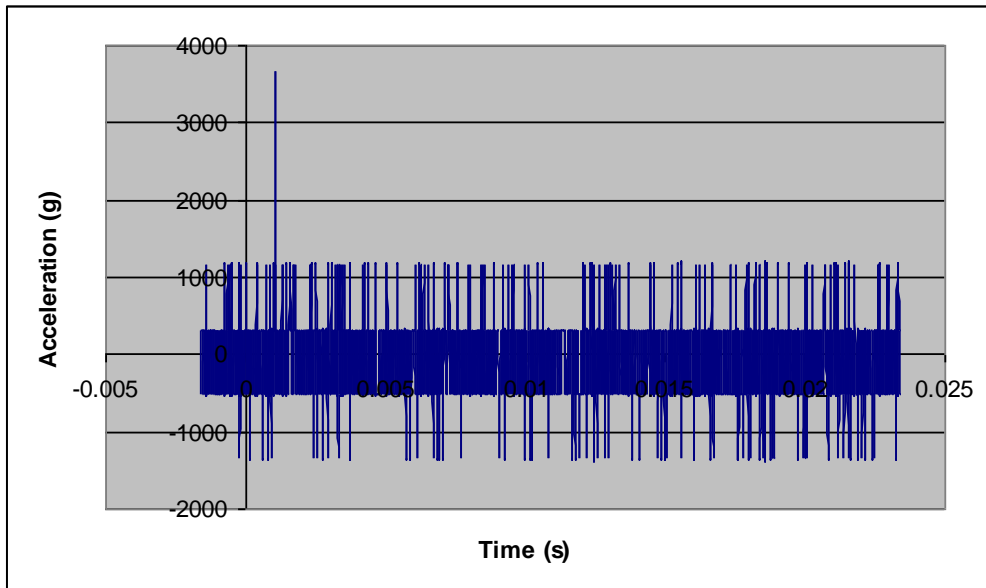


Figure 62: Graph showing the acceleration signal recorded on SA Waterman #3 (behind the uniform only interface).

6.4 BOP Injury Calculations and Analysis

6.4.1 Analysis of SA Waterman face-on pressure measurements and CWVP injury calculations

The peak positive pressures all occur at approximately the same time (See Figure 60). This was expected as the transducers mounted on the SA Waterman torso surrogates were approximately equidistant from the centre of the charge. Unfortunately, the pressure profile for the transducer behind the lexin interface appears corrupted as the extremely high negative pressure values were not expected and the approximately 25 ms duration of the negative pressure peak was not realistic. Thus it was assumed that the transducer was damaged (perhaps due to water leakage from the SA Waterman). The signals that were left to analyse were those obtained behind the foam and the uniform only interfaces as shown in Figure 63.

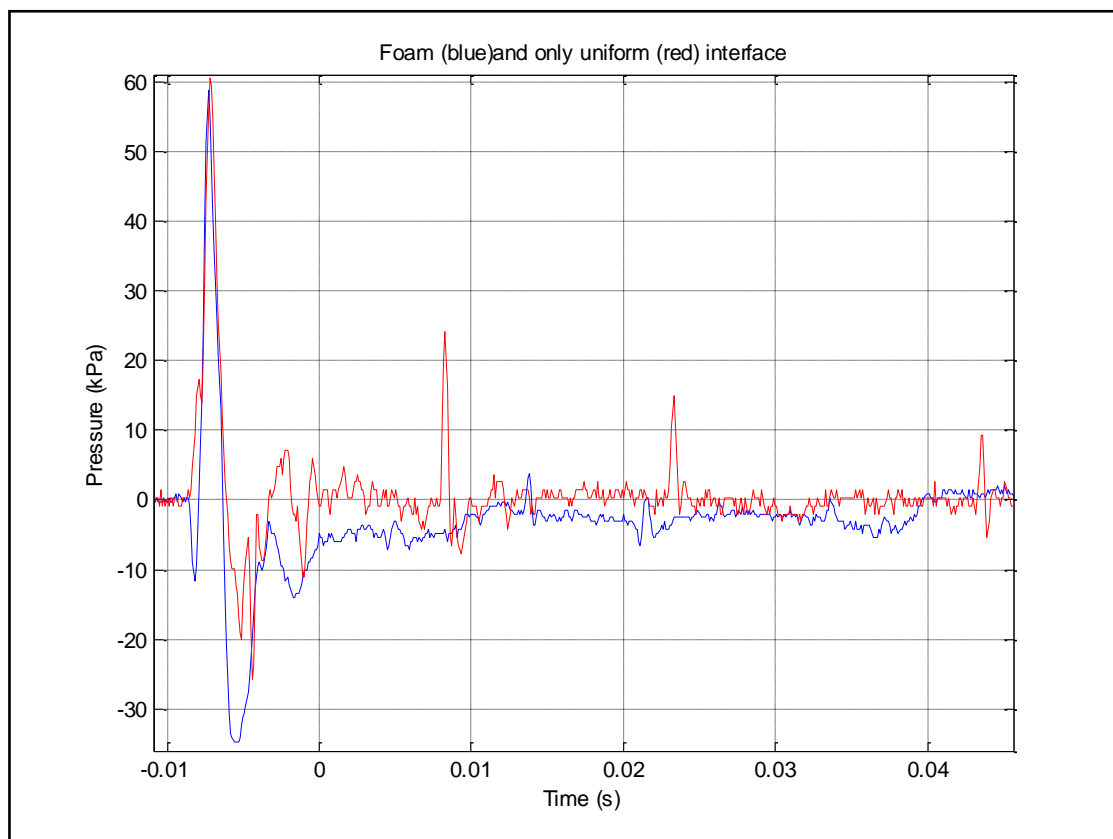


Figure 63: Graph of the pressure profiles captured by transducers mounted behind the foam (blue) and the uniform only (red) interfaces.

In order to verify the results, the pressure values predicted at various distances from a 100 g spherical TNT charge were obtained from the BECV4 calculator and are shown in Table 16 and Figure 64.

Table 16: Peak face-on pressure, peak side-on pressure and positive phase duration at various distances from a 100 g TNT charge from BECV4.

Distance from charge (m)	Peak face-on (reflected) pressure (kPa)	Peak side-on pressure (kPa)	Positive phase duration (ms)
0.5	6630	1156	0.9
0.7	2497	545	1.0
1.0	842	239	1.0
2.0	138	56	1.6

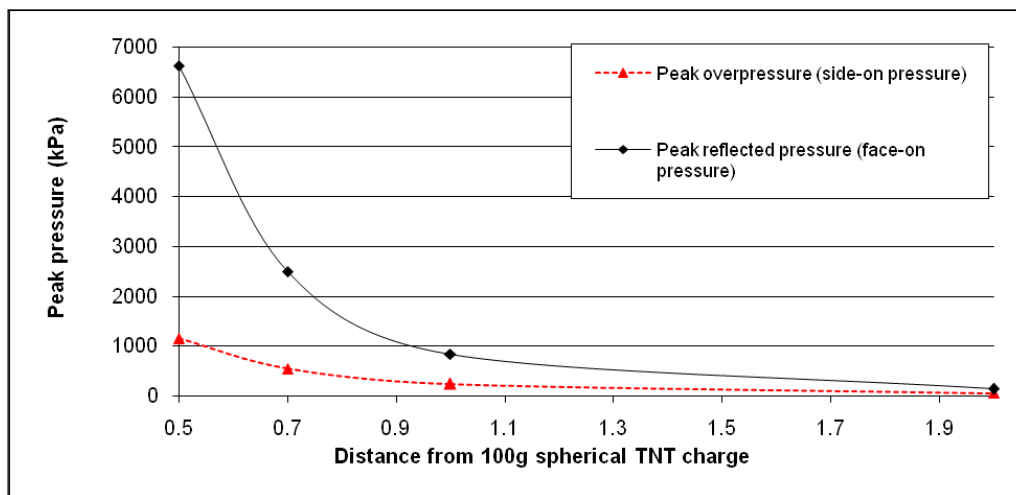


Figure 64: Graph showing the peak reflected and side on pressure values at various distances from a 100 g TNT charge as obtained from BECV4.

The transducers mounted on the SA Waterman Surrogates were face-on transducers, so the expected peak reflected pressure, as predicted by BECV4, was 2497 kPa at 0.7 m from a 100 g TNT charge. However, the BECV4 predictions are for the no protection case, where no interfaces between the charge and the pressure transducer are present. The peak pressure value obtained with the foam interface was approximately 59 kPa and with the uniform only interface the peak pressure was approximately 60 kPa. It was not expected that these interfaces would reduce the peak as significantly as they did.

The sample rate of 10 kHz may be insufficient to record the actual peak. To confirm this theory, further tests must be conducted including a test where no interfaces are present (although there would be a higher risk of damage to the transducers by particles accelerated by the explosive event if no protection or interface is). A sample rate of no less than 200 kHz should be used.

Although it was suspected that reflected pressure profiles that were recorded by the transducers mounted on the SA Waterman torso surrogates were underestimates of the actual peak pressures experienced, these face-on measurements were used to calculate the CWV [Axelsson and Yelverton: 1996]. The CWV that was calculated for the uniform only interface is plotted in Figure 65.

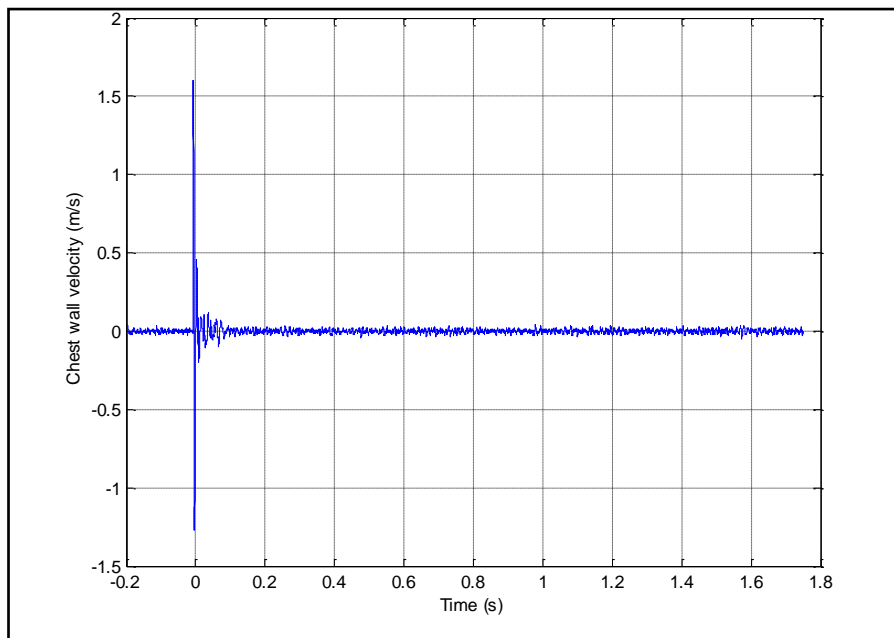


Figure 65: Graph of the calculated CWV using the pressure measured behind the uniform only interface.

The maximum CWV that was calculated for the uniform only interface was 1.6 m/s which was below the threshold for lung damage which occurs at 3.6 m/s [Axelsson and Yelverton: 1996]. Similarly, the CWV was calculated for the foam interface of 1.5 m/s which is also below the threshold for lung injury.

These predicted BOP injuries (based on the actual recorded reflected pressure measurements) do not correlate with the BOP injuries obtained using empirical BECV4

predictions that were discussed earlier. This adds evidence to the argument that the actual experimental measurements were not recorded using a sufficient sample rate.

Although the pressure profile for the lexin interface was determined to be invalid, the CWV was calculated to be 8.89m/s. This high CWV was due to the relatively long duration of the high negative overpressure. If this was a valid pressure measurement this would represent moderate to extensive [Axelsson and Yelverton: 1996] overpressure injuries.

6.4.2 Analysis of free-field pencil probe side-on pressure measurement and injury predictions (using Bass *et al.* [2006a] BOP injury curves)

The free-field pencil probe recorded a peak pressure of approximately 270 kPa (with positive phase duration of 1 ms) (See Figure 61). As shown in Table 16, BECV4 predicts a peak pressure of 545 kPa (with a positive phase duration of 1 ms) at 0.7 m from a 100 g TNT charge. The measured value was less than the value predicted by BECV4. A possible reason for this could be the sample rate as the signal was only sampled at 100 kHz and not at the recommended rate of above 200 kHz. Thus, the actual peak could have gone undetected. Another possible reason for the deviation could be that the values predicted by BECV4 were specified for a spherical charge whereas the actual test charge was cylindrical.

If the BOP injury curve from Bass *et al.* [2006a] is used, the side-on pressure measured by the pencil probe represents injuries that are just below the threshold for lung damage.

Using the empirical BECV4 peak side-on pressure value, the risk of BOP injury was found to exceed the threshold for lung damage, but with a greater than 50% chance of survival (using the Bass *et al.* [2006a] injury curve).

6.4.3 Analysis of SA Waterman #3 accelerometer measurement

The accelerometer mounted on SA Waterman #3 (uniform only interface) recorded the signal shown in Figure 62. The accelerometer was chosen based on tests conducted in [Bouamoul *et al.*: 2007]. The pressure recorded 2.5 m from a 5 kg C4 charge produced a peak pressure reading of 500 kPa which was similar to the 545 kPa predicted pressure by BECV4 at 0.7 m from a 100 g TNT charge. The acceleration measured by a torso

surrogate in [Bouamoul *et al.*: 2007] was approximately 12 755 g. Thus as the acceleration was expected to be greater than 12 755 g, the 100 000 g accelerometer was chosen as the only transducers available for testing at the time were 5 000 g or 100 000 g. Unfortunately, either the acceleration was too low for the transducer to record a reliable signal or the transducer itself was faulty. The peak acceleration recorded was 3658 g, but unfortunately this value was based on only one sample point and thus the result was considered unreliable. In future it is recommended that more suitable accelerometers for the predicted accelerations are used.

6.4.4 Analysis of PPE test standards in the demining scenario

As discussed in the introduction of this chapter, current internationally recognised test standards for PPE in the demining scenario do not require assessment of risk of BOP injuries. Empirical predictions show that with a medium size AP mine (100 g TNT equivalent) at a distance of 0.7 m, the threshold for lung injury would be exceeded. The IMAS standard recommends the use of 240 g TNT mine surrogate at a distance of 0.6 m for testing of PPE for use in demining applications. This is more than double the charge size and the subject is closer to the charge than was considered in this preliminary study, thus, theoretically, the threshold for lung injury would be exceeded. This highlights the need to explore contradictions between what is measured and stated in test standards, versus what is measured in experimental setups or predicted using empirical pressure profiles.

6.5 Summary of Chapter Outputs

- The SA Waterman surrogates provided an inexpensive representative mass on which to mount the transducers. However, the shape of the brackets and the SA Waterman does not allow for a uniform to be fitted as it would be on personnel. It is recommended that an improved instrumented torso surrogate be developed in order to be used in future AP blast mine experiments.
- The reflected pressure measurements that were obtained by the transducers mounted on the SA Waterman surrogates were used with the CWVP criterion and the results were below the threshold for BOP injuries. However, the sample rate was too low and thus the peak pressures may have been underestimated.

- Although current test standards for validation of PPE for use in the demining environment do not require the assessment of risk of BOP injuries, empirical pressure profiles of the same test charges, used together with BOP injury criteria, show that the threshold for lung damage would be exceeded in the specified scenarios. This contradiction should be explored further.
- A comment on how different materials mounted on the torso may influence the pressure measurements was not achieved as the sample rate at which the pressure was recorded was too low to provide reliable results. The brackets mounted on the SA Waterman torso surrogates worked well to prevent direct impact of the pressure transducer by the uniforms and other materials mounted on the torso.

7 DEVELOPMENT OF THE SOUTH AFRICAN TORSO SURROGATE (SATS) AND AP MINE SCENARIO INVESTIGATION (SCENARIO D)

7.1 Introduction

In Chapters 3, 4, 5 and 6, preliminary experimental results were correlated with empirical predictions and test standards were assessed in their ability to predict the risk of these injuries to determine their relevance in that particular scenario. A summary of the four scenarios that were considered, the test standards that were evaluated and a comment on their adequacy in the predicting BOP injuries is provided in Table 17.

Table 17: Summary of comments on applicability of test standards and BOP injury criteria applied in the various scenarios described in this study.

Scenario Description	Blast Test Standards Applied	Comments
Vehicle validation testing (Against threat from blast landmines and IEDs)	AEP-55 Volume 2 [2006], NATO-RTO-TR-HFM-148 [2012]	Standard Adequate. CWVP and VC injury criteria applied.
Explosive event inside vehicle or enclosed space	N/A	Although this scenario is relevant in terrorist attack scenarios, no current test standards exist to evaluate risk of injury should the event originate within the vehicle.
Assessment of BOP injuries from a close contact with a fragmentation hand grenade detonation	N/A	Theoretically, BOP injuries would occur close to the hand grenade, but the fragments are the primary injury mechanism, thus a standard for testing for BOP injuries for a fragmentation munition is not relevant to this study.
Demining scenario (PPE validation testing)	NATO PPE IMAS	Standards Not Adequate. Limited confidence in injury criteria when applied to very short duration overpressure exposures.

The demining scenario was shown to be an area of particular interest as empirical pressure profiles predicted that the threshold for lung damage would be exceeded in a typical demining setup. However, current personal protective equipment (PPE) test standards do not mandate the measurement of pressure profiles to determine the risk of blast overpressure (BOP) injuries (the focus is on the ballistic performance of the PPE).

Whilst the SA Waterman surrogates provided an inexpensive representative mass and torso shape on which to mount the transducers, the shape of the brackets and the SA Waterman itself did not allow for a uniform to be fitted as it would have been on a person. It was recommended that an improved instrumented torso surrogate be developed in order to conduct further research into test standards and injury criteria to be applied in the evaluation of PPE in the demining scenario. Thus, a prototype South African Torso Surrogate (SATS) was developed and tested in an AP mine scenario.

7.1.1 Chapter aims

The aims of this chapter are:

- To develop a SATS prototype and determine the suitability of the apparatus to provide measurements which can be used to investigate BOP effects. Specifically,
 - Do polyvinylidene fluoride (PVDF) foil gauges show promise in obtaining time of arrival measurements of the shock/pressure wave at the surface of and through the body of the SATS?
 - Can the chest plate face-on pressure, side on pressure and acceleration measurements be correlated with one another and used to predict injuries based on currently available injury criteria (i.e. Bass/Bowen/CWVP for pressure and C/VC for acceleration).
- Use pressure measurements obtained using the SATS, and empirical BECV4 [2000] pressure profiles, to determine whether BOP injuries are significant in a typical demining scenario (using a large AP landmine at a standoff of 0.6 m).
- Comment on whether current PPE test standards adequately assess the risk of BOP injuries to the thorax and abdomen due to a large AP mine.

7.1.2 Chapter Outline

The design considerations for the SATS are outlined, followed by a description of the method that was followed and the materials that were used to manufacture the prototype SATS. The transducers with which the SATS was equipped were listed.

A preliminary AP mine test was then conducted using the SATS prototype to determine which measurements were useful, or potentially useful, in the research of injuries caused by explosive events.

SATS pressure measurements were used to calculate the CWVP to predict the risk of BOP injuries (primary injuries). Secondary injuries were noted (as it was necessary to protect the SATS transducers from fragments/soil ejecta from the blast), but tertiary injuries such as behind armour blunt trauma, injuries caused by the global movement of the body as it is thrown backwards or burn injuries were not considered in this study.

The BOP injuries predicted as a result of the blast were compared to empirical BOP injury predictions (using BECV4 generated pressure profile data). The contradictions between currently available overpressure injury threshold values and adequate BOP injury assessment in recognised PPE test standards were then discussed.

7.2 Method

7.2.1 Design and development of the SATS prototype

The SATS was designed to enable the exploration of BOP and blunt trauma effects across various blast scenarios. However, in this thesis, the SATS was used only in the demining scenario.

The SATS was required to be relatively inexpensive and robust so that it could be directly exposed to explosive events (as in the demining scenario). Although this prototype SATS was not designed to be used initially as part of a PPE test standard, the materials selected and method in which it was created were chosen to allow for the process to be repeated as closely as possible should further SATS rigs be required in the future.

Various torso rigs and ATDs were reviewed prior to the development of the SATS in order to select appropriate materials with which to simulate the torso and specifically

the chest wall and abdomen deflection, velocity and acceleration characteristics (due to an impact or pressure wave exposure). These included:

- The **Hybrid III 50th percentile male ATD** which was originally developed for vehicle safety purposes [NHTSA: no date]. This ATD represents the average male of a USA-population between the 1970s and the 1980s with a height of 1.72 m, an erect sitting height of 0.88 m and a weight of 78 kg. The weights of the Hybrid III upper and lower torso are 17.2 kg (37.9 lbs) and 23.0 kg (50.8 lbs) respectively [NHTSA: no date] (Total torso weight: 40.2 kg). The upper torso contains 6 high strength steel ribs with polymer based damping material to simulate human chest force-deflection characteristics and the standard instrumentation includes a thorax rotary potentiometer to measure the chest deflection (or sternum deflection). The lower torso contains an abdominal insert of urethane foam with a vinyl skin that can be removed to access the lumbar spine instrumentation. The standard abdominal insert does not contain instrumentation.

The major advantage of using this ATD is that the response to impact is well characterised and chest displacement values can be related to a risk of thoracic injury using established injury criteria and injury assessment reference values that were developed for the Hybrid III specifically.

Disadvantages are that the Hybrid III ATD is very expensive and the validity of measurements taken during blast loading are not well validated and similarly the injury criteria associated with the Hybrid III ATD are mostly only valid for automotive impacts which are slower than blast events.

- The original **blast test device (BTD)**, as described by Axelsson and Yelverton [1996] was used in the development of the chest wall velocity predictor (CWVP). The BTD consists of a cylinder that represents the human torso, on which four pressure transducers can be mounted.

An advantage of using this rig is that the response can be directly related to an injury criterion that was developed for use in blast testing (i.e. the CWVP). A disadvantage is that deming PPE or body armour cannot be easily mounted on the cylinder as it does not closely resemble a human thorax.

- **Plate “chest simulator”** [Nerenberg *et al.*: 2000] was developed by Med-Eng Systems Inc. was used to evaluate stackings of armour materials or lamination samples in Nerenberg *et al.* [2000]. The “chest simulator” consists of a rigid, non-compliant, curved aluminium plate that is 12.7mm thick and has a contour that is roughly similar to the human torso (See Figure 66). Pressure transducers are mounted flush at the surface. Results obtained using the “chest simulator” were shown to reflect similar trends in protection offered by various lamination samples as those obtained using a Hybrid II ATD [Nerenberg *et al.*: 2000].

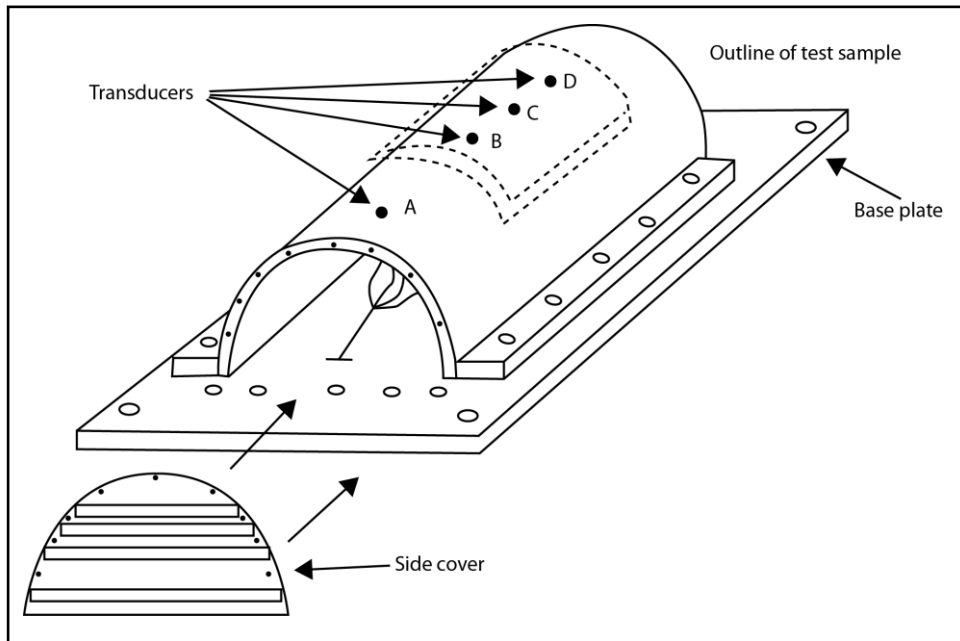


Figure 66: A diagram showing the location of the pressure transducers and the structure of the “chest simulator” used to evaluate stackings of armour materials or lamination samples (From [Nerenberg *et al.*: 2000]).

- **The Mannequin for the Assessment of Blast Incapacitation and Lethality (MABIL)** developed by Defence R&D Canada, Valcartier [Oullet and Williams: 2008] (See Figure 67). The MABIL is essentially a deformable polyurethane thoracic surrogate whose shape is base on the 1988 US Army anthropometric database and is considered to be representative of the 50th percentile Canadian soldier. It is instrumented with accelerometers located at the mid-sternum and navel position. The membrane thickness at the front and sides is 20 mm increasing to about 150 mm at the back to give a spine-like rigidity.



Figure 67: The Mannequin for the Assessment of Blast Incapacitation and Lethality (MABIL) developed by Defence R&D Canada, Valcartier [Bouamoul *et al.*: 2007].

The MABIL torso surrogate membrane is cast from Shore A 70 (PU70) polyurethane which is a visco-elastic material that has been used to represent the behaviour of the human thorax under dynamic loading caused by behind armour blunt trauma [Bouamoul *et al.*: 2007].

- Other rigs developed for behind armour blunt trauma (BABT) effects, include DSTL's BABT thoracic rig and the DRDC Valcartier and Biokinetics and Associates Ltd. BABT rigs [Bourget *et al.*: 2002]. These are membranes shaped in a curve to represent the thorax and mounted on a rigid plate. The deformation corridors were then established due to various impacts and compared to established corridors for the human thorax and pig thorax. The third generation thorax developed by Biokinetics and Associates Ltd. comprised of a 30 mm thick membrane and the Shore A hardness of the materials under consideration for use as a thorax stimulant ranged between 20 and 50.

Taking the above thorax designs into account, a well defined silicone was selected to allow for repeatable casting procedures should more SATS test rigs be required. As the thorax was to comprise of two lungs with a solid section between them that would add stiffness to the frontal impact direction of the thorax, a Shore A hardness of 40 was selected. SORTA-ClearTM 40 was selected. It cures at room temperature with

negligible shrinkage and has a tensile strength of 800 psi which would make the SATS robust.

An abdominal insert of Dragon Skin™ was cast to represent the fleshy organs of the abdomen with a Shore A hardness of 20.

The abdominal insert was cast and allowed to cure overnight prior to casting the outer membrane of the SATS. The dimensions of the abdominal insert were 125 mm by 295 mm, tapering in depth towards the groin area. A mould was created by hot moulding a lexin sheet around shaped florists foam (Oasis) (See Figure 68).



Figure 68: Photograph of the mould created in order to cast the abdominal insert of the SATS.

The florists foam was then removed and the Dragon Skin™ was poured into the mould.

It is worth noting that the procedure to prepare both the Dragon Skin™ and the SORTA-Clear™ 40 involved mixing Part A and Part B of the mixtures and then placing the solution under vacuum suction to ensure that air bubbles introduced during the mixing process were removed (See Figure 69) (air bubbles could influence the properties specified for the silicone materials).



Figure 69: Photograph showing vacuum generated to remove air bubbles from the Dragon Skin™ mixture.

The abdominal insert was then placed together with a steel “skeleton” into a torso mannequin mould. The two hollow air-containing lungs with a hollow trachea exiting at the neck were created by placing a shaped mould made out of florists foam (Oasis) into the torso mould before the silicone was poured (See Figure 70). The foam was later scraped out via the trachea once the silicone had set. The outer layer of the thorax and abdomen was cast using SORTA-Clear™ 40 which was chosen to simulate the deflection characteristics of the chest wall.

During the casting process, experimental piezoelectric polyvinylidene fluoride (PVDF) film gauges were attached at points through the abdomen and thorax as follows:

- Abdomen front: on the front outside of the torso (See Figure 72),
- Abdomen middle: on the front of the abdominal insert (See Figure 70),
- Abdomen back: on the back of the abdominal insert prior to casting the outer layer of the torso (See Figure 71),
- Thorax front: on the front outside of the torso (See Figure 73),
- Thorax middle: on the wall of the lung cavity that is closest to the front of the torso,
- Thorax back: on the wall of the lung cavity that is closest to the back of the torso.

The aim of the PVDF gauges was to see whether the time of arrival of the shock wave at various locations in the SATS could be determined during an explosive test. The remainder of the instrumentation was installed after the SATS had been cast. The final weight of the SATS was 39.0 kg.

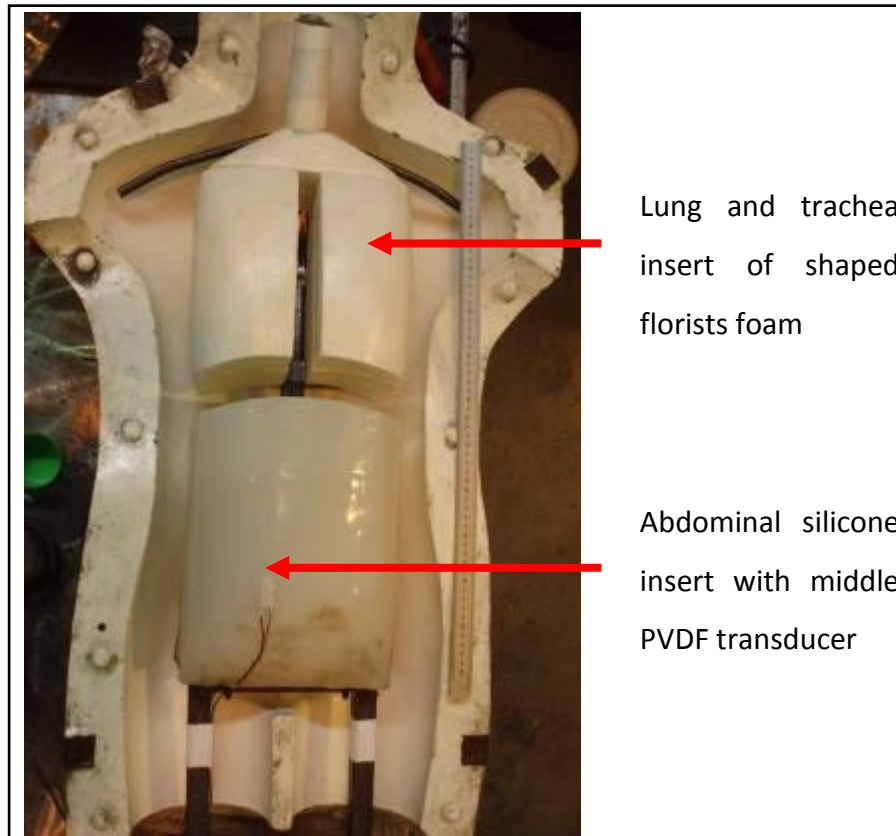


Figure 70: Photograph of the lungs and abdominal insert secured on a steel frame prior to casting the outer layer of the SATS.



Figure 71: Photograph of the abdominal insert prior to casting the outer layer of the SATS with the back PVDF transducer.



Figure 72: Photograph of the abdominal section of the SATS, after casting the outer layer, with the front PVDF transducer positioned (above the top of the middle PVDF transducer that cannot be seen here).

7.2.2 SATS instrumentation

The SATS was instrumented with a number of transducers in order to monitor various parameters during the explosive event. Table 18 shows the full list of transducers that were installed in the SATS.

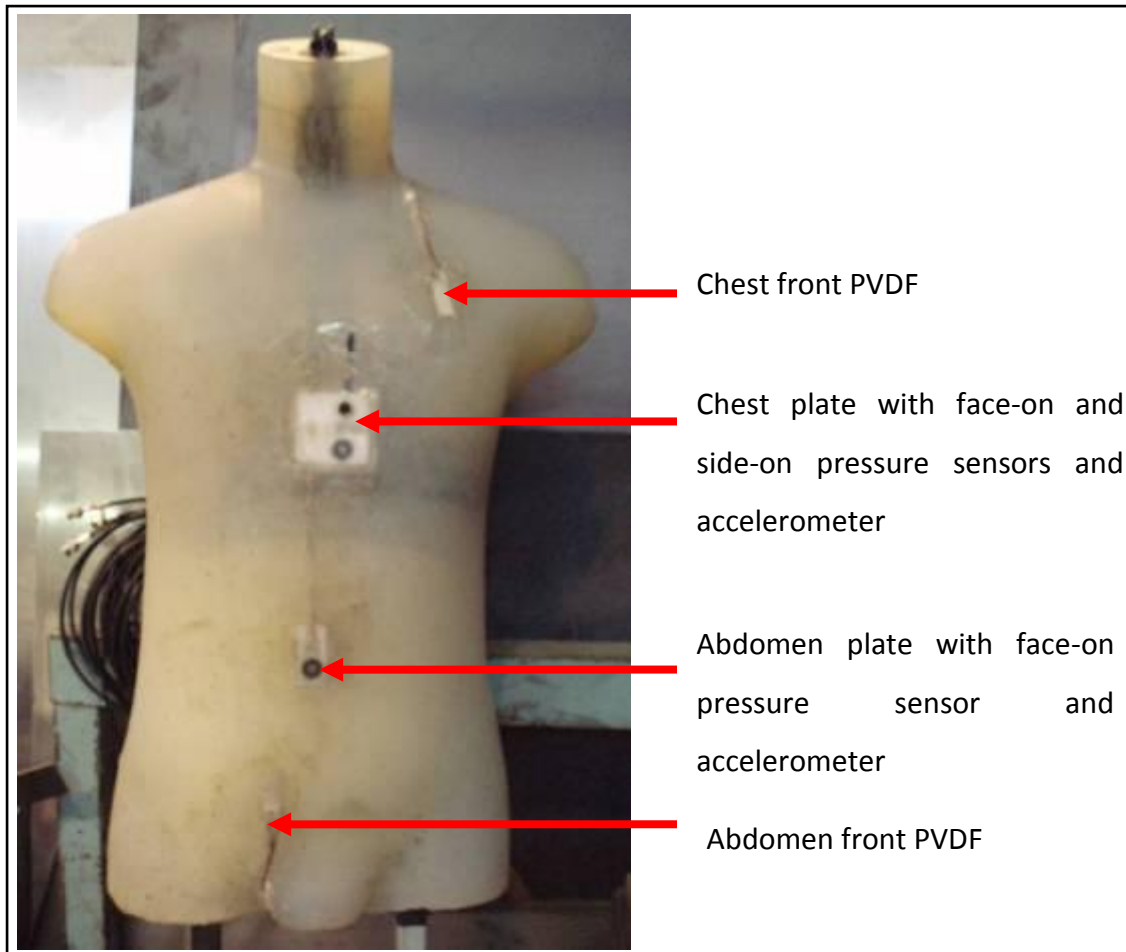


Figure 73: Labelled photograph of the SATS to show transducers.

Table 18: Sensor specification for the SATS.

Sensor description	Model	Serial number	Range	Sensitivity
Chest Accelerometer	350B03	26525	10000g	0.397 mV/g (@100 Hz)
Abdomen Accelerometer	350C02	26570	50000g	0.097 mV/g (@100 Hz)
Chest face-on pressure sensor	109B01	6370	551580 kPa for 6V output	10.48 mV/MPa
Abdomen face-on pressure sensor	109B01	6369	551580 kPa for 6V output	10.48 mV/Mpa
Chest plate side mounted pressure sensor	102A12	13120	1379 kPa for 5V output, 2758 kPa for 10V output	(average 3.6 mV/kPa)
Abdomen internal face-on pressure	102A12	16887	1379 kPa for 5V	(average 3.6 mV/kPa)

Sensor description	Model	Serial number	Range	Sensitivity
sensor			output, 2758 kPa for 10V output	
Head Acceleration (Ax)	350B50	26295	10000g	0.541mV/g (@ 100Hz)
Head Acceleration (Ay)	350B50	26295	10000g	0.524mV/g (@ 100Hz)
Head Acceleration (Az)	350B50	26295	10000g	0.548mV/g (@ 100Hz)
Chest front PVDF	Piezo	n/a	None	None
Chest middle PVDF	Piezo	n/a	None	None
Chest back PVDF	Piezo	n/a	None	None
Abdomen front PVDF	Piezo	n/a	None	None
Abdomen middle PVDF	Piezo	n/a	None	None
Abdomen back PVDF	Piezo	n/a	None	None

The SATS was fitted with a hard plastic chest plate (similar to that described in AEP-55 [2006] and NATO-RTO-TR-HFM-148 [2012]) in which a face-on pressure sensor and accelerometer were mounted (See Figure 74). A section of steel pipe was threaded through the plastic plate and connected to flexible plastic pipe that travelled into the lung cavity and out of the back of the torso. A pressure sensor was mounted side-on to the pipe with the purpose of measuring the unobstructed pressure wave moving through the pipe.

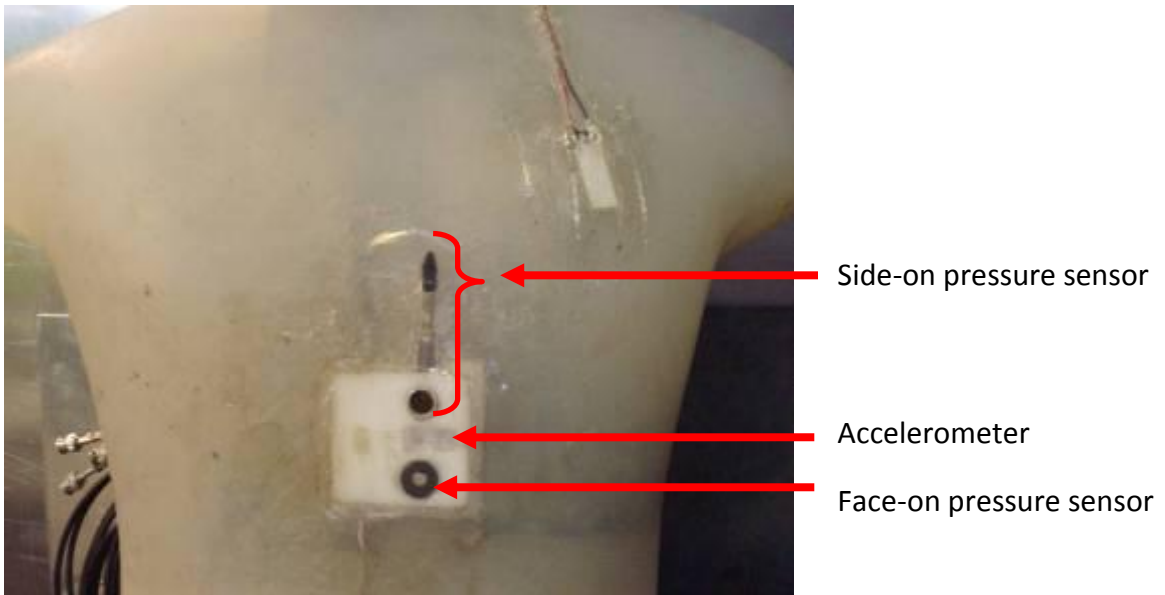


Figure 74: Labelled photograph of the SATS chest plate to show the chest accelerometer, chest face-on pressure sensor and the chest side-on pressure sensor with vent hole through the torso.

The cables were routed through the lung cavities and through sealable holes in the back of the torso and secured with bolts onto the steel frame on the back of the torso (See Figure 75).



Figure 75: Labelled photograph of the SATS to show transducers.

Although a number of measurements were recorded for basic research purposes, only the chest face-on pressure measurement was necessary to calculate the CWVP injury criterion used to predict possible BOP injuries.

7.2.3 Ethical considerations for AP mine test

Table 19 shows the Safe Operating Procedure (SOP) for performing blast tests at the CSIR Detonics, Ballistics and Explosive Laboratory (DBEL). This was part of the ethical considerations of this work as safety is paramount when conducting tests using explosives.

Table 19: DBEL Safe Operating Procedure (SOP) specifications

SOP Title:	DURING BLAST TESTING
SOP number:	DBEL – 990003 - 103
SOP Title:	SAFE OPERATING PROCEDURE FOR THE FIRING OF EXPLOSIVES USING FS-43 FIRING PACK
SOP number:	DVEL – 990013 - 103

7.2.4 AP mine and SATS test setup and data processing

A stand was manufactured in order to suspend the SATS in a position to simulate kneeling and leaning over a mine (See Figure 76). The centre of the chest of the SATS was 0.60 m from the AP mine and the nose of the SATS was 0.62 m from the AP mine.

The rig was designed such that the SATS was free to fall over backwards to simulate the tertiary effects (i.e. the effect of being propelled backwards) of the explosive event. Foam mats were positioned behind the SATS to prevent damage to the SATS should it fall backwards during the event.

The SATS was clothed in a bomb suit with ballistic protection to ensure that it was not severely damaged during the test. The suit consisted of a NomexTM (245 gsm) outer shell, inserts of multiple layers of KevlarTM and a clear polycarbonate chest plate insert.

A 208 g pentolite charge was used to represent a large AP mine (See Figure 77) and it was buried at a depth of 0.02 m.



Figure 76: Photograph showing the positioning of the SATS (wearing protective clothing) and the stand in relation to the AP mine and the splinter proof shelter.



Figure 77: Photograph of the 208 g pentolite charge.

The protection against fragments was assessed to ensure that the SATS transducers were not compromised during the blast. The European Committee for Standardisation CEN Workshop Agreement [2007] was employed which specifies a woven cotton fabric witness sheet covered with a non-adhesive cling film. For this test Mutton cloth (Builder's Pride™) was stretched over the SATS (See Figure 78) and covered with Gladwrap™.



Figure 78: Photograph of the SATS covered with a Mutton cloth layer to test for any penetration effects.

All data acquisition equipment was positioned inside a mobile splinter proof shelter (See Figure 79).



Figure 79: Photograph of the mobile splinter proof shelter in which the data acquisition equipment was placed.

Three data acquisition units were used to record measurements during the blast (See Figure 80):

- Scope1 (Tektronix TPS 2024),
- Scope2 (Tektronix TPS 2024) and
- GraphtecTM (Graphtec Corporation, GL1100).

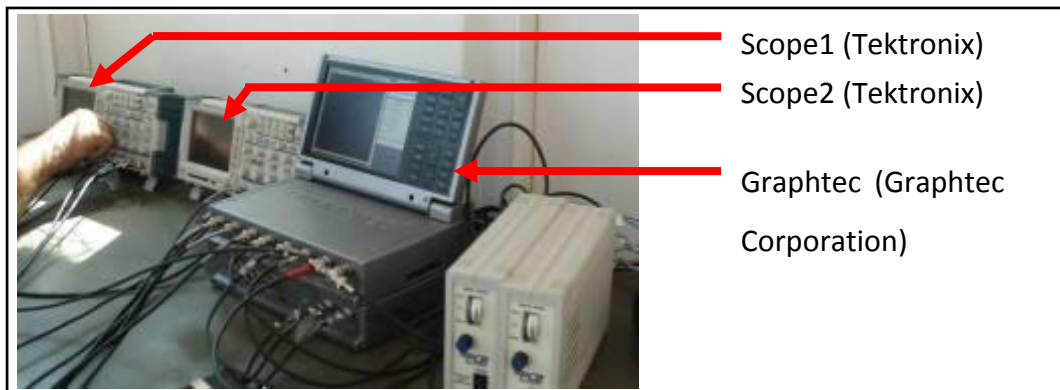


Figure 80: Labelled photograph of the data acquisition equipment inside the mobile splinter proof shelter.

The description of which data acquisition unit and which channel number was used to record the signals from each transducer was recorded in Table 20. The GraphtecTM sampled the data at 1 MHz for 65 ms (including 40 ms of pre-trigger data), whilst Scope1 and Scope2 sampled the data at 100 kHz for 25 ms seconds (including 2.5 ms of pre-trigger data).

Table 20: Record of data acquisition unit and channel number associated with each SATS transducer for the AP mine test.

Sensor description	Data acquisition unit	Channel number
Chest Accelerometer	Graphtec Scope1	1 1
Abdomen Accelerometer	Graphtec	2
Chest face-on pressure sensor	Graphtec	3
Abdomen face-on pressure sensor	Graphtec	4
Chest plate side mounted pressure sensor	Graphtec	5
Abdomen internal face-on pressure sensor	Graphtec	6
Head Acceleration (Ax)	Graphtec	7
Head Acceleration (Ay)	Graphtec	8
Head Acceleration (Az)	Graphtec	9
Chest front PVDF	Scope1	2
Chest middle PVDF	Scope1	3
Chest back PVDF	Scope1	4
Abdomen front PVDF	Scope2	2
Abdomen middle PVDF	Scope2	3
Abdomen back PVDF	Scope2	1

The aim was to trigger all data acquisition units (including the camera) and to detonate the explosive charge simultaneously. This was to enable SATS transducer measurements to be compared to the camera footage to see if the visual time of arrival of the blast wave front could be correlated with a time of arrival indicator in the measurements. In order to accomplish this, the trigger cable was run from the firing unit to the mobile splinter proof shelter to trigger all the data acquisition units. The

control unit was inside the main splinter proof shelter (from which the explosive charge was detonated and from which researchers observe the event) approximately 70 m from the explosive. The camera was also triggered using the output from the control unit and was positioned next to the main splinter proof shelter (See Figure 81).



Figure 81: Photograph of the test setup in relation to the main splinter proof shelter and to the camera.

The camera that was used was a portable, rugged Photron Ultima APX-RS Fastcam camera that can withstand shocks of up to 100 g. It can record up to 10 000 fps at full resolution (1024 x 1024) and up to 250 000 fps at reduced resolution. For this test the camera was set to record at 20 000 fps.

Data Processing and BOP Injury Predictions

The recorded measurements were processed and plotted in MATLABTM using the code saved as *plot_SATS_041108_plotfinal.m* (See Appendix D1). The input pressure was obtained from the SATS chest face-on pressure recording and the ambient pressure on the day of testing (also required for the CWVP calculation) was recorded as 101.33 kPA.

The chest plate acceleration was integrated to obtain the chest plate velocity and the chest plate displacement was also used to predict possible thoracic injuries. This was performed in MATLABTM using the file saved as *plot_SATS_041108_chestdispandvel.m* (See Appendix D1).

The velocity obtained from the CWVP criterion was compared with the velocity obtained using the chest plate acceleration and the injuries that were predicted were discussed.

7.3 Results

During the test, the SATS was thrown backwards onto the foam mats (See Figure 82). The front collar of the bomb suit was found approximately 3 m from the SATS and the back collar was found approximately 20 m from the SATS. The polycarbonate protective insert in the suit was shattered.



Figure 82: Photograph of the SATS after the AP mine test.

When the suit was removed, it was found that only a single penetration had occurred. Although the actual penetration hole was very small, it could be easily identified by inspecting the Mutton cloth (See Figure 83 and Figure 84).



Figure 83: Photograph of the SATS with protective clothing removed to enable the Mutton cloth layer to be inspected for signs of penetrations.



Figure 84: Photograph showing a penetration of the Mutton cloth layer by a small stone on the right shoulder of the SATS.

Data was captured by all of the transducers, except the triaxial accelerometer in the upper neck/head region of the SATS. This was due to the cable detaching from the transducer during the event, possibly due to the air compressing in the lung cavities and moving up through the trachea cavity. It can be seen in Figure 85 that the mounting of the transducer was bent upwards.



Figure 85: Photograph of damaged triaxial head accelerometer.

Although the abdomen face-on pressure sensor, the abdomen accelerometer, the chest plate side mounted pressure sensor and the abdomen internal pressure sensor all captured data, the data was found to be corrupt (containing discontinuities at different times) and thus could not be used for analysis.

That left the PVDF signals, the chest plate acceleration and chest plate pressure profile for analysis.

The abdominal and chest PVDF signals for the first 25 ms of the blast are shown in Figure 86 and Figure 87 respectively (See Section 8.2.1 for a description and photographs of the positioning of the PVDF sensors in the SATS). It must be noted that the units of the PVDF signal are arbitrary as they have not been calibrated, thus only the time axis should be considered relevant.

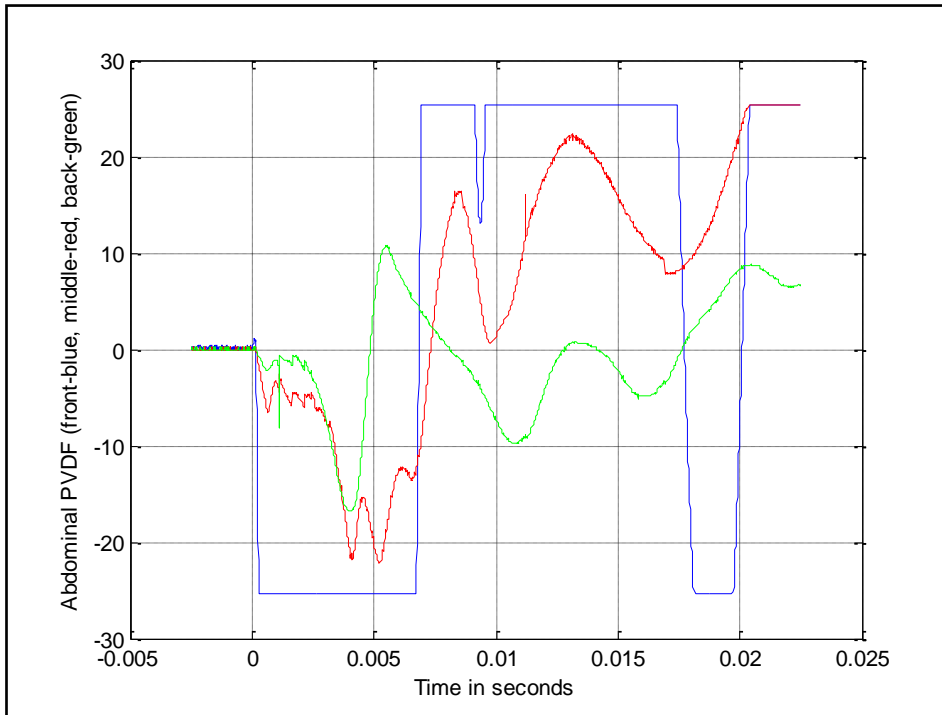


Figure 86: Graph of abdominal PVDF signals (front – blue; middle – red; back – green).

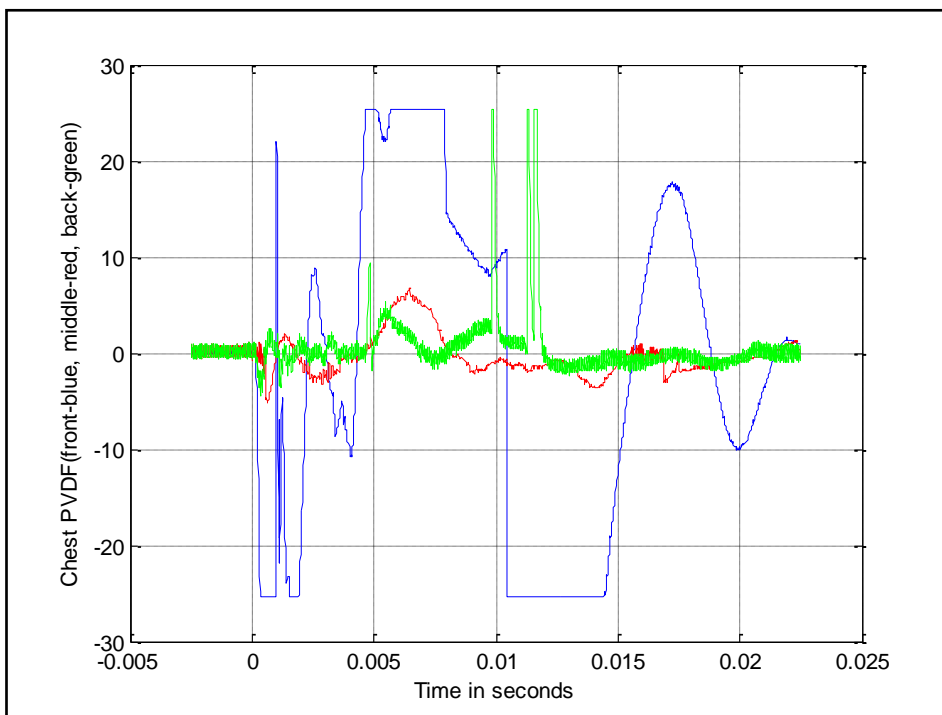


Figure 87: Graph of chest PVDF signals (front – blue; middle – red; back – green).

The chest plate acceleration measurement was set up to be captured by both Scope1 and the Graphtec data acquisition unit at the same time to enable the process of simultaneous data collection to be assessed. These signals are shown in Figure 88.

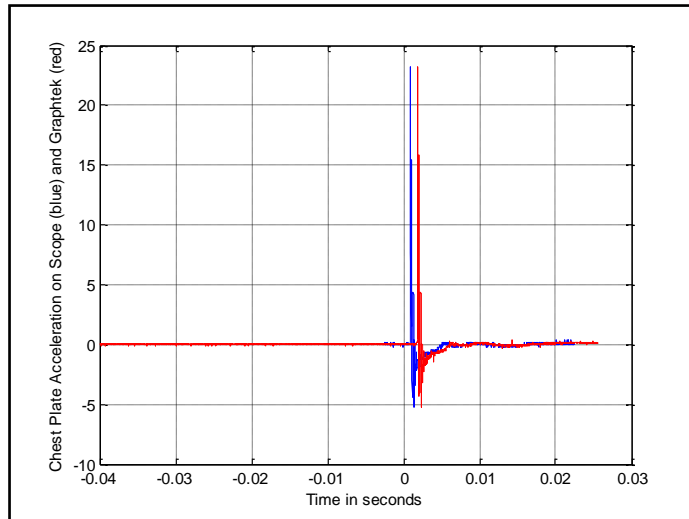


Figure 88: Graph showing the chest plate acceleration signal recorded by both the Scope1 (blue) and the Graphtek (red) data acquisition units.

The chest face-on pressure measurement shown in Figure 89 (Note that to calculate the CWVP, the “spikes” in the data were filtered whilst ensuring that the peak pressure was not compromised. This will be discussed further in the next section).

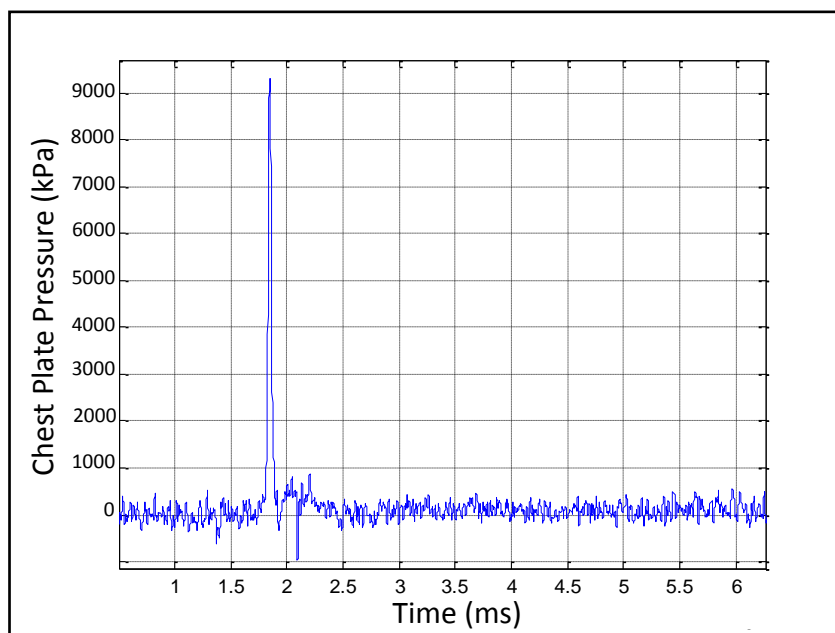


Figure 89: Pressure profile obtained from the SATS chest plate face-on pressure sensor.

Still frames of camera footage recorded during the AP mine test will be discussed in the following section.

7.4 BOP Injury Predictions and Analysis

7.4.1 Correlation of SATS measurements and camera footage

All data acquisition units (including the camera) were triggered simultaneously with the detonation signal so that it could be determined which phases of the blast the various transducers were capturing. In particular, the PVDF gauges were explored to determine whether they were able to respond to the time of arrival of the shock wave (pressure wave) and to provide insights as to how the wave travels through the SATS.

However, this proved more complicated than expected as the data acquisition units were not triggered simultaneously with one another. This was observed by linking the chest acceleration signal to both Scope1 and to the Graphtec™ data acquisition unit and comparing the recorded data. Figure 88 in the results section shows the same signal as recorded by the two different data acquisition units. Figure 90 shows the delay of approximately a 1 ms between the start of the acceleration signal captured by the Scope1 unit and the signal captured by the Graphtec unit. This delay is almost as long as the duration of the signal itself which is significant. This delay must be taken into account when comparing the timing of events based on data captured by different data acquisition units.

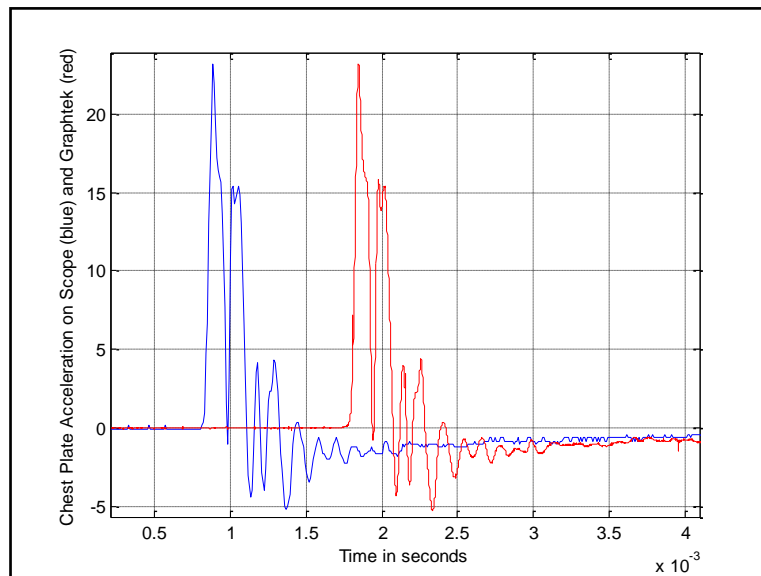


Figure 90: Graph showing the chest plate acceleration signal recorded by both the Scope 1 (blue) and the Graphtec (red) data acquisition units (zoomed in view).

To give an indication of the significance of this time delay, the camera footage at 0.9 ms (the start of the chest plate acceleration signal recorded by Scope 1 is at about 0.8 ms) and at 2.0 ms (the start of the chest plate acceleration signal recorded by the Graphtec data acquisition unit is at about 1.8 ms) is shown in Figure 91.



Figure 91: Still frames of the camera footage from the blast at 0.9 ms (left) and 2 ms (right).

The cause of this delay may be due to the time taken for the signal to travel through the connecting nodes of the coaxial cable. This was not expected to be a problem as the cable linking the data acquisition units was approximately 0.5 m. However, in the field of detonics and explosive effects, where crucial events happen so quickly when the area of interest is very close to the explosive charge, a small time delay can negatively influence the accuracy of results. This is a good example of why understanding what transducers are actually measuring versus what one expects them to measure, or what they are designed to measure, is so important.

Another delay was found in the triggering of the camera and the triggering of the detonation. The camera shows the start of the fireball of the blast and soil ejecta prior to the camera being triggered (i.e. this initial phase of the blast was captured by the pre-trigger data recorded by the camera, instead of the camera being triggered

simultaneously with the detonation signal). Figure 92 shows the camera footage captured at -0.05 ms where the light from the detonation can already be seen and by 0.00 ms the detonation is well underway. This shows that the camera was only triggered after the detonation had already begun.



Figure 92: Still frames of the camera footage from the blast at -0.05 ms (left) and 0 ms (right).

Again, this may be due to the speed of the signal travelling through the different cables that were used to trigger the camera and the explosive charge. However, this is a smaller time delay than that observed between the chest acceleration signals as captured by the two different data acquisition units.

The PVDF film sensors were used to see if the time of arrival of the shock/pressure wave through the SATS (from front to back) could be determined. The zoomed in view of the first 1 ms of the data captured by the sensors mounted through the abdomen is shown in Figure 93.

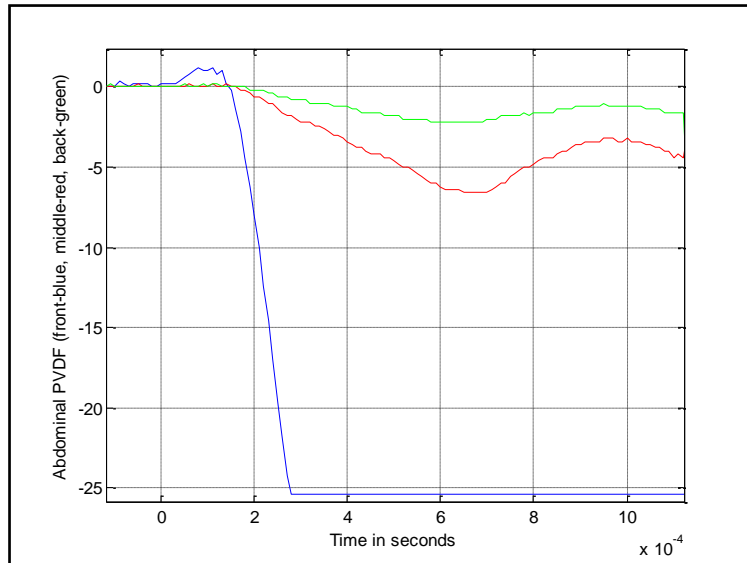


Figure 93: Graph of abdominal PVDF signals (front – blue; middle – red; back – green) zoomed in view of the first 1 ms.

As mentioned previously, the magnitude of the curves was not meaningful as the sensors were not calibrated, but the time of arrival (when a signal appears from the noise) could be determined. Figure 93 showed that the front of the abdomen responded to the blast first (blue), at about 0.03 ms after Scope 2 data acquisition unit was triggered. The middle PVDF sensor (mounted on the front of the abdominal insert) responded next (red) at about 0.15 ms and finally, at about 0.18 ms the back PVDF sensor (mounted on the back of the abdominal insert) responded (green).

Looking at the chest section of the SATS (See Figure 94), the PVDF on the front of the chest responded to the blast first (blue), at about 0.07 ms after Scope 1 data acquisition unit was triggered. The back PVDF sensor (mounted on the wall of the lung cavity that is closest to the back of the torso) responded next (red) at about 0.17 ms and, at about 0.4 ms the middle PVDF sensor (mounted on the wall of the lung cavity that is closest to the front of the torso) responded (green).

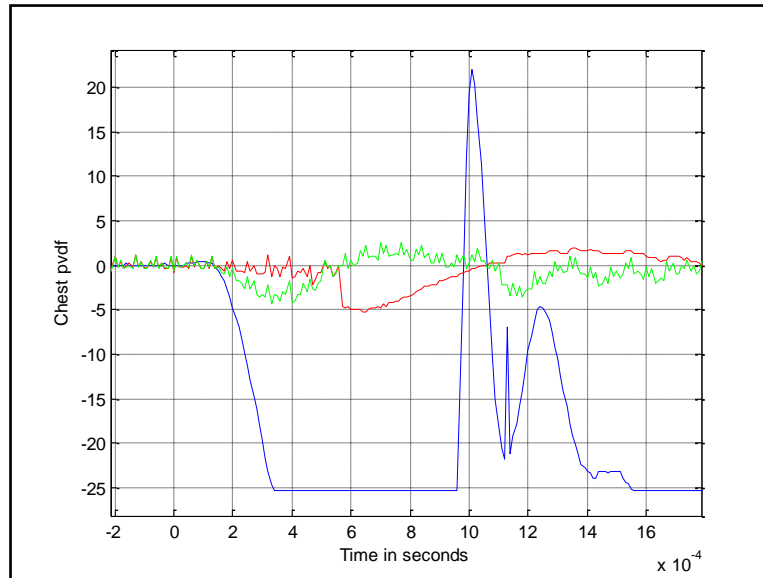


Figure 94: Graph of chest PVDF signals (front – blue; middle – red; back – green) zoomed in view of the first 3 ms.

This was not as expected as the front sensor was expected to respond first, followed by the middle sensor and finally the back sensor – as was the case with the PVDF sensors mounted through the abdominal section of the SATS. This could be due to poor attachment of the PVDF films inside the lung cavity as it was difficult to get the film to adhere to the wall which was not as easy to access as the outside surface of the SATS. In the abdominal section of the SATS, the middle and back PVDF films were cast firmly and permanently in place between the abdominal insert and the outer layer of silicone.

Looking the speed at which the PVDF sensors respond compared to, for example, the accelerometer sensor, Figure 95 shows the front chest PVDF signal (blue) and the chest plate acceleration signal (red) that were both captured by Scope1. The chest PVDF responds much more quickly to the blast event, at about 0.07 ms, than the chest plate accelerometer which first records a signal at about 0.8 ms. In fact, all the PVDF sensors, throughout the SATS, responded within 0.4 ms of the triggering of Scope 1. Thus, the PVDF film sensors show good potential for use in time of arrival studies or to determine the speed at which a wave arrives at or passes through an object. There are however disadvantages to using these sensors, such as susceptibility to temperature changes.

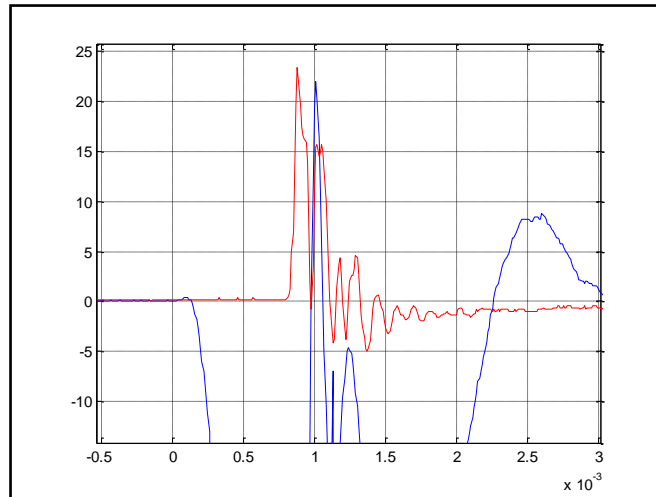


Figure 95: Graph of front chest PVDF signals (blue) and chest plate acceleration (red) zoomed in view of the first 3 ms (both captured by Scope 1).

In terms of predicting BOP injuries, the chest plate pressure is significant as it is used to calculate the CWVP injury criterion which, in turn, gives an indication of the severity of possible BOP injuries. The time at which the chest plate pressure sensor starts to respond is the same as the time at which the chest plate accelerometer starts to respond (See Figure 96). This was as expected as both transducers were mounted on the same hard plastic chest plate. This provides confidence in the pressure signal that will be used to calculate the risk of BOP injury in the next section.

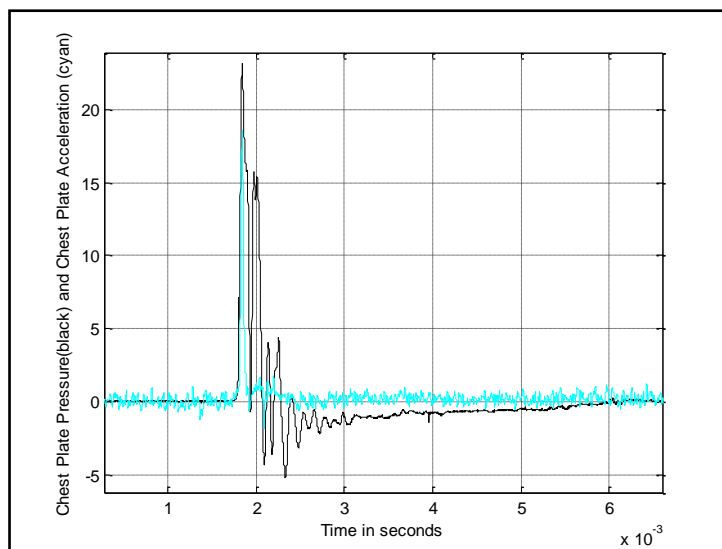


Figure 96: Graph of chest plate pressure signals (cyan) and chest plate acceleration (black) zoomed in view of the first 7 ms (both captured by the Graphtec data acquisition unit).

Although it is uncertain which phase of the explosion (as seen in the camera footage) is captured by the pressure sensor and the accelerometer, the BOP injury criteria were derived based on pressure measurements that were correlated with BOP injury severity.

7.4.2 BOP injury prediction based on experimental SATS test results

In order to predict BOP injuries to the thorax and abdomen caused by the detonation, the face-on pressure signal from the chest plate of the SATS was used (See Figure 97). The peak pressure value was 9230 kPa.

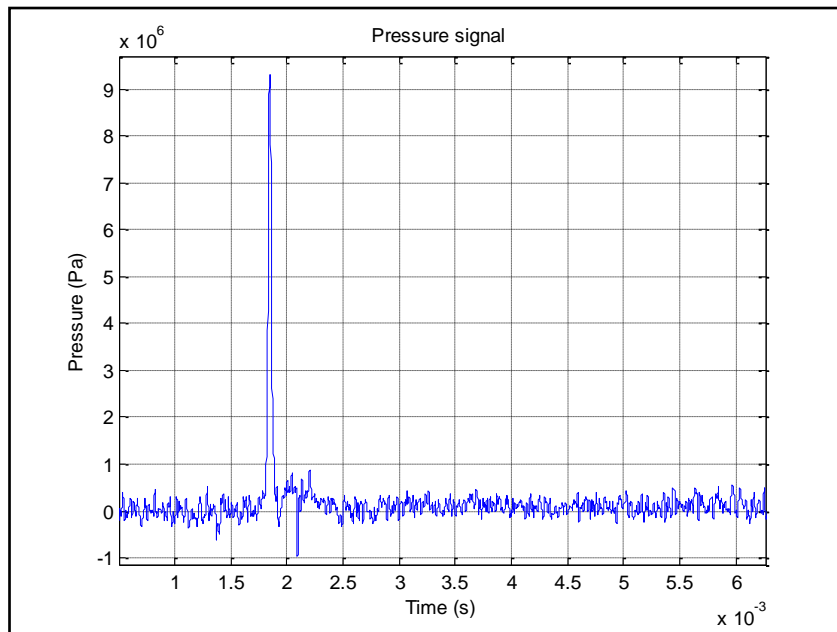


Figure 97: Pressure profile obtained from the SATS chest plate face-on pressure sensor.

As it was a complex wave environment behind the body armour, the CWV [Axelsson and Yelverton: 1996] was calculated based on the pressure signal. The peak CWV was determined to be 10.3 m/s (See Figure 98). This represented moderate to extensive injury levels, but was still less than 12.8 m/s, above which the chance of survival would be less than 50%.

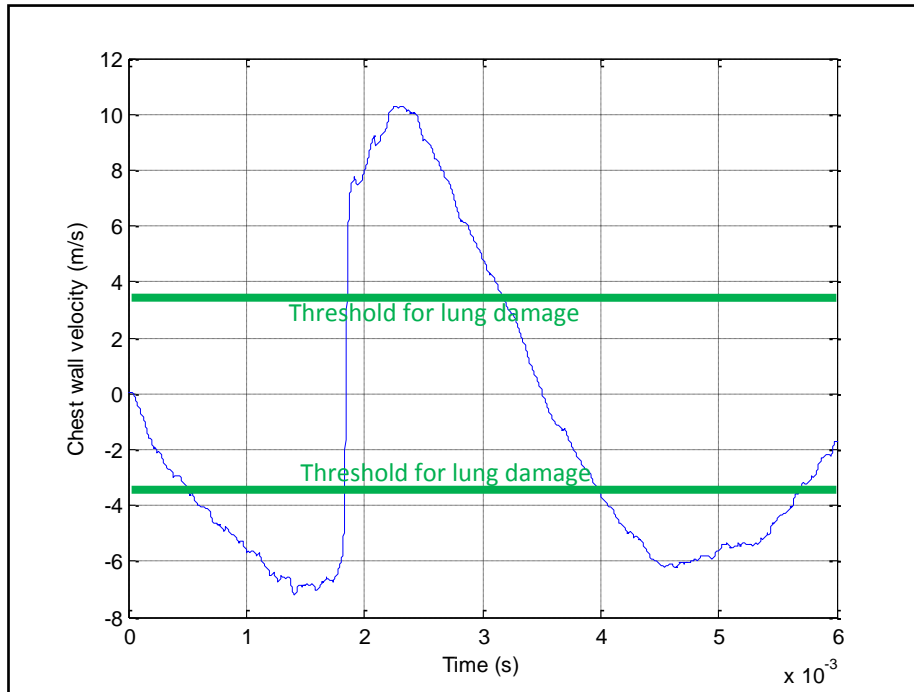


Figure 98: Calculated CWV from the pressure profile obtained from the SATS chest plate face-on pressure sensor.

Further injury calculations using the chest acceleration measurements and empirical BECV4 predicted pressure profiles will be discussed in Chapter 9. A general discussion of the applicability of various injury criteria (i.e. The Compression Criterion (CC) and the Viscous Criterion (VC)) to be used in the demining scenario will also be investigated in Chapter 9.

7.5 Summary of Chapter Outputs

- The SATS was developed and tested in the demining scenario. Although some of the data was found to be corrupt, the PVDF measurements, chest plate face-on pressure measurement and the chest plate acceleration measurement were obtained. Thus,
 - the PVDF film gauges provided promising time of arrival results which could possibly be used to investigate which phase of the blast is responsible for causing BOP injuries.
 - The SATS fulfilled its goal to provide measurements with which the risk of BOP injury could be calculated.

- BOP injuries were found to be significant in a typical demining scenario based on injury predictions from both the SATS experimental measurements and BECV4 empirical pressure profiles.
- Current internationally recognised PPE test standards do not adequately assess the risk of BOP injuries to the thorax and abdomen due to a large AP mine.
 - The SATS predicted moderate to severe overpressure injuries due to the recorded pressure measurements. However, it is unclear whether the currently available injury criteria are suitable for predicting these types of injuries caused by AP landmines. In addition, no current internationally recognised PPE test standards include the measurement of pressure behind body armour. This issue requires further investigation as the experimental results together with the currently available injury criteria highlights the fact that overpressure injuries may in fact be more severe with the use of body armour than if no armour was used. This conclusion has appeared in the literature, but the results do not agree with the injuries reported in the DDAS (or statements in many PPE test standards).

8 GENERAL DISCUSSION OF CHAPTER OUTPUTS

The aim of the study was to evaluate the adequacy of internationally accepted test standards in determining the level of protection offered against blast overpressure injuries.

A test standard will be deemed *adequate* if:

- BOP injuries are not predicted in the scenario under consideration, thus the evaluation of protection against these injuries is not necessary;
- OR

The test standard mandates that the risk of BOP injury be determined using currently available measurement methods and injury criteria for the scenario under consideration

AND

the limitations of the test standard are fully described/disclosed. (i.e. the reasons for selecting the best available injury criteria, whether they under or over predict injuries for certain scenarios, for which conditions they are strictly valid, the assumptions made when test charge surrogates/torso surrogates are used, for which conditions the test scenario reflects the operational scenario).

In order to reach conclusions regarding the above, the following questions were posed in the preceding chapters of this thesis:

- What are BOP injuries?
- How are BOP injuries identified?
- How can we predict possible BOP injuries?

The first two questions lead to a discussion as to whether BOP injuries are a cause for concern in each of the scenarios considered in this thesis (See Section 8.1 and Section 8.2). As the demining scenario was identified for further exploration, the rest of the discussion considers the adequacy (or availability) of test standards to evaluate

protection concepts for this scenario. Section 8.3 looks at the ability of various injury criteria to predict BOP injuries in the demining scenario based on SATS test results and empirical BECV4 predictions.

The adequacy of test standards used to evaluate BOP injury risk and the limitations of these predictions are discussed (See Section 8.4) and some of the contradictions that were found between test standard specifications, predicted BOP injuries and real BOP injuries are explored (See Section 8.5).

The implications of the limitations of internationally recognised test standards on the development of BOP injury protection strategies will then be considered (See Section 8.6).

8.1 Identification and Prevalence of BOP Injuries

In most blast scenarios, a number of different blast injury mechanisms occur simultaneously which makes it difficult to assess the true effect of BOP. In addition, the methodology used to assess the injuries will influence which injuries are detected [Mayorga: 1997].

The identification and quantification was studied in Chapter 3 using rat lungs exposed to shock tube generated BOP. Although the results were not as expected, the difficulties inherent in tests using animal subjects were discovered. The MATLAB™ program reduces the subjectivity involved in the process of visually identifying the percentage lung contusion based on photographs of lung samples. The ability to identify and quantify injuries was highly dependent on methodology specifications (such as the perfusion process). It was also noted that many other studies did not include sham or control subjects, thus making comparison of injured and uninjured subjects impossible.

The ability to correctly identify BOP injuries will influence the reported prevalence of BOP injuries. Kirkman *et al.* [2011] suggest that the occurrence of BOP (blast lung) injuries may be underestimated in current military casualties as blast lung injuries are often excluded when they co-exist with other injury types (such as fragment injuries to the torso or broken ribs).

There is much debate regarding the prevalence of BOP injuries in general. Cooper [1996] reports that blast lung was a common injury amongst soldiers killed by explosions in Northern Ireland, where 11% of them sustained lung damage with no other apparent injuries. However, most often, BOP injuries are grouped together with blast injuries in general (including fragment injuries etc.) and thus it is difficult to ascertain the prevalence of BOP injuries in particular.

In the armoured vehicle scenario, ear drum ruptures, lung and intestinal injuries are reported, but the assumption hold true that if the vehicle integrity is assured (i.e. No breach of the occupant compartment) then BOP injuries are unlikely [Dosquet *et al.*: 2004; Nelson *et al.*: 2008; Ramasamy *et al.*: 2011; Radonic *et al.*: 2004; Medin *et al.*: 1998]. However, one point to note in this scenario is that when injuries do occur in this scenario, they are usually serious and often fatal [Radonic *et al.*: 2004].

Examples of the scenario where an explosive event occurs inside a vehicle or enclosed space, could occur in terrorist attacks such as bombs or IEDs detonated within busses, cars or trains. These incidents result in a high number of BOP injuries (most often along with mutilating and/or penetrating injuries). For example, Katz *et al.* [1989] described injuries due to a 6 kg TNT bomb explosion in a civilian bus in Jerusalem. BOP injuries were found in the 29 people that were hospitalised, with 76% showing ear drum perforations, 38% showing blast lung and 14% with abdominal blast injuries (including bowel perforations). Other terrorist attacks include the London Underground 7/7 attacks where 56 people were killed and the Madrid train bombings where 191 people died with 63% of the critically ill patients having blast lung injuries [de Ceballos *et al.*: 2005; Hepper *et al.*: 2011]. In a military scenario, shaped charges or explosively formed projectiles (EFPs) may breach the occupant compartment, however, the peak BOP measured experimentally are too low to cause significant BOP injuries [Jacobson and Schmidt: 1999; Held: 2008].

In the close proximity to a hand grenade in open space scenario, if a person is close enough to the hand grenade to be injured by BOP injuries, the fragmentation effects and mutilating blast effects will be the main concern for protection standards.

In the demining scenario, people may be injured by BOP, mutilating effects if in direct contact with the mine (brisance or shattering effect), fragmentation effects and whole body motion due to blast winds. According to the United States Department of Defense Humanitarian Demining R&D Program, mine and explosive remnant of war casualties occur in every region of the world and cause 15 000 to 20 000 injuries each year [United States Department of Defense (U.S. DoD) Humanitarian Demining R&D Program: 2013]. They say the numbers of casualties are increasing due to local recycling of unexploded ordinance for its scrap metal value.

The injury mechanisms described in NATO-RTO-TR-HFM-089 [2004] are burns, BOP and fragmentation, where direct injuries include respiratory tract injuries, ear injuries. Indirect injuries include those due to the elastic deformation of PPE caused by the push of the air shock and detonation products, body translation and fragmentation [NATO-RTO-TR-HFM-089: 2004]. The AP mine case and internal trigger mechanism become fragments that can cause injury and soil ejecta, small stones or other environmental debris can become secondary fragments as the blast propels them away from the origin of the blast [NATO-RTO-TR-HFM-089: 2004]. The injuries that occur depend largely on the position of the victim relative to the mine. The BOP decreases exponentially as a victims distance from the mine increases and thus the risk of BOP injury decreases. Whilst test standards do exist for this scenario, they do not require protection against BOP to be assessed. This will be discussed further in this chapter.

8.2 Prediction of BOP Injuries in Background Scenario Investigations

The aim of chapters 3, 4, 5 and 6 was to determine which operational scenarios – involving blasts which may cause BOP injuries – were of the greatest concern (in terms of likelihood of BOP injuries and adequacy of currently available test standards).

8.2.1 BOP injury prediction in the validation testing of landmine protected vehicles (LPVs) or armoured vehicles (AVs)

In Chapter 3, the scenario where AVs are subjected to a blast, face-on pressure measurements were recorded during vehicle validation tests. The risk of BOP injuries was determined by calculating the chest wall velocity predictor (CWVP). Although

BOP injuries were predicted in the case of one IED test (where the vehicle hull was breached), the remainder of vehicle testing results did not show evidence that BOP injuries would occur (if the vehicle hull remains intact during the blast). AEP-55 volume 2 [2006] and NATO-RTO-TR-HFM-148 [2012] include a general criterion that the integrity of the vehicle crew compartment (or the vehicle hull) is assured during the explosive event. This general “no penetration” criterion is backed up by the used of the CWVP criterion and BOP injuries covered as a fail-safe to assure the integrity of the vehicle crew compartment. In addition, although the chest compression criterion (C) and the Viscous Criterion (VC) are not validated for use in explosive event scenarios, they have been included in this scenario to cover blunt trauma injuries that may occur. As the exact mechanisms of BOP injury are not clearly understood, this provides further confidence that torso injuries would not occur. Thus, the risk of BOP injuries is adequately covered by the current test standards.

8.2.2 Explosive charge within a vehicle or enclosed space

Chapter 4 considered possible BOP injuries to vehicle occupants if a charge was detonated within the vehicle. The predicted BOP injuries were severe even with a relatively small amount of explosive. This demonstrated the increase in the risk of injury of a complex wave environment in enclosed spaces compared to free field empirical equivalents. Although there are no test standards available to validate protection against this scenario, there are test standards to evaluate vehicles from an outside threat. The test standards do not allow the explosion to breach the vehicle and if the vehicle integrity remains intact (i.e. No penetrations by anti-armour ammunition or IEDs (AEP-55 vol. 2 (Edition 1) [2006]; NATO-RTO-TR-HFM-148 [2012]), injury to vehicle occupants is unlikely (as discussed in the Chapter 3)). For this specific scenario, with the threat originating inside the vehicle, no test standards exist and thus they cannot be assessed in this study. However, this scenario demonstrated the high risk of injury in a complex wave environment and it is recommended that a test standard be developed to allow protection concepts for this scenario to be evaluated. Terrorist attacks involving blast on busses and trains can also be described by this scenario (e.g. Katz *et al.* [1989]; de Ceballos *et al.* [2005]; Hepper *et al.* [2011]).

8.2.3 Case study involving a hand grenade explosion in very close proximity to people

The scenario in which people are directly exposed to an explosive event (i.e. not protected by a vehicle or PPE) was then explored through a hand grenade case study in Chapter 5. Although the BOP injuries would influence the severity of injury, as in this study the victims were extremely close to the explosive device, this is a fragmentation hand grenade and the high velocity fragments that it expels (to a range of up to 230m) would be the primary concern when protection against such a threat is concerned. However, by simulating the BOP profile of the hand grenade, possible BOP injuries were predicted. Insights were gained regarding the validity of empirical BOP injuries predicted based on pressure profiles with positive phase durations less than 0.4 ms (less than 0.5 m from the hand grenade). The validity of the Bowen criterion for pressure profiles with positive phase durations less than 0.2 ms [Bowen *et al.*: 1968] or 0.4 ms for the CWVP criterion [Axelsson and Yelverton: 1996] has yet to be determined. The Bass *et al.* [2006a] criterion can be used for durations as short as 1 ms, but, as with the other criteria, there were few experiments with positive phase duration of less than 1 ms and limited experimental data across the range of durations and pressures for threshold injury tolerance [Bass *et al.*: 2006a]. Further research is required to develop BOP injury criteria suitable for this loading regime. This scenario was not considered further in this discussion as the focus is on the primary injury mechanism of BOP effects, rather than secondary injury mechanisms from fragments (which are the dominant injury mechanism in the case of a hand grenade).

8.2.4 The South African Waterman exposed to anti-personnel (AP) mine blast

The demining scenario was introduced in Chapter 6, where protection against BOP injuries must be provided at close range, and where BOP, rather than fragments, was the primary injury mechanism. The South African Waterman was instrumented and face-on pressure measurements were used to calculate the risk of BOP injury. Lessons were learned regarding placing test equipment in direct contact with an explosive charge and, as in the vehicle validation testing scenario, the importance of an adequately high sample rate when pressure is measured during an explosive event. As discussed

previously, current internationally recognised test standards for PPE in the demining scenario do not require assessment of risk of BOP injuries. Although the preliminary experiment using the SA Waterman did not result in the prediction of BOP injuries, this was probably due to the insufficient sample rate. Empirical predictions, based on a medium size AP mine (100 g TNT equivalent), indicate that at a distance of 0.7 m the threshold for lung injury would be exceeded. This highlighted the need to explore contradictions between what is measured and stated in test standards, versus what is measured in experimental setups or predicted using empirical pressure profiles. It was concluded that the SA Waterman surrogates provided an inexpensive representative mass on which to mount the transducers. However, the shape of the brackets and the SA Waterman does not allow for a uniform to be fitted as it would be on personnel. It was thus recommended that an improved instrumented torso surrogate be developed in order to be used in future AP blast mine experiments.

A summary of the outcomes of the various scenarios is shown in Table 21. These outcomes lead to Chapter 6 in which the demining scenario was further investigated by developing and testing the South African Torso Surrogate (SATS) rig.

Table 21: Summary of the outcomes regarding the available test standards and injury criteria based on the scenario investigations.

Scenario Name and Description	Test Standards Available and BOP Injury Criteria Specified?	Outcome
Scenario A - Indirect blast exposure of vehicle occupant (threat outside vehicle)	AEP-55 vol.2 (Edition 1) [2006], AEP-55 vol.2 (Edition 2) [2011], NATO-RTO-TR-HFM-148 [2012] CWVP [Axelsson and Yelverton: 1996]	Test standards adequate. No need to study further.
Scenario B- Direct blast exposure within a vehicle or enclosed space (threat inside vehicle) <i>e.g. confined spaces, in vehicle/bus or building, in trench etc.</i>	None	No test standards to evaluate. Recommend testing in future studies.
Scenario C - Direct blast exposure to fragmentation munitions (close contact)	None	Fragmentation and mutilating injuries dominate. Not studied further.
Scenario D – Demining	NIJ public safety bomb suit standard - 0117.00 [NCJ 227357: 2012] NATO AP demining PPE standard [NATO-RTO-TR-HFM-089: 2006] International Mine Action Standards (IMAS) 10.3 [2009] and CEN workshop agreement for guidance on the test and evaluation of PPE (CWA 15756) [2007]	No evaluation of BOP or blunt trauma injuries to the torso and no torso injury criteria are used in any of the standards. Test standards are not adequate based on test and empirical pressure results. This will be discussed further in this section.

8.3 Ability of Injury Criteria to Predict BOP Injuries in the Demining Scenario

8.3.1 Factors that influence the development of injury criteria

The literature review showed some of the difficulties inherent in animal testing which is conducted to establish injury criteria. The following are parameters which will influence the accuracy of the injury criteria derived from these tests.

The animal subjects used in the tests

The size and anatomical structure of the animal will influence results substantially. For example, a mouse has a 50% chance of mortality at a pressure of about 7 times less than the pressure at which a sheep has the same chance of mortality (See Figure 99 from [Richmond *et al.*: 1968]).

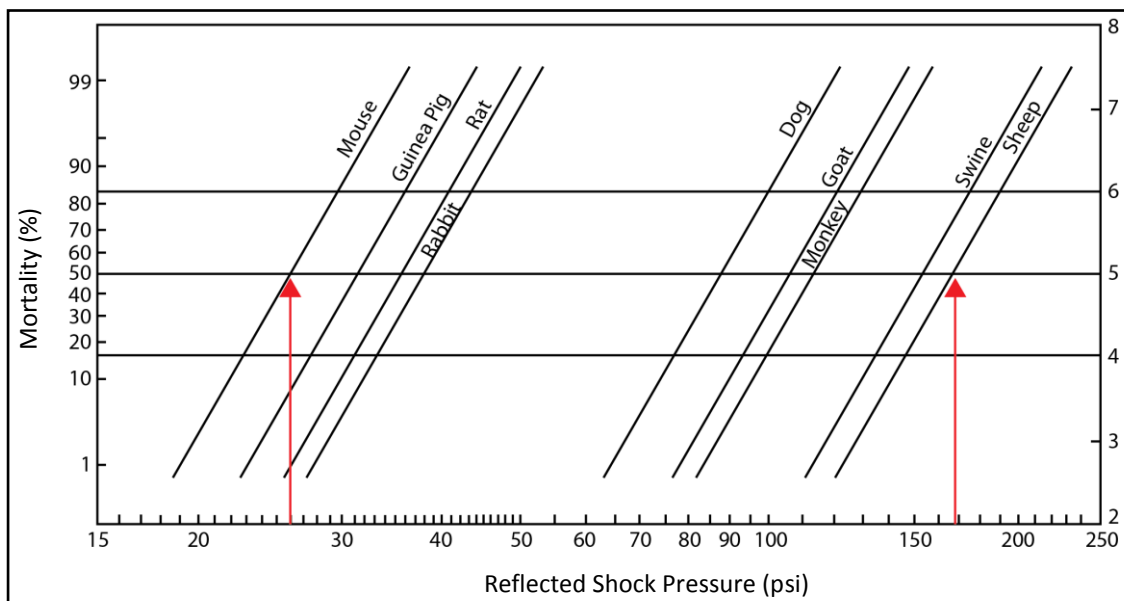


Figure 99: Mortality curves for different animal species exposed to “short” duration reflected pressures (after Richmond *et al.* [1968]).

Method used to determine the pressure dose

Teland and van Doormaal [2012] quote the original Kingery and Bulmash [1984] report wherein Kingery and Bulmash express doubts about the accuracy of the experimental data for the positive phase duration as, “...it is very difficult to determine the time of which the overpressure changes to an underpressure. There can be large variations in the individual interpretations of the positive duration of the blast wave.” This will

directly affect BOP injury predictions that rely on CONWEP to obtain the peak BOP and the positive phase duration.

The positive phase duration data was also used in the development of the Bass *et al.* [2006a] BOP injury criterion itself.

It is useful to know that CONWEP may under predict BOP outputs for smaller charges and close-in targets (as discussed in Johnson and Claber [2000]) as this may make injury criteria that are based on these inputs non-conservative.

Method of injury assessment and injury severity scores used

A common scoring protocol [Yelverton: 1996] [Axelsson and Yelverton: 1996] includes the “Grade” of the injury (or percentage lung contusion), the “Extent” of the injury (or how many different lung sections show injury), the “Type” of injury (such as small bruises or lung rupture) and the “Depth” of injury (how many lung layers or sections have been affected) [Yelverton: 1996]. However, Carneal *et al.* [2012] found the “Depth” and “Grade” scores were the most sensitive to changing threat levels. Some studies make use of the lung weight to body weight ratio [Cooper *et al.*: 1991], which others claim is not a good indicator of the severity of BOP lung injury [Jankui *et al.*: 1996].

8.3.2 Injury predictions and comparison of injury criteria (using SATS test results)

In Chapter 7, the development of the SATS rig was described. The chest plate of the SATS contained a face-on pressure transducer and an accelerometer to measure BOP effects behind the protective armour. The CWVP [Axelsson and Yelverton: 1996] was calculated based on the SATS chest pressure profile recorded during an AP mine test (208 g pentolite charge (Equivalent to approximately 240 g TNT), buried at a depth of 0.02 m, with SATS kneeling/leaning over the mine (chest to mine distance of 0.60 m)). In this section, additional injury criteria will be assessed and their ability to predict BOP injuries in this scenario will be compared.

Experimental SATS results and application of iInjury criteria

The peak CWV [Axelsson and Yelverton: 1996] that was calculated based on the chest plate pressure profile was 10.3 m/s (See Chapter 8 for further details). This represented moderate to extensive injury levels, but was still less than 12.8 m/s, above which the chance of survival would be less than 50%.

The velocity of the chest plate was calculated from the chest plate accelerometer so that it could be compared to the CWV calculated using the pressure profile obtained from the chest plate face-on pressure transducer. The chest plate acceleration signal is shown in Figure 100 and the velocity profile that was obtained by integrating the acceleration curve in MATLAB™ (See Figure 100).

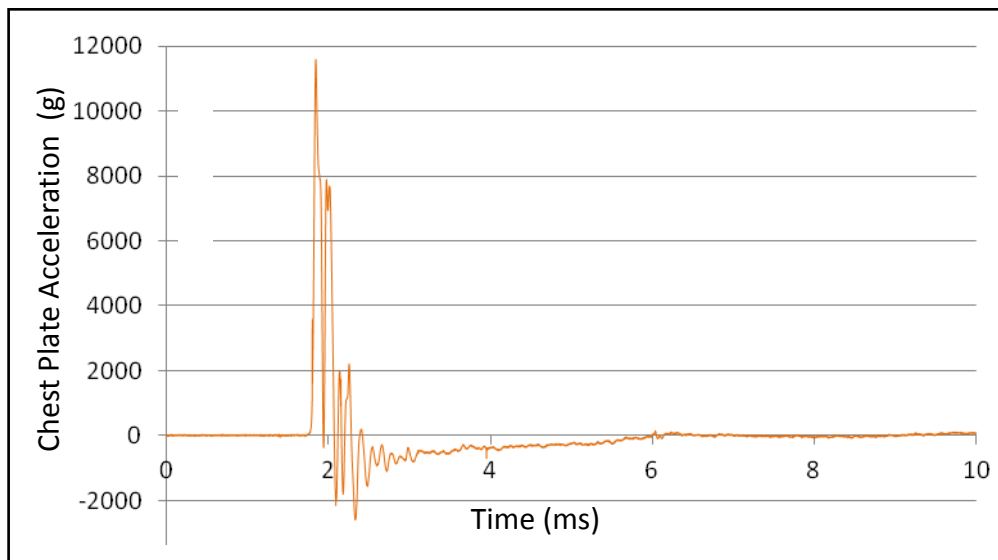


Figure 100: Acceleration signal recorded by the SATS chest plate accelerometer during an AP mine test.

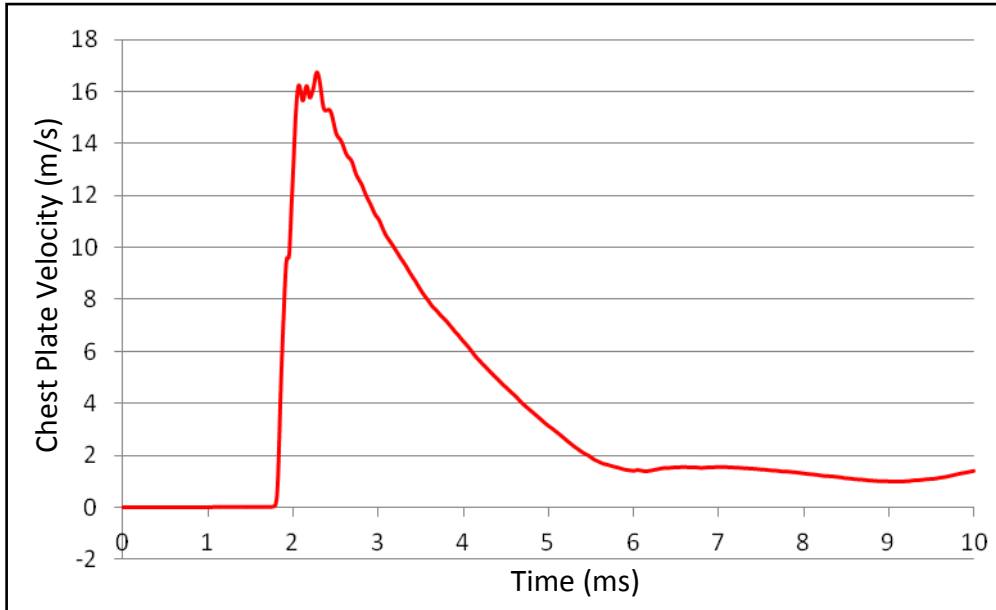


Figure 101: Calculated chest plate velocity from the SATS chest plate accelerometer.

As previously discussed, for short duration impacts, velocity is more suitable for use to determine injuries than acceleration (Accelerations in excess of 100g may not be harmful to man provided they are less than 2.5 ms in duration Hirsh [1964]). The peak chest plate velocity calculated from the acceleration signal was 16.7 m/s and occurred at about 2.4 ms after detonation. The peak CWV, calculated from the pressure signal, was 10.3 m/s and occurred at about 2.3 ms after detonation. Both the chest plate acceleration signal and the chest plate pressure signal from which these velocities were derived were recorded by the Graphtec™ data acquisition unit and they both started at about 1.75 ms and peaked at about 1.85 ms after detonation. Thus, the timing of the signals correlates well and provides confidence in the results.

The chest plate displacement (See Figure 102) was also obtained by further integrating the chest plate velocity derived from the acceleration signal. The maximum chest plate displacement attained during the recording period was about 0.036 m.

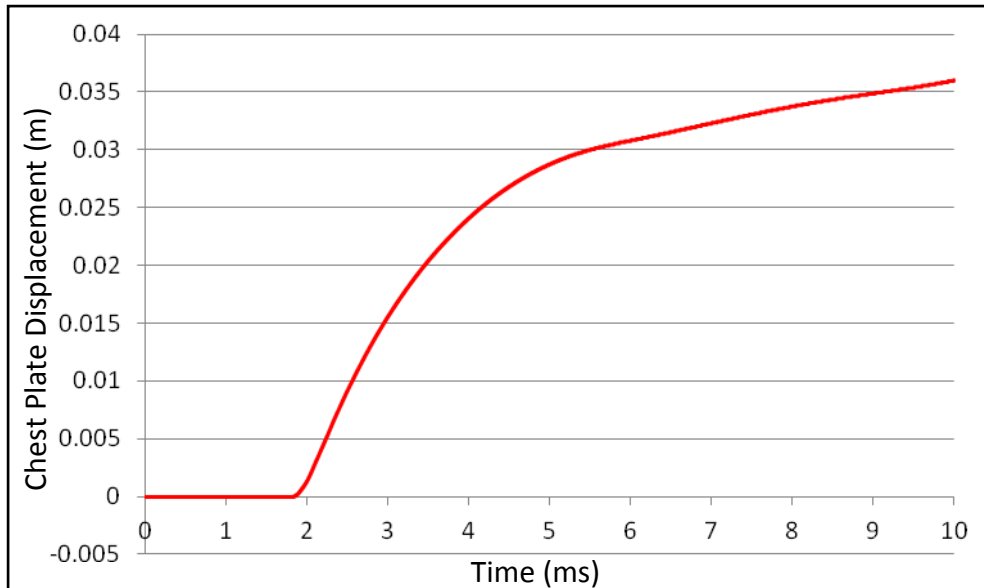


Figure 102: Calculated chest plate displacement from the SATS chest plate accelerometer.

In order to identify an applicable injury criterion and threshold value, the mechanism of injury must be determined [Bir: 2000]. At impact velocities of less than 1 m/s, the injury is mainly due to a crush mechanism (in the automotive field) [Lau and Viano: 1986]. The chest compression (C) is best predictor of this type of injury as it reflects that the chest cannot compress beyond a certain value without injury, even if the velocity has become very low. When the impact velocity is between 3 and 30 m/s, the injury tolerance becomes rate sensitive and the VC has been proven to best predict these injuries [Lau and Viano: 1986; Horsh *et al.*: 1985; Bir: 2000].

Although chest compression injury threshold values were developed for the Hybrid III ATD, applying these to the maximum SATS chest plate deflection, 36 mm corresponds to approximately a 20% risk of Abbreviated Injury Scale (AIS) 3+ (See Figure 103). AIS 3+ thoracic injuries are classified as serious injuries (for example, lung contusion, minor hear contusion, 4 or more rib fractures on one side or 2 to 3 rib fractures with hemo/pneumothorax [AAAM: 2005]). The vehicle test standards AEP-55 volume 2 [2006] and NATO-RTO-TR-HFM-148 [2012] specify a maximum limit of 50 mm deformation that corresponds to a 50% risk of AIS 3 + injuries [Mertz *et al.*: 1991]. It must be noted that the structure of the SATS is different from that of the Hybrid III ATD and thus the applicability of limit values developed for the Hybrid III ATD to the SATS displacement results is not strictly accurate.

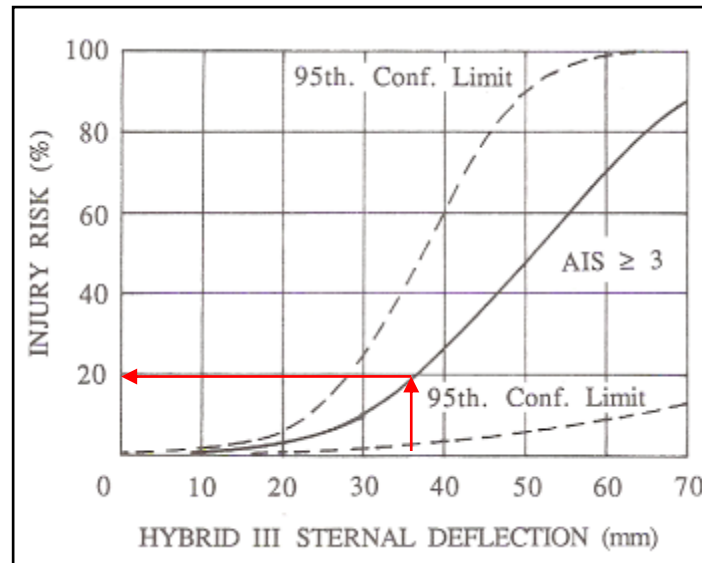


Figure 103: Injury risk curve for Hybrid III sterna deflection and associated 95% confidence bands for AIS 3+ thoracic injury (after Mertz *et al.* [1991]).

The VC was developed by [Viano and Lau: 1985] where the chest compression (C) was defined as the displacement of the chest in relationship to the spine, normalized by the initial thickness of the thorax. The VC_{max} is the maximum of the momentary product of the thorax deformation speed (V) and the thorax deformation (C). The VC was found in various studies to predict injuries such as heart rupture [Kroel *et al.*: 1986], cardiac arrhythmia [Bir and Viano: 1999] and severe liver lacerations [Horsch *et al.*: 1985]. The VC_{max} for frontal impact in the automotive field is calculated from the Hybrid III ATD chest deflection (i.e. the instantaneous displacement between the sternum and the spine [Berthet and Vezin: 2006]). As the proposed human tolerance was derived from cadaver data, a scaling needed to be performed to relate the anteroposterior deformation measured externally to the cadaver to the internal value of the Hybrid III ATD. Thus,

$$VC_{max} = 1.3 (V(t)C(t))_{max},$$

where the compression $C(t)$ is related to the chest deflection $D(t)$ by

$$C(t) = D(t)/0.229 \text{ for the Hybrid III ATD.}$$

However, on the SATS, the acceleration transducer from which the displacement was calculated is not inside the chest cavity (as is the case in the Hybrid III ATD), thus the

scaling of 1.3 is not necessary. The initial torso thickness of the SATS is approximately 0.205 m, thus,

$$VC_{max} = V(t)C(t)/0.205 \text{ m/s.}$$

Figure 104 shows a plot of $V(t)C(t)$. The peak $V(t)C(t)$, which occurs at 3.2 ms, is then divided by thickness of the SATS initial torso thickness to give $VC_{max} = 0.176/0.205 = 0.9 \text{ m/s}$. A VC_{max} of 0.9 m/s reflects a 20% chance of an AIS 4+ injury to the thorax which translates to severe to fatal thoracic injuries.

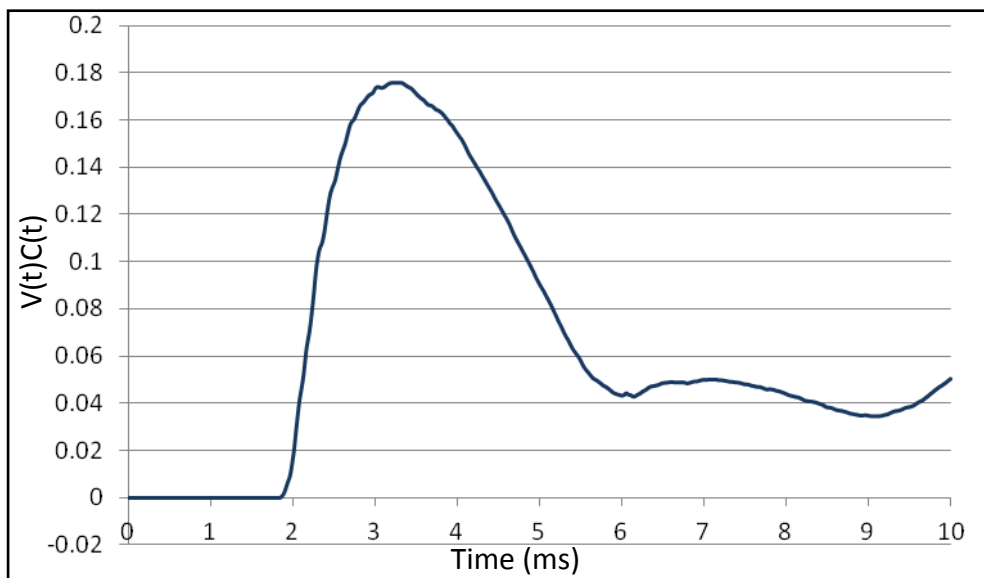


Figure 104: $V(t)C(t)$ calculated based on the SATS rig acceleration data in order to obtain VC_{max} .

Empirical BOP Injury Predictions

The purpose of the empirical predictions was to ascertain whether, based on an empirical pressure profile of the same test charge, BOP injuries were likely to occur. The empirical predictions could then be compared to the injuries that were predicted based on the experimental data.

BECV4 [2000] was used to predict the empirical peak overpressure (side-on pressure) and positive-phase duration at various distances from the test charge. As a 208 g pentolite charge was used in the test with the SATS, an equivalent spherical charge of 240 g TNT in free field was chosen for the empirical predictions (See Table 22).

Table 22: Peak face-on pressure, peak side-on pressure and positive phase duration at various distances from a 240 g TNT charge from BECV4 [2000].

Distance from charge (m)	BECV4 peak face-on pressure (kPa)	BECV4 peak side-on pressure (kPa)	BECV4 positive phase duration (ms)
0.2	86326	9272	0.1
0.4	23657	3195	0.3
0.6	8913	1457	1.0
0.8	3996	781	1.4
1.0	2059	469	1.3

The severity of lung overpressure injuries at various distances from the 240 g TNT charge were then predicted using the Bowen *et al.* [1968] and the Bass *et al.* [2006a] curves.

The survival curves predicted for a 70 kg man applicable to a free field situation, where the long axis of the body is perpendicular to the blast wind [Bowen *et al.*: 1968], were used to predict the chance of survival due to lung BOP injuries. Within 1.0 m of the charge, the threshold for lung damage was exceeded. At 1.0 m, 0.8 m, 0.6 m, 0.4 m from the charge, the predicted chance of survival due to BOP injuries, was greater than 99%, between 90% and 99%, between 10% and 50% and between 50% and 90% respectively. However, the validity of the Bowen *et al.* [1968] curves for durations less than 4 ms has been debated.

The Bass *et al.* [2006a] curves (See Figure 105) were specifically derived for short-duration blasts (< 30 ms) by reanalysing existing blast literature, including the data used in the development of the Bowen *et al.* [1968] curves, together with additional, more recent, test data. The empirical predicted overpressure injuries at various distances from a 240 g TNT charge, as shown in Table 22, were plotted on Figure 105 using large “+” symbols.

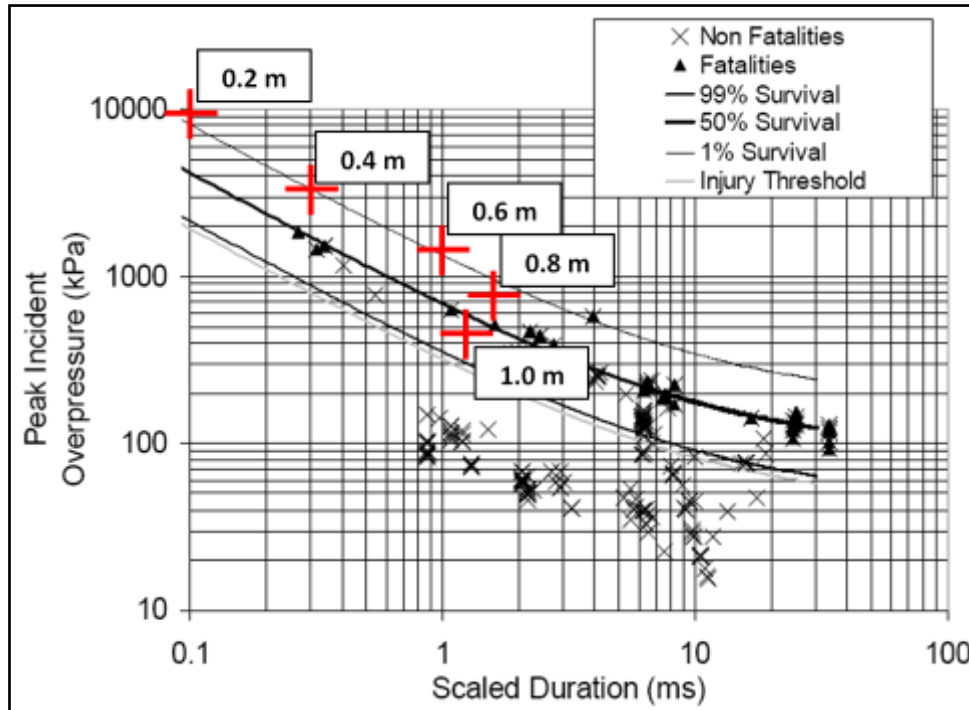


Figure 105: Calculated nonlinear logistic regression model for survival or threshold for injury for a 70 kg man using scaled duration and side-on pressure (after Bass *et al.* [2006a]) applicable to a free field situation where the long axis of the body is perpendicular to the blast winds with indicators showing the predicted overpressure injuries at various distances from a 240 g TNT charge as determined in Table 22.

Within 1 m of the charge, the predicted BOP injuries were above the threshold for lung damage. The chance of survival due to these lung injuries were 1% or less within 0.6 m of the charge. At 0.8 m from the charge, the chance of survival is still less than 50% and at 1 m from the charge, the chance of survival is greater than 50%, but less than 99%. A summary of the BOP injury predictions based on the empirical BECV4 pressure profiles is provided in Table 23.

Table 23: Chance of survival due to BOP injury as predicted using empirical BECV4 pressure profiles and Bowen *et al.* [1968] and Bass *et al.* [2006a] injury criteria at various distances from a 240 g TNT charge.

Distance from charge	Bowen <i>et al.</i> [1968] predicted injury level	Bass <i>et al.</i> [2006a] predicted injury level
0.2 m	n/a	Above the threshold for lung damage and less than 1% chance of survival
0.4 m	Above the lung injury threshold, but between 50% and 90% chance of survival	Above the threshold for lung damage and less than 1% chance of survival
0.6 m	Above the lung injury threshold, but between 10% and 50% chance of survival	Above the threshold for lung damage and less than 1% chance of survival
0.8 m	Above the lung injury threshold, but between 90% and 99% chance of survival	Above the threshold for lung damage and between 1% and 50% chance of survival
1.0 m	Above the lung injury threshold, but a greater than 99% chance of survival	Above the threshold for lung damage, but between 50% and 99% chance of survival

The Bass *et al.* [2006a] curves were found to recommend lower blast lung injury tolerances than the Bowen *et al.* [1968] curves (See Table 23). Although injury predictions were provided for 0.4 m and 0.2 m distances from the charge, these results were displayed in red as the validity of the predictions for positive-phase duration less than 1 ms were unreliable [Bass *et al.*: 2006a]. As the Bass *et al.* [2006a] curves were specifically derived for short-duration blasts (< 30 ms) and were derived from a data set

including additional more recent test data than that used in [Bowen *et al.*: 1968], the Bass *et al.* [2006a] predictions were used in the remainder of this discussion.

Comparison of injury predictions using empirical and experimental SATS test results

The reflected pressure value recorded by the SATS at 0.6 m from the AP mine was 9230 kPa. This was about 3% higher than the empirical BECV4 predicted peak pressure value of 8913 kPa. It must be emphasised that the theoretical results are empirical fits, or approximations, that were primarily based on much larger charges (typically > 1 kg TNT). This introduces uncertainty in the empirical pressure profile predictions or the PPE worn by the SATS amplified the BOP effects of the blast (See Section 8.5.3 in this chapter for further discussion regarding PPE).

The BOP injuries predicted using the SATS face-on chest pressure and acceleration measurements (measured at 0.6 m from a 208 g pentolite (equivalent to 240 g TNT) cylindrical charge) behind PPE. The CWVP [Axelsson and Yelverton: 1996], chest compression [Mertz *et al.*: 1991] and VC [Lau and Viano, 1986] injury predictions are shown in Table 24, together with the Bass *et al.* [2006a] empirical side-on BECV4 predictions.

Table 24: Chance of survival due to BOP injury as predicted by empirical BECV4 pressure profiles for a 240 g TNT spherical charge and 208 g pentolite charge at 0.6 m.

Injury criterion and source of pressure/acceleration data	Predicted injury level at 0.6 m from the charge
Bass <i>et al.</i> [2006a] using BECV4 side-on pressure data (hemispherical charge in free field)	Above the threshold for lung damage and less than 1% chance of survival.
Chest Wall Velocity Predictor (CWVP) [Axelsson and Yelverton: 1996] and SATS chest plate face-on pressure data (behind PPE jacket)	CWV = 10.3 m/s which relates to moderate to severe BOP injuries, but a greater than 50% chance of survival.
Chest compression and SATS chest plate acceleration data (behind PPE jacket)	Compression = 36 mm which relates to a 20% chance of AIS3+ injuries which are serious thoracic injuries.
Viscous Criterion (VC) [Lau and Viano, 1986] and SATS chest plate acceleration data (behind PPE jacket)	VCmax = 0.9 m/s which relates to a 20% chance of AIS 4+ injuries which are severe to fatal thoracic injuries.

The VCmax predicts more severe injuries than the chest compression. This was expected as VC is valid for higher loading rates than the compression criterion which does not take into account the dynamic movement of the chest.

The Bass *et al.* [2006a] curves used with the empirical BECV4 pressure profiles (at 0.6 m from a 240 g TNT spherical charge) predict BOP injuries with a less than 1% chance of survival. The CWVP [Axelsson and Yelverton: 1996] (based on chest plate face-on pressure data) indicated moderate to severe BOP injuries, but with a greater than 50% chance of survival.

The empirical pressure profiles used with the Bass *et al.* [2006a] curves did not include the use of PPE as was worn by the SATS when the pressure measurement was recorded,

thus, the injuries predicted based on the experimental results would be expected to be less severe than if no PPE was worn (See Section 8.5.3 of this chapter for more discussion of the influence of PPE on BOP injuries). Although one must be wary of comparing the injuries predicted based on experimental results and those predicted using the empirical BECV4 pressure profiles, both methods indicate that BOP injuries need to be considered in demining and EOD/IED PPE test protocols.

Comparing the suitability of these injury criteria for use in the testing of demining PPE, the CWVP is the most suitable as it is valid for complex wave environments and makes use of face-on or reflected pressure measurements. The VCmax is also recommended as the results correlate well with the CWVP and should the armour result in blunt trauma injury mechanisms (for which the CWVP is not valid), the VCmax would predict these injuries. So, the minimum measurements for a torso surrogate should be chest face-on pressure and chest acceleration. However, of these two measures, the chest face-on pressure is most important as it is less dependent on the physical properties of the torso surrogate than the VCmax.

8.4 Test Standards to Evaluate BOP Injury Risk in the Demining Scenario

Available test standards were then assessed in their ability to evaluate possible protection concepts developed for the demining scenario against BOP injuries. The standards were summarised in Table 21 and are discussed individually below.

8.4.1 National Institute of Justice (NIJ) Public Safety Bomb Suit Standard (NIJ Standard - 0117.00) [NIJ: 2012]

Although this standard focuses on evaluating bomb suits against IEDs, the scenario is similar to that of the demining scenario.

The standard recommends the use of the Hybrid III ATD in kneeling posture with the exterior of the bomb suit 0.6 m from the 0.6 kg C4 (equivalent to 0.7 kg TNT from BECV4 [Swisdak: 2000]) test charge (this is the setup simulated in the SATS AP mine test described in this section, but the charge size in the SATS test was only 0.240 kg TNT equivalent).

The NIJ states the following under the scope of the document, “This standard addresses blast overpressure only in terms of bomb suit integrity. As of the date of the document, blast overpressure protection test measures did not provide sufficient confidence levels to recommend test methods and protective performance requirements.” The integrity test specifies that all protective elements must remain secured on the surrogate and protective elements covering the thorax/abdomen and pelvis shall remain attached to the bomb suit in the donned position. These protective elements shall maintain shape integrity and show no evidence of collapse. Cosmetic damage is permissible as long as such damage does not compromise the integrity of the protective layers within the bomb suit. Rips or holes are permissible as long as they do not perforate the innermost fabric ballistic protection layer. No gaps that expose the surface of the test surrogate are allowed.

During this test, the polycarbonate chest insert was shattered and sections of the outer layer of Kevlar were ripped or penetrated by soil ejecta. Perhaps if insert had remained in-tact, the chest face-on pressure and the chest acceleration would not have resulted in severe thoracic injury predictions. However, the charge size was only about 30% of that recommended in this standard and the inner layer of protection was not perforated as described in the integrity test. This indicates that BOP injuries should be evaluated by test standards for this scenario, even though this standard does not recommend this testing. This contradiction will be explored further in Section 9.5.

8.4.2 North Atlantic Treaty Organisation (NATO) Test Methodologies for PPE Against Anti-Personnel (AP) Mine Blast [NATO-RTO-TR-HFM-089: 2006]

The NATO-RTO-TR-HFM-089 [2006] also recommends the use of a Hybrid III ATD in a kneeling position. The explosive threat is smaller than that used in the NIJ standard, 0.1 to 0.2 kg C4 or PE4 (equivalent to 0.1 to 0.3 kg TNT), short cylinder (35% height to diameter ratio), plastic casing with 2mm max thickness and is buried with 20mm overburden.

The current NATO standard (NATO-RTO-TR-HFM-089 [2006]) also does not mandate the evaluation of possible BOP injuries. It was stated in NATO-RTO-TR-HFM-089 [2006] that, “The loads generated by an AP mine, for the body positions considered,

were well below the threshold required for blast lung injury,” however, “Ear pressure was found to often exceed the acceptable threshold for eardrum rupture...current helmet designs can increase the overpressure at the ear level...presence of a visor was found to lessen these effects significantly.”

Each participant of the HFM-089/TG-024 that contributed to the development of this standard provided test setup examples for various trials that were performed. A few of these setups included pressure sensors mounted flush on head at ear location and on the thorax (“skin”) surface of the ATD but do not describe the BOP injury criteria that they use with these sensors. DSTL, Porton Down, described a thoracic rig that they used to measure chest wall acceleration. Selected test setups suggested the use of the Bowen *et al.* [1968] risk curves, but applied to free-field side-on overpressure that the standard states should be measured to monitor the repeatability and quality of the explosive charges. These curves do not take into account the complex wave environment existing behind body armour or the ability of certain armour materials to enhance or reduce the coupling of the stress wave into the thorax and abdomen.

8.4.3 International Mine Action Standards (IMAS) 10.3 [2009] - Specifications for PPE to protect against unexploded ordnance (UXO) and AP landmines (And CEN workshop agreement (CWA 15756) [2007] (provisionally withdrawn))

It is stated that the minimum requirement for demining PPE is that it, “Shall be capable of protecting the parts of the body that are covered against the blast effects of 240 g of TNT at distances appropriate to the wearer’s activity.” The minimum requirements for protection of the torso body region are:

- Protection against fragments as outlined in the North Atlantic Treaty Organisation (NATO) Standardization Agreement (STANAG) 2920 [2003] for V50 rating (dry) of 450 m/s for 1.102g fragments.
- Protection of the chest, abdomen and groin area against blast effects of 240 g of TNT at 0.6 m from the closest part of the body.

The IMAS 10.3 [2009] referred to The European Committee for Standardisation (CEN) Workshop Agreement [2007] for guidance on the test and evaluation of PPE.

The European Committee for Standardisation (CEN) Workshop Agreement [2007] agreement was provisionally withdrawn by the CEN as “The measurement of the quantity of explosive, necessary to carry out the tests, is inaccurate. Pending the recalculation of this parameter, a revised CWA in which the incriminated clause will be removed will be soon posted on this web page. New tests will have to be carried out before a complete CWA can be finalized and published.” [The European Committee for Standardisation (CEN) Workshop Agreement Withdrawn, no date]. However, at the time of submitting this thesis, the document had not been updated and The European Committee for Standardisation (CEN) Workshop Agreement [2007], or any later or previous version, was not available online. As this standard provided guidelines focussing on the testing of PPE for mine action against AP blast mines, it was considered to be worth discussing.

Based on “effectiveness of ppe for use in demining ap landmines” – Chinchester *et al.* [2001] UXO conference, the The European Committee for Standardisation (CEN) Workshop Agreement [2007] stated that “blunt trauma on the torso has been demonstrated not to be critical with a chest-mine distance of 60 cm. This appears to be reinforced with the data from the DDAS (Database of Demining Accidents [Smith: no date]).”

Or again, “the blunt trauma from a blast has not been demonstrated to be a significant contributing (life threatening) factor, for the conditions tested, to deminer injuries, as presented in “A methodology for evaluating demining PPE for AP landmines. A number of simplifications have, therefore, been made to ensure more effective application for the mine action environment. The threat increases with proximity to the charge and the assumption is made that a reasonable distance is maintained between the deminer and the hazard.”

8.5 Contradictions between Test Standard Specifications, Predicted BOP Injuries and Real BOP Injuries

This section looks at possible reasons for the contradictions between test standard specification, predicted BOP injuries and real BOP injuries.

8.5.1 Injury criteria inadequacy and incomplete understanding of BOP injury mechanisms

It was difficult to define the direct BOP torso injury mechanisms for the AP blast mine scenario. The effect of PPE on the BOP injuries was at the centre of this debate. The NATO-RTO-TR-HFM-089 [2004] describes the “elastic deformation of the PPE due to the push of the air shock and detonation products,” as an indirect blast effect. However, the BOP transferred by the PPE to the torso may be a direct effect. Understanding which phase of the event causes which injuries and how to measure these effects is key to predicting BOP injuries. The exact mechanisms and the ability of certain materials to amplify BOP effects are not yet fully understood, but it is important that a surrogate captures the influence of PPE or the interaction of the BOP with the PPE effect [Ouellet: 2008]. Another injury mechanism at play occurs later in the event when the whole body begins to move, but this is not within the scope of this study.

There is also much debate regarding the validity of blast prediction or calculations and injury criteria when the subject is very close to explosive charges (or high peak pressures with short positive phase durations). The validity of the Bowen criterion for pressure profiles with positive phase durations less than 0.2 ms [Bowen *et al.*: 1968] or 0.4 ms for the CWVP criterion [Axelsson and Yelverton: 1996] has yet to be determined. The [Bass *et al.*: 2006a] criterion can be used for durations as short as 1 ms, but, as with the other criteria, there were few experiments with positive phase duration of less than 1 ms and limited experimental data across the range of durations and pressures for threshold injury tolerance [Bass *et al.*: 2006a]. Injury criteria that were developed using CONWEP data may under predict BOP outputs for smaller charges and close-in targets (as discussed in Johnson and Claber [2000]). This may make injury criteria that are based on these inputs non-conservative. This could be dangerous as the risk of and severity of BOP injuries that are predicted may be less than

could actually occur. Further research is required to develop criteria suitable for the blast loading regime.

8.5.2 BOP injuries caused by AP mine incidents may be under-reported

The Database of Demining Accidents (DDAS) [Smith: no date] is an open online database where actual incidents are described. There are few serious BOP injuries reported in this database. This may be due to difficulties with reporting the incident (time lapse between incident and the reporting), insurance issues, “field control inadequacy” is often stated as the cause of the incident and follow up reporting is often difficult in the regions where mines are prevalent. The details are often unclear and some victims even “disappeared” prior to incident investigations.

It could be that BOP injuries were not diagnosed due to other more obvious external injuries or that the BOP injuries took time to develop or that by the time of reporting, mild BOP injuries had resolved. Elsayed and Gorbunov [2006] found that a single exposure to low level BOP ($62.0 \text{ kPa} \pm 2.0 \text{ kPa}$) causes notable changes in the lungs. These effects increased significantly with time from 1 to 24 h. Raghavendran *et al.* [2005] conducted a similar study of the evolution of lung contusion, but from blunt chest trauma, rather than BOP. The rats in this study showed that lung injury was the most severe in the acute period (between 8 minutes and 24 hours), but by 48 hours, the arterial oxygenation and blood markers were almost normal. It is mentioned in Raghavendran *et al.* [2005] that this patterns of inflammation peaking by 24 h, followed by subsequent signs of healing has also been noted in humans with lung contusion.

8.5.3 Differences in pressure profiles predicted using empirical blast calculation software or computational fluid dynamics (CFD) simulation software

The empirical blast calculation software used in this thesis was BECV4 and the computational fluid dynamics (CFD) programs that were used in this study were ProSAir and ANSYS AUTODYN.

A comparison of ProSAir and ANSYS AUTODYN is currently underway at Cranfield University and a description of preliminary results and basic differences between the codes can be found in Appendix F [Forth and Sharma: 2014]. Preliminary results

revealed that using an equivalent mesh size, there was little difference between peak BOP predicted by the code at large scaled distances (>0.4 m). However, as the scaled distance decreased (<0.2 m), ProSAir predicted nearly double the peak BOP that was predicted by ANSYS AUTODYN. However, the validity of CFD software, empirical software and experimental results at such small scaled distances is questionable. For the purpose of this thesis, where scaled distances were greater than 0.4 m for the scenarios considered, it would be assumed that if similar simulation parameters were used, that ProSAir and ANSYS AUTODYN would produce similar results.

Another limitation that applies to both ProSAir and ANSYS AUTODYN is that they ignore the effects of afterburning which may result in a greater impulse exposure in a real scenario. This means that BOP injuries could be underpredicted if CFD software is used to obtain BOP profiles on which to base injury predictions.

When comparing the BOP profiles, it must be noted that spherical charges were used, whereas BECV4 predictions were based on hemispherical charges. A hemispherical charge would produce a greater peak BOP than a spherical charge of the same weight at the same distance [Chichester *et al.*: 2001]. Thus, the simulations were expected to produce lower peak BOP than the BECV4 software at the same distance and charge size.

The limitations of blast calculators must also be considered when using setups that vary from those under which the underlying experimental data is based. When this is not the case, one should keep in mind that the algorithms used to for example, scale the data or account for alternative weather conditions, are not absolute values, but rather approximations that may be based on limited data. The empirical data was gathered from a limited set of data which was collected during the detonation of very large charges. Thus, the accuracy of empirical equations decreases as the explosive event becomes increasingly near field [Remennikov: 2003].

In the field of BOP injury research, the charges are usually much smaller than those used in the development of the blast calculation software and they are positioned close to the subject. This is important when reviewing injury criteria that were developed making use of these calculators and when comparing experimental blast results to those

predicted by the blast calculators for relatively small charges that are close to the subject.

The importance of conducting actual blast trials or experiments is acknowledged as there is still much debate as to the accuracy of empirical blast calculators, especially when looking at small charges, close-in, as is the case in this thesis. It would be dangerous if only blast calculators were used to predict BOP injuries as the BOP outputs are sometimes under-predicted which could lead to a higher risk of more severe BOP injuries for a particular scenario.

However, blast calculators are useful to allow comparisons with experimental results, provided the limitations of the blast calculators are understood.

8.5.4 Real scenario differs from simulated or test scenario

The empirical predictions are based on a hemi-spherical test charge in free field whereas the preliminary SATS test was conducted using a cylindrical buried charge. Another major factor is the PPE which was worn in the preliminary SATS test to protect it from penetration of soil ejecta whereas in the empirical predictions do not include the use of PPE. The influences of the differences between the real scenario and the test scenario are described here.

Environmental conditions

Weather effects may significantly influence low pressure measurements and thus results may differ significantly from the empirical Kingery-Bulmash curves [Swisdak: 1994].

Far from the origin of the blast, the atmospheric conditions start to notably influence the BOP, as the properties of the blast wave differ from those of an ideal pressure profile that is transmitted through a homogeneous atmosphere. Very far from the origin of the blast, the peak pressures are really sound pressures and can be up to ten times greater or more than ten times less than the ideal pressures for a homogenous atmosphere [UFC: 2008].

Body positioning or orientation of a person relative to the origin of the blast

The position of a person relative to an explosive blast has a significant effect on the BOP dose to which a person is exposed and thus the predicted injury outcomes.

The extremes of how a person's orientation is able to influence the BOP injury dose to which they are exposed are described by Stuhmiller *et al.* [1991]. A person oriented end-on to a blast, as would be the case if a person was lying down with either their head or feet pointed toward the blast, has a small surface area to offer resistance against the dynamic pressure component of the wave, and the side-on pressure would be the pressure dose to which the person is exposed. For a person standing and facing the blast, for example, the pressure dose would be from both the dynamic pressure and the incident pressure, the sum of which gives the face-on pressure.

In the DDAS, the demining personnel were often not positioned as they were trained to be, this may also lead to confusion regarding actual injuries that do not correlate well with predicted injuries.

Blast cone and depth of burial of AP landmine, buried IED charges and shape of charge

The blast cone and depth of burial all influence the BOP to which a person is exposed during an explosive event [NATO-RTO-TR-HFM-089: 2004].

The depth of burial of a landmine or IED will influence the BOP as some of the energy of the blast is transferred into kinetic energy of the soil particles. The deeper the charge is buried, the less the peak BOP at the same distances from the charge [NATO-RTO-TR-HFM-089: 2004]. However, the impulse transferred by the soil ejecta may introduce additional injury mechanisms (such as global movement due to impact with body), even though the peak BOP may be less.

The shape of the charge also influences results. The outputs of a cylindrical charge, for example, depend on the relative dimensions as well as the bulk explosive weight of the charge and the BOP will depend on the charge orientation (height to diameter) as well as the orientation of the person with respect to the charge [Knock and Davies: 2013]. The empirical data (from BECV4) used for predictions in this thesis was based on test

conducted using hemispherical charges, rather than the cylindrical charge used in the SATS tests or the spherical charges used in the ProSAir and ANSYS AUTODYN simulations. For an equal mass of explosive, the BOP from a hemispherical charge is stronger than that produced by a spherical blast detonated in air [Chichester *et al.*: 2001]. This means that the simulations used in this thesis predict lower BOP profiles than those predicted by empirical data based on hemispherical charges such as BECV4.

Making use of PPE

The SATS was clothed in a bomb suit with ballistic protection to ensure that it was not severely damaged during the AP mine test. The suit consisted of a NomexTM (245 gsm) outer shell, inserts of multiple layers of KevlarTM and a clear polycarbonate chest plate insert. Although the polycarbonate chest plate insert was cracked, the inner layer of KevlarTM underneath the plate was not penetrated. The peak pressure recorded on the chest plate of the SATS was 9230 kPa. The peak reflected pressure predicted by BECV4 was 8913 kPa. Although the predictions are empirical fits or approximations (and were based on larger charges), this result may indicate that the PPE worn by the SATS amplified the BOP effects of the blast. This amplification effect of certain materials has been described by several authors [Cooper *et al.*:1991; Cooper: 1996; Hattings and Skews: 2001; Trimble *et al.*: 2001; Rabet *et al.*: 2006; Oullet *et al.*: 2008; Ouellet and Williams: 2008]. However, internationally recognised test standards still do not mandate measurements behind body armour or PPE.

8.6 Implications for Development and Testing of BOP Protection Strategies for the Demining Scenario

This study focussed on the test standards used to evaluate BOP protection rather than the BOP protection (such as PPE) concepts themselves. However, the results of tests to determine the protection offered by PPE will ultimately determine the level of protection offered to people exposed to blast events.

It was determined that test standards used in the evaluation of PPE were not adequate as severe BOP injuries were predicted in typical PPE scenarios, however, the test protocol does not require the testing of PPE ensembles for BOP protection offered. BOP injuries do occur in reality and unlike the vehicle hull which will protect against blast provided

it is not compromised, body armour does not guarantee the same protection if it remains intact. Armour may even enhance BOP injury, but research has shown that the transmitted BOP can be effectively reduced by making use of various combinations soft ballistic protection, rigid plates, foams and air gaps.

Although limitations exist in the ability of injury criteria and measurement methods to accurately predict BOP injuries, generally a conservative approach should be taken, so even if it is a first attempt at testing for BOP injuries. The alternative is to possibly pass PPE (according to internationally accepted test standards) which may in-fact enhance BOP injuries (which may otherwise have been prevented through simple countermeasures).

9 CONCLUSIONS

Blast Overpressure (BOP) injuries occur in a number of different scenarios. Internationally recognised test standards were adequate in predicting BOP injuries in vehicle validation testing against improvised explosive devices (IEDs) and landmines. Test standards are not available for the explosive charge within a vehicle scenario and the close proximity to a hand grenade scenario.

In the demining scenario,

Moderate to severe BOP injuries were predicted using both measurements obtained from the South African Torso Surrogate (SATS) and empirical pressure profiles. The Viscous Criterion (VC) and the Chest Wall Velocity Predictor (CWVP) were found to be the most suitable injury criteria to predict these injuries.

AND

Current internationally recognised personal protective equipment (PPE) test standards do not mandate that the risk of BOP be evaluated.

Thus, **internationally recognised PPE test standards** (used in the demining scenario) **do not adequately assess the risk of BOP injuries** to the thorax and abdomen.

Although limitations exist in the ability of injury criteria and measurement methods to accurately predict BOP injuries, generally a conservative approach should be taken. Thus, it is **recommended** that the **risk of BOP injuries** should be **evaluated in PPE test standards**.

10 REFERENCES

Association for the Advancement of Automotive Medicine (AAAM), 2005. *AIS 2005: Abbreviated Injury Scale 2005*. Gennarelli, T. and Wodzin, E. Editors. Barrington, IL 60011, U.S.A.

Allied Engineering Publication (AEP)-55, 2006. *Procedures for Evaluating the Protection Level of Logistic and Light Armoured Vehicles, Volume 2 (Edition 1) for Mine Threat*. North Atlantic Treaty Organisation (NATO), Neuilly-sur-Seine Cedex, France.

Allied Engineering Publication (AEP)-55, 2011. *Procedures for Evaluating the Protection Level of Logistic and Light Armoured Vehicles, Volume 2 (Edition 2) for Mine Threat*. North Atlantic Treaty Organisation (NATO), Neuilly-sur-Seine Cedex, France.

Anctil, B., Keown, M., Williams, K., Manseau, J., Dionne, J.P., Jetté, F. and Makris, A. 2004. Development of a Mannequin for Assessment of Blast Incapacitation and Lethality. *In Proceedings of the Personal Armour Systems Symposium (PASS)*, pp. 332-344, The Netherlands.

Axelsson, H. and Yelverton, J. 1996. Chest Wall Velocity as a Predictor of Nonauditory Blast Injury in a Complex Wave Environment, *The Journal of Trauma*, Vol. 40 (3S), pp. S31-S37.

Backaitis, S. and Mertz, H. 1994. *Hybrid III: the first human-like crash test dummy*. SAE International, PT-44, USA.

Bass, C., Rafaels, K. and Salzar, R. 2006a. Pulmonary Injury Risk Assessment for Short-Duration Blasts. *In Proceedings of the Personal Armour Systems Symposium (PASS)*, Manchester, UK.

Bass, C., Rafaels, K., Salzar, R. 2008. Pulmonary Injury Risk for Short-duration Blasts, *The Journal of Trauma*, Vol. 65, No. 3, pp. 604-615.

Begeman, P. and Prasad, P. 1990. *Human Ankle Impact Response in Dorsiflexion*. In: S. Backaitis, S. and Mertz, H. ed. 1994. *Hybrid III: The First Human-like Crash Test Dummy*, USA: SAE International, PT-44.

Berthet, P. and Vezin, P. 2006. *Review of Thorax Injury Criteria*. France: Institut National de Recherche sur les Transports et leur Sécurité (INRETS), Integrated Project on Advanced Protection Systems (APROSYS), AP-SP51-0038B.

Bir, C. 2000. The Evaluation of Blunt Ballistic Impacts of the Thorax. Doctor of Philosophy Dissertation, The Graduate School of Wayne State University Detroit, Michigan.

- Bir, C. and Viano, D. 1999. Biomechanical Predictor of Commotio Cordis. *Journal of Trauma*, Vol. 47, pp. 468-473.
- Bir, C., Viano, D. and Kind, A. 2004. Development of biomechanical Response Corridors of the Thorax to Blunt Ballistic Impacts. *Journal of Biomechanics*, Vol. 37, pp. 73-79.
- Bouamoul, A., Williams, K. and Levesque, H. 2007. Experimental and Numerical Modelling of a Mannequin for the Assessment of Blast Incapacitation and Lethality under Blast Loading. *In Proceedings of the 23rd International Symposium of Ballistics*, Tarragona, Spain.
- Bourget, D., Anctil, B., Doman, D. and Cronin, D. 2002. Development of a Surrogate Thorax for BAPT Studies. *Personal Armour Systems Symposium*, The Netherlands.
- Bowen, I., Fletcher, E. and Richmond, D. 1968. *Estimate of Man's Tolerance to the Direct Effects of Blast*. Washington, DC: Defence Atomic Support Agency, Department of Defense, Technical progress report no. DASA-2113.
- Carneal, C., Merkle, A., Cernak, I., Tenore, F., Romano, R., Carboni, M., DeCristofano, B., Januszkiewicz, A. and Meaffeo, M. 2012. Thoraco-abdominal Organ Injury Response Trends due to Complex Blast Loading. *In Proceedings of Personal Armour Systems Symposium (PASS)*, Nuremberg, Germany.
- Ceh, M., Fall, R., Bergeron, D., El-Maach, I., Jetté, F. and Dionne, J.P. 2005. *Protocols to Test Upper Body PPE Against AP Blast Mines*. Defence R&D Canada (DRDC) Technical Memorandum, DRDC Suffield TM 2005-216.
- Chichester, C., Bass, C., Boggess, B., Davis, M., Sanderson, E., Di Marco, G., Andrefsky, W. And Hess, W. 2001. *A Test Methodology for Assessing Demining Personal Protective Equipment (PPE)*. USA: US Army Developmental Test Command, Volume 1, Report number ATC-8437.
- Clasper, J. 2014. Personal communication via discussions held at Cranfield University on 4 June. Cranfield University, Shrivenham, U.K.
- CONWEP: Conventional Weapons Effects Program, 1991. Prepared by DW Hyde, ERDC, U.S. Army Corps of Engineers, Vicksburg, MS.
- Cooper, G., Townsend, D., Cater, S. and Pearce, B. 1991. The Role of Stress Waves in Thoracic Visceral Injury from Blast Loading: Modification of Stress Transmission by Foams and High-density Materials. *Journal of Biomechanics*, Vol. 24, No. 5, pp. 273-284.

- Cooper, G. 1996. Protection of the Lung from Blast Overpressure by Thoracic Stress Wave Decouplers. *The Journal of Trauma*, Vol. 40 (3s), pp. 105S-110S.
- Cooper, G., Pearce, B., Sedman, A., Bush, I. and Oakley, C. 1996. Experimental Evaluation of a Rig to Simulate the Response of the Thorax to Blast Loading. *The Journal of Trauma*, Vol 40 (3S) Supplement, pp. 38S-41S.
- Courtney A, Courtney M. 2009. A Thoracic Mechanism of Mild Traumatic Brain Injury Due to Blast Pressure Waves. *Medical Hypotheses*, Volume 72 (1), pp. 76-83.
- Cripps, N. And Cooper, G. 1997. Risk of Late Perforation in Intestinal Contusions caused by Explosive Blast. *British Journal of Surgery*, Vol. 84, pp. 1298-1303.
- Dearden, P. 2001. New Blast Weapons. *Journal of the Royal Army Medical Corps*, Vol. 147, pp. 80-86.
- De Ceballos J., Turegano-Fuentes F., Perez-Diaz D., Sanz-Sanchez M., Martin-Llorente C., Guerrero-Sanz J. 2005. 11 March 2004: The Terrorist Bomb Explosions in Madrid, Spain – An Analysis of the Logistics, Injuries Sustained and Clinical Management of Casualties Treated at the Closest Hospital. *Critical Care*, Vol. 9, pp. 104–111.
- Denel, [no date]. *M26 HE Hand Grenade*. Available from: <http://www.denel.co.za/Landsystems/LS_PyrotechnicsGrenades.pdf> [Accessed on 02 November 2007].
- Department of Defense Explosives Safety Board (DDESB), [no date]. *TP17- DDESB Blast Effects Computer Version 6 User's Manual and Documentation*. Available at <www.ddesb.pentagon.mil/techpapers.html> [Accessed on 29 April 2013].
- Dionne, J.P. and Makris, A. 2011. Increased Blast Injury Potential in the Vicinity of Reflecting Surfaces and VBIEDs. In *Proceeding of North Atlantic Treaty Organisation (NATO), Research and Technology Organisation (RTO), The RTO Human Factors and Medicine Panel (HFM) Task Group TG-207 (NATO-RTO-TR-HFM-207), A Survey of Blast Injury across the Full Landscape of Military Science*, Halifax, Canada.
- Dodd, K., Yelverton, J., Richmond, D., Morris, J. and Ripple, G. 1990. Nonauditory Injury Threshold for Repeated Intense Free Field Impulse Noise. *Journal of Occupational Medicine*, Vol. 32, pp. 260-266.
- Dosquet, F., Niew, O. and Lammers, C. 2004. Test Methodology for Protection of Vehicles Occupants against IED. In *Proceedings of 18th Symposium of Military Aspects of Shock and Blast*, Germany.
- Elsayed, N. 1997. Toxicology of Blast Overpressure. *Toxicology*, Vol. 121, pp. 1-15.

- Elsayed, N. and Gorbunov, N. 2007. Pulmonary Biochemical and Histological Alterations after Repeated Low-Level Blast Overpressure Exposures, *Toxicological Sciences*, Vol. 95(1), pp. 289-296.
- Forth, S. 2012. ProSAir 2012.5 User Guide. Applied Mathematics and Scientific Computing, CDS Shrivenham, Swindon, SN6 8LA, UK.
- Forth, S. and Sharma, M. 2014. Personal communication via discussions held at Cranfield University on 6 June. Cranfield University, Shrivenham, U.K.
- Gartner, L. and Hiatt, J. 1994. *Colour Atlas of Histology*. Edition 2. Hagerstown, Maryland, U.S.A: Lippincott Williams & Wilkins.
- Geneva International Centre for Humanitarian Demining (GICHD), [no date]. Introduction to mine action. Available from: < <http://www.gichd.org> > [Accessed on 4 November 2004].
- Goodman, H. 1960. *Compiled Free Air Blast Data on Bar Spherical Pentolite*. BRL Report 1092, Aberdeen Proving Ground, Maryland, 1960. In: *Unified Facilities Criteria (UFC) 3-340-02. 2008. Structures to Resist the Effects of Accidental Explosions*. Department of Defense, USA.
- Gondusky, J. and Reiter, M. 2005. Protecting Military Convoys in Iraq: An Examination of Battle Injuries Sustained by a Mechanized Battalion During Operation Iraqi Freedom II. *Military Medicine*, Vol.170(6), pp. 546-549.
- Global Security .Org. [no date]. *Hand Grenades*. Available from: <<http://www.globalsecurity.org/military/library/policy/army/fm/3-23-30/appe.htm>> [Accessed on 02 November 2007].
- Harrison, C., Bebarta, V., Xydakis, M., Grant, G. and Conner, J. 2006. Tympanic-membrane Perforation as a Biomarker of Barotrauma After Blast Exposure in Iraq. *New England Journal of Medicine*, Vol. 357, pp. 830-831.
- Hattingh, T. and Skews, B. 2001. Experimental Investigation of the Interaction of Shock Waves with Textiles. *Shock Waves*, Vol. 11, pp. 115-123.
- Hayda, R., Harris, R. and Bass, C. 2004. Blast Injury Research: Modeling Injury Effects of Landmine, Bullets, and Bombs. *Clinical Orthopaedics and Related Research*, Vol. 422, pp. 97-108.
- Held, M. 2008. Behind Armour Effects at Shaped Charge Attacks. In *Proceedings of the 24th International Symposium on Ballistics (ISB)*, New Orleans, U.S.A.

Hepper, A., Pope, D., Bishop, M., Kirkman, E., Sedman, A., Mahoney, P., Clasper, J. and Russell, R. 2011. Modelling the Blast Environment and Relating this to Clinical Injury. In *Proceeding of North Atlantic Treaty Organisation (NATO), Research and Technology Organisation (RTO), The RTO Human Factors and Medicine Panel (HFM) Task Group TG-207 (NATO-RTO-TR-HFM-207), A Survey of Blast Injury across the Full Landscape of Military Science*, Halifax, Canada.

Hoge, C., McGurk, D., Thomas, J., Cos, A., Engel, C. and Castro, C. 2008. Mild Traumatic Brain Injury in U.S. Soldiers Returning from Iraq. *New England Journal of Medicine*, Vol. 358, pp. 453-463.

Horrocks, C. 2001. Blast Injuries: Biophysics, Pathophysiology and Management Principles. *Journal of the Royal Army Medical Corps*, Vol. 147, pp. 28-40.

Horsch, J., Lau, I., Viano, D. and Andrzejack, D. 1985. Mechanism of Abdominal Injury by Steering Wheel Loading. In *the Proceedings of the 29th Stapp Car Crash Conference*, Warrendale, PA: Society of Automotive Engineers, SAE 851724.

Hull, J. and Cooper, G. 1996. Pattern and Mechanism of Traumatic Amputation by Explosive Blast. *Journal of Trauma*, Vol. 40(S), pp. S198-S205.

Hyde, D. 1992. *User's guide for microcomputer program CONWEP: applications of TM 5-885-1*. Fundamental of protective design for conventional weapons, Instruction report SL-88-1.

International Mine Action Standards (IMAS). 2009. *IMAS 10.3: Safety and Occupational Health – Personal Protective Equipment*. Second edition. Available at: <[http://www.mineactionstandards.org/IMAS_archive/Final/IMAS%2010.30%20SOH%20PPE%20\(Edition%202\).pdf](http://www.mineactionstandards.org/IMAS_archive/Final/IMAS%2010.30%20SOH%20PPE%20(Edition%202).pdf)>.

Iremonger, M. 1997. Physics of Detonations and Blast-Waves. In: Cooper G., Dudley H. and Gann D. Eds. *Scientific Foundations of Trauma*. Oxford, UK: Butterworth-Heinemann, Section 3, Chapter 15, pp. 189-199.

Johnson, N. and Claber, K. 2000. Blast Measurements – Trends and Anomalies (Revised Paper). In *Proceedings of the 16th International Symposium and Military Aspects of Blast and Shock*, Keble College, Oxford.

Joynt, V. 2008. Course Notes: Light Armoured Vehicle Design Course. Cranfield University, Shrivenham, UK.

Katz, E., Ofek, B., Adler, J., Abramovitz, H., Krausz, M. 1989. Primary Blast Injury After a Bomb Explosion in a Civilian Bus. *Annals of Surgery*, Vol. 209(4), pp.484-488.

- Kingery, C. 1966. Air blast parameters vs. Scaled distance for hemispherical TNT surface burst, BRL report 1344. In: Swisdak, M. 1994. Simplified Kingery Airblast Calculations, *In the Proceedings of the 26th DoD Explosives Safety Seminar*, Miami, Florida, USA.
- Kingery, C. and Bulmash, G. 1984. *Airblast Parameters from TNT Spherical Air Burst and Hemispherical Surface Burst*. U.S. Army BRL, Aberdeen Proving Ground, MD, Report ARBL-TR-02555.
- Kingery, C. and Pannill, B. 1964. *Peak Overpressure vs. Scaled Distance for TNT Surface Bursts (Hemispherical Charges)*. U.S. Army BRL, Memorandum Report 1518.
- Kinney, G. and Graham, K. 1985. *Explosive Shocks in Air*. Second edition. New York, U.S.A.: Springer-Verlag New York Inc, ISBN 3-540-15147-8.
- Kirkman, E., Watts, S. And Cooper, G. 2011. Blast Injury Research Models. *Philosophical Transactions of the Royal Society Biological Sciences*, Vol. 366, pp. 144-159.
- Kluger, Y., Nimrod, A., Bidernan, P., Mayo, A. and Sorkin, P. 2007. The Quinary Pattern of Blast Injury. *American Journal of Disaster Medicine*, Vol. 2, pp. 21-25.
- Knock, C. and Davies, N. 2013. Blast Waves from Cylindrical Charges. *Shock Waves*, Vol. 23, pp. 337-343.
- Köhler, J. and Meyer, R. 1993. *Explosives: Fourth, revised and extended edition*. U.S.A: VCH Publishers, ISBN 1-56081-266-4.
- Kroell, C., Schneider, D. and Nahum, A. 1971. Impact Tolerance and Response of The Human Thorax. *15th Stapp Car Crash Conference*, SAE Paper No. 710851.
- Kroell, C., Allen, S., Warner, C. and Perl, C. 1986. Interrelationship of Velocity and Chest Compression in Blunt Thoracic Impact to Swine II. *30th Stapp Car Crash Conference*, SAE Paper No. 861881.
- Lau, I. and Viano, D. 1986. The Viscous Criterion - Bases and Applications of an Injury Severity Index for Soft Tissues. *In Proceedings of the 30th Stapp Car Crash Conference*, Warrendale, Pa, Society of Automotive Engineers (SAE) Paper No. 86182123.
- Lee, E., Hornig, H. and Kury, J. 1968. *Adiabatic Expansion of High Explosive Detonation Products*, Lawrence Radiation Laboratory, University of California, Livermore. Reproduced by United States Department of Energy: Oak Ridge, Tennessee, Document number: UCRL-50422.

- Leerdam, P.J. 2002. Research Experiences on Vehicle Mine Protection. *In Proceedings of First European Survivability Workshop (ESW)*, Germany.
- Lewis, E. 2006. Between Iraq and a Hard Plate: Recent Developments in UK Military Personal Armour. *In Proceedings of the Personal Armour Systems Symposium (PASS)*, Manchester, UK.
- Loiseau, O., Cheval, K. and Kevorkian, S. 2009. Laboratory Scale Tests for the Assessment of Solid Explosive Blast Effects. *Eurosafe Forum*, Brussels, Belgium. Available from: <<http://www.eurosafe-forum.org/>> [Accessed on: 10 June 2014].
- Mayorga, M. 1997. The Pathology of Primary Blast Overpressure Injury. *Toxicology*, Vol. 121, pp. 17-28.
- McKay, B., Foster, C., Depinet, P. and Bir, C. 2010. A Biofidelic Lower Extremity Surrogate for Evaluating Military Vehicle Occupant Injury in Underbelly Blast Impacts. *In Proceedings of the Personal Armour Systems Symposium (PASS)*, Quebec, Canada.
- Medin, A., Axelsson, H. and Suneson, A. 1998. The reactions of the crew in an armoured personnel carrier to an anti-tank mine blast: A Swedish incident in Bosnia 1996. *FOA Defence Research Establishment*, ISSN 1104-9154.
- Meel, B. 2007. Lightning Fatalities in the Transkei Sub-region of South Africa. *Medical Science and Law*, Vol. 47(2), pp. 161-164.
- Meel, B. 2008. Personal communications with Professor Meel, including descriptions and photographs of M26 hand grenade incident that occurred near Mthatha in 1998. Walter Sisulu University, Mthatha, South Africa (Email communications in possession of the author).
- Meel, B., Whyte, T. and Kaswa, R. 2009. Accidental Hand-Grenade Injuries in the Transkei Region of South Africa: A Case Report. *South African Family Practise*, Vol. 51(4), pp. 348-350.
- Mertz, H., Horsch, J., Horn, G. and Lowne, R. 1991. *Hybrid III Sternal Defelction Association with Thoracic Injury Severities of Occupants Restrained with Force Limiting Belts*. Warrendale, Pa, Society of Automotive Engineers (SAE) PT-92.
- National Center for Injury Prevention and Control, Division of Injury Response, Centers for Disease Control and Prevention (CDC) CS218119-A, [no date]. *Blast Injuries: Fact sheet for professionals*. U.S. Department of Health and Human Services, U.S.A. Available from: <<http://emergency.c.c.gov/BlastInjuries>> [Accessed on: 22 February 2013].
- National Highway Traffic Safety Administration (NHTSA), [no date]. *Biomechanics and Trauma*. Available from: <www.nhtsa.gov/Research> [Accessed on 18 May 2013].

North Atlantic Treaty Organisation (NATO), Research and Technology Organisation (RTO), Human Factors and Medicine Panel (HFM) Task Group TG-022 (NATO-RTO-TR-HFM-022), 2003. *Reconsideration of the Effects of Impulse Noise*. Neuilly-sur-Seine Cedex, France, Technical report (TR) 017 AC/323 TP/17.

North Atlantic Treaty Organisation (NATO), Research and Technology Organisation (RTO), Human Factors and Medicine Panel (HFM) Task Group TG-024 (NATO-RTO-TR-HFM-089), 2004. *Test Methodologies for Personal Protective Equipment Against Anti-Personnel Mine Blast*. Neuilly-sur-Seine Cedex, France.

North Atlantic Treaty Organisation (NATO), Research and Technology Organisation (RTO), Human Factors and Medicine Panel (HFM) Task Group TG-25 (NATO-RTO-TR-HFM-090), 2007. *Test methodology for protection of vehicle occupants against anti-vehicular landmine effects*. Neuilly-sur-Seine Cedex, France.

North Atlantic Treaty Organisation (NATO), Research and Technology Organisation (RTO), Human Factors and Medicine Panel (HFM) Task Group TG-148 (NATO-RTO-TR-HFM-148), 2012. *Test methodology for protection of vehicle occupants against anti-vehicular landmine and/or IED effects*. Neuilly-sur-Seine Cedex, France.

North Atlantic Treaty Organisation (NATO) Standardization Agreement (STANAG) 2920, 2003. *Ballistic Test Method for Personal Armour Materials and Combat Clothing*. Neuilly-sur-Seine Cedex, France. Annex B, edition 7.

National Institute of Justice (NIJ), 2008. *Ballistic Resistance of Body Armor (NIJ-0101.06)*. U.S.A, Washington, U.S. Department of Justice Office of Justice Program. Available from: <www.ojp.usdoj.gov/nij> [Accessed on: 13 May 2013].

National Institute of Justice (NIJ), 2008. *Draft NIJ Bomb Suit Standard for Law Enforcement (NIJ Standard-0117.00)*. U.S. Department of Justice Office of Justice Program. No longer available online.

National Institute of Justice (NIJ), 2009. *National Law Enforcement and Correction Technology Centre, A program of the National Institute of Justice, Bomb Suit Standard, Fall 2009 TechBeat Report*. U.S. Department of Justice Office of Justice Program. Available from: <<http://www.justnet.org/TechBeat%20Files/Bomb%20Suite%20Standard.pdf>> [Accessed on: 14 June 2010].

National Institute of Justice (NIJ), 2010. *NIJ Bomb Suit Standard for Public Safety June 2010 Fact Sheet*. National Law Enforcement and Correction Technology Centre, A program of the U.S. National Institute of Justice. Available from: <http://www.justnet.org/Lists/JUSTNET%20Resources/Attachments/2025/Bomb_Suit_Handout.pdf> [Accessed on: 14 June 2010].

National Institute of Justice (NIJ), 2012. *Public Safety Bomb Suit Standard (NIJ Standard-0117.00)*. U.S.A, Washington, DC 20531, U.S. Department of Justice Office of Justice Program, NCJ 227357.

National Institute of Justice (NIJ), 2012. *Public Safety Bomb Suit Certification Program Requirements (NIJ CR-0117.00)*. U.S.A, Washington, DC 20531, U.S. Department of Justice Office of Justice Program, NCJ 237910. Available from: <www.ncjrs.gov/pdffiles1/nij/237910.pdf> [Accessed on: 13 May 2013].

Nelson, T., Clark, T., Stedje-Larsen, E., Lewis, C., Grueskin, J., Echols, E., Wall, D., Felger, E. and Bohman, H. 2008. Close Proximity Blast Injury Patterns from Improvised Explosive Devices in Iraq: A Report of 18 Cases. *The Journal of Trauma*, Vol. 65, pp. 212-217.

Nerenberg, J., Makris, A. and Kleine, H. 2000. The Effectiveness of Different Personal Protective Ensembles in Preventing Injury to the Thorax from Blast-Type Anti-Personnel Mines. *The Journal of ERW and Mine Action*, Issue 4.2. Available from: <<http://maic.jmu.edu/journal/4.2/focus/effectiveness/effect.htm>> [Accessed on: 11 May 2013].

Office of the Assistant Secretary of Defense for Special Operations/Low Intensity Conflict (OASD(SO/LIC)), 2000. *Landmine Casualty Data Report: Deminer Injuries*. U.S. Department of Defense.

Ouellet, S., Levine, J. And Dionne, J.P. 2008. Parametric Study on Rigid Plates, Compressible Foams and Air Gaps Combinations for Mitigating Blast in Personal Protection Applications. *In Proceedings of the Personal Armour Systems Symposium (PASS)*, Brussels, Belgium.

Ouellet, S. and Williams, K. 2008. Characterisation of Defence Research and Development Canada's Mannequin for the Assessment of Blast Incapacitation and Lethality (DRDC MABIL). *In Proceedings of the Personal Armour Systems Symposium (PASS)*, Brussels, Belgium.

Peare, A. 2013. Personal communication via email with Alan Peare during the 2013/2014 academic year. Cranfield University, Shrivenham, U.K. (Email communication in possession of the author).

Peters, P. 2011. Primary Blast Injury: An Intact Tympanic Membrane Does Not Indicate the Lack of a Pulmonary Blast Injury. *Military Medicine*, Vol. 176(1), pp. 110-115.

Petes, J. 1968. Blast and Fragmentation Characteristics. In: Weyer, E. Ed. *Prevention Of and Protection Against Accidental Explosion of Munitions, Fuels and Other Hazardous Mixtures*. New York Academy of Sciences, Annals, 152, Part 1.

- Phillips, Y. and Richmond, D. 1991. Primary Blast Injury and Basic Research: A Brief History. In: R.F. Bellamy and R. Zajtchuk (Eds), *Textbook of Military Medicine, Part I, Vol. 5, Conventional Warfare, Ballistic, Blast, and Burn Injuries*. Washington, DC: Office of the Surgeon General, Department of The Army, pp. 221 -240.
- Rabet, L., Scheppers, J., Verpoest, I., Pirlot, M., Desmet, B., Gilson, L. and Pirard, P. 2006. Development of Low Cost Composite Plates for Humanitarian Demining Operations. *Journal de Physique IV France*, Vol. 134, pp. 1225-1230.
- Radonic, V., Giunio, L., Biocic, M., Tripkovic, A., Luksic, B. and Primorac, D. 2004. Injuries form Antitank Mines in Southern Croatia. *Military Medicine*, Vol. 169.
- Raghavendran, K., Davidson, B., Helinski, J., Marschke, C., Manderscheid, P., Woytash, J., Notter, R. and Knight, P. 2005. A Rat Model for Isolated Bilateral Lung Contusion from Blunt Chest Trauma. *Anesthesia and Analgesia*, Vol. 101, pp. 1482-1489.
- Ramasamy, A., Masouros, S., Newell, N., Hill, A., Proud, W., Brown, K., Bull, A. and Clasper, J. 2011. In-Vehicle Extremity Injuries From Improvised Explosive Devices: Current and Future Foci. *Philosophical Transactions of the Royal Society Biological Sciences*, Vol. 366, pp. 160-170.
- Remennikov, A. 2003. A Review of Methods for Predicting Bomb Blast Effects on Buildings. *Journal of Battlefield Technology*, Vol. 6(3).
- Richmond, D., Damon, E., Fletcher, E., Bowen, I. and White, C. 1968. The Relationship Between Selected Blast-Wave Parameters and the Response of Mammals Exposed to Air Blast. In: Weyer, E. Ed. *Prevention Of and Protection Against Accidental Explosion of Munitions, Fuels and Other Hazardous Mixtures*. New York Academy of Sciences, Annals, 152, Part 1.
- Schmitt, K., Niederer, P. and Walz, F. 2004. *Trauma Biomechanics: Introduction to Accidental Injury*. Berlin, Heidelberg, New York: Springer-Verlag.
- Sharpnack, D., Johnson, A., Phillips, Y. 1991. The Pathology of Primary Blast Injury. In: Bellamy, R. and Zajtchuk, R. Eds. *The Textbook of Military Medicine – Conventional Warfare: Ballistic, Blast, and Burn Injuries*. Washington, DC: Department of the Army, Office of the Surgeon General, pp. 271-294.
- Shirinov, A. and Schomburg, W. 2008. Pressure Sensor From a PVDF Film. *Sensors and Actuators A: Physical*, Vol. 142, Issue 1, pp.48 – 55.
- Singleton, J., Gibb, I., Bull, A., Mahoney, P. and Clasper, J. 2013. Primary Blast Lung Injury Prevalence and Fatal Injuries from Explosions: Insights from Postmortem Computed Tomographic Analysis of 121 Improvised Explosive Device Fatalities.

Smith, A, [no date]. Database of Demining Accidents (DDAS). Available from: <<http://www.ddasonline.com>>.

Smith, P. and Hetherington, J. 1994. *Blast and Ballistic Loading of Structures*. Butterworth-Heinemann, ISBN 0750620242, 9780750620246.

Smith, S., Stuhmiller, J. and Januszkiewicz, A. 1996. Evaluation of Lethality Estimates for Combustion Gases in Military Scenarios. *Toxicology*, Vol. 115, pp. 157-165.

Snyman, I. 2008. Personal communication with Izak Snyman. Council for Scientific and Industrial Research (CSIR), Pretoria, South Africa (Emailed data in possession of the author).

Stewart, C. 2006. Blast Injuries: Preparing for the Inevitable. *Emergency Medicine Practice*, Vol. 8(4), pp. 1-28. Available from: <EBMedicine.net> [Accessed: 22 January 2013].

Stiff, P. 1986. *Taming the landmine*. Alberton, South Africa: Galago Publishing.

Stuhmiller, J., Phillips, Y. and Richmond, D. 1991. The Physics and Mechanisms of Primary Blast Injury. In: Bellamy, R. and Zajtchuk, R. Eds. *The Textbook of Military Medicine – Conventional Warfare: Ballistic, Blast, and Burn Injuries*. Washington, DC: Department of the Army, Office of the Surgeon General, pp. 241-270.

Suneson, A., Hansson, H. and Seeman, T. 1987. Peripheral High-Energy Missile Hits Cause Pressure Changes and Damage to the Nervous System: Experimental Studies on Pigs. *The Journal of Trauma*, Vol. 27(7), pp. 782-789.

M. Swisdak. 1975. *Explosion Effects and Properties, Part 1, Explosion Effects in Air*. Naval Surface Weapons Center White Oak Lab Silver Spring MD. 20910. Reproduced by U.S. Department of Commerce, National Technical Information Service, Springfield, VA 22161.

Swisdak, M.M. Jr. 1994. Simplified Kingery Airblast Calculations, Proceedings of the twenty sixth DoD Explosives Safety Seminar, Miami, FL on 16-18 August.

Swisdak, M.M. Jr. 2000. *Blast Effects Computer Version 4.0 (BECV4)*[Computer program]. Department of Defense Explosives Safety Board. Available from: <<http://orise.orau.gov/emi/hazards-assessment/files/resources/BlastEffectsComputer4.0Description.pdf>> [Accessed: 19 January 2013].

Swisdak, M. and Absil, L. 2000. 40 Tonne Event: A Comparison of Predicted and Measured Airblast Results. *Minutes of the 29th DoD explosives Safety Seminar*, U.S.A., New Orleans.

Swisdak, M., Ward, J. and Jerry, M. 2000. The DDESB Blast Effects Computer – Version 4. *Minutes of the 29th DoD explosives Safety Seminar*, U.S.A., New Orleans.

Taber , K., Warden, D. and Hurley R. 2006. Blast-related Traumatic Brain Injury: What is Known? *Journal of Neuropsychiatry and Clinical Neuroscience*, Vol. 18, pp. 141-145.

Tatic, V., Ignjatovic, D., Jevtic, M., Jovanovic, M., Draskovic, M. and Durdevic, D. 1996. Morphologic Characteristics of Primary Nonperforative Intestinal Blast Injuries in Rats and their Evolution to Secondary Perforations. *The Journal of Trauma*, Vol. 40(3S), pp.94S-99S.

Teland, J. and van Doormaal, J. 2012. Blast Wave Injury Predictions for Complex Scenarios. *In Proceedings of 22nd Military Aspects of Blast and Shock (MABS)*, Bourges, France.

The European Committee for Standardisation (CEN) Workshop Agreement, 2007. *Humanitarian Mine Action (HMA) – Personal Protective Equipment (PPE) – Test and Evaluation*. CWA 15756.

The European Committee for Standardisation (CEN) Workshop Agreement Withdrawn, [no date]. *Provisionally Withdrawn: Humanitarian Mine Action (HMA) – Personal Protective Equipment (PPE) – Test and Evaluation* (CWA 15756). Acquired from: <<http://www.mineactionstandards.org/withdrawn.htm>> and <<http://www.cen.eu/cen/Sectors/TechnicalCommitteesWorkshops/Workshops/Pages/ws26.aspx>> [Accessed on: 2 February 2010].

Trimble, K., McLean, D., Sedman, A. and Watkins, P. 2002. Modulation of Primary Pulmonary Blast Injury by a New Body Armour. *Journal of Bone and Joint Surgery – British Volume*, Vol 84(B), pp. 171.

Unified Facilities Criteria (UFC), 2008. *Structures to resist the effects of accidental explosions (UFC 3-340-02)*. Department of Defense, USA.

United States Department of Defense (U.S. DoD) Humanitarian Demining R&D Program. 2013. *Landmine Threats Continuing Injuries*. Available at: <www.humanitarian-demining.org/2010Design/Threats_Injuries.asp> [Accessed on 11 May 2013].

van der Horst, M., Leerdam, P.J., Manseau, J., Lafont, D., Dosquet, F., Bir, C., Philippens, M., Vezin, P., Reinecke, D., Whyte, T., Svensson, L., Arborelius, U. and Frydman, A. 2010. Criteria and Test Methodologies for Injury Assessment of Vehicle

Occupants Threatened by Landmines and/or IED: An Approach by HFM-148/RTG. *In Proceedings of Personal Armour Systems Symposium (PASS)*, Quebec, Canada.

van der Horst, Leerdam, P.J., Manseau, J., Dosquet, F., Svensson, L., Axelsson, H., Lafont, D., Lemasle, R. and Wolfe, G. 2006. Occupant Safety Measurements and Injury Assessment for the Anti-Vehicular Landmine Threat; An Approach by HFM-090/TG-25. *In Proceedings of the Third European Survivability Symposium*, Toulouse, France.

van de Vord, P., Bolander, R., Sajja, V., Hay, K. and Bir, C. 2012. A Mild Neurotrauma Indicates a Range-Specific Pressure Response to Low Level Shock Wave Exposure. *Annals of Biomedical Engineering*, Vol. 40 (1), pp. 227-236.

Viano, D. and Lau, I. 1985. Thoracic Impact: A Viscous Tolerance Criterion. *In Proceedings of the Tenth International Conference on Experimental Safety Vehicles*, Oxford, England.

Viano, D. and Lau, I. 1988. A Viscous Tolerance Criterion for Soft Tissue Injury Assessment. *Journal of Biomechanics*, Vol. 21, pp. 387–399.

White, C. 1968. The Scope of Blast and Shock Biology and Problem Areas in Relating Physical and Biological Parameters. In: Weyer, E. Ed. *Prevention Of and Protection Against Accidental Explosion of Munitions, Fuels and Other Hazardous Mixtures*. New York Academy of Sciences, Annals, 152, Part 1.

Whyte, T. 2007. Investigation of Factors Affecting Surrogate Limb Measurements in the Testing of Landmine Protected Vehicles. Thesis presented for the degree of Master of Science in Mechanical Engineering, University of Cape Town, South Africa.

Whyte, T., Snyman, I.M. and Meel, B.L. 2008. Prediction of Injuries Caused by Explosive Events: A Case Study of a Hand Grenade Incident in South Africa. *In Proceedings of Science real and relevant: 2nd Council for Scientific and Industrial Research (CSIR) biennial conference*, Pretoria, South Africa.

Wightman, J. and Gladish, S. 2001. Explosions and Blast Injuries. *Annals of Emergency Medicine*, Vol. 37, pp. 664-678.

Wildegger-Gaissmaier, A. 2003. Aspects of Thermobaric Weaponry. *ADF Health*, Vol. 4, pp. 3-6.

Wilkinson, A. 2003. International Mine Action Standards: Future Development of PPE Standards. *Journal of Mine Action*, Issue 7.1.

Wolf, S., Bebarta, V., Bonnett, C., Pons, P. and Cantrill, S. 2009. Blast Injuries. *The Lancet*, Vol. 374, pp. 405-415.

Xydakis, M., Bebarta, V., Harrison, C., Conner, J., Grant, G. and Robbins, A. 2007. Tympanic-Membrane Perforation as a Marker of Concussive Brain Injury in Iraq. *New England Journal of Medicine*, Vol. 357, pp. 830-831.

Yelverton, J. 1996. Pathology Scoring System for Blast Injuries. *The Journal of Trauma*, Vol. 40(3S), pp. 111S-115S.

Yelverton, J. 1997. Blast Biology. In: Cooper, G., Dudley, H., Gann, D., Little, R. and Maynard, R. Eds. *Scientific Foundations of Trauma*. UK: Reed Educational and Professional Publishing Ltd.

Zajtchuk, R. 1990. *Conventional Warfare: Ballistic, Blast, and Burn Injuries*. Textbook of Military Medicine: Warfare, Weaponry, and the Casualty, Volume 5 Part 1. Defence Dept., Army, Office of the Surgeon General, Borden Institute.

Zuckerman, S. 1941. The Problem of Blast Injuries. *Proceedings of the Royal Society of Medicine*, Vol. 34, pp. 171-188.

11 APPENDICES

APPENDIX A: SUPPLEMENTARY INFORMATION FOR CHAPTER 3

APPENDIX A1: MATLAB Simulink™ Diagram to Calculate the Chest Wall Velocity Predictor (CWVP)

Figure B1 shows the feedback loop generated in MATLAB Simulink™ to calculate the chest wall velocity. The inputs required are the measured face-on pressure signal in kPa (pdata) and the atmospheric pressure (Po). The program outputs the chest wall velocity (vel) which is the required parameter for the CWVP injury risk values.

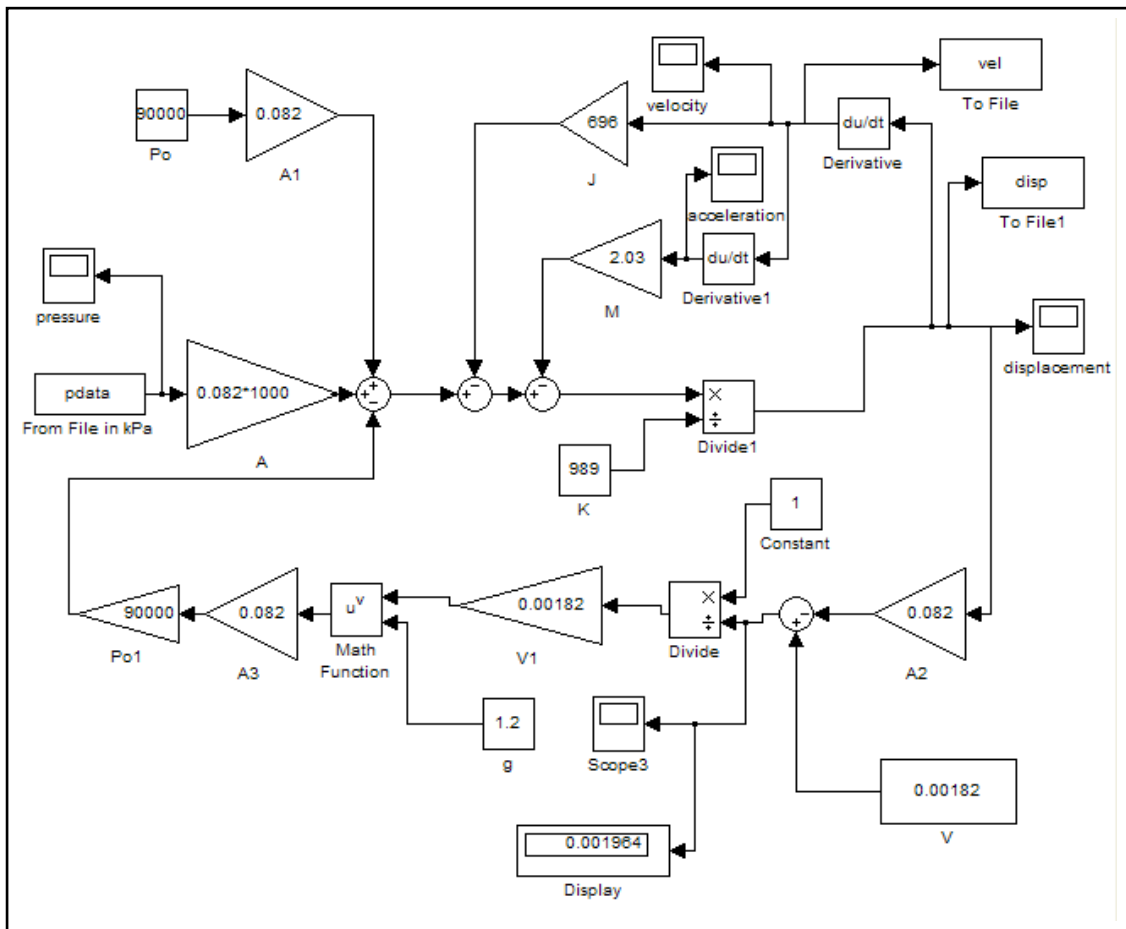


Figure A1: MATLAB Simulink™ Diagram to Calculate the Chest Wall Velocity Predictor (CWVP)

APPENDIX B: SUPPLEMENTARY INFORMATION FOR CHAPTER 4

APPENDIX B1: MATLAB Code to Process and Plot the ProSAir Simulation Results

plot_ProSAir_results.m

```
%Plots results of ProSAir tests
%saved as plot_ProSAir_results.m

clear all;

load('time');
load('olthorax');

time=time';
olthorax=olthorax';
t(1:1199)=0;
olthoraxval(1:1199)=0;
olthoraxref(1:1199)=0;
cf=3.5; %conversion factor calculated from BECV4 to convert the
pressure from side-on to reflected pressure

for loop=1:1199
    t(loop)=time{loop};
    olthoraxval(loop)=olthorax{loop};
    olthoraxref(loop)=olthorax{loop}*cf;
end;

time=t;
olthorax=olthoraxval;
save('olthoraxref','olthoraxref');
save('t','t');

plot(t,olthorax,'r');
xlabel('Time in ms');
ylabel('Occupant 4 Thorax (Side-on Pressure in kPa)');
grid on;

pause;
hold on;

plot(t,olthoraxref,'b');
xlabel('Time in ms');
ylabel('Occupant 4 Thorax (Side-on and Reflected Pressure in kPa)');
grid on;
pause;

tstart=0.050930306;
tend=10.0057926;
tstep=(tend-tstart)/(1198);
```



```

timefixedstep=(tstart:tstep:tend);

plot(timefixedstep,olthoraxref,'g');
grid on;

pause;
hold off;

[maxolthorax,imaxolthorax]=max(olthorax);%maximum or peak side-on
pressure
timemaxolthorax=t(imaxolthorax);%time at which this peak occurs
[maxolthoraxref,imaxolthoraxref]=max(olthoraxref);%maximum or peak
reflected pressure
timemaxolthoraxref=t(imaxolthoraxref);%time at which this peak occurs

disp('Peak side-on pressure is ')
disp(maxolthorax);
disp('and occurs at time ')
disp(timemaxolthorax);
disp('Peak reflected pressure is ')
disp(maxolthoraxref);

%now need to load the time and reflected pressure files that were
saved for
%each target point and calculate the cwvp

```

plot_prosair_cwvp

```
%plot prosair results, convert to face-on or reflected pressure and
%calculate the cwvp

%saved as plot_prosair_cwvp

clear all;

load('olthorax');

cf=3.5; %conversion factor for side-on to face-on for occupant 1
thorax

tend=1198*0.000008303;
time=(0:0.000008303:tend);%in seconds

for loop=1:1199
    olthoraxval(loop)=olthorax{loop};
    olthoraxref(loop)=olthorax{loop}*cf;
end;

cp=olthoraxref.*1000; %to convert to Pa
pressure=cp;

%calculating cwvp

plot(time,pressure,'r');
xlabel('Time in seconds');
ylabel('Chest reflected pressure in Pa');
grid on;
pause;

%*****
%*****
%CHEST CRITERIA
%*****
%*****
pressurefn=[time;pressure];

save('pressurefn','pressurefn');

t = sim('cwvmodel_prosair');%name of specific simulink file to handle
this data format-note time spans must be specified in the simulink
file
%also note that pressurefn needs to have same sample rate as that of
the
%time sampling (left click on pressurefn block in simulink to change
the
%sample time!!)
```

```

load('vel');
load('displ');

plot(vel(1,:),vel(2,:));
tcwv=vel(1,:);
cwv=vel(2,:);
grid on;
%title('Chest wall velocity calculated for target point');
xlabel('Time (s)');
ylabel('Chest wall velocity (m/s)');

[peakvel,i1]=max(vel(2,:));
minvel=min(vel(2,:));
stnum=num2str(peakvel);
disp(['Maximum chest wall velocity: ',stnum,'m/s.']);

stnum=num2str(minvel);
disp(['Minimum chest wall velocity: ',stnum,'m/s.']);

%set to columns so easy to copy to excel
tcwv=tcwv';
cwv=cwv';
time=time';
pressure=pressure';

```

APPENDIX C: SUPPLEMENTARY INFORMATION FOR CHAPTER 6

APPENDIX C1: MATLAB Code to Process and Plot the SA Waterman Demining Scenario Results

watermen_viewer_version1.m

```
%09/2007 watermen_viewer_version1.m
%This code processes data and calculates all relevant injury levels

%setting up data before processing can begin
%ATD1 DAQ - serial no. 02062006
g1=237.79;
g2=239.66;
g3=240.34;
g4=241.61;
g5=196.5;
g6=83.862;
g7=85.681;
g8=148.65;
g9=944.63;
g10=1956.2;
g11=1948.6;
g12=705.04;%seat load cell
g13=715.11;
g14=1363.5;
g15=1948;
g16=1923.1;
g17=1140.8;
g18=1149.4;
g19=1637.5;
g20=1135.4;
g21=1144.9;
g22=898.82;
g23=2399.1;
g24=1141;

e1=4.979;
e2=4.994;
e3=4.991;
e4=4.994;
e5=4.980;
e6=4.985;
e7=4.976;
e8=4.973;
e9=4.966;
e10=5.002;
e11=4.974;
e12=4.963;
e13=4.988;
e14=4.973;
e15=4.990;
e16=4.987;
e17=4.981;
```

```

e18=4.975;
e19=4.958;
e20=4.975;
e21=4.970;
e22=4.960;
e23=4.973;
e24=4.983;

```

```

%***CHECK ALL ACCS AND PRESSURES FOR AT 5V EXCITATION AND NOT 10V
%EXCITATION
s1=0.037708;      %headax mV/g at 10v 0.2584
s2=0.01885;      %headay at 10v 0.2474
s3=0.01885;      %headaz at 10v 0.2335
s4=0.037708;      %lumbaray at 10V excitation %0.1075 at 5V
excitation
s5=0.0993;        %lumbaraz at 10V %0.0993 at 5V excitation
s6=0.1190;        %right foot az at 10v 0.2380
s7=0.303;         %pressure chest plate mV/kPa at 10Vdc 0.606
s8=0.037708;      %pressure right ear in mV/kPa transducer model
1471 - 250psi
s9=1.8879*e9/11120.6;      %right lower tibia fx %output at
capacity(mV/V)*excitation voltage/capacity(N) gives sensitivity in
mV/N
s10=1.0616*e10/11120.6;    %right lower tibia fz
s11=1.0418*e11/11120.6;    %right upper tibia fz
s12=1.5*e12/(1000*9.81);    %right lower tibiamx %1.5mV/V at 5V
excitation as is 3mV/V at 10V
s13=3.0000*e13/395.4;      %right lower tibiamy
s14=1.5186*e14/15568.8;    %right ankle fz
s15=0.9427*e15/13344.7;    %lumbar fz
s16=1.0877*e16/11120.6;    %left lower tibia fz
s17=1.6789*e17/8896.4;     %upper neck fx
s18=1.6195*e18/8896.4;     %upper neck fy
s19=1.3267*e19/13344.7;    %upper neck fz
s20=1.6413*e20/282.5;      %upper neck mx
s21=1.6427*e21/282.5;      %upper neck my
s22=2.2967*e22/282.5;      %upper neck mz
s23=0.9247*e23/13344.7;    %lower neck fz
s24=1.7080*e24/451.9;      %lower neck my

```

```

%old values

```

```

k1=1/(g1*s1/1000);
k2=1/(g2*s2/1000);
k3=1/(g3*s3/1000);
k4=1/(g4*s4/1000);
k5=1/(g5*s5/1000);
k6=1/(g6*s6/1000);
k7=1/(g7*s7/1000);
k8=1/(g8*s8/1000);
k9=1/(g9*s9/1000);
k10=1/(g10*s10/1000);
k11=1/(g11*s11/1000);
k12=1/(g12*s12/1000);
k13=1/(g13*s13/1000);
k14=1/(g14*s14/1000);
k15=1/(g15*s15/1000);
k16=1/(g16*s16/1000);
k17=1/(g17*s17/1000);

```

```

k18=1/(g18*s18/1000);
k19=1/(g19*s19/1000);
k20=1/(g20*s20/1000);
k21=1/(g21*s21/1000);
k22=1/(g22*s22/1000);
k23=1/(g23*s23/1000);
k24=1/(g24*s24/1000);

%DAQ module calibration factors
lsb1=5138541;
lsb2=5137644;
lsb3=5138743;
lsb4=5139510;
lsb5=5143096;
lsb6=5144681;
lsb7=5144548;
lsb8=5143030;
lsb9=5143034;
lsb10=5144864;
lsb11=5141033;
lsb12=5140608;
lsb13=5146051;
lsb14=5144106;
lsb15=5141500;
lsb16=5146931;
lsb17=5146575;
lsb18=5143842;
lsb19=5142372;
lsb20=5142923;
lsb21=5144268;
lsb22=5144068;
lsb23=5144033;
lsb24=5143722;

os1=3509254;
os2=3707103;
os3=3535372;
os4=3517065;
os5=-22553994;
os6=-22672507;
os7=-22635456;
os8=-22688160;
os9=-41378200;
os10=-41212233;
os11=-41296774;
os12=-41343432;
os13=-41276693;
os14=-41297240;
os15=-41161695;
os16=-41358444;
os17=-11757656;
os18=-11697527;
os19=-11742609;
os20=-11771349;
os21=-11717166;
os22=-11722145;
os23=-11739478;
os24=-11783587;

```

```

fn='LEGS_060907_1506.dlp';%data file

textname=( [fn(1:16), '_watermen_summary'] );
fnt=fopen(textname, 'wt');

kall=[k1;k2;k3;k4;k5;k6;k7;k8;k9;k10;k11;k12;k13;k14;k15;k16;k17;k18;k
19;k20;k21;k22;k23;k24];
channelall=[1;2;3;4;5;6;7;8;9;10;11;12;13;14;15;16;17;18;19;20;21;22;2
3;24];
lsball=[lsb1;lsb2;lsb3;lsb4;lsb5;lsb6;lsb7;lsb8;lsb9;lsb10;lsb11;lsb12
;lsb13;lsb14;lsb15;lsb16;lsb17;lsb18;lsb19;lsb20;lsb21;lsb22;lsb23;lsb
24];
osall=[os1;os2;os3;os4;os5;os6;os7;os8;os9;os10;os11;os12;os13;os14;os
15;os16;os17;os18;os19;os20;os21;os22;os23;os24];
col=['r';'g';'b';'c'];

fid=fopen(fn, 'r');
[f,lengthfile]=fread(fid);
fclose(fid);
nchannel=length(channelall);
endn=20000;%(lengthfile/nchannel);
for loopk=1:nchannel;
fid=fopen(fn, 'r');
k=kall(loopk);
os=osall(loopk);
lsb=lsball(loopk);
channel=channelall(loopk);

n=1;
t=-0.25;
fs=10000;
h=1/fs;

while n<endn+1;
    A=fread(fid,24, 'ubit16');

    B=A(channel);

    %Swap upper and lower bytes
    X=rem(B,256);
    Y=fix(B/256);
    Z=(256*X)+Y;

    %Apply correction for "sign"
    if Z>(2^15);
        Z=Z-(2^16);
    end;

    Data(n)=k*((lsb*1e-9*Z)-(os*1e-9));
    %Data(n)=k*(20/(2^12))*Z;
    time(n)=t;
    n=n+1;
    t=t+h;
end;%while
fclose(fid);
data{loopk}=Data;

end;%for

```

```

%*****
%*****
%Filtering and subtracting offset from data
%*****
%*****
t0=-0.2;
t1=t;
time=time(501:20000);%to eliminate first 0.05s (index to 501) of
pretrigger data
Data=data{1};
c1=Data(501:20000)-mean(Data(200:500));%not using first 0.05s of
pretrigger data which is 1:501
Data=data{2};
c2=Data(501:20000)-mean(Data(200:500));
Data=data{3};
c3=Data(501:20000)-mean(Data(200:500));
Data=data{4};
c4=Data(501:20000)-mean(Data(200:500));
Data=data{5};
spineaz=Data(501:20000)-mean(Data(200:500));
spineaz=spineaz.*-1;
Data=data{6};
footaz=Data(501:20000)-mean(Data(200:500));
Data=data{7};
pressurechest=Data(501:20000)-mean(Data(200:500));
%gives pressure in kPa
Data=data{8};%right ear pressure
pressureright=Data(501:20000)-mean(Data(200:500));
%gives pressure in kPa
Data=data{9};
rlovertibiafx=Data(501:20000)-mean(Data(200:500));
Data=data{10};
rlovertibiafz=Data(501:20000)-mean(Data(200:500));
Data=data{11};
ruppertibiafz=Data(501:20000)-mean(Data(200:500));
Data=data{12};
seatload=Data(501:20000)-mean(Data(200:500));
Data=data{13};
rlovertibiamy=Data(501:20000)-mean(Data(200:500));
Data=data{14};
ranklefz=Data(501:20000)-mean(Data(200:500));
Data=data{15};
lumbarfz=Data(501:20000)-mean(Data(200:500));
Data=data{16};
llovertibiafz=Data(501:20000)-mean(Data(200:500));
Data=data{17};
uneckfx=Data(501:20000)-mean(Data(200:500));
Data=data{18};
uneckfy=Data(501:20000)-mean(Data(200:500));
Data=data{19};
uneckfz=Data(501:20000)-mean(Data(200:500));
Data=data{20};
uneckmx=Data(501:20000)-mean(Data(200:500));
Data=data{21};
uneckmy=Data(501:20000)-mean(Data(200:500));
Data=data{22};
uneckmz=Data(501:20000)-mean(Data(200:500));
Data=data{23};
lneckfz=Data(501:20000)-mean(Data(200:500));

```



```

Data=data{24};
lneckmy=Data(501:20000)-mean(Data(200:500));

plot(time,c1,'b');
grid on;
title('Foam (blue)and only uniform (red) interface');
xlabel('Time (s)');
ylabel('Pressure (kPa)');
hold on;

plot(time,c3,'r');
grid on;
pause;
hold off;
%*****
%*****
%CHEST CRITERIA
%*****
%*****
pressurefn=[time;c2*1000];

save('pressurefn','pressurefn');

t = sim('cwvmodel_25072007');%name of specific simulink file to handle
this data format-note time spans must be specified in the simulink
file

load('vel');
load('displ');

plot(vel(1,:),vel(2,:));
grid on;
title('Chest wall velocity calculated for waterman');
xlabel('Time (s)');
ylabel('Chest wall velocity (m/s)');

[peakvel,i1]=max(vel(2,:));
minvel=min(vel(2,:));
stnum=num2str(peakvel);
disp(['Maximum chest wall velocity: ',stnum,'m/s.']);

stnum=num2str(minvel);
disp(['Minimum chest wall velocity: ',stnum,'m/s.']);

```

APPENDIX D: SUPPLEMENTARY INFORMATION FOR CHAPTER 7

APPENDIX D1: MATLAB Code to Process and Plot the South African Torso Surrogate (SATS) Results

plot_SATS_041108_final.m

```
%Plots results of tests conducted with SATS on 04/11/2008
%saved as plot_SATS_041108_final

clear all;

load('c1');
load('c2');
load('c3');
load('c4');
load('c5');

load('c6');
load('c7');
load('c8');
load('c9');

cacc=c1;%in g
aacc=c2;%in g
cp=c3.*1000;%to convert from MPa to kPa
ap=c4.*1000;%to convert from MPa to kPa
csp=c5;%in kPa
aip=c6;%in kPa

tend=(length(c1)*1.0000e-006)-(0.04+1.0000e-006);
time=(-0.04:1.0000e-006:tend);
time=time';
%plot(time,cacc);
%hold on;

%subtracting offsets
cacc=cacc-mean(cacc(1:10000));
aacc=aacc-mean(aacc(1:10000));
cp=cp-mean(cp(1:10000));
ap=ap-mean(ap(1:10000));
csp=csp-mean(csp(1:10000));
aip=aip-mean(aip(1:10000));

%filtering the acceleration signals
fs=1/0.000001;
[b,a]=butter(2,(1.25*40000*2/fs));
fcp=filtfilt(b,a,cp);
[b,a]=butter(2,(1.25*1650*2/fs));%cfc600 filter for acc as in vehicle
testing
```

```

fcacc=filtfilt(b,a,cacc);

%can't filter below signals as all are corrupt with discontinuities -
have
%no idea why!!
faacc=aacc;%filtfilt(b,a,aacc);
fap=ap;%filtfilt(b,a,ap);
fcsp=csp;
fcsp=filtfilt(b,a,csp);
faip=aip;%filtfilt(b,a,aip);

%only look at relevant part of signal - pre trigger data not important
partfcacc=fcacc(40001:60000,:);
partfaacc=faacc(40001:60000,:);
partfap=fap(40001:60000,:);
partfcp=fcp(40001:60000,:);
partfcsp=fcsp(40001:60000,:);
partfaip=faip(40001:60000,:);
timepart=time(40001:60000,:);

%plotting all data
hold off;
plot(time,cp,'b');
grid on;
xlabel('Time in seconds');
ylabel('Chest reflected pressure in kPa');
hold on;
plot(time,fcp,'g');
plot(timepart,partfcp,'r');
hold off;

pause;
plot(time,ap,'b');
grid on;
xlabel('Time in seconds');
ylabel('Abdominal reflected pressure in kPa');
hold on;
plot(time,fap,'g');
plot(timepart,partfap,'r');
hold off;

pause;
plot(time,csp,'b');
grid on;
xlabel('Time in seconds');
ylabel('Chest plate side-mounted pressure in kPa');
hold on;
plot(time,fcsp,'g');
plot(timepart,partfcsp,'r');
hold off;

pause;
plot(time,aip,'b');
grid on;
xlabel('Time in seconds');

```

```

ylabel('Abdominal internal pressure in kPa');
hold on;
plot(time, faip, 'g');
plot(timepart, partfaip, 'r');
hold off;

pause;
plot(time, cacc, 'b');
grid on;
xlabel('Time in seconds');
ylabel('Chest wall acceleration in g');
hold on;
plot(time, fcacc, 'g');
plot(timepart, partfcacc, 'r');

hold off;
pause;
plot(time, aacc, 'b');
grid on;
xlabel('Time in seconds');
ylabel('Abdominal wall acceleration in g');
hold on;
plot(time, faacc, 'g');
plot(timepart, partfaacc, 'r');
pause;
hold off;

%calculating cwvp

pressure=cp.*1000;%pressure in Pa
%pressure((45001:60000),:)=0;
plot(time, pressure, 'b');
xlabel('Time in seconds');
ylabel('Chest reflected pressure in Pa');
hold on;

%filtering the spikes out of the chest pressure signal
fs=1/0.000001;
[b,a]=butter(2, (1.25*40000*2/fs));
pressure=filtfilt(b,a,pressure);

plot(time, pressure, 'r');
xlabel('Time in seconds');
ylabel('Chest reflected pressure in Pa');
hold off;
pause;

pressure=pressure(40001:60000,:);
fcppart=pressure;

pressure=pressure';
time=time(40001:60000,:);

```

```

%*****
*****
%CHEST CRITERIA
%*****
*****
time=time';
plot(time,pressure,'b');
grid on;
xlabel('Time (s)');
ylabel('Pressure (Pa)');

pressurefn=[time;pressure];

save('pressurefn','pressurefn');
title('Pressure signal ');
xlabel('Time (s)');
ylabel('Pressure (Pa)');

pause;

t = sim('cwvmodel_sim');%name of specific simulink file to handle this
data format-note time spans must be specified in the simulink file

load('vel');
load('displ');

plot(vel(1,:),vel(2,:));
grid on;
title('Chest wall velocity calculated for ATD');
xlabel('Time (s)');
ylabel('Chest wall velocity (m/s)');

[peakvel,i1]=max(vel(2,:));
minvel=min(vel(2,:));
stnum=num2str(peakvel);
disp(['Maximum chest wall velocity: ',stnum,'m/s.']);

stnum=num2str(minvel);
disp(['Minimum chest wall velocity: ',stnum,'m/s.']);

```

plot_SATS_041108_chestdispanvel.m

```
%Plots results of tests conducted with SATS on 04/11/2008
%saved as plot_SATS_041108_chestdispanvel.m

clear all;

load('c1');
load('c2');
load('c3');
load('c4');
load('c5');

load('c6');
load('c7');
load('c8');
load('c9');

cacc=c1;%in g
aacc=c2;%in g
cp=c3.*1000;%to convert from MPa to kPa
ap=c4.*1000;%to convert from MPa to kPa
csp=c5;%in kPa
aip=c6;%in kPa

tend=(length(c1)*1.0000e-006)-(0.04+1.0000e-006);
time=(-0.04:1.0000e-006:tend);
time=time';

%subtracting offsets
cacc=cacc-mean(cacc(1:10000));

%***
%calculating chest wall velocity from acc signal
%this set to use unfiltered acc data

%integration of chest acceleration

tend=(length(c1)*1.0000e-006)-(0.04+1.0000e-006);
time=(-0.04:1.0000e-006:tend);
tstarti=40001%40001 is time of trigger;
tstart=(tstarti*1.0000e-006)-(0.04+1.0000e-006);
tendi=65536%40001+(0.010/1.0000e-006): for first 10 ms %65536%60000%;
tend=(tendi*1.0000e-006)-(0.04+1.0000e-006);
cacc=cacc(tstarti:tendi);
hf1=cacc(1)*9.81;%to get a in m/s^2

[b,a]=butter(2,(1.25*1650*2/100000));%CFC1000 as descibed in AEP-55
VOL 2
fcacc=cacc;%filtfilt(b,a,cacc);

dt=0.000001;
```

```

time=(tstart:dt:tend);
plot(time,cacc,'b');
grid on;
xlabel('Time in seconds');
ylabel('Chest wall acceleration in g (unfiltered - blue, filtered -
red)');
hold on;

cacc=fcacc;

plot(time,fcacc,'r');
hold off;

%endt=200001;
vplate(1)=dt*(hf1);%0.5*dt*(h2+h1);%

for loopv=2:(tendi-tstarti+1)
    hf1=cacc(loopv)*9.81;%to get a in m/s^2
    vplate(loopv)=(dt*hf1)+vplate(loopv-
1);%0.5*dt*(h2+h1)+v(loopv-1);
end;
[maxplatev,imaxplatev]=max(vplate);

pause;
plot(time,vplate);
grid on;
xlabel('Time in seconds');
ylabel('Chest wall velocity in m/s');

%integrate velocity to get displacement

hf1=vplate(1);

dispchest(1)=dt*(hf1);%0.5*dt*(h2+h1);%

for loopv=2:(tendi-tstarti+1)
    hf1=vplate(loopv);
    dispchest(loopv)=(dt*hf1)+dispchest(loopv-
1);%0.5*dt*(h2+h1)+v(loopv-1);
end;
[maxdispchest,imaxdispchest]=max(dispchest);

hold off;

for vclloop=1:(tendi-tstarti+1)
    vc(vclloop)=(vplate(vclloop)*dispchest(vclloop));
end;

pause;
plot(time,dispchest);
grid on;
xlabel('Time in seconds');
ylabel('Chest wall displacement in m');

```

```
peakvel=max(vplate);  
minvel=min(vplate);  
stnum=num2str(peakvel);  
disp(['Maximum chest wall velocity: ',stnum,'m/s.']);  
  
stnum=num2str(minvel);  
disp(['Minimum chest wall velocity: ',stnum,'m/s.']);
```


APPENDIX E: PUBLICATIONS

The research output from this study in the form of papers and presentations are listed below.

- van der Horst, M., Leerdam, P.J., Manseau, J., Lafont, D., Dosquet, F., Bir, C., Philippens, M., Vezin, P., Reinecke, D., Whyte, T., Svensson, L., Arborelius, U. and Frydman, A. 2010. Criteria and Test Methodologies for Injury Assessment of Vehicle Occupants Threatened by Landmines and/or IED: An Approach by HFM-148/RTG. *In Proceedings of Personal Armour Systems Symposium (PASS)*, Quebec, Canada. .
- Whyte, T. and Horsfall, I. 2010. The Development of a South African Torso Surrogate (SATS) to Explore Contradictions in Personal Protective Equipment (PPE) Test Standards and Methodologies Regarding Primary Blast Overpressure Injuries. *In Proceedings of Personal Armour Systems Symposium (PASS)*, Quebec, Canada. .
- Meel, B., Whyte, T. and Kaswa, R. 2009. Accidental Hand-Grenade Injuries in the Transkei Region of South Africa: A Case Report. *South African Family Practise*, Vol. 51(4), pp. 348-350.
- Whyte, T., Snyman, I.M. and Meel, B.L. 2008. Prediction of Injuries Caused by Explosive Events: A Case Study of a Hand Grenade Incident in South Africa. *In Proceedings of Science real and relevant: 2nd Council for Scientific and Industrial Research (CSIR) biennial conference*, Pretoria, South Africa.

APPENDIX F: PERSONAL COMMUNICATION WITH S. FORTH AND M. SHARMA

This appendix is based on discussions held at Cranfield University on 6 June 2014 with Mayank Sharma and Shaun Forth.

A major difference between ProSAir and ANSYS AUTODYN is that ProSAir uses ideal gas model equations whereas ANSYS AUTODYN uses JWL equations.

Preliminary results from comparison trials at various distances from 1 kg spherical TNT charge (with a diameter of 52.7 mm) gave the following results:

Distance from charge (m)	ProSAir Peak BOP (kPa)	ANSYS AUTODYN Peak BOP (kPa)
0.14	17800	9500
0.40	4280	4269
0.60	2600	2599
1.00	1010	974
4.00	148	142

Using an equivalent mesh size, autodyn took about 5 half hours to run whereas ProSAir took about 25 mins. This may be due to the generality options in ANSYS AUTODYN, whereas prosair is specifically used for blast simulations, thus the capabilities and hence the complexities are limited